ABSTRACT

Title of Dissertation: INVESTIGATING PAIR-RULE GENE ORTHOLOGS IN AN INTERMEDIATE GERM BEETLE, *DERMESTES MACULATUS*

Jie Xiang, Doctor of Philosophy, 2017

Dissertation directed by: Professor Leslie Pick
Department of Entomology
University of Maryland, College Park

Insects share a body plan based on repeating segments. Segmentation has been well characterized in *Drosophila melanogaster*, in which segments are established by a genetic hierarchy including gap, pair-rule and segment polarity genes. Pair-rule genes (PRGs) are a key class of segmentation genes as they are the first cohort of genes expressed in a periodic pattern. Segments are established simultaneously in *Drosophila* in early embryos, while most other insects add segments sequentially as the embryo elongates. Our goal is to understand molecular mechanisms controlling segment formation and to determine the extent of their conservation during evolution. Here, we established the hide beetle *Dermestes maculatus*, an intermediate germ developer, as a new model system for studying segmentation patterning. We first established a lab colony and studied early embryogenesis in *Dermestes*. All nine PRG orthologs were isolated using degenerate PCR and RACE, and their expression

patterns were examined with *in situ* hybridization. Except for *opa*, all *Dermestes* PRG orthologs are expressed in PR-like striped patterns. Gene functions were tested using RNA interference (RNAi). We examined both hatched and unhatched larvae to uncover defects with different severities. Both *Dmac-prd* and -*slp* knockdown resulted in typical PR defects, suggesting that they are "core" PR genes. *Dmac-eve*, -*run* and -*odd* have dual roles in germ band elongation and in PR segmentation, as severe knockdown caused anterior-only, asegmental embryos while moderate knockdown resulted in PR-like defects. Elongated but asegmental germ bands resulted from *Dmac-prd* and -*slp* double knockdown, suggesting decoupling of germ band elongation and PR segmentation. Extensive cell death prefigured the cuticle patterns after knockdowns, seen long ago for *Drosophila* PR phenotypes, although disrupted cell mitosis was also observed after *Dmac-eve* knockdown. We propose that PRGs have retained basic roles in PR segmentation during the transition from short-to-long germ development and share evolutionary conserved functions in promoting cell viability. Finally, I also present detailed protocols on *Dermestes* lab rearing, embryo collection and fixation, *in situ* hybridization and RNAi. The technical information described here will provide useful information for other genetic studies in this new model system.

INVESTIGATING PAIR-RULE GENE ORTHOLOGS IN AN INTERMEDIATE GERM BEETLE, *DERMESTES MACULATUS*

by

Jie Xiang

Dissertation submitted to the Faculty of the Graduate School of the
University of Maryland, College Park, in partial fulfillment
of the requirements for the degree of
Doctor of Philosophy
2017

Advisory Committee:
Dr. Leslie Pick, Chair
Dr. Alexa Bely
Dr. Eric Haag
Dr. Steve Mount
Dr. Jian Wang

Dedication

To Mingxuan, Yuhuan and my parents

Acknowledgements

First, I would like to express my gratitude to my advisor, Dr. Leslie Pick, for her great support and generous advice during my study. Her knowledge, understanding, patience and enthusiasm have made my time in graduate school enjoyable and rewarding. I am really grateful to other committee members, Dr. Eric Haag, Dr. Steve Mount, Dr. Alexa Bely and Dr. Jian Wang for their advice and help on this project through years.

Next, I would like to thank all previous and current members of the Pick lab, especially Alison Heffer and Yong Lu for teaching me basic techniques and giving me advice, Katie Reding for helping me with beetles rearing, RNAi and manuscript preparation, and Iain Forrest for his help on several experiments. I also need to thank other lab mates, Amanda Field, Mengyao Chen, Alys Jarvela, Patricia Graham and Faith Kung for your help and friendship.

I would like to thank my friends in other labs and departments, especially Lijuan Du, Xiangying Meng, Hsiao-ling Lu, Chyong-yi Wu, for their help, support, and friendship. They made my life here in College Park much better with lots of fun. I would also like to extend my thanks to people in Entomology Department, BISI program, and several research facilities for their help on my study and experiments.

To my parents, thank you for your unconditional love and support. You allow me to explore the world and have always been there, listening to me and guiding me through all the difficulties. To my son Yuhuan, I am very grateful for your coming into my life and all the joy you bring. You make me happier and become a better

person. To my husband Mingxuan, thank you for your support and encouragement during the past 10 years. I wouldn't have gone this far without you.

Table of Contents

List of Tables

List of Figures

Figure 4-14. *Dermestes* PRG orthologs required for elongation and PR-like segmentation.

List of Abbreviations

A. mellifera or *Am*: *Apis mellifera*

AEL: after egg laying

anti-PH3: anti-phospho Histone H3

B. mori or *Bmor*: *Bombyx mori*

bp: base pair

C. maculatus: *Callosobruchus maculatus*

CNS: central nervous system

COI: cytochrome c oxidase subunit I

D. frischi: *Dermestes frischi*

D. maculatus or *Dmac*: *Dermestes maculatus*

D. melanogaster or *Dm*: *Drosophila melanogaster*

Dcp-1: Droshphila caspase-1

dsRNA: double-stranded RNA

en/En: *engrailed*/Engrailed

eRNAi: embryonic RNA interference

eve: *even-skipped*

ftz: *fushi tarazu*

G. bimaculatus or *Gb*: *Gryllus bimaculatus*

gsb: *gooseberry*

gsb-n: *gooseberry-neuro*

h: *hairy*

h: hour(s)

HD: homeodomain

hl: head lobe

MUSCLE: multiple sequence comparison by Log-Expectation

N. vitripennis or *Nv*: *Nasonia vitripennis*

O. fasciatus or *Of*: *Oncopeltus fasciatus*

odd: *odd-skipped*

OP: octapeptide

opa: *odd-paired*

P. americana or *Pa*: *Periplaneta americana*

paf: posterior amniotic fold

PD: paired domain

prd: *paired*

PRG: pair-rule gene

pRNAi: parental RNA interference

ps: parasegment

RACE: rapid amplification of cDNA ends

RNAi: RNA interference

run: *runt*

S. americana: *Schistocerca americana*

S. gregaria: *Schistocerca gregaria*

SAZ: segment addition zone

slp: *sloppy paired*

SPG: segment polarity gene

sw: serosal window

T. castaneum or *Tc*: *Tribolium castaneum*

vf: ventral furrow

Chapter 1: Introduction

Arthropods are the largest group of animals, representing over 80% of known animal species (Zhang, 2011). Though they occupy all kinds of habitats, range in size and display distinct as well as intriguing morphologies, repeated metameric units along the anterior-posterior axis is a shared feature among them. This segmented body plan, along with associated jointed appendages, are thought to provide functional flexibility for arthropods to adapt to different environments. This likely has contributed largely to the great success of this group of animals (Jarvis et al., 2012). Interesting questions regarding arthropods body plan patterning include to what extent the patterning mechanism is conserved, and how segmentation genes and gene regulatory networks evolved. To address these questions, comparative studies on developmental processes in different species (evo-devo) are required.

Among arthropods, insects are the largest group with great morphological diversity. Generally, insects have small body size, a relatively short life cycle and high fecundity. Insect rearing in a lab environment is feasible and cheap. With the technical advances during the past two decades in this group, including genome sequencing and RNA interference (RNAi), insects provide a good repertoire for comparative developmental genetics studies for reconstructing the evolutionary path of basic body plan patterning.

1.1 Early embryogenesis in *Drosophila melanogaster*

Drosophila melanogaster (*D. melanogaster*, common name: fruit fly) is the most well-studied representative of Arthropods. As a holometabolous insect, its

development undergoes embryonic, several larval instars, pupal and adult stages. With a short life cycle, high fecundity and the ease of husbandry, *D. melanogaster* has emerged as an ideal model for studying genetics and development. The steps involved in early embryogenesis have been well characterized in this species (Figure 1-1) (Campos-Ortéga and Hartenstein, 1997; Gilbert, 2010). After the fusion of male and female pronuclei, nuclear division initiates and occurs in the anterior of the embryo during the first several rounds of division. Later, nuclei spread out along the anterior-posterior (AP) axis and gradually move towards the egg surface. Except for a few moving to the posterior pole or remaining in the yolk, nuclei arrive at the egg periphery at cell cycle 10, establishing a syncytial blastoderm (a common cytoplasm shared by all nuclei). Following three more nuclear division cycles, a cellular blastoderm is established as cell membranes invaginate between individual energids (nucleus surrounded by cytoplasm). Soon after cellularization, gastrulation proceeds with dramatic morphological movements to establish three germ layers with invaginated mesoderm and endoderm (reviewed in (Campos-Ortéga and Hartenstein, 1997; Gilbert, 2010). During gastrulation, a germband is formed, consisting of the primodium of future trunk. The germ band extends and then folds over within the egg shell. The first morphological sign of segments appear well after gastrulation (Martinez-Arias and Lawrence, 1985).

Figure 1-1. Early embryogenesis in *D. melanogaster*. During the first 9 cell cycles, nuclei divide in the center of the embryo. Most nuclei arrive at the egg surface at cycle 10. After several rounds of division at the egg periphery, a cellular blastoderm is established at cycle 14. Figure from Developmental Biology. 6th edition, Gilbert S.F., 2000.

1.2 A genetic hierarchy determining segmentation in *D. melanogaster*

In 1980, Christiane Nüsslein-Volhard and Eric Wieschaus published their pioneer genetic screen for zygotic mutations causing segmentation defects in *D. melanogaster* (Nüsslein-Volhard and Wieschaus, 1980). Before this work, maternal effect mutants lacking the anterior, posterior or terminal regions, as well as homeotic mutants with mis-specified segment identity had been reported in *D. melanogaster* (see below). However, the processes for establishing segments in *D. melanogaster* were still unknown at that time. Based on the phenotypes discovered in (Jürgens et al., 1984; Nüsslein-Volhard and Wieschaus, 1980; Nüsslein-Volhard et al., 1984; Wieschaus et al., 1984b), mutants were assigned to three classes (Figure 1-2): 1. Loss of several consecutive segments (gap mutants), 2. Deletion in every other segment

(pair-rule, PR mutants) and 3. Abnormality in every segment, usually mirror-image duplication associated with deletion (segment polarity mutants).

Since then, genes responsible for these segmentation defects have been isolated and investigated. A sequential mechanism subdividing the *D. melanogaster* embryo into increasingly specified and ultimately repeated metameric units along the anterior-posterior axis has been revealed (Akam, 1987; Gilbert, 2010; Lawrence, 1992; Lewis, 1978; Nüsslein-Volhard et al., 1985; Nüsslein-Volhard and Wieschaus, 1980; Wakimoto et al., 1984). The hierarchy is initiated by maternal effect genes. Transcripts from maternal effect genes are deposited into the egg during oogenesis. Protein products activate or repress zygotic gene expression and the basic axes of the embryo are determined. For example, *bicoid* (*bcd*) mRNA is localized in the most anterior region in early embryos. Bcd translated from the transcripts diffuse freely in the syncytial blastoderm and form a gradient with the highest concentration in the most anterior region. In *bcd* mutants, the anterior region including head and thorax are missing (Driever and Nüsslein-Volhard, 1988; Driever et al., 1990). Maternal effect genes regulate gap genes, which are expressed in one or sometimes more broad domains. Gap genes determine broad regions in embryo, as evidenced by loss of a set of segments in gap gene mutants. For example, *Krüppel* (*Kr*) mutants lack thoracic and anterior abdominal segments (Nüsslein-Volhard and Wieschaus, 1980; Wieschaus et al., 1984a). Pair-rule genes (PRGs), most of which are expressed in 7-striped patterns, promote the development of body segments. Their expression patterns are staggered along the anterior-posterior axis in the embryo. PRG mutants display similar but non-identical defects, emphasizing the importance of combined

contributions from this cohort of genes (Gergen and Wieschaus, 1985; Nüsslein-Volhard and Wieschaus, 1980). For examples, seven even-numbered parasegments are missing in *fushi tarazu* (*ftz*) mutants while seven odd-numbered parasegments are missing in even-skipped (*eve*) (Nüsslein-Volhard and Wieschaus, 1980; Wakimoto et al., 1984). Segment polarity genes (SPGs) determine anterior-posterior polarity in each segment and establish parasegmental boundaries. *engrailed* (*en*), a segment polarity gene, is expressed in 14-stripes in the posterior region of every segment. *en* is important for maintaining compartment boundaries. Fused segments in *en* mutants suggest failure in segmentation (Kornberg, 1981). Lastly, homeotic genes determine the unique identities of each segment. Ectopic expression of homeotic gene leads to a 'homeotic transformation', defined by Bateson in 1894 as the replacement of one body part with an alternate body part (Bateson, 1894). For example, *Antennapedia* (*Antp*) plays a crucial role in the second thoracic (T2) segment. When it is ectopically expressed in the head, antennae are transformed to T2 legs (Schneuwly et al., 1987).

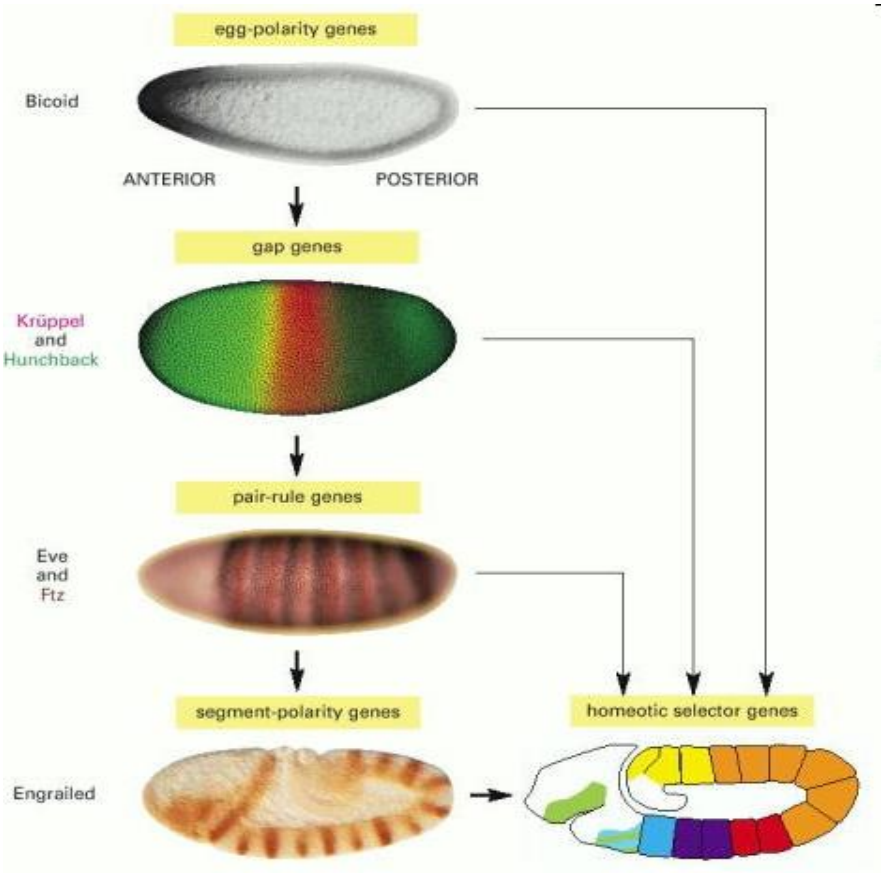

Figure 1-2. The genetic hierarchy determining segmentation in *D. melanogaster* embryogenesis. Maternal effect genes establish embryonic polarity. They regulate gap genes, which divide the embryo into large regions covering consecutive segments. Gap genes regulate pair-rule genes (PRGs), which further promote segmentation. Segment polarity genes (SPGs) are controlled by PRGs and determine AP polarity in each segment. Lastly, homeotic genes specify unique segment identities. In general, segmentation genes are expressed in the primordia of tissue lost or affected in mutants. Figure from Molecular Biology of the Cell. 4th edition, Alberts B. Johnson A, Lewis J, et al. 2002

1.3 PRGs in *D. melanogaster*

Except for *ftz-f1* (*fushi tarazu factor 1*) and *odd-paired* (*opa*), *D. melanogaster* PRGs are expressed in alternating parasegments or segments, the primordia of regions missing in the corresponding mutants. With the expression of the cohort of PRGs, upstream aperiodic information is converted into periotic output with offset register. In total, nine PRGs have been reported in *D. melanogaster*

(Jürgens et al., 1984; Nüsslein-Volhard and Wieschaus, 1980; Nüsslein-Volhard et al., 1984; Wakimoto et al., 1984; Yu et al., 1997). They are *eve*, *runt* (*run*), *hairy* (*h*), *odd-skipped* (*odd*), *paired* (*prd*), *sloppy paired* (*slp*), *odd-paired* (*opa*), *ftz* and its cofactor *ftz-f1*.

A large body of literature is focused on this cohort of genes, giving insights into their expression, function, downstream targets, genetic interactions and transcriptional regulation. Mainly based on regulatory interactions among them, a hierarchical PRG network model was proposed (Akam, 1989; Ingham, 1988; Ingham and Martinez-Arias, 1986). Maternal effect and gap genes regulate expression of primary PRGs. Primary PRGs interact with each other and define their expression. Secondary PRGs are regulated by primary PRGs, and there is also interactions among secondary PRGs. Secondary PRGs are thought to regulate expression of segment polarity genes thus establishing parasegmental boundaries more directly (Akam, 1989; Ingham, 1988; Ingham and Martinez-Arias, 1986). In general, resolved striped expression of primary PRGs is slightly earlier than other PRGs (Ingham, 1988). Furthermore, mainly after investigating the regulatory elements of *ftz*, *h* and *eve*, it was proposed that 7-striped patterns of primary PRGs are generated by separate stripe-specific *cis*-regulatory elements, while 7-striped patterns of secondary PRGs are driven by primary PRGs via zebra elements (Akam, 1989; Goto et al., 1989; Harding et al., 1989; Hiromi and Gehring, 1987; Hiromi et al., 1985; Howard et al., 1988; Ingham, 1988).

Later, lines of evidence suggested that the above model is oversimplified. For example, the establishment of secondary PRGs - *ftz* and *prd* - stripes require upstream

aperiodic input (Gutjahr et al., 1993a; Yu and Pick, 1995). These two secondary PRGs also regulate primary PRG such as *run* (Klingler and Gergen, 1993). Shroeder et al. performed a computational prediction, and they found that there are two *odd* upstream modular elements: *odd_(-3)* drives expression in stripe 3 and 6, while *odd_(-5)* drives an anterior striped expression (stripe 1) and a posterior broad expression domain (probably stripe 5 and 6) (Schroeder et al., 2004). *odd* thus behaves in a primary PRG manner. Altogether, the regulatory network of PRGs is much more complicated than we thought before and cannot fit perfectly into the hierarchical model.

1.4 Diverse modes of segmentation in insects

In 1939, Krause reported his observations regarding insect embryogenesis and embryo morphologies (Krause, 1939). By observing early embryogenesis and manipulating embryos, Krause and other researchers found that in some species, such as *D. melanogaster*, segments are specified almost at the same time during blastoderm stages (long germ mode or simultaneously segmenting mode). In contrast, in some other species, such as *Tribolium castaneum* (*T. castaneum*), only head segments are specified at the end of blastoderm stage. Other posterior segments are added sequentially from posterior segment addition zone (SAZ) (Figure 1-3) (Janssen et al., 2011). Intermediate germ species like *Dermestes maculatus* develop somewhere between the above two extremes. Head and thoracic segments are specified in the germ anlage (embryonic rudiment) prior to gastrulation. Because

posterior segments are added sequentially in short and intermediate germ developers, these are both referred to as sequential segmentation.

Krause also observed that long germ insects usually have a large initial germ anlage (relative to their egg sizes) at the end of blastoderm stage, while short germ developers have a small germ anlage at the same stage. For example, in *D. melanogaster*, almost all the cells in the cellular blastoderm form future germ anlage. In extreme short germ species, such as the grasshopper *Schistocerca gregaria* (*S. gregaria*), only a very small portion of cells located in the ventral posterior contribute to the future germ anlage (Akam and Dawes, 1992).

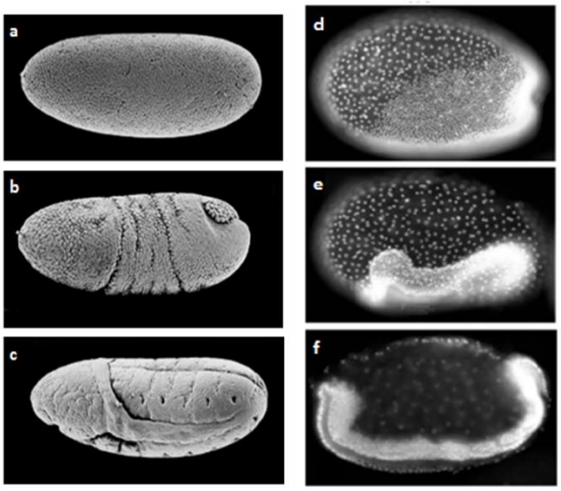

Figure 1-3. Long and short germ segmentation modes are employed in *D. melanogaster* and *T. castaneum* embryogenesis, respectively. (a,b,c) SEM photographs of *D. melanogaster* embryogenesis. Adapted from http://labs.fhcrc.org/parkhurst/embryo.html; (d,e,f) DAPI nuclear staining of *T. castaneum* embryogenesis. Modified from (van der Zee et al., 2005). (a) About 6000 cells are distributed on the periphery of the egg at the end of the cellular blastoderm stage. (b) *D. melanogaster* embryo then starts gastrulation, during which, cephalic furrow and anterior and posterior transversal furrows become obvious. (c) An extended segmented germ band is evident after germ band extension. (d) For *T. castaneum* embryogenesis, at the end of blastoderm stage, a population of cells migrates to the posterior ventral region to form the germ rudiment. (e) At the early germ band stage, head lobes and a posterior growth zone are visible. (f) During germ

band extension, more segments are formed. In *D. melanogaster* embryogenesis, all segments are specified almost simultaneously at the onset of gastrulation. For *T. castaneum*, only anterior segments are specified prior to gastrulation; posterior segments are added sequentially from the posterior end (SAZ).

While short and intermediate germ modes appear to be more widely distributed in different insect orders, the long germ mode appears to exclusively exist in holometabolous insects (Figure 1-4) (Davis and Patel, 2002; Liu and Kaufman, 2005b; Stahi and Chipman, 2016). Basally branching insects seem to use short and/or intermediate germ modes while derived Diptera fulfill their body plan using long germ modes. Both short and/or intermediate and long germ modes have been reported in several major holometabolous orders, including Lepidoptera, Coleoptera and Hymenoptera. These observations suggest that the short germ mode is likely to be an ancestral state and the long germ mode an invention in some Holometabola (Liu and Kaufman, 2005b).

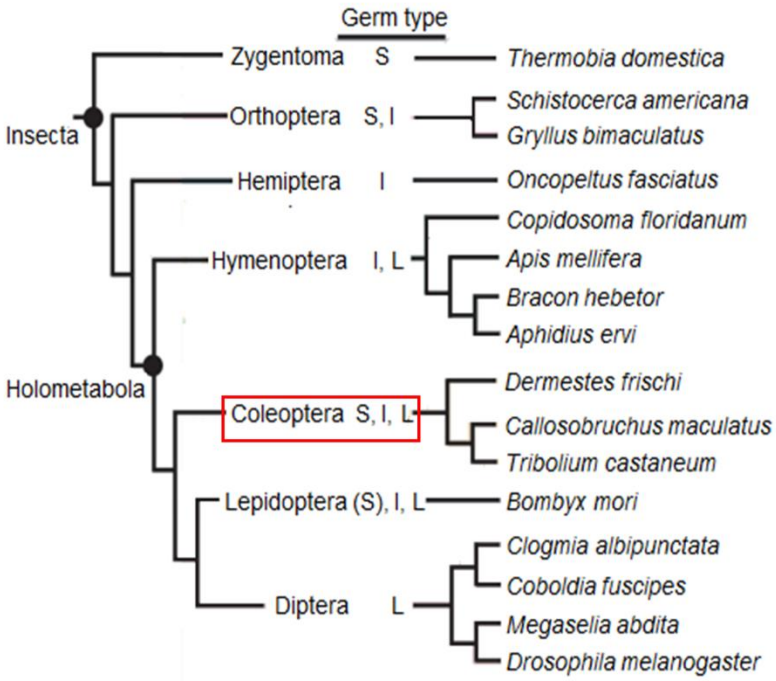

Figure 1-4. Different modes of segmentation are widespread during insect evolution. While short and intermediate germ types have been reported throughout Insecta, the long germ mode is restricted to Holometabola. Figure adapted from (Liu and Kaufman, 2005b).

1.5 Hypotheses on the short-to-long transition

As previously introduced, in *D. melanogaster*, the segmentation hierarchy was activated in blastoderm stage embryos, where molecules can diffuse freely to establish morphogen gradients critical for initiating the hierarchy. Segments are patterned almost simultaneously in *D. melanogaster*, In contrast, in sequentially segmenting species with short or intermediate germ modes, posterior segments added after gastrulation are formed in an obviously different environment – a cellular environment. Therefore, it is reasonable to speculate that a different route would be taken to achieve a segmented body plan in sequentially segmenting species, at least for posterior segments generated after gastrulation. There is also a particular interest in investigating the segmentation network in species with intermediate germ modes, as this mode may be an intermediate state during the short-to-long germ mode transition. So far, there are several hypothesis regarding the cause of the transition.

In *D. melanogaster*, maternal inputs localized at both poles are required for patterning. In short germ species, such as *Schistocerca* and *Atrachya menetriesi*, germ band development seems normal after manipulating the anterior half of the embryo (Miya and Kobayashi, 1974; Sander, 1976). These results indicated that an anterior localized organizing center is not required in these species (Davis and Patel, 2002). Indeed, compared to the posterior organizing center, the anterior organizing center is less conserved in insects (Liu and Kaufman, 2005b; Peel et al., 2005). Consistent with this hypothesis, nurse cells, which provide maternal inputs, are not present in most

insects outside of Holometabola (Davis and Patel 2002). Taken together, this suggests that the enrichment of maternal patterning information may have played a role in the short-to-long germ transition. However, there is some contradictory evidence. For example, both anterior and posterior organizing centers exist in short germ *Bombyx mori* (*B. mori*) (Nakao, 2012).

Recent studies in *T. castaneum* revealed that some PRG orthologs (*eve, odd*) show clock-like dynamic expression, reminiscent of somitogenesis-related gene expression in vertebrates (El-Sherif et al., 2012; Sarrazin et al., 2012). Similar dynamic expression of *h* has been shown in a chelicerate and some basally branching insects, although whether or not *h* is actually involved in a germ band elongation driven by a clock-like mechanism is still under debate (Kainz et al., 2011; Mito et al., 2011; Pueyo et al., 2008; Schoppmeier and Damen, 2005b; Stollewerk et al., 2003). It has been proposed that a primary oscillator of PRGs in sequentially segmenting ancestors may have been replaced by gap genes, thus triggering the short-to-long germ transition. Notably, some gap gene expression shifts towards the anterior over time. Such dynamic expression pattern is very similar to the reported "wave" of PRG ortholog expression in *T. castaneum* (El-Sherif and Levine, 2016; Verd et al., 2016). Clark et al. hypothesized that during the short-to-long transition, gap genes acquired the oscillatory feature and gradually replaced the PRGs-related oscillator (Clark, 2017).

Germ anlage in short germ species are located in the ventral posterior end of the blastoderm before gastrulation. In long germ species, the germ anlage is relatively large, covering anterior regions (Davis and Patel, 2002; Krause, 1939). A study

showed that knockdown of *zerknüllt1* (*zen1*) in *T. castaneum* resulted in loss of serosa (van der Zee et al., 2005). Interestingly, after *zen1* knockdown, the germ anlage expanded anteriorly, showing long germ mode features. Moreover, the overall expression patterns of PRG orthologs shifted towards the anterior, reminiscent of PRG expression in long germ *D. melanogaster* (van der Zee et al., 2005). This study thus indicated that there might be an association between extraembryonic tissue specification and germ mode: reduced extraembryonic tissue in short germ developers may cause the transition towards long germ segmentation mode.

To summarize, the appearance of a syncytial blastoderm stage, enrichment of maternal inputs, reduced requirement for oscillatory features of PRGs, and loss of extraembryonic tissue may be prerequisites or even direct causes for the short-to-long germ transition. Based on the distribution of segmentation modes on the phylogenetic tree of insects, a long germ segmentation mode may have arisen several times independently within different orders in Holometabola (Davis and Patel, 2002; Liu and Kaufman, 2005b). Thus, even if direct causes of short-to-long transition were to be demonstrated someway in some systems, there might be other routes to reach long germ segmentation modes in other lineages.

1.6 PR or not PR? - early PRG orthologs expression studies

In the early 1990s, several insect models were developed to study segmentation. Functional tools were not available when these early studies were performed, thus conclusions were drawn from embryonic expression patterns of segmentation gene orthologs.

The grasshopper *Schistocerca americana* (*S. americana*, grasshopper, Orthoptera) is an extreme short germ insect with several notable features correlated with a primitive segmentation mode. Only a very small number of cells in late blastoderm stage contribute to the germ anlage (Akam and Dawes, 1992). All or most segments are patterned after gastrulation (Sander, 1976). Another feature is that it has panoistic ovaries, which lack nurse cells and the corresponding maternal inputs (Davis and Patel, 2002; Patel et al., 1994). Using an antibody raised against grasshopper Eve, expression was examined in *S. americana* (Patel et al., 1992). Eve was expressed in a segmentally repeated pattern in a subset of homologous neurons in both *D. melanogaster* and *S. americana*, suggesting its conserved function in both insects (Doe et al., 1988; Patel et al., 1992). At early developmental stages, after gastrulation, Eve was detected in the posterior region of the germ band, following the appearance of two *en* stripes, but Eve expression never resolved into a striped or periodic pattern (Patel et al., 1992).

Consistent with this finding, a *ftz* ortholog from a different Orthopteran species (*S. gregaria*) showed a very similar pattern. Posterior expression never resolved into a PR-like pattern (Dawes et al., 1994). Together, this suggests that these two PRG orthologs, which are crucial players in *D. melanogaster* PR patterning, do not function similarly in grasshopper. At that time, this result casted doubt on the existence of PR patterning in short germ species, and indicated that even if PR patterning is still required in these insects, the components as well as the mechanism are substantially different.

Data from another sequentially segmenting species, the short germ beetle *T. castaneum*, revealed a different scenario. Sommer and Tautz (Sommer and Tautz, 1993) performed *in situ* hybridization to investigate *Tc-h* expression. Striped expression was detected at early blastoderm stage in a PR-like pattern. A primary *Tc-h* stripe pattern later resolved into secondary segmental striped expression, probably by stripe splitting (Sommer and Tautz, 1993). Appearance of secondary segmental stripes from a primary PR pattern of PRGs also occurs in *D. melanogaster* (*eve* (Macdonald et al., 1986); *odd* (Coulter et al., 1990); *slp* (Grossniklaus et al., 1992); *prd* (Kilchherr et al., 1986); *run* (Klingler and Gergen, 1993). *ftz* expression was analyzed in this short germ beetle as well. Resolved *ftz* stripes overlap with every other En stripe, displaying typical PR expression pattern (Brown et al., 1994a). This indicates that PR patterning is present in species with a short germ mode. Using a cross-acting antibody, Patel et al. examined Eve expression in three beetles, including *T. castaneum* (Patel et al., 1994). Though with distinct germ types, Eve was expressed in similar patterns in all these species: primary stripes appear sequentially in an anterior-to-posterior order from a broad posterior expression. Primary stripes then split into pairs of secondary stripes. The major difference between the different species seems to be the number of primary stripes before gastrulation, with 2 in *T. castaneum*, 4 in intermediate germ *Dermestes frischi* (*D. frischi*), and 6 in the long germ *Callosobruchus maculatus* (*C. maculatus*) (Patel et al., 1994).

In more recent years, the number of species in which PRG ortholog expression has been examined increased. Most of these studies focused on a subset of PRGs, especially *eve, h, run, odd, ftz* and *prd*/*pairberry*, from species representing

Diptera, Lepidoptera, Coleoptera and Hymenoptera. Early studies showed PR-like patterns, indicating that they may be involved in PR patterning in these Holometabolous species with distinct germ modes (Section 1.7 and Figure 1-5).

Information from more basally branching insects outside of Holometabola is sparse. To date, variation in PRG ortholog expression has been observed. For example, besides posterior expression in grasshopper, *eve* is also expressed in a broad domain in the posterior of milkweed bug *Oncopeltus fasciatus* (*O. fasciatus*) and cricket *Gryllus bimaculatus* (*G. bimaculatus*) embryos (Liu and Kaufman, 2005a; Mito et al., 2007). Periodic patterns resolve from posterior expression, though the registers of those stripes have not been fully determined yet (Section 1.7 and Figure 1-5).

Taken together, early studies, based solely on expression patterns, suggested that PR patterning is largely conserved, at least within Holometabola. These studies suggested that several orthologs of *D. melanogaster* PRGs are required for dividing tissue into repeated metameric units in insects with distinct germ modes.

1.7 PRG functions vary in insects

When and where a gene is expressed can provide clues about the gene's function. However, it is not always the rule. For examples, modifications such as post-transcriptional and post-translational regulation can affect gene activity. For some PRG products, activity is also limited by interaction with coactivators or corepressors. Therefore, although expression patterns indicate that some PRG orthologs are involved in segmentation patterning in other species, functional studies are required to assess PRG orthologs' function. To our knowledge, such studies have

only been reported in a limited number of insect species, including *B. mori* (short germ; Lepidoptera), *T. castaneum* (short germ; Coleoptera), *Nasonia vitripennis* (*N. vitripennis*, long germ; Hymenoptera), *Apis mellifera* (*A. mellifera* long germ; Hymenoptera), *O. fasciatus* (intermediate germ, Hemiptera), *G. bimaculatus* (intermediate germ, Orthoptera). Surprisingly, PRG orthologs show divergent function, even within so few examined insects.

*1.7.1 Coleoptera (*T. castaneum*)*

As a worldwide pest of stored grain products, *T. castaneum* has been developed into a new model insect system during the past two decades with a sequenced and annotated genome, and techniques for genetic studies, such as RNAi, germline transformation and CRISPR/Cas-9 (Bucher et al., 2002; Lorenzen et al., 2003; Posnien et al., 2009; Richards et al., 2008). Recent progress on imaging cellular dynamics using transient fluorescence labeling facilitated the study of embryogenesis in wild-type or genetically manipulated *T. castaneum* individuals (Benton et al., 2013). As introduced previously, *T. castaneum* represents a short germ insect, developing into a segmented germ band differently than *D. melanogaster* (Davis and Patel, 2002; Patel et al., 1994) and Section 1.4). Together with available tools and resources, *T. castaneum* thus became an important representative for comparative studies of segmentation.

A number of studies have examined the expression patterns of *Tc-eve, run, odd, prd, slp, ftz,* and *h.* These genes are all expressed in PR-like patterns, indicating that they have conserved roles in PR segmentation in this short germ beetle (Aranda

et al., 2008; Brown and Denell, 1996; Brown et al., 1994a; Brown et al., 1997; Choe and Brown, 2007; Choe et al., 2006; Eckert et al., 2004; Patel et al., 1994; Sommer and Tautz, 1993) and section 1.4). Stuart et al. generated a large genome deficiency in the *T. castaneum* Homeotic complex. The *Tc-ftz* locus was deleted in this deficiency, however, no PR-like phenotype was revealed (Stuart et al., 1991). Thus, it appears that *Tc-ftz* is not involved in PR patterning despite the fact that it is expressed in a PR-like striped pattern (section 1.6; (Brown et al., 1994a). Schröder et al. studied *Tc-eve* function using chromophore-assisted laser inactivation (CALI) (Schröder et al., 1999). Anterior patterning defects were observed after inactivating *Tc*-Eve function (Schröder et al., 1999). The defects appeared to be PR-like, restricted in anterior segments, leaving entire abdominal segments unaffected, although they were observed with low frequency.

The first systematic analysis of PRG orthologs in species other than *Drosophila* was carried out in *T. castaneum* by (Choe et al., 2006). *T. castaneum* PRG orthologs' expression patterns were reexamined in this study. The results were very similar to those previously reported. *Tc-eve* is expressed in a posterior domain in embryos at both blastoderm and germ band stages. Striped expression of *Tc-eve* segregates from the posterior expression domain in an anterior-to-posterior sequence. Primary stripes split into pairs of secondary stripes due to fading expression in the center of each stripe (Brown et al., 1997; Patel et al., 1994). *Tc-h* expression is dynamic in the posterior region of the embryo. PR-like primary stripes appear sequentially and split into secondary segmental stripes (Aranda et al., 2008; Eckert et al., 2004). *Tc-odd* is expressed in a PR-like pattern complimentary to *Tc-eve* (Choe et

al., 2006). *Tc-run* and *-ftz* show primary PR-like striped expression pattern without secondary segmental striped expression (Brown and Denell, 1996; Brown et al., 1994a; Choe et al., 2006). *Tc-slp* and *prd* secondary stripes appear by *de novo* intercalation and splitting, respectively (Choe and Brown, 2007; Choe et al., 2006). One or two primary PRG stripes are established in *T. castaneum* before gastrulation, consistent with its short germ segmentation mode (Brown and Denell, 1996; Davis and Patel, 2002).

In *T. castaneum*, injected dsRNA can be taken up by gonads and cause defects in offspring (Bucher et al., 2002). This type of RNA interference thus is named parental RNAi (pRNAi). To demonstrate the role of PRG orthologs during segmentation in *T. castaneum*, Choe et al. performed functional studies using pRNAi (Choe et al., 2006). *Tc-eve*, *Tc-run* and *Tc-odd* pRNAi resulted in truncated, asegmental embryos, with only spherical head cuticle left (Choe and Brown, 2009; Choe et al., 2006). Unlike *Tc-eve*, *-run*, and *-odd*, knockdown of *Tc-prd* and *Tc-slp* resulted in typical, *Drosophila*-like pair-rule phenotypes (Choe and Brown, 2007; Choe et al., 2006). Odd- and even-numbered segments were missing in *Dmac-prd* and *Dmac-slp* RNAi embryonic cuticles, respectively (Choe and Brown, 2007, 2009; Choe et al., 2006).

Further investigation of gene expression patterns after knockdown indicated that *Tc-eve, -run* and *-odd* act at a higher functional level than *Tc-prd* and *-slp* (Choe et al., 2006). In addition, a genetic circuit for *T. castaneum* was proposed: *Tc-eve* activates *Tc-run*, which in turn activates *Tc-odd*, and *Tc- eve* is repressed by Tc-*odd*. This circuit is involved in forming an elongating germ band. Knockdown of any

member disrupted this self-regulatory network and thus resulted in truncated embryos (Choe et al., 2006). Choe et al. proposed that a clock-like mechanism exists in short germ *T. castaneum* (Choe et al., 2006). Such a mechanism has been reported in vertebrate presomitic mesoderm segmentation (reviewed in (Pourquié, 2011), non-insect arthropod species (Stollewerk et al., 2003), and the centipede *Strigamia maritima* (Chipman et al., 2004). Recent studies provided more convincing data on the existence of a clock-like mechanism in *T. castaneum* (El-Sherif et al., 2012; Sarrazin et al., 2012).

Heffer et al. investigated the function of *Tc-ftz-f1* (Heffer et al., 2013). *Tc-ftz-f1* is first expressed uniformly in early embryo. Later, it is expressed as a single stripe in late blastoderm stage embryos. *Tc-ftz-f1* stripes arise sequentially during germ band elongation, and the register of the stripes was confirmed as PR stripes (Heffer et al., 2013). *Tc-ftz-f1* pRNAi affected egg laying (Heffer et al., 2013; Xu et al., 2010). Therefore, embryonic RNAi, which requires direct injection of dsRNA into individual early embryos, was performed (Heffer et al., 2013). Reduced Engrailed expression in alternate segments revealed the PR-like segmentation function of *ftz-f1* in *T. castaneum* (Heffer et al., 2013).

Unlike *Tc-eve, -run, -odd, -ftz, -prd* and *-slp*, which all play crucial roles in segmentation patterning in *T. castaneum*, knockdown of *Tc-ftz* or *-opa* didn't produce any trunk segmentation defects (Choe et al., 2006). *Tc-h* RNAi caused defects but only in head patterning (Aranda et al., 2008; Choe et al., 2006).

In *D. melanogaster*, each PRG is necessary for segmentation patterning. PRG mutants all display similar but non-identical PR phenotypes. In PRG mutants,

interactions among the PRGs are disrupted, causing altered expression of downstream targets, including segment polarity genes. In *T. castaneum,* 3 PRG orthologs (*Tc-ftz*, *-opa* and *-h*) are not required for trunk segmentation. Knockdown of *eve*, *run* and *odd* in *T. castaneum* caused truncated instead of PR defects. These results indicate that the functions of PRG orthologs as well as the interactions among them differ between short germ *T. castaneum* and long germ *D. melanogaster*.

*1.7.2 Hymenoptera (*A. mellifera*)*

Hymenoptera branched at the base of the holometabolous group. Studying species from this lineage will help to reveal conserved features in Holometabola (Schmidt-Ott and Lynch, 2016). Phylogenetic studies indicate that the long germ mode of segmentation in this order was independently acquired (Sander, 1976; Savard et al., 2006). The development of molecular genetic tools such as RNAi and germline transformation approaches in honeybee *A. mellifera* (*Am*), together with its well annotated and assembled genome, provide valuable tools and resources for addressing genetic questions, such as segmentation patterning in this species (Schmidt-Ott and Lynch, 2016).

Expression of *Am-eve*, *-run*, *-ftz* and *-h* was examined by *in situ* hybridization (Wilson and Dearden, 2012). All of these genes show maternal expression in oocytes and nurse cells. *Am-eve, -run* and *-ftz* are expressed in a broad domain spanning the central regions of the early embryo. Later, striped expression appears sequentially in an anterior-to-posterior order. It seems that there is no early broad domain expression of *Am-h. Am-h* is expressed in a broad stripe in the anterior of the embryo and in PR-

like stripes in the trunk region (Wilson and Dearden, 2012). The function of PRG orthologs in honeybee was tested by embryonic RNAi (Wilson and Dearden, 2012). Knockdown of *Am-eve* produced defective cuticles with different severities, from fusions in the posterior regions to complete lack of trunk segmentation. *Am-run* knockdown resulted in PR-like defects: fewer segments were present and the remaining segments were wider. *Am-h* knockdown caused fused segments in the thorax and anterior abdomen. Fusion of all segments was observed in severely affected embryos after *Am-h* knockdown. These *Am-h* RNAi defects were similar to the mild defects after knockdown of anterior patterning genes in honeybee (*orthodenticle-1* and *hunchback*). *Am-ftz* RNAi produced cuticles without anterior segmentation, but the thorax and abdomen appeared to be unaffected. Severe segmentation defects, together with their expression during oogenesis in *A. mellifera* indicate that these PRG orthologs may play roles at a more upstream level in a segmentation patterning network than their counterparts in *D. melanogaster*. The expression of several gap gene and maternal patterning gene were examined after *Am-eve, -run* and *-ftz* knockdowns. The authors observed shifted, reduced or abolished gap gene and maternal patterning gene expression. Therefore, *Am-eve, -run* and *-ftz* appear to be required for early patterning.

*1.7.3 Hymenoptera (*N. vitripennis*)*

N. vitripennis, the jewel wasp, also shows long germ segmentation, as do *A. mellifera* and *D. melanogaster*. *N. vitripennis* have relatively large germ anlage and two signaling centers, features typical of long germ species (Davis and Patel, 2002;

Lynch et al., 2006; Sander, 1976). As introduced above, recent phylogenetic studies placed Hymenoptera at the base of Holometabola, thus indicating that the long germ segmentation mode in *N. vitripennis* evolved independently of *D. melanogaster* (Savard et al., 2006).

Rosenberg et al. studied the expression and function of *N. vitripennis* PRG orthologs (Rosenberg et al., 2014). Using *in situ* hybridization, the authors showed that *Nv-eve, -odd, -run* and *-h* are all expressed in PR-like expression patterns (Rosenberg et al., 2014). The first 5 *Nv-eve* primary stripes resolve from two broad expression domains and split into secondary stripes. The remaining *Nv-eve* stripes emerge from a posterior broad domain. When germ band elongation is completed, a total of 16 *Nv-eve* secondary stripes were detected. The first 3 *Nv-odd* stripes resolve from a broad domain in the central of the embryo. Stripe 4-6 are expressed in a "wave" from a cap-like expression in the posterior. The cap itself resolves into the last two *Nv-odd* stripes. *Nv-run* primary stripes appear sequentially in an anterior-to-posterior manner in alternate segments. Secondary segmental expression appears later when the germ band is completely extended. For *Nv-h,* the second primary stripe arises first, followed by appearance of the first stripe anteriorly. Stripe 3-5 emerge sequentially in the center of the embryo, while stripes 6, 7 and 8 appear posteriorly. A cap-like expression in the anterior initiates around the beginning of gastrulation and becomes more visible and broader afterwards. After germ band retraction, faint *Nv-h* seems to be expressed uniformly and also in a faint segmental striped pattern. In summary, these PRG orthologs in *N. vitripennis* display PR-like expression patterns.

Also, their posterior expression arises more or less sequentially. Stripes are either added *de novo* or resolved using a wave-like mechanism (Rosenberg et al., 2014).

pRNAi in *N. vitripennis* was less efficient in targeting late-acting zygotic genes compared to early-acting genes such as maternal and early-acting zygotic genes, thus morpholino knockdown was performed to investigate the function of PRG orthologs in this long germ wasp (Rosenberg et al., 2014). Knockdown of *Nv-eve*, *-odd* and *-h* all caused a similar graded series of defects, from fused segmental boundaries in the least affected larvae to truncated posterior in the most severely affected ones. Fused segmental boundaries were found in an anterior region covering T1 to A4 segments, indicating PR-like defects in the anterior, reminiscent of typical *D. melanogaster* PR mutants. Posteriorly truncated defects were similar to the head-only cuticles seen after *Tc-eve*, *-odd* and *-run* knockdowns (Section 1.7.1).

In sum, *N. vitripennis* appears to display a mixed mode of segmentation using *eve, odd* and *h* differently in the anterior and posterior regions of the embryo. These PRG orthologs function in PR patterning in segments anterior to A5 and they are also involved in posterior elongation. Rosenberg et al. interpreted the results as reflecting retention of an ancestral simultaneous segmentation mechanism in patterning posterior segments in this long germ species. Thus, *N. vitripennis* was proposed to represent an intermediate state in the short-to-long segmentation mode transition (Rosenberg et al., 2014).

*1.7.4 Lepidoptera (*B. mori*)*

The silkworm, *B. mori*, is a cultivated species of great economic importance. Establishing genetic approaches in this species is important for understanding its basic biology. Multiple techniques have been successfully applied for genetic manipulation in this species, including RNAi and CRISPR/Cas9 genome editing (summarized in (Schmidt-Ott and Lynch, 2016; Xu and O'Brochta, 2015). There is special interest in studying segmentation in *B. mori* as it is thought to have both short and long germ features (Davis and Patel, 2002; Nakao, 2015). The short germ feature is that there is no syncytial blastoderm stage during *B. mori* early embryonic development, and segments are generated sequentially in a cellular environment (Nagy et al., 1994). However, *B. mori* have relatively large germ anlage, rapid embryonic development as well as two signaling centers, usually features of a long germ segmentation mode (Davis and Patel, 2002; Nakao, 2012, 2015).

Bmor-eve PR-like stripes appear sequentially from a broad posterior expression domain (Nakao, 2010), as previously reported in several other insects (Mito et al., 2007; Patel et al., 1994). This expression pattern is consistent with that previously reported by (Xu et al., 1997). *Bmor-odd* is expressed in a dynamic pattern (Nakao, 2015). Its first two stripes resolve from a broad expression located in the posterior half of the embryo. Later, the domain divides into two narrower domains with stripe 3 to 5 emerging from the anterior narrow domain and the last two stripes appearing from the posterior narrow domain. *Bmor-run* transcripts were detected as early as in the ovaries of fifth-instar larvae (Liu et al., 2008). Anterior primary *Bmor-run* stripes appear to resolve from a broad expression domain. Posterior stripes then

appear sequentially. PR-like primary stripes seem to split into secondary segmental stripes (Liu et al., 2008).

RNAi targeting *Bmor-eve, -odd* and *-run* all resulted in truncated asegmental cuticles without posterior gnathal structure or any thoracic and abdomen tissue (Nakao, 2015). Similar defects were also observed by (Liu et al., 2008). Therefore, *Bmor-eve, -odd* and *-run* appear to play roles in germ band elongation. Nakao studied interactions among these PRG orthologs in *B. mori* by examining their expression after each gene knockdown (Nakao, 2015), and comparing that with previous results from *T. castaneum* (Choe et al., 2006). In *B. mori*, *odd* represses *run*, which represses *eve*. It seems that these three genes do not form a circuit or negative feedback loop, thus the mechanism proposed for *T. castaneum* may not apply in *B. mori*, despite similar defects after gene knockdown (Nakao, 2015). This study in *B. mori* (Nakao, 2015) also revealed altered PRG expression after gap gene knockdown, similar to *D. melanogaster*. The authors suggested that the input controlling the genetic circuit composed of *eve*, *run* and *odd* in short germ species (*T. castaneum*) was replaced by gap genes. This replacement may have triggered the short-to-long transition (Nakao, 2015).

1.7.5 Non-holometabolous insects

In insect orders other than Holometabola, evidence for PRG ortholog function is sparse. In an intermediate germ insect, the milkweed bug *O. fasciatus*, segmental *eve* stripes appear sequentially in an anterior to posterior order from a posterior expression domain during both blastoderm and germ band stages (Liu and Kaufman,

2005a). Both parental and embryonic RNAi resulted in similar defects, including defective posterior segmentation in mildly affected individuals to complete loss of body segments in severely affected animals. Expression of two gap genes expression was disrupted after *Of-eve* knockdown, indicating that it regulates gap genes (Liu and Kaufman, 2005a).

In the cricket *G. bimaculatus*, which is an intermediate germ insect, *eve* transcripts were first detectable in three broad domains in the very early germ rudiment (Mito et al., 2007). These domains then resolve into three stripes and the posterior two later split into four secondary stripes. Posterior stripes appear from a broad domain in the posterior. It is difficult to determine if they arise in PR pattern and then split into segmental stripes or if they arise directly in a segmental pattern. Fused thoracic and abdominal segments were detected after embryonic RNAi (Mito et al., 2007). Also, reduced segment number was observed in some cases. By examining expression of a segment polarity gene, several *Hox* and gap genes, a mixed mode of *Gb-eve*'s role was revealed. It appears that *Gb-eve* functions as a PR gene in anterior patterning. In the posterior, *Gb-eve* RNAi caused large deletion of thorax and abdomen. Together with altered gap gene (*hunchback* and *Krüppel*) expression after *Gb-eve* knockdown, these data indicated that *Gb-eve* has a gap-like function in posterior patterning (Mito et al., 2007). The posterior segmentation defects were interpreted as gap-like defects in the above two studies, although they appear to be similar to truncated asegmental defects when germ band elongation was affected in other sequentially segmenting species.

Results from the American cockroach *Periplaneta americana* (*P. americana*) showed that *Pa-h* is expressed in stripes with segmental register. After *Pa-h* RNAi, abdominal segmentation was disrupted, indicating that *h* is involved in posterior segmentation in this hemimetabolous insect (Pueyo et al., 2008).

1.7.6 Evidence from more basal arthropods

Expression and functional evidence summarized above clearly reveals the existence of PR patterning in sequentially segmenting insects. PRG ortholog expression was also examined in other arthropod species to address the question of the requirement of PRG in segmentation in arthropods outside of Insecta (Figure 1-5).

Centipedes always have an odd number of trunk segments, though the number varies among species, within populations of the same species and even between two sexes (Damen, 2004; Hughes and Kaufman, 2002a). This mysterious feature led researchers to wonder if PR-like or any other double-segmental mechanism is involved in segment formation in this group of arthropods. *eve* expression was examined first in *Lithobius atkinsoni* (*L. atkinsoni*) using *in situ* hybridization (Hughes and Kaufman, 2002a). Broad dynamic posterior expression of *Latk-eve* resolved into striped expression in newly formed segments. There was no splitting or intercalation of new stripes, indicating the striped pattern was segmental instead of PR-like. Contradicting evidence arose by investigating expression pattern of another PRG ortholog, *odd*, in *Strigamia maritima* (*S. maritima*) (Chipman et al., 2004). Similar to *Latk-eve*, an *odd* ortholog in *S. maritima* (*Smar-odr1*) was expressed dynamically in the posterior region. However, it resolved into a striped pattern with double segment periodicity first, then secondary *Smar-odr1* stripes were added

between two primary stripes to establish the final segmental striped expression pattern. This observation of intercalation of *Smar-odr1* secondary stripes indicates that there is at least transient double-segment periodic expression of *Smar-odr1* (Chipman et al., 2004). Moreover, it implies that a double-segment periodic mechanism establishing *Smar-odr1* expression may provide a constraint on developing odd-numbered trunk segments in centipede (Damen, 2004). Primary expression of *eve*, *h* and *run* orthologs in *S. maritima* all displayed double-segment periodicity, with secondary segmental striped expression resolved later for some orthologs (Chipman and Akam, 2008; Green and Akam, 2013). Interestingly, a *S. maritima eve* ortholog is only expressed in single-segment periodicity when generating the most posterior segments (the last 3 to 15 segments) (Brena and Akam, 2013). In a millipede, *Glomeris marginata* (*G. marginata*), *eve*, *run*, *h*, *Pax3/7* and *slp* orthologs also showed transient double-segment periodic expression at blastoderm stage but only single-segment periodic expression at later stages (Janssen et al., 2011; Janssen et al., 2012).

Within the group of Chelicera, delayed striped expression of a *prd* homolog in alternate segments was detected in the two-spotted spider mite, *Tetranychus urticae* (Davis et al., 2005; Dearden et al., 2002). Together, data from Chelicera and Myriapoda indicates that PR patterning is also involved in these two groups of arthropods.

eve expression in a broad posterior region of embryos seems to be conserved, indicating it may have a conserved role in segment addition and patterning (Damen et al., 2000; Schönauer et al., 2016). Based on their spatio-temporal expression patterns

in several species, *eve* and *run* may function at upstream levels within a segmentation network (Damen et al., 2005; Green and Akam, 2013). *ftz* arose as a *Hox* gene and has evolved a striped pattern at the base of insects and then PR function within Holometabola (Heffer et al., 2010). *h* is involved in *Notch*-mediated segment addition in a spider (Stollewerk et al., 2003). Whether the *Notch*-mediated segmentation exists in insects is still debatable (Kainz et al., 2011; Mito et al., 2011; Pueyo et al., 2008).

While the function and expression of PRG orthologs are surprisingly divergent, a segmented body is still persistent in all arthropods. A bottom level segmentation module composed of secondary PRG ortholgs (*slp* and *prd*) and SPG orthologs (*wingless* and *engrailed*) is highly conserved (Green and Akam, 2013; Janssen et al., 2011). This observation strongly suggests that the segmentation network is highly robust at this level as SPG orthologs can resist the disturbance caused by the re-wiring of PRG orthologs (Green and Akam, 2013; Peel et al., 2005). Being a perfect example of developmental system drift (True and Haag, 2001), the evolutionary constraint on this module is intriguing and still remains to be discovered.

				eve		*run*		*odd*		*h*		*prd/Pax3/7*		*slp*		*ftz*		*ftz-f1*		*opa*	
				Expr.	Func.	Expr.	Func.	Expr.	Func.	Expr.	Func.	Expr.	Func.	Expr.	Func.	Expr.	Func.	Expr.	Func.	Expr.	Func.
Insecta	Holometabola	Diptera	*Drosophila melanogaster* (fruit fly)	B-PR-SS	PR/A	PR-SS	PR	PR-SS	PR	PR	PR	PR-SS	PR	PR-SS	PR	PR	PR	U	PR	U-SS	PR
			Megaselia abdita (scutter fly)	PR-SS																	
			Clogmia albipunctata (moth midge)	B-PR																	
			Coboldia fuscipes (minute black scavenger fly)	PR-SS																	
			Anopheles gambiae (African malaria mosquito)	B-PR																	
		Lepidoptera	*Meduca sexta* (tobacco hornworm)			PR-SS															
			Bombyx mori (domestic silkworm)	P-PR	T	P-PR-SS	T	B-PR	T												
		Coleoptera	*Tribolium castaneum* (red flour beetle)	P-PR-SS	PR(a)/T	P?-PR	T	P-PR-SS	T	PR-SS	PR(h)	PR-SS	PR	PR-SS	PR	PR	NS	PR	PR	SS?	NS
			Callosobruchus maculatus (bean beetle)	P-PR-SS																	
			Dermestes frischi (hide beetle)	P-PR-SS																	
		Hymenoptera	*Nasonia vitripennis* (jewel wasp)	B-PR-SS	PR(a)&T	PR-SS		B-PR&P-PR	PR(a)&T	PR	PR(a)&T	S									
			Copidosoma floridanum (wasp)	B-SS																	
			Bracon hebetor (parasite wasp)	B-PR-SS																	
			Aphidius ervi (parasitic wasp)	NS																	
			Apis mellifera (honey bee)	U-B-PR-SS	A	B-PR-SS	PR			PR	A	PR-SS				B-PR	A(a)				
	Hemiptera		*Oncopeltus fasciatus* (milkweed bug)	P-SS	T																
		Orthoptera	*Schistocerca gregaria* (desert locust)													P					
			Schistocerca americana (American grasshopper)	P								PR-SS									
			Gryllus bimaculatus (two-spotted cricket)	P-PR-SS	PR(a)&T																
	Blattodea		*Periplaneta americana* (American cockroach)							P-SS	A(p)										
	Zygentoma		*Thermobia domestica* (firebrat)													S					

Figure 1-5. Summary of PRG orthologs expression and function in arthropods (Part I – Insects). Species name with red color indicates that the species has a long germ segmentation mode. Blue indicates an intermediate germ mode. Green indicates a short germ mode. Abbreviations: **Expr.**, exression; **Func.**, function; **PR**, pair-rule pattern or defect; **SS**, segmental striped pattern; **B**, broad domain expression; **P**, dynamic posterior expression; **U**, ubiquitous expression; **S**; striped pattern is reported but the register remains to be determined; **H**, *Hox*-like expression; **H***, fading *Hox*-like expression; **T**, truncated defect; **A**, disrupted segmentation;

		eve		*run*		*odd*		*h*		*prd/Pax3/7*		*slp*		*ftz*		*ftz-f1*		*opa*	
		Expr.	Func.	Expr.	Func.	Expr.	Func.	Expr.	Func.	Expr.	Func.	Expr.	Func.	Expr.	Func.	Expr.	Func.	Expr.	Func.
Crustacea	*Artemia salina* (brine shrimp)													H*					
	Artemia franciscana (brine shrimp)	P-S								P-SS									
	Daphnia pulex (common water flea)													H					
	Mysidium columbiae (reef mysid)									P-SS									
	Sacculina carcini (crab)													NH, NS					
Myriapoda	*Strigamia maritima* (coastal centepede)	P-PR(a)-SS		P-PR-SS		P-PR-SS		P-PR-SS		SS		SS		PR-SS				SS	
	Lithobius atkinsoni (lithobiomorph centipede)	P-SS								SS				H-SS					
	Glomeris marginata (pill millipede)	P-PR(a)-SS		P-PR(a)-SS		NS(a),P-SS		PR(a)-SS		PR(a)-SS		PR(a)-SS		H-SS				U(a)-PR(a)-SS	
Chelicerata	*Tetranychus urticae* (two-spotted spider mite)			SS						PR(a)-SS									
	Archegozetes longisetosus (oribatid mite)													H					
	Schizocosa ocreata (wolf spider)									P-SS									
	Cupiennius salei (tiger wandering spider)	P-S		P-S		S		P-S		P-SS		S		H				S	
	Limulus polyphemus (horseshoe crab)									SS									

Figure 1-5. Summary of PRG orthologs expression and function in arthropods (Part II- Non-insect arthropods). Continued- **(a)** indicates that the expression pattern or the defects were observed only in anterior segments; **(h)** indicates that the defects was observed only in the head; **NS**, no striped expression or no segmentation defects; - indicates that an early expression pattern resolves into a later expression pattern. For example, P-PR-SS indicates that dynamic posterior expression resolves into PR striped expression. Later, secondary segmental stripes appear. & indicates that different defects were reported in one study. / indicates that different defects were reported in different studies. **?** indicates that the pattern was mentioned by personal communication but not reported in literature. Note that for expression pattern, only segmentation-related patterns are listed here. Many PRG orthologs have head or CNS expression, which are not included in this figure. References for information listed in this figure that is not included in the text: (Binner and Sander, 1997; Brena and Akam, 2013; Chipman and Akam, 2008; Copf et al., 2003; Davis et al., 2001; Goltsev et al., 2004; Grbic et al., 1996; Grbić and Strand, 1998; Hughes and Kaufman, 2002a, b; Hughes et al., 2004; Janssen and Damen, 2006; Janssens et al., 2014; Keller et al., 2010; Kraft and Jäckle, 1994; Mouchel-Vielh et al., 2002; Osborne and Dearden, 2005; Papillon and Telford, 2007; Rohr et al., 1999; Schoppmeier and Damen, 2005a; Telford, 2000).

1.8 Challenges for studying segmentation network evolution

Though progress has been made in understanding the function of PRG orthologs in different species and the evolution of the segmentation network, still, there are some challenges for these comparative studies.

1.8.1 Inappropriate reference due to differences in embryogenesis

In *D. melanogaster*, early morphogens diffuse in a syncytial blastoderm, which is formed by superficial cleavage. However, a syncytial blastoderm stage is transient or even lacking in some species (Section 1.5). Detailed information about the presence and duration of a syncytial blastoderm stage is crucial as it provides information about how segments are patterned in different kinds of environment. If a species lacks a syncytial blastoderm stage, all segments are determined in a cellular environment. In this scenario, *Drosophila*-like hierarchical activation in a syncytium may not exist in this species.

The assignment of germ mode (long, intermediate, short) was mainly classified by the number of segments specified in the early embryo, revealed by embryo manipulation experiments in the early days (Davis and Patel, 2002; Krause, 1939). With the development of molecular genetics, determination of whether or not segments are specified in early embryo relies on the number of PRG or SPG stripes observed before gastrulation. The start point of gastrulation is not always the same in different species, even in closely related ones. For example, gastrulation starts posteriorly in *T. castaneum* but ventrally in *D. maculatus* (Handel et al., 2000) and Chapter 2). Gastrulation is even difficult to directly observe in the cricket (Donoughe and Extavour, 2016). As a result, lack of consistent morphological markers (reference

points) for the start of gastrulation makes it difficult to determine and compare the number of specified segments in different species at the same developmental stage. Taken together, it is critical to first examine and compare embryogenesis thoroughly before comparing underlying mechanisms of segmentation in different species.

1.8.2 Technical issues (inefficient knockdown and inappropriate data interpretation)

The most direct and definite way to reveal gene function is to find out what the defects look like when inactivate that gene activity. Thus, loss of function analysis to partially or completely abolish gene product is critical to determine gene function. Most functional studies in insects have been carried out using RNAi. Due to limitations of techniques, gene activity may not be effectively targeted. The knockdown efficiency for RNAi depends on lots of factors, such as the RNAi machinery in the animal, the gene itself, the timing or developmental stage for knockdown, and the quality of dsRNA. RNAi efficiency varies among closely related species and even different strains (Dönitz et al., 2015; Kitzmann et al., 2013).

If a gene is involved in multiple biological processes, the final phenotype after manipulating the gene function may be difficult to sort out. An example here is from the cricket *G. bimaculatus* (Kainz et al., 2011). *Delta* eRNAi caused segmentation-like defects. However, early expression of a segment polarity gene, *hedgehog*, appeared to be normal. The authors examined the defects after RNAi over time, and they found that the defects were caused by delayed development instead of disrupted segmentation (Kainz et al., 2011). To study the function of such a pleiotropic gene function during segmentation patterning, spatiotemporal-specific gene targeting approach are critical.

1.8.3 Limited understanding based on previous knowledge from D. melanogaster

For decades, researchers have been expanding segmentation studies to other insect models by investigating the expression and functions of segmentation gene orthologs. In this way, we are able to track the evolution of known segmentation genes in Insecta. However, we cannot neglect the fact that there are genes not involved in segmentation in *D. melanogaster* but function in segmentation patterning in other species. For example, *E75A*, which encodes a nuclear receptor does not have any segmentation function in *D. melanogaster*, but is involved in PR-like patterning in *O. fasciatus* (Erezyilmaz et al., 2009). Defective boundaries between adjacent segments were observed frequently in a PR-like pattern after *E75A* knockdown in *O. fasciatus* (Erezyilmaz et al., 2009). While we keep comparing orthologs of known PRGs, we cannot exclude the possibility that there might be other PRG candidates in other systems.

Researchers aim to observe *D. melanogaster* -like segmentation phenotypes when investigating PRG ortholog function in other species. However, sometimes the defects are hard to discern. An example here is the severe defects after *eve* knockdown in *O. fasciatus* and *G. maculatus* (Liu and Kaufman, 2005a; Mito et al., 2007). With large disrupted posterior regions, the defects were interpreted as gap-like defects. However, defects in germ band elongation also display disrupted posterior segmentation. *eve* in both *O. fasciatus* and *G. maculatus* is expressed in the posterior region in elongating germ band (Liu and Kaufman, 2005a; Mito et al., 2007).

Therefore, whether *eve* indeed functions as a gap gene, or the defects are actually caused by failure in germ band elongation still needs further investigation.

1.8.4 Problem raised by selection of model systems

Within Holometabola, where diverse modes of segmentation have been reported, functional studies of PRG ortholog have been carried out in Lepidoptera, Hymenoptera and Coleoptera other than long germ Diptera. As previously introduced, a short germ to long germ evolution probably occurred several times independently in different insect lineages. The studies discussed above were performed in either only one representative in each lineage (*T. castaneum* in Coleoptera; *B. mori* in Lepidoptera) or two representatives in a single clade but with the same segmentation mode (*A. mellifera* and *N. vitripennis* in Hymenoptera). Thus, until now, information about conservation and variation between segmentation in representatives with distinct segmentation modes from one lineage is still lacking. Comparing closely related species within the same lineages displaying differences in segmentation mode is critical for understanding germ mode evolution. With species displaying all distinct segmentation modes, Coleoptera (beetles) provides a great repertoire for studying segmentation patterning evolution within a single insect order.

1.9 Conclusions

Often, expression data does not faithfully predict gene function (Section 1.7 and Figure 1-5). For example, in *T. castaneum*, *Tc-ftz* and *-h* are expressed in PR-like patterns, but RNAi experiments showed that neither is required for trunk segmentation (Choe et al., 2006). Thus, performing functional studies in new model

species is required to acquire definitive information for accurate and comprehensive understanding of the evolution of the PRG network.

As I introduced in a previous section, within the order Coleoptera, short, intermediate, and long modes of segmentation all have been reported. Thus, it is an interesting order for comparative studies (Figure 1-6). Furthermore, being the largest order of insects, beetles are underrepresented by having only one well-established model, *T. castaneum*. More model systems in this order are necessary to understand basic beetle biology and for genetic approaches to control pest species. Taken together, studying segmentation in a new beetle model with a distinct segmentation mode would give more insight into the short-to-long germ mode transition within one lineage. Tools successfully applied in this study would be helpful for performing genetic studies in this beetle and provide a potential way for controlling this pest species.

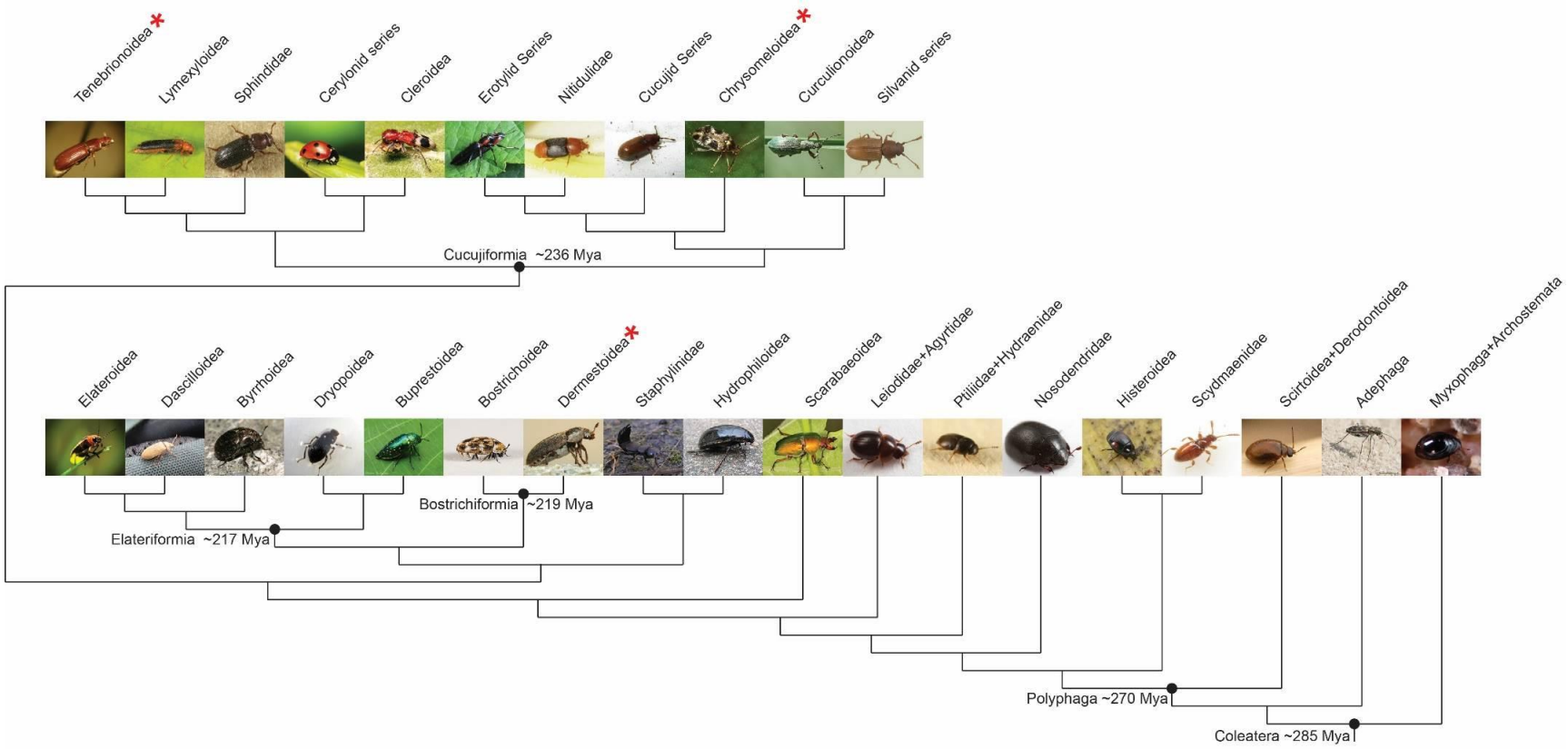

Figure 1-6. The phylogenetic tree of beetles. The phylogeny is based on (Hunt et al., 2007). Red asterisks indicate the examined three beetle with distinct segmentation modes. *Tribolium castaneum*, a short germ bettle, belongs to the Tenebrionoidea superfamily. *Dermestes maculatus*, an intermediate germ beetle, belongs to the superfamily of Dermestoidea. *Callosobruchus maculatus*, a long germ beetle, belongs to the superfamily of Chrysomeloidea.

In this work, I established an intermediate germ beetle, *D. maculatus* as a new model insect to study PRG ortholog function. I first established a stable lab colony and examined early embryogenesis in this species. I successfully applied techniques for molecular genetics in *D. maculatus*. After isolating all nine PRG orthologs using degenerate PCR and RACE, expression was examined with *in situ* hybridization and function was investigated with parental or embryonic RNAi. All *D. maculatus* PRG orthologs show PR-like expression except for *opa*. Both *Dmac-prd* and *-slp* RNAi-mediated knockdown resulted in typical PR defects, suggesting that they are "core" PR genes. Severe knockdown of *Dmac-eve*, *-run* or *-odd* resulted in anterior-only, asegmental embryos while moderate knockdown resulted in PR-like defects. These three genes thus have dual roles in germ band elongation and in PR segmentation. Elongated but asegmental germ bands resulted from *Dmac-prd* and *-slp* double knockdown, confirming their exclusive roles in PR segmentation. Moreover, the result suggested that germ band elongation and PR segmentation are two decoupled processes in *D. maculatus*. Disrupted cell mitosis in the posterior germ band was observed after *Dmac-eve* knockdown. Extensive cell death generally prefigured the cuticle patterns after knockdowns, seen long ago for *Drosophila* PR phenotypes. We propose that PRGs have retained basic roles in PR segmentation during the transition from short to long germ development and share evolutionary conserved functions in promoting cell viability.

Chapter 2: *Dermestes maculatus*: an intermediate-germ beetle model system for evo-devo **[Published: Xiang, Forrest and Pick, *EvoDevo*, 2015]**

2.1 Abstract

Background: Understanding how genes change during evolution to direct the development of diverse body plans is a major goal of the evo-devo field. Achieving this will require the establishment of new model systems that represent key points in phylogeny. These new model systems must be amenable to laboratory culture, and molecular and functional approaches should be feasible. To date, studies of insects have been best represented by the model system *Drosophila melanogaster*. Given the enormous diversity represented by insect taxa, comparative studies within this clade will provide a wealth of information about the evolutionary potential and trajectories of alternative developmental strategies.

Results: Here we established the beetle *Dermestes maculatus*, a member of the speciose clade Coleoptera, as a new insect model system. We have maintained a continuously breeding culture in the lab and documented *Dermestes maculatus* embryogenesis using nuclear and phalloidin staining. Anterior segments are specified during the blastoderm stage before gastrulation, and posterior segments are added sequentially during germ band elongation. We isolated and studied the expression and function of the pair-rule segmentation gene *paired* in *Dermestes maculatus*. In this species, *paired* is expressed in stripes during both blastoderm and germ band stages:

four primary stripes arise prior to gastrulation, confirming an intermediate-germ mode of development for this species. As in other insects, these primary stripes then split into secondary stripes. To study gene function, we established both embryonic and parental RNAi. Knockdown of *Dmac-paired* with either method resulted in pair-rule-like segmentation defects, including loss of Engrailed expression in alternate stripes.

Conclusions: These studies establish basic approaches necessary to use *Dermestes maculatus* as a model system. Methods are now available for use of this intermediate-germ insect for future studies of the evolution of regulatory networks controlling insect segmentation, as well as of other processes in development and homeostasis. Consistent with the role of *paired* in long-germ *Drosophila* and shorter-germ *Tribolium, paired* functions as a pair-rule segmentation gene in *Dermestes maculatus.* Thus, *paired* retains pair-rule function in insects with different modes of segment addition.

2.2 Introduction

Understanding the basis for the diversity of plant and animal systems on our planet will require studies of the mechanistic basis of body patterning and developmental stratgies used in different species and an understanding of how these mechanisms evolved (evo-devo). It is crucial that these studies include sampling of species from a broad range of taxa that represent distinct branches of the tree of life (reviewed in (Cheatle et al., 2015). Rapid progress in the development of genomic technologies has made it possible to readily identify genes in diverse species.

However, understanding how these genes control developmental processes will require establishment of model systems in which gene function can be assessed.

Arthropods represent ~ 80% of all described species; among them, insects are the dominant taxa, representing ~ 65% of all animal species on the planet (Zhang, 2011). Insects are easy to experimentally manipulate, can often be readily cultured in the laboratory, producing large numbers of embryos with reasonable generation time, and their enormous diversity makes them an ideal group for comparative studies to probe phenotypic diversity and unravel ancestral mechanisms. Among insects, the most sophisticated model system available to date is *Drosophila melanogaster* (*D. melanogaster*). *D. melanogaster* serves as a reference species for any study of insects, or other new animal model, with more than one hundred years of study by thousands of researchers throughout the world, a plethora of genetic tools to assess gene function, and progress on every type of 'omics' analysis (Wangler et al., 2015). *D. melanogaster* is a member of the group of holometabolous insects thought to have arisen 300-400 million years ago (Mya) (Misof et al., 2014), which includes >80% of all extant insect species (Grimaldi and Engel, 2005). Additional models are needed from this group to understand diversity in Holometabola. The most speciose order of holometabolous insects is Coleoptera (beetles), with >350,000 named species representing ~ 40% of all insect species (Bouchard et al., 2009; Hammond, 1992; Zhang, 2011). Coleoptera are thought to have arisen ~ 285 Mya (Hunt et al., 2007) and have radiated to occupy a broad variety of niches on our planet including those with extreme environments, such as the Arctic, high mountain altitudes and dry, desert terrains. Beetles range in size from <0.5mm to >15cm in length and feed on

everything from other insects, to fungus, decaying wood, a wide variety of plants, animal debris and even dung. The most sophisticated coleopteran model system developed to date is the flour beetle, *Tribolium castaneum* (*T. castaneum*; (Brown et al., 2009; Denell, 2008; Richards et al., 2008)), providing a frame of reference for the development of additional beetle systems to represent the diversity of this large clade.

Segmentation is a highly conserved feature shared by all panarthropods (Blair, 2008; Gabriel and Goldstein, 2007; Janssen and Budd, 2013; Janssen et al., 2011; Schoppmeier and Damen, 2005a). Despite this similarity, the ways in which segments form and the genes that control this process vary among taxa (Davis and Patel, 2002; Peel et al., 2005; Rosenberg et al., 2009). Krause first classified insect embryogenesis into short-, intermediate- and long-germ modes based on the relative size of the germ anlage prior to gastrulation (Krause, 1939). These different modes of segmentation can be distinguished by the number of segments established in the germ rudiment before gastrulation: long-germ (all or most segments are established more or less simultaneously), short-germ (only anterior segments are specified) and intermediate-germ (head and thorax segments, and sometimes anterior abdominal segments are specified). Both short- and intermediate-germ insects differ from long-germ insects in that posterior segments are added sequentially from a posterior segment addition zone (SAZ) or growth zone. This strategy of 'sequential addition' of segments is thought to be ancestral to arthropods and it is only in holometabolous insects that long-germ development has been observed (Liu and Kaufman, 2005b). Phylogenetic studies and accumulating molecular evidence indicate that long-germ development in different orders of Holometabola has evolved independently (Davis and Patel, 2002;

Rosenberg et al., 2014). How modes of segment formation switched without disrupting the segmented body plan itself is unclear. The presence of nurse cells, enlarged germ size, acquisition of an anterior patterning center, shifted gap gene expression boundaries, and diminished activity of a segmentation clock have been proposed as prerequisites for long-germ development (Davis and Patel, 2002; El-Sherif et al., 2012; Peel et al., 2005; Rosenberg et al., 2014; Rosenberg et al., 2009; Sarrazin et al., 2012). Studies of the mechanisms underlying segmentation in an intermediate-germ insect, which may reflect an intermediate state between short- and long-germ modes of segmentation, will yield information on the transition from ancestral sequential specification to long-germ development. In addition, since long-germ development appears to have evolved several times independently within Holometabola, it will be of interest to compare mechanisms in species within a single clade rather than just comparing all sequentially segmenting species to *D. melanogaster*. These comparative studies will distinguish stages in the evolution of the long-germ mode which may have been gradual, with increasing numbers of segments specified simultaneously in different species, or may have occurred in a punctuated fashion, reflecting developmental constraints that remain to be discovered.

The two best-developed insect systems, *D. melanogaster* and *T. castaneum*, represent different modes of segment addition with *D. melanogaster* displaying the long-germ mode and *T. castaneum* specifying segments sequentially. Genetic screens in *D. melanogaster* identified a group of pair-rule segmentation genes (PRGs) that control the formation of body segments, and many of these also function in segmentation in *T. castaneum* (Choe and Brown, 2007; Choe et al., 2006; Heffer et

al., 2013). However, their specific roles in the segmentation process often differ and some genes involved in segmentation in *D. melanogaster* do not function in segmentation in *T. castaneum* (Choe et al., 2006; Stuart et al., 1991). Work from other insects suggests that new genes may be recruited into PRG networks and that PRG orthologs have acquired novel function in different lineages (Erezyilmaz et al., 2009; Wilson and Dearden, 2012). To understand the extent to which mechanisms regulating segmentation vary, the genetic underpinnings of this process must be examined in different species. As first pointed out by Patel and Davis, Coleoptera are an ideal order for this comparison, as short-, intermediate- and long-germ development have all been observed in beetles (Davis and Patel, 2002; Patel et al., 1994; Sander, 1976). Comparison of gene function in species within the same clade displaying these different developmental strategies will provide information about the extent of variation among segmentation regulatory networks, the impact of these changes on downstream targets, and clues about how changes in gene expression and function drive the evolution of alternative developmental modes.

Here we have established *Dermestes maculatus* (*D. maculatus*) as a system for comparative studies within Coleoptera. *T. castaneum* and *D. maculatus* diverged close to the time of origin of this clade ~ 250 Mya, (Hedges et al., 2015), making this pair of species ideal for comparative studies, as they represent divergent lineages within the order Coleoptera. *D. maculatus* display an intermediate-germ mode of segmentation compared to the shorter-germ mode of *T. castaneum*. *D. maculatus* are easy to rear in the lab, with high fecundity and a short life cycle. We characterized the early steps of nuclear division in *D. maculatus* embryos and isolated an ortholog of

the *D. melanogaster* PRG, *paired (prd). Dmac-prd* has pair-rule-like expression and function, regulating the expression of alternate stripes of the segment polarity gene *engrailed* (*en*). These studies support the conclusion that the function of *prd* as a PRG is highly conserved across holometabolous taxa. Additionally, these studies establish methods for *in situ* hybridization, antibody staining, and both parental and embryonic RNAi in *D. maculatus*.

2.3 Methods and materials

Dermestes *species verification using DNA barcoding*

D. maculatus adults and larvae were purchased from Carolina Biological Supply Company. To verify the identity of the species, we amplified the mitochondrial cytochrome c oxidase subunit I (COI) gene (Bely and Weisblat, 2006; Folmer et al., 1994). Genomic DNA was extracted using a DNeasy Tissue kit (Qiagen). Only wings and legs were taken from four *Dermestes* adults to avoid contamination by gut content. PCR using primers (Appendix I) amplified an approximately 700 base pair (bp) fragment. The sequence of this fragment matched *D. maculatus* COI (GenBank ID HM909035.1) except at position 581 (C to T transition; Appendix II; Figure 2-1).

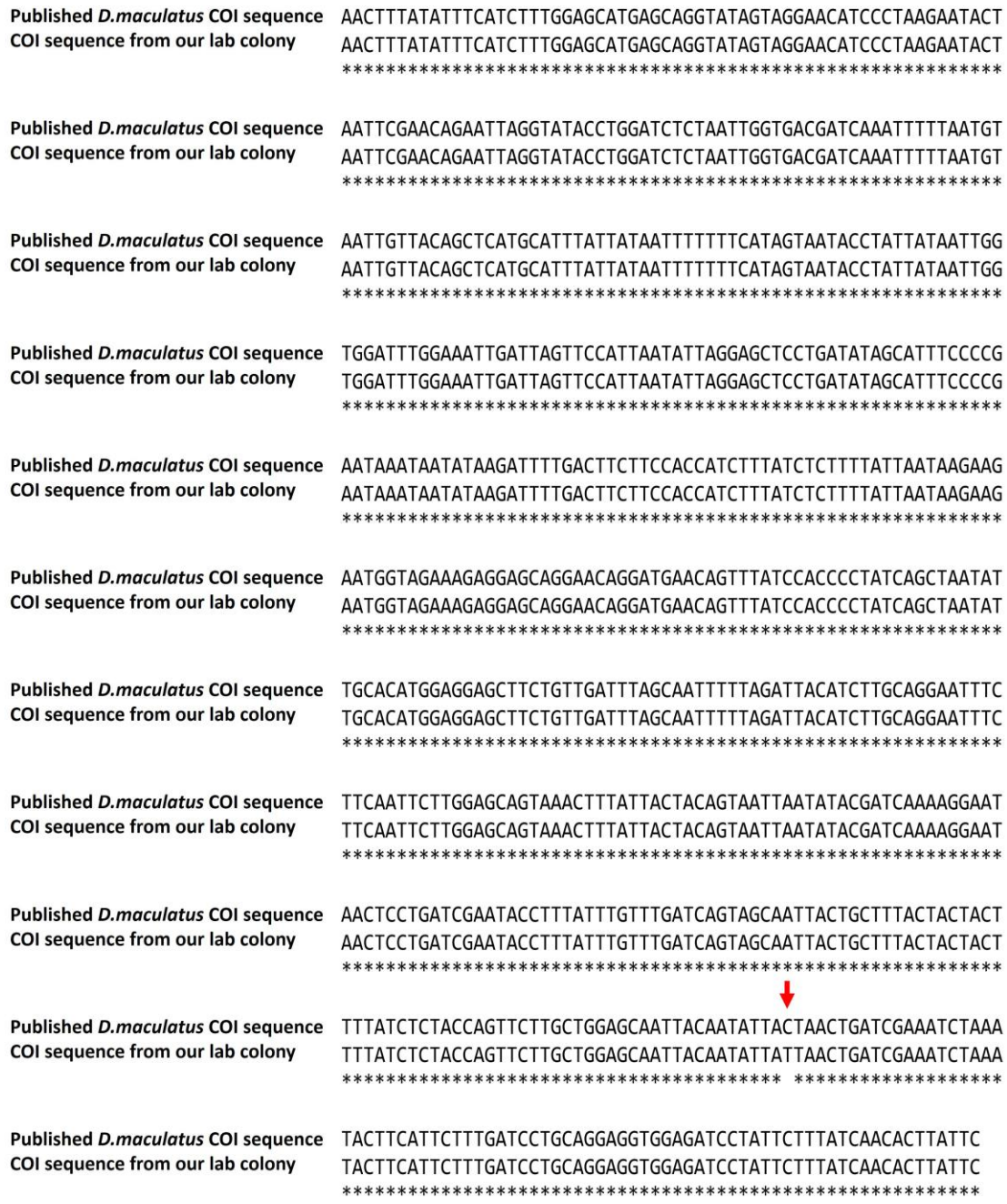

Figure 2-1. COI identification of laboratory reared species. The COI gene from our lab *D. maculatus* colony was compared to the published *D. maculatus* COI sequence (GenBank ID HM909035.1). Red arrow shows mismatch. Alignment was performed using ClustalW2.

Rearing of D. maculatus

D. maculatus were kept in large plastic cages (14.5 inches long × 8.5 inches wide × 10 inches high) with a thin layer of wood shavings spread on the bottom. The beetles were fed cat food (Fancy Feast) placed in a small weigh boat and changed twice a week. No water was added to avoid fungal growth. As immobile final instar larvae and pupae would be slaughtered by younger larvae, chunks of styrofoam were placed in the cages for the larvae to crawl into and hide before eclosion. Mesh cloth was used to cover the cages to prevent beetle escape while keeping the cages well ventilated. Cages were placed in incubators at 25° C or 30° C for colony maintenance. To collect embryos, newly eclosed *D. maculatus* were selected from the colony and placed in small plastic cages (9 inches long × 6 inches wide × 6.5 inches high) without wood shavings. They were fed daily to provide sufficient food. Cotton balls were stretched out and placed in the cage for egg laying. The cages were held at either 25° C or 30° C degrees for developmental staging.

Embryo collection and fixation

The protocol for fixation of *D. maculatus* embryos was modified from standard *D. melanogaster* and *Oncopeltus fasciatus* (*O. fasciatus*) embryo fixation protocols (Kosman et al., 2004; Liu and Kaufman, 2009) as follows. Cotton balls were carefully torn apart to let embryos fall onto a black sheet of paper. Embryos are white, approximately 0.2 cm in length, and can be easily seen against the black background. Embryos were transferred into small beakers and treated with 50% bleach for 4 minutes followed by several water rinses. Embryos were then transferred into 1.5 ml Eppendorf tubes with distilled H_2O (approximately 200 µl of embryos in

1000 µl of distilled H_2O). Tubes were placed in boiling water for 3 minutes and then on ice for 7 minutes to swell the eggshell, making embryos easier to dissect before staining. Embryos were then fixed in heptane: 4% PFA 1:1 for 20 minutes on a shaker at high speed (~ 250 rpm). PFA (lower phase) was removed and MeOH was added and the tube was shaken vigorously for 20 seconds. After several MeOH washes, embryos were stored at -20°C in MeOH. A detailed *D. maculatus* embryo fixation protocol is provided (Appendix III).

prd *gene cloning and identification*

To isolate *prd* from *D. maculatus* embryonic mRNA, total RNA was extracted from 0-1 day (0-1d) after egg laying (AEL) embryos developing at 30° C using TRIzol (Invitrogen) and an RNeasy mini kit (Qiagen). Reverse transcription was performed using the QuantiTect Reverse Transcription kit (Qiagen) to prepare 0-1d embryonic cDNA. Two rounds of degenerate PCR were performed using primers as in (Davis et al., 2001) (Appendix I), generating a product of approximately 600 bp length. After purification and insertion into pGEM-T Easy Vector (Promega) by TA cloning, sequencing of individual clones revealed partial *Dmac-prd*, as well as partial sequences of the *Pax3/7* family genes *Dmac-gooseberry (gsb)* and *Dmac-gooseberry-neuro* (*gsb-n*) (Baumgartner et al., 1987; Bopp et al., 1986; Gutjahr et al., 1993b). The 3' end of the *Dmac-prd* coding sequence and 3' UTR were isolated through two rounds of 3'RACE using gene specific primers and the FirstChoice RLM-RACE kit (Ambion) following the manufacturer's instructions (Appendix I). A contiguous fragment spanning part of the paired domain (PD) through the stop codon was

verified using gene specific primers (Appendix I). The region coding for the C-terminus of the PD through the stop codon was inserted into the XhoI and XbaI restriction sites of a KS vector for use as template for RNA *in situ* hybridization probe and double-stranded RNA (dsRNA) syntheses (KS-*Dmac-prd*).

Embryo developmental staging, RNA in situ hybridization and antibody staining

For *D. maculatus* developmental staging, embryos were collected every 2 hours (h) AEL over an 18-h period. After fixation, as described above, MeOH was removed and embryos were transferred into glass dishes with PBST. They were then hand-dissected with Dumont #5 forceps to remove the eggshell. For staging, embryos were incubated with 1:1000 SYTOX Green (Invitrogen) in the dark for 30 minutes at room temperature. They were then washed three times with PBST and visualized under fluorescence microscopy (Olympus SZX12, Leica 501007 or Leica SP5X). *D. melanogaster* protocols were followed for tracking the cytoskeletal dynamics using phalloidin and DAPI nuclear staining (Ramos et al., 2010). For phalloidin staining, 80% EtOH was used instead of MeOH for fixation. After hand-dissection in PBTA (1×PBS, 0.1% TritonX-100, 0.02% sodium azide), embryos were incubated with Alexa Fluor 488 phalloidin (1:200; Molecular probes) overnight at 4° C and then washed several times with PBST. Embryos were mounted in Vectashield mounting solution with DAPI (Vector Laboratories) and visualized with confocal microscopy (Leica SP5X). For *in situ* hybridization, digoxygenin-labeled *Dmac-prd* probes were synthesized using T7 polymerase (antisense) or T3 polymerase (sense) (Roche). *in situ* hybridization was performed following modifications of a standard *D.*

melanogaster RNA *in situ* hybridization protocol (Kosman and Small, 1997) (see Appendix III for details). Briefly, fixed embryos were hand-dissected in PBST. Embryos were pre-hybridized in hybridization solution for one h at 60° C. After overnight incubation with 1:50 of digoxygenin-labelled probe (~500 ng/µl) at 60° C, embryos were washed in hybridization solution and PBST. AP conjugated sheep anti-digoxygenin antibody (1:2000; Roche) was added. Embryos were incubated for one h at room temperature. Following four washes with PBST, NBT/BCIP (Roche) was used for detection. Antibody staining was performed following a standard *D. melanogaster* protocol (Gutjahr et al., 1994; Nagaso et al., 2001). Hand-dissected fixed embryos were incubated with anti-En 4D9 primary antibody (1:5 dilution of antibody stock provided by the Developmental Studies Hybridoma Bank at 53 µg/ml) and then with biotinylated anti-mouse antibody (1:500; Vector Laboratories). A color reaction was performed after ABC (Vector Laboratories) incubation using DAB (Sigma). Embryos were incubated with SYTOX Green in PBST, washed three times in PBST, and visualized with Olympus SZX12, Leica 501007 or Zeiss SteREO Discovery V12 microscopy. Embryos at germ band stages were hand-dissected to remove yolk before visualization.

Parental and embryonic RNA interference and phenotypic analysis

Primers with T7 promoter sequence at their 5' ends were used to amplify fragments from KS-*Dmac-prd* (Appendix I). The PCR products were used as templates for dsRNA syntheses. MEGAscript T7 Transcription kit (Ambion) was used to make dsRNA according to the manufacturer's instructions. For parental

RNAi, pupae were selected from the *D. maculatus* colony. Female and male pupae were separated by visualizing their genitalia (Figure 2-2). 2 µl of dsRNA (2 µg/µl) was injected into the abdomen of each newly eclosed female. After one day recovery at 30° C, injected females were mated by placing them in small plastic cages with an equal number of uninjected males. After allowing them to mate for one day, cotton balls were added to cages and embryos were collected daily for phenotypic analysis. For embryonic RNAi, 0-3 h AEL embryos (pre-cellular blastoderm) were collected at 25° C and aligned on glass slides. Approximately 50 to 100 ng (3 ug/ul) dsRNA was injected into each embryo using a micromanipulator within 5 h AEL. To examine morphological defects, hatched larvae were collected and fixed in #1184C Pampel's solution (BioQuip Products, Inc.) at 4° C overnight before visualization. To screen for segmentation defects, each larva was streched out using forceps under a dissecting microscope. To examine Engrailed (En) expression, embryos at appropriate stages were fixed and stained, as described above.

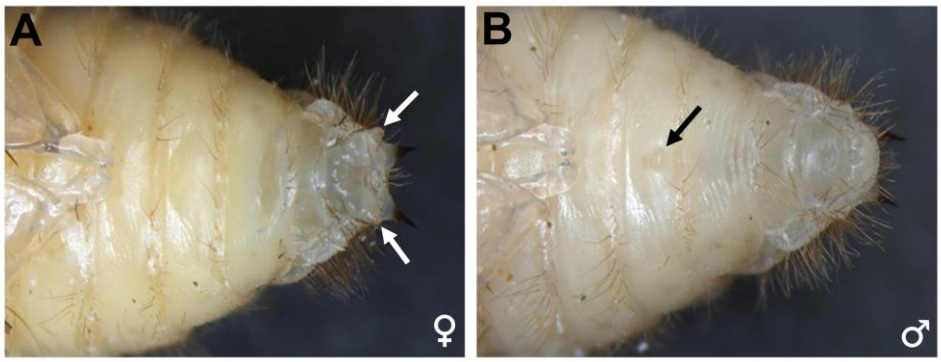

Figure 2-2. Female and male *D. maculatus* pupae. Morphology used to distinguish female and male *D. maculatus* is shown in this photograph. (A) Two genital papillae at the posterior end of a female pupa (white arrows). (B) Male pupa has a median sternal lobe on the ventral side of the posterior abdomen (black arrow).

2.4 Results

2.4.1 *Early embryogenesis in* D. maculatus

Since little was known about the early stages of *D. maculatus* embryonic development, we tracked nuclear and cytoskeletal dynamics using SYTOX Green, DAPI and phalloidin staining (Figure 2-3). Progression of embryogenesis was monitored at 25° C to slow development and capture all stages. Zygotic nuclei were first observed dividing multiple times in the center of the embryo, forming a syncitium (0-6 h AEL, Figure 2-3A-C). At very early stages, female and male pronuclei were evident inside the embryo (white arrow, Figure 2-3A), while the polar body nuclei were at the surface of the embryo (red arrow, Figure 2-3A). After several divisions, zygotic nuclei gradually distributed along the length of the embryo (Figure 2-3B) and, after additional divisions, began migrating toward the egg surface (Figure 2-3C). Between 6 and 8 h AEL, most of the nuclei had migrated to the periphery of the egg, forming a syncytial blastoderm (Figure 2-3D). “Cap”-like phalloidin staining was detected in some embryos at this stage, suggesting that nuclei arriving at the surface of the embryo are surrounded by cytoplasmic islands containing cytoskeleton (Figure 2-3E). These phalloidin-stained actin caps protruded at the embryo surface, similar to cytoskeletal events that occur at a comparable stage in *D. melanogaster* (cell cycle 9/10; (Foe et al., 1993; Gilbert, 2010)). Later, cell membranes formed between individual energids (nucleus with associated cytoplasm) as “furrow canal”-like phalloidin staining appeared, and a cellular blastoderm was established (8-10 h AEL, Figure 2-3G). This is similar to cellularization events in *D. melanogaster* at cell cycle 14 (Foe et al., 1993; Gilbert, 2010). In *D. maculatus*, we were able to capture

embryos in which dividing cells with two nuclei still sharing cytoplasm were visible at the cellular blastoderm surface (arrows, Figure 2-3H), while cells that had finished cytokinesis each exhibited one nucleus enclosed by its own, individual membrane (Figure 2-3I).

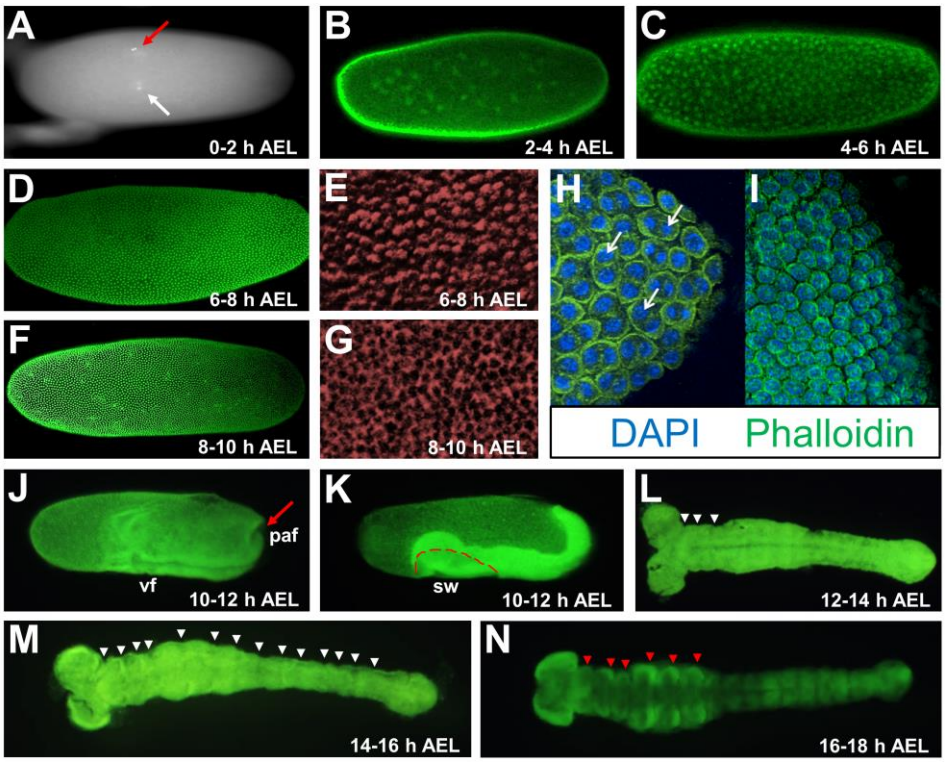

Figure 2-3. Early *D. maculatus* embryogenesis. Photographs of *D. maculatus* embryos are shown, documenting key steps of nuclear division and early embryonic development. (A) DAPI nuclear staining of a 0-2 h AEL *D. maculatus* embryo. (B-D, F, J-N) Nuclear staining using SYTOX Green of *D. maculatus* embryos between 2 and 18 h AEL, as indicated. (E, G) F-actin phalloidin staining of 6-8 h and 8-10 h AEL *D. maculatus* embryos (recolored red). (H, I) Merge of DAPI (blue) and phalloidin (green). (A) White arrow indicates pronuclei. Red arrow indicates polar body nuclei. (B) Nuclei have divided and spread in the central portion of the embryo. (C) Nuclei continue to divide and migrate towards the egg surface. (D) Most nuclei have arrived the periphery of the egg. (E) "Cap"-like phalloidin staining suggests the arrival of nuclei at the surface. (F) Cells have rearranged as some are closely clustered together in the ventral posterior area. (G) "Furrow canal"-like phalloidin staining appears during this stage. (H, I) Fully cellularized embryo. White arrows indicate cells at telophase of mitosis on the egg surface. (J) The ventral furrow (vf) has invaginated and posterior amniotic fold (paf, red arrow) has appeared. (K) The germ band has coalesced and begun to extend towards the dorsal side of the embryo. Red dashed line indicates serosal window (sw). (L) An extending germ band stage

embryo with bilateral head lobes. White arrowheads show segmental furrows. (M) Segmental furrows appear in more posterior regions as the germ band elongates (white arrowheads). (N) A fully elongated germ band with morphological segments and appendage primordia (red arrowheads indicate appendage primordia). Embryos were reared at 25° C and photographed with Olympus SZX12, Leica 501007 or Leica SP5X confocal microscopy. A, E, G, H and I were prepared by Iain Forrest.

Between 10 and 12 h AEL, the *D. maculatus* embryo was rapidly transformed from a uniform cellular blastoderm to an elongating germ band (Figure 2-3J, K; Figure 2-4). In late cellular blastoderm, cells in the ventral posterior region packed together, forming the germ rudiment (Figure 2-4A). The first detectable sign of gastrulation was the formation of a ventral furrow (vf), which appeared as a shallow broad furrow in the mid-ventral region (Figure 2-4B, B'). Shortly after, several transverse folds emerged (Figure 2-4B). As the ventral furrow further invaginated into the interior of the egg, it elongated towards the ventral posterior end (Figure 2-4C'). The anterior-most fold embedded deeper while other short-lived transverse folds became invisible due to cell movements (Figure 2-4C, C'). The dorsal embryonic region condensed while the dorsal anterior extraembryonic region expanded with gastrulation progression (compare Figure 2-4B and C, arrowheads indicate the boundary between extraembryonic region and the embryo proper). Gastrulation proceeded as the ventral furrow became narrower and reached the posterior end (Figure 2-3J; Figure 2-4D, D'). Head lobes (hl) were visibly distinguished from surrounding extraembryonic tissue (Figure 2-3J; Figure 2-4D，D'). During the same time period, a posterior amniotic fold (paf) emerged and, shortly after, covered the posterior end of the germ anlage (red arrow in Figure 2-3J; red arrowhead in Figure 2-4D). It continued to proceed anteriorly along the ventral

side as the germ band elongated (red arrowhead, Figure 2-4E, E'). By approximately 12 h AEL, an early germ band with serosal window (sw) was established (Figure 2-3K, red dashed line). The germ band further extended dorsally over the next 4 h and segmental furrows appeared in an anterior to posterior progression (12-16 h AEL; white arrowheads in Figure 2-3L, M). Morphological segments as well as appendage primordia were seen at 16-18 h AEL (red arrowheads in Figure 2-3N).

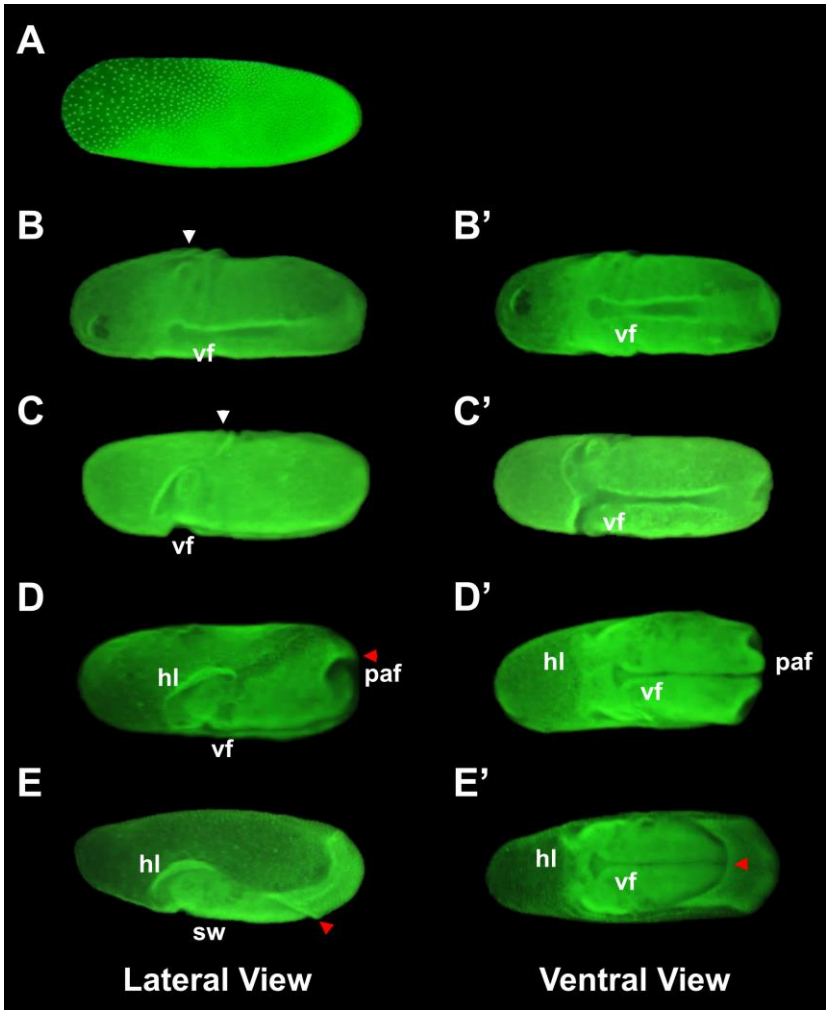

Figure 2-4. Gastrulation in *D. maculatus* embryos. Embryos were stained with SYTOX Green. (A) Embryo from overnight collection. Note that nuclei are closely packed together posteriorly with large and loosely arranged nuclei in the anterior dorsal region. (B-E) embryos were collected between 10 and 12 h AEL at 25° C. Left

column, lateral view; right column, ventral view of same embryo. (B, B') The ventral furrow (vf) and several transverse folds appear as signs of early gastrulation. White arrowhead indicates the boundary between the embryo proper and extraembryonic tissue on the dorsal side. (C, C') Ventral furrow invaginates towards the yolk. The anterior fold separates the head lobes from the anterior extraembryonic tissue. The boundary between the embryo proper and extraembryonic tissue is indicated by the white arrowhead. (D, D') The narrower and deeper ventral furrow reaches the posterior end. The amnion folds over the posterior end of the germ rudiment, forming the posterior amniotic fold (paf). Involuting head lobes (hl) are visible. Red arrowhead shows the edge of the paf. (E, E') The amnion, together with the serosa, moves anteriorly on the ventral side of the embryo, leaving an open serosal window (sw). Red arrowhead indicates the posterior edge of sw.

In sum, *D. maculatus* embryogenesis progressed through pre-blastoderm, cellular blastoderm, gastrulation and germ band extention stages within the first 18 h AEL at 25° C. At 30° C, embryos developed faster, as expected: a cellular blastoderm formed and gastrulation began between 4 and 6 h AEL. An early germ band was established 6-8 h AEL and the embryo reached late germ band stages within 10 h AEL (Table 2-1).

Table 2-1. *D. mauclatus* early embryogenesis at 25° C and 30° C. Embryos were collected every 2h AEL at 25° C or 30° C over an 18-h or a 10-h period, respectively. *D. maculatus* embryogenesis was examined using nuclear and phalloidin staining. Embryos at the end of 8-10 h AEL at 30° C are roughly equivalent to 14-16 h AEL embryos at 25° C.

	25° C	30° C
0-2 hr AEL	Male and female pronuclei fuse	Male and female pronuclei fuse, zygotic nuclei divide in the center of the egg
2-4 hr AEL	Zygotic nuclei divide in the center	Most nuclei migrate toward the egg periphery, a syncytial blastoderm forms
4-6 hr AEL	Zygotic nuclei divide and gradually distribute along the embryo	Cellular blastoderm forms, gastrulation starts
6-8 hr AEL	Most nuclei migrate toward the egg periphery, a syncytial blastoderm forms	Gastrulation completes, germband extention begins
8-10 hr AEL	Cellular membrane form between individual energids, a cellular blastoderm forms, gastrulation starts	Serosal window closes, germband extends dorsally
10-12 hr AEL	Gastrulation proceeds, an early germ band with an open serosal window is established	
12-14 hr AEL	Germ band extends, head segmental furrows become visible	
14-16 hr AEL	Germ band extends dorsally, thoracic segmental furrows become visible	
16- 18 hr AEL	Germ band is fully extended, abdominal segments become obvious, appendage buds form	

2.4.2 *Isolation of* prd *from* D. maculatus

To identify *Dmac-prd* ortholog(s), degenerate primers were designed based on conserved sequences in the paired domain (PD) and the homeodomain (HD) in Pax3/7 orthologs (Bopp et al., 1986; Burri et al., 1989; Davis et al., 2001; Frigerio et al., 1986). An approximately 600 bp fragment isolated by PCR amplification using *Dmac* 0-1d cDNA was extended by two rounds of 3'RACE to generate a 1,341 bp fragment that encodes a PD and a HD (Figure 2-5; *Dmac*-Prd sequence see Appendix II). An octapeptide sequence (OP) is present in most Pax3/7 orthologs but is absent from Prd from *D. melanogaster*, *T. castaneum*, *Apis mellifera* (*A. mellifera*) and *Nasonia vitripennis* (*N. vitripennis*) (Keller et al., 2010; Noll, 1993). This OP was not

found in the *Dmac*-Prd sequence, consistent with this being an ortholog of *prd*, rather than another family member. The HD of this predicted *Dmac*-Prd has a serine residue at position 50 (red arrow, Figure 2-5), which is vital for the DNA-binding specificity of Prd-family homeodomains (Choe and Brown, 2007; Davis et al., 2001; Keller et al., 2010; Treisman et al., 1989). As shown in Figure 2-5, the PD and the HD from *D. maculatus, T. castaneum* and *D. melanogaster* are similar. The PD of *Dmac*-Prd is 97% identical to that of *Tc*-Prd, with only 3 amino acid differences between *Dmac*-Prd and *Tc*- PDs in the N-terminal portion of the PD, and is 84% identical to that of *Dm*-Prd. The *Dmac*-Prd HD is 98% identical to that of *Tc*-Prd, with only the most C-terminal amino acid different, and 92% identical to the *Dm*-Prd HD. Blastx searches using sequences of other TA cloning products identified orthologs of *gsb* and *gsb-n* in that their predicted protein sequences possess a PD, a HD and a Gsb- or Gsb-n-type OP (Gsb and Gsb-n sequences see Appendix II; Figure 2-6).

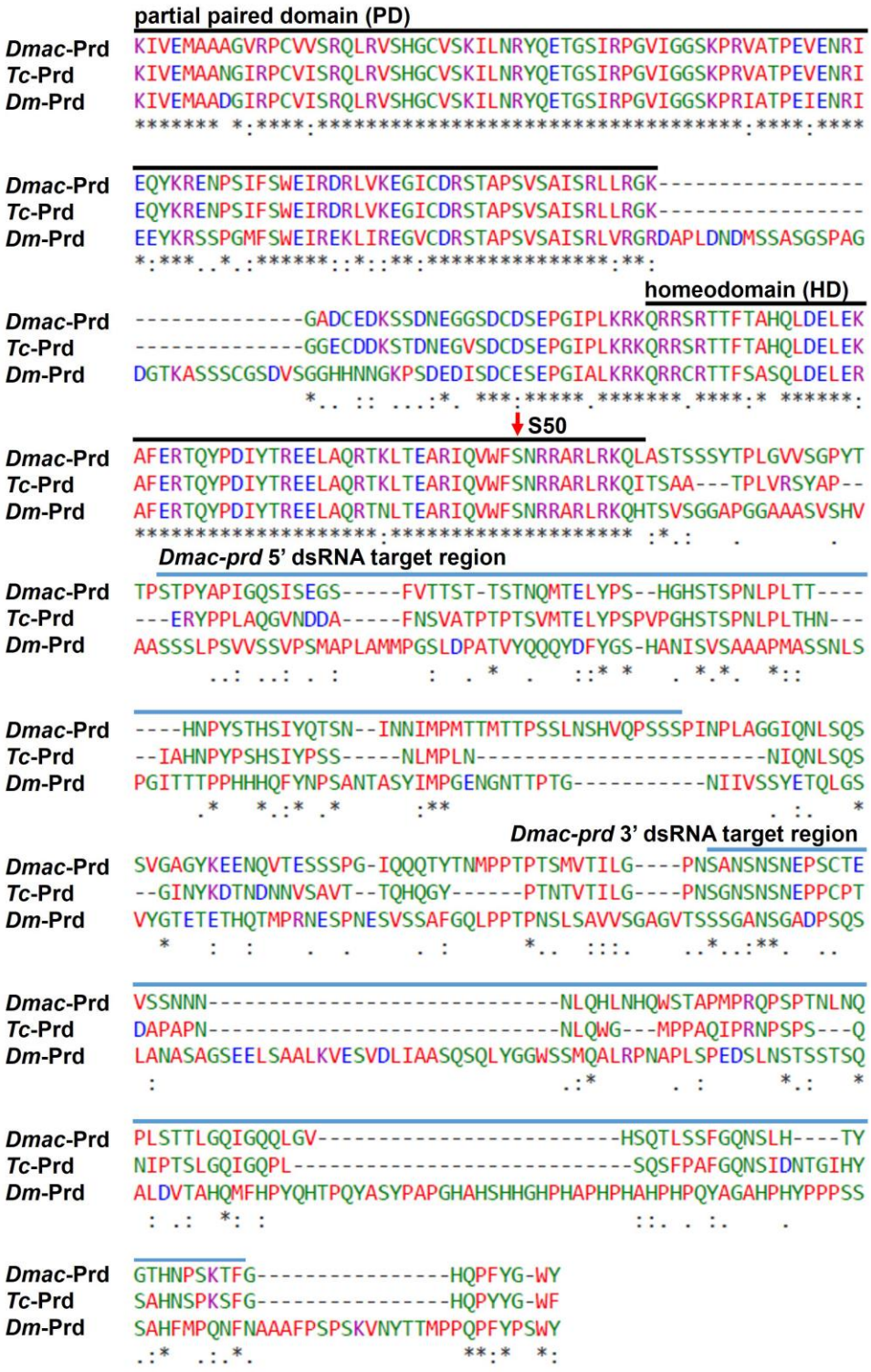

Figure 2-5. *Dmac*-Prd is similar to Prd from other insects. Alignment of partial Paired (Prd) sequences from *D. maculatus*, *T. castaneum*, and *D. melanogaster* is shown. Black lines indicate the paired domain (PD) and homeodomain (HD). Red arrow indicates S50 in the HD, critical for DNA binding specificity. The regions used for RNAi experiments are overlined in blue. Protein sequence alignment was

performed using ClustalW2. * indicates identical residues; : indicates conserved substitutions; . indicates weakly similar substitutions. Colors indicate residues classified into groups according to their physicochemical properties. Red: Nonpolar side chain; Green: Polar side chain; Blue: Negatively charged side chain; Magenta: Positively charged side chain.

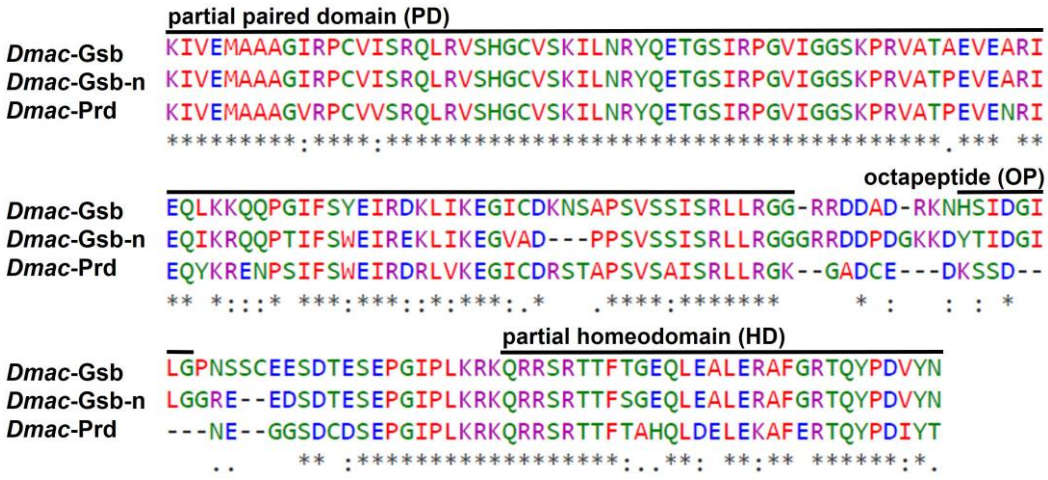

Figure 2-6. Alignment of partial *Dmac*-Gsb, Gsb-n, and Prd protein sequences. Black lines indicate the paired domain (PD), octapeptide (OP) and homeodomain (HD). Note that *Dmac*-Prd is lacking the OP motif. Gsb has a Gsb-type OP: HSIDGILG. Gsb-n has a Gsb-n type OP: YTIDGILG. Protein sequence alignment was performed using ClustalW2. * indicates identical residue, : indicates conserved substitutions, . indicates weakly similar substitutions. Colors indicate residues are classified into groups according to their physicochemical properties. Red: Nonpolar side chain; Green: Polar side chain; Blue: Negatively charged side chain; Magenta: Positively charged side chain.

2.4.3 Dmac-prd *is expressed in stripes*

To investigate the expression of *prd* in *D. maculatus*, RNA *in situ* hybridization in early embryos was performed. No specific staining pattern was detectable using a sense probe (data not shown). Using an antisense probe, *Dmac-prd* transcripts were initially detected as a single stripe at approximately 50% of the blastoderm length (black arrow, Figure 2-7A). Posterior *Dmac-prd* stripes emerged sequentially in an anterior to posterior fashion (Figure 2-7B-N). The first primary

Dmac-prd stripe resolved into a more clearly detectable thin stripe and remained undivided (black arrow, Figure 2-7B and C). The second and the third primary *Dmac-prd* stripes first appeared as weak broad stripes in the posterior half of the embryo (red arrows, Figure 2-7B and C). These two primary stripes split into pairs of thin secondary stripes (red arrowheads, Figure 2-7D and E). By the time the fourth primary *Dmac-prd* stripe arose in the posterior region (late cellular blastoderm, red arrow, Figure 2-7D), the second primary stripe had completed its split into two secondary stripes (red arrowheads, Figure 2-7D), and the third primary stripe began to split (black arrowhead, Figure 2-7D). At the onset of gastrulation when the ventral furrow emerged, the anterior-most undivided *Dmac-prd* stripe, four anterior secondary stripes and a fourth primary stripe were clearly observed (Figure 2-7E).

During gastrulation, when the ventral furrow had invaginated further into the yolk and several transverse folds appeared, the fourth primary stripe had resolved into secondary stripes (arrowheads, Figure 2-7F and G) and a fifth primary stripe was detected (red arrow, Figure 2-7G). When the posterior invagination and the ventral furrow became more prominent (black arrowhead), a total of eight *prd* stripes (5 primary stripes, among which the first remained undivided, three middle stripes split into 6 secondary stripes, and a fifth newly arisen stripe, red arrow) were detected (Figure 2-7H). Anterior stripes started to fade while posterior stripes were embedded into the posterior end due to the SAZ invagination (Figure 2-7I, J). As gastrulation proceeded, the embryonic rudiment with bilateral head lobes was clearly distinguishable from the extraembryonic tissue (Figure 2-7I and J, red dashed line in I indicates the anterior boundary of the germ rudiment). In the embryonic rudiment,

secondary stripes resolved from the fifth primary stripe (red arrowheads, Figure 2-7I and J) and a weak sixth primary stripe (red arrow, Figure 2-7I and J) was detected.

As the germ band extended, new *prd* stripes arose from the region anterior of the SAZ and resolved into thin secondary stripes by fading expression in the center (Figure 2-7K-N and P-R), as reported in other species (Choe and Brown, 2007; Gutjahr et al., 1993a; Kilchherr et al., 1986; Osborne and Dearden, 2005). There was no obvious intensity or width difference within pairs of *Dmac-prd* secondary stripes in the blastoderm or the germ band (Figure 2-7E-G and P-R). As posterior *Dmac-prd* stripes were added sequentially, anterior *prd* stripes became weak and eventually invisible (Figure 2-7K-N). Gnathal, thoracic and abdominal *prd* stripes dissapeared gradually during germ band extension (Figure 2-7L-N). During later embryogenesis, *prd* was strongly expressed in appendage primordia in gnathal segments (black arrows, Figure 2-7O). Together, the conserved protein sequence, expression in stripes, and the characteristic splitting of primary stripes into secondary stripes in early embryos, suggested that *Dmac-prd* is involved in pair-rule patterning. The finding that a total of four primary *Dmac-prd* stripes are present at the onset of gastrulation is consistent with the assignment of *D. maculatus* as an intermediate-germ insect.

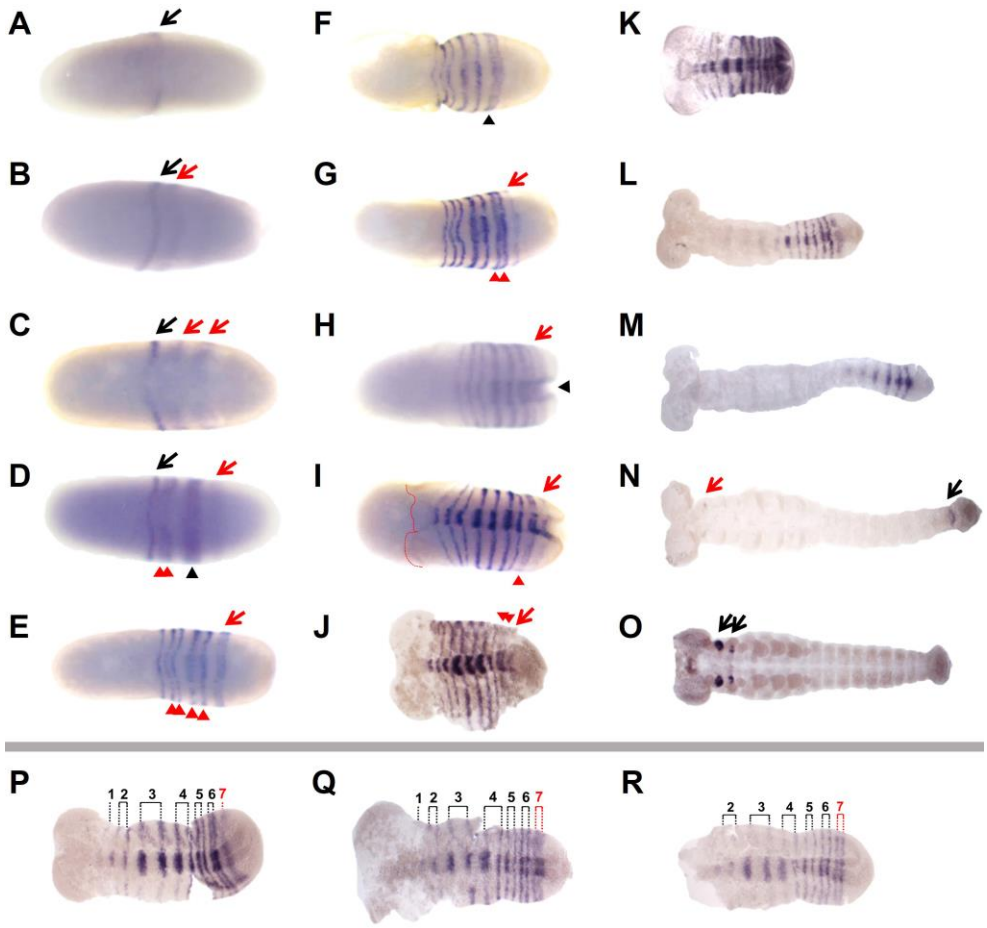

Figure 2-7. *Dmac-prd* is expressed in stripes during embryogenesis. Expression of *Dmac-prd* examined by *in situ* hybridization. Throughout, arrows and arrowheads indicate primary and secondary stripes, respectively. Black arrows show "old" primary stripes while red arrows indicate "new" primary stripes. Black arrowheads show splitting primary stripes, and red arrowheads indicate resolved secondary stripes. (A) A single weak stripe in early blastoderm (black arrow). (B) The first stripe becomes clearly detectable (black arrow). The second stripe emerges posterior to the first stripe (red arrow). (C) Two broad primary stripes appear (red arrows). (D) A late blastoderm stage embryo. The first primary stripe remains undivided (black arrow). The second primary stripe has divided into two secondary stripes (red arrowheads). The third primary stripe is splitting (black arrowhead). The fourth primary stripe is showing up *de novo* (red arrow). (E) When the broad shallow ventral furrow appears, the first undivided stripe, four secondary stripes (red arrowheads) and a fourth primary stripe are detected (red arrow). (F) Fading expression is detected in the center of the newly arisen stripe (black arrowhead). (G) The fourth primary stripe has divided into two stripes (red arrowheads). A weak fifth stripe appears (red arrow). (H) During gastrulation, a total of 8 *Dmac-prd* stripes are detectable. Black arrowhead indicates the posterior end of the ventral furrow. Red arrow indicates the posterior-most *Dmac-prd* stripe. (I, J) As gastrulation proceeds, a 6th primary stripe arises; bilateral head lobes become visible. Red arrowheads indicate the dividing

stripe. Red arrow indicates the newly emerged stripe. Red dashed line in I shows the anterior edge of the germ rudiment. (K) Embryo during early germ band elongation with striped *Dmac-prd* expression across the whole germ band. (L, M) Elongating embryo with faint *Dmac-prd* stripes in anterior segments. Posterior segments have strong striped *Dmac-prd* expression. (N) Embryo at late germ band elongation stage. Stripes have faded except for the most posterior segment (black arrow). Hint of *Dmac-prd* expression appears in the mandibles (red arrow). (O) Later embryo showing *Dmac-prd* expression in the head (black arrows). (P-R) Detailed view of stripe splitting. (P) A total of 7 primary stripes have developed. The first stripe remains undivided. The next 5 primary stripes have resolved to secondary stripes. The 7th primary stripe emerges from the anterior region of the posterior end of the embryo as a broad weak stripe. (Q) Anterior striped expression fades. The expression in the center of the 7th stripe becomes fuzzy and faint. (R) The 7th stripe has divided into two thin secondary stripes as there is no expression in the center. All embryos are shown with anterior to the left.

2.4.4 *RNAi knockdown of* Dmac-prd *results in defects in segmentation*

To investigate the function of *prd* in *D. maculatus*, and to determine whether RNA interference (RNAi) is effective in this species, we performed embryonic RNAi (eRNAi). *Dmac-prd* 3' dsRNA, corresponding to a 254 bp region downstream of the HD, was injected into pre-blastoderm stage embryos (target region is indicated in Figure 2-5). After injection, all hatched offspring from control embryos injected with *gfp* dsRNA were wild-type in appearance with head, three thoracic segments and ten abdominal segments (Figure 2-8A). In contrast, over 85% (18/21) of the newly hatched larvae after *Dmac-prd* 3' dsRNA injections showed segmentation defects with one or several fused segmental boundaries (T2/T3, A1/A2, A3/A4, A5/A6, A7/A8; black arrows in Figure 2-8B-D), reminiscent of the segmentation phenotype produced by *eve* eRNAi in cricket (Mito et al., 2007). Some cases included loss of or abnormal development of T2 legs (red arrow, Figure 2-8D).

Injection of dsRNA into pupal or adult females can result in phenotypes evident in their offspring. This phenomenon was named parental RNAi (pRNAi) and

has been observed in *T. castanum*, *O. fasciatus*, *Gryllus bimaculatus*, *Blattella germanica, N. vitripennis,* and other species (Bucher et al., 2002; Ciudad et al., 2006; Liu and Kaufman, 2004; Lynch et al., 2006; Mito et al., 2005). To determine whether pRNAi functions in *D. maculatus,* and to verify the segmentation phenotypes observed with *Dmac-prd* eRNAi, *Dmac-prd* 3' dsRNA was injected into newly eclosed virgin females and their offspring were examined. To ensure specificity, a second dsRNA was generated from a non-overlapping target region (*Dmac-prd* 5', 256 bp; Figure 2-5). There was no significant difference in the offspring yield or hatch rates between *gfp* dsRNA injected and *Dmac-prd* 5' or 3' dsRNA injected females (data not shown). Segmentation in all hatched offspring from control females injected with *gfp* dsRNA appeared to be wild-type (Figure 2-8E). In contrast, over 50% (100/184) of hatched offspring collected on the 3rd day after injection from *Dmac-prd* 3' dsRNA injected females and ~ 73% (66/91) from *Dmac-prd* 5' dsRNA injected females displayed segmentation defects (Figures 2-8F-H and 2-9A). The percentage dropped to less than 30% (51/195) and ~ 39% (52/135) on the 4th day after injection for *Dmac-prd* 3' and *Dmac-prd* 5', respectively (Figure 2-9A). On the 5th day after injection, less than 3% of embryos hatched with segmentation defects (*Dmac-prd* 5', 6/202; *Dmac-prd* 3' 9/305; Figure 2-9A). Only very few embryos collected on the 6th day after injection hatched with fused segments (2/234, *Dmac-prd* 5'; 1/282, *Dmac-prd* 3'; Figure 2-9A).

Analysis of segmentation defects revealed a range of defects, phenocopying an allelic series. In mildly affected larvae, partial or complete fusion was observed for one pair of adjacent segments, most often A5/A6 (Figures 2-8F, 2-9B). In other cases,

fusions were detected between two, three or four pairs of adjacent segments (Figures 2-8G, H and 2-9C). The fusions occurred in the same alternating fashion as observed for eRNAi (Figures 2-8F-H, 2-9B). Missing or defective T2 legs were also observed in some severe cases. Very often, the defective T2 legs projected from the lateral edge of instead of the ventral-lateral side of the T2 segment (red arrow, Figure 2-8H').

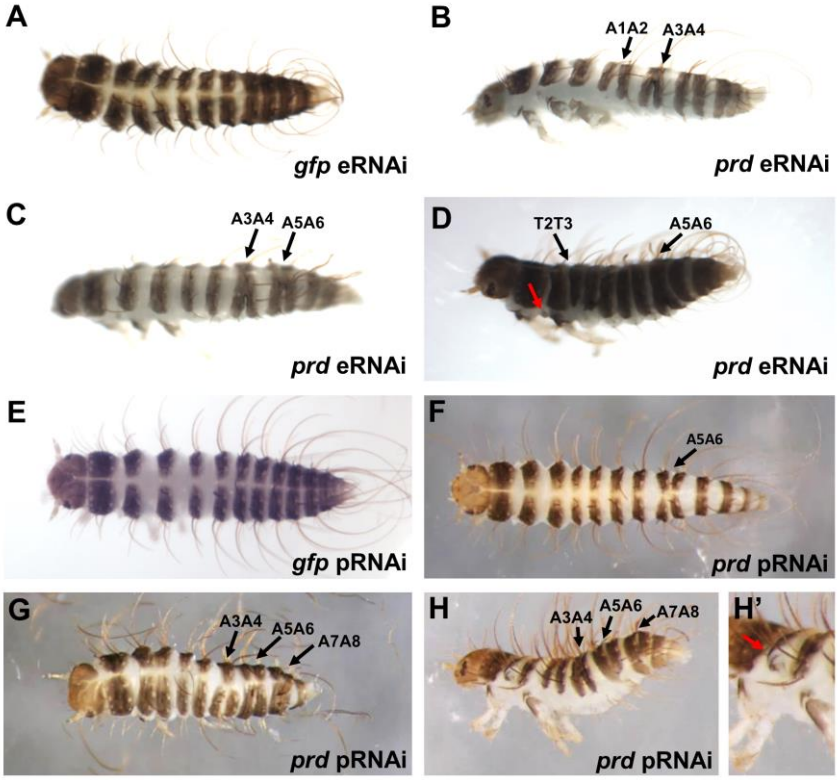

Figure 2-8. Knockdown of *Dmac-prd* with RNAi causes segmentation defects. *Dmac-prd* or *gfp* RNAi was carried out, as indicated. *gfp* dsRNA was injected as negative control. (A-D) embryonic RNAi. (E-H) parental RNAi. (A) Dorsal view of a first instar *D. maculatus* larva after *gfp* dsRNA injection showing wild-type phenotype with head, three thoracic segments and ten abdominal segments. (B) A hatched first instar larva after *Dmac-prd* dsRNA injection contains fused A1/A2 and A3/A4 segments (black arrows). (C) Lateral view of a larva with fused A3/A4 and A5/A6 segments after *Dmac-prd* eRNAi (black arrows). (D) T2 legs are missing in hatched larva with severe phenotype after *Dmac-prd* eRNAi (red arrow). Black arrows indicate fused T2/T3 and A5/A6 segments. (E) Offspring produced by *gfp* dsRNA injected female are viable until hatching and show wild-type phenotype (dorsal view). (F) Dorsal view of a hatched offspring with fused A5/A6 segments from *Dmac-prd* 3' dsRNA injected female (black arrow). (G, H) First instar larva after *Dmac-prd* (3' and 5', respectively) pRNAi with shortened body length as well as

fused segments. Black arrows indicate fusions of adjacent segments. (H') Red arrow indicates defective T2 legs.

To further analyze the role of *Dmac-prd* in segmentation, defects were quantitated in hatched embryos collected on the third day after injection. More than 70% of *Dmac-prd* 5' dsRNA offspring displayed some type of defect (Figure 2-9A). Of these, ~ 40% displayed one segmental fusion while nearly 60% hatched with more than one segment fused (35% with two fusions, 12% with three fusions and 12% with four fusions; Figure 2-9C). The percentage of *Dmac-prd* 3' dsRNA affected offspring was over 50% (Figure 2-9A). Of these, 54% had one segmental fusion, 36% had two, 9% had three, and 1% had four segments fused (Figure 2-9C). Overall, segments A5/A6 were most commonly affected by *Dmac-prd* knockdown, with over 80% of either *Dmac-prd* 5' or 3' dsRNA affected larvae displaying fusion of these segments (Figure 2-9B). Fusion of A3/A4 was seen in 68% and 48% of *Dmac-prd* 5' and 3' affected larvae, respectively. Fusion of A7/A8 was detected in 27% and 51% of *Dmac-prd* 5' and 3' affected larvae, respectively. Fusions of T2/T3 and A1/A2 had lower frequencies (11% and 4% for fused T2/T3 in *Dmac-prd* 5' and 3' affected larvae, respectively; 8% and 4% for fused A1/A2 in *Dmac-prd* 5' and 3' affected larvae, respectively). These differences in frequency suggest differential susceptibility of different parasegments to *Dmac-prd* knockdown (Figure 2-9B).

In sum, both eRNAi and pRNAi were effective tools to analyze gene function in *D. maculatus*. Analysis of the morphology of larvae hatched after knockdown of *Dmac-prd* indicates a role for *prd* in segmentation in this species.

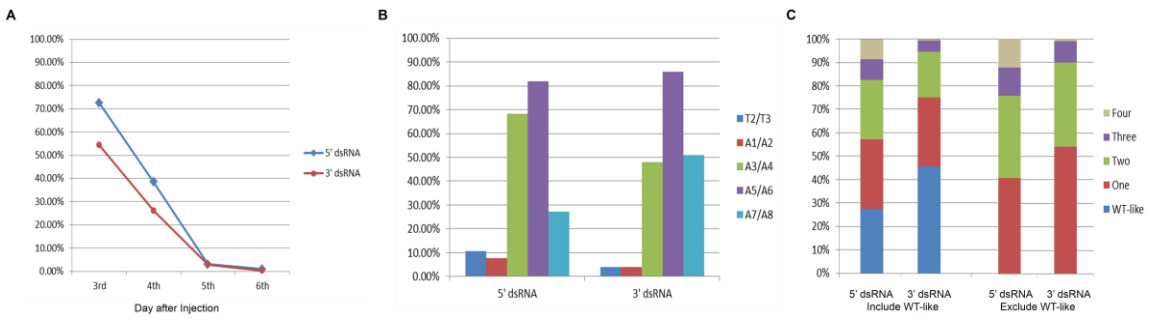

Figure 2-9. Quantitation of *Dmac-prd* pRNAi segmentation defects. Offspring produced by twelve of either *Dmac-prd* 5' or 3' dsRNA injected females, as indicated. Each hatched larva was stretched out using tweezers and examined under a dissecting microscope. (A) Percent of hatched pRNAi offspring showing segmentation phenotypes. (B-C) Embryos were collected on the third day after the injection and segmentation defects were scored. (B) Frequency of fusion of specific pairs of adjacent segments. Note that some larvae had more than one pair fused. (C) Frequency of types of segmentation defects observed. Left bars, percentage of hatched larvae with wild type segmentation, and those displaying one, two, three or four segmental fusions; right bars, percentage of hatched larvae with one, two, three or four segmental fusions among those with observable segmentation defects.

2.4.5 Dmac-prd *is necessary for the expression of alternate Engrailed stripes*

In both *D. melanogaster* and *T. castaneum*, *prd* functions as a pair-rule gene and regulates *en* expression in odd-numbered segments (Choe and Brown, 2007; DiNardo and O'Farrell, 1987). We therefore asked if *Dmac-prd* functions similarly to regulate the expression of alternate En stripes in *D. maculatus*. Embryos injected with buffer alone showed equally strong En expression in every segment (Figure 2-10A). In contrast, loss of En expression in alternating segments was evident in over 50% (25/46) of extended germ bands after *Dmac-prd* eRNAi (asterisks, Figure 2-10C, E). Germ band morphology was also analyzed using nuclear staining with SYTOX Green. This revealed partial or even complete fusion of pairs of adjacent segments into a wider segment (asterisks, Figure 2-10D, F).

Since injection of embryos may have caused damage that precluded a more careful analysis of En expression, embryos laid by *Dmac-prd* dsRNA-injected females were also examined. While offspring from the *gfp* dsRNA control injected females displayed wild-type-like En expression (Figure 2-10G), loss of or reduced En expression in the labium, T2, A1, A3, A5, A7 and A9 segments were detected in over 60% (112/179) of extended germ band stage embryos from *Dmac-prd* dsRNA injected females (asterisks, Figure 2-10I). Segmental fusion was observed in the posterior region of odd-numbered segments following nuclear staining in the regions where loss of En expression was detected (asterisks, Figure 2-10J).

The decreased expression of alternate En stripes, as well as the segmentation defects observed in embryos in which *Dmac-prd* was knocked down, indicate that *Dmac-prd* functions as a pair-rule segmentation gene in *D. maculatus*.

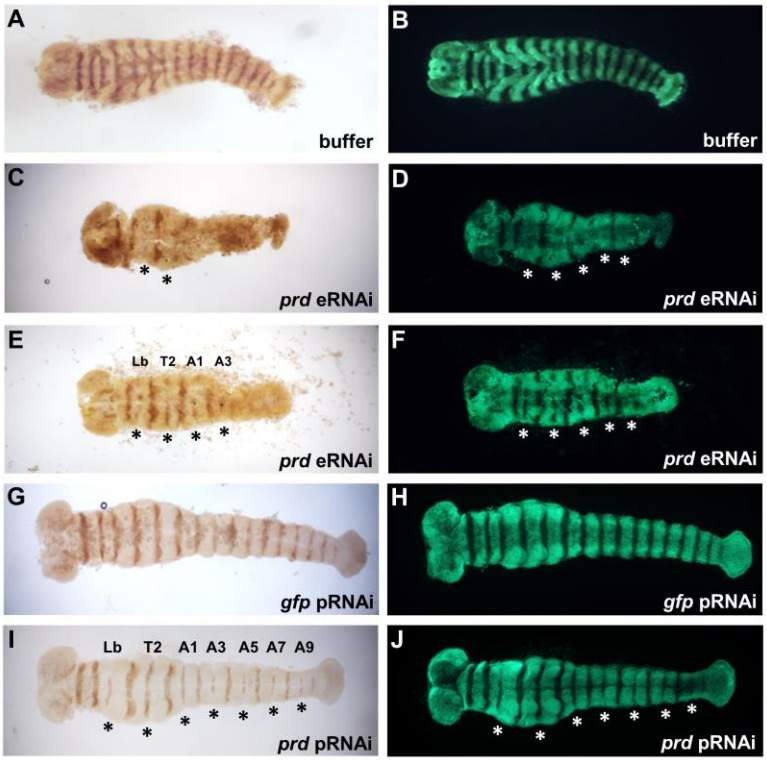

Figure 2-10. Reduced expression of alternate Engrailed stripes after *Dmac-prd* RNAi. (A-F) embryonic RNAi. (G-J) parental RNAi. (A, C, E, G, I) Injected embryos 24-27 h AEL (eRNAi) or 0-1d AEL embryos from injected females (pRNAi), as indicated were fixed and stained using anti-En 4D9 primary antibody and DAB staining. (B, D, F, H, J) SYTOX Green nuclear staining of same embryos for visualization of morphological defects. Asterisks indicate reduced En expression, fused segments or partial fusion between two neighboring segments.

2.5 Discussion

Here we have established *D. maculatus* as a new system for studying embryonic development, gene expression and gene function. *D. maculatus* were maintained in long-term culture in the lab and large numbers of embryos were readily collected and processed. The timing and progression of nuclear divisions, cellularization, gastrulation, and germ band development were described (Figures 2-3, 2-4). Genes of the *Pax3/7* family were isolated (Figures 2-5, 2-6) and the *Dmac-prd* ortholog was found to be expressed in stripes in blastoderm, gastrulation and germ band extension stages embryos, with additional stripes added from the posterior region (Figure 2-7). Both eRNAi and pRNAi were effective in this species, revealing a role for *Dmac-prd* in pair-rule patterning (Figures 2-8, 2-9, 2-10), similar to that seen in other insects (Choe and Brown, 2007; Choe et al., 2006; Gutjahr et al., 1993a; Kilchherr et al., 1986; Maderspacher et al., 1998; Nüsslein-Volhard and Wieschaus, 1980). These findings suggest that the role of *prd* in pair-rule patterning is shared among holometabolous insects with different modes of embryonic development.

Our studies support the classification of *D. maculatus* as an intermediate-germ beetle, as four primary *prd* stripes were established in late blastoderm (Figure 2-7D). In contrast, only one Prd/*prd* stripe was seen in *T. castaneum* embryos prior to

gastrulation (Choe and Brown, 2007; Davis et al., 2001). In *T. castaneum*, the pair-rule segmentation genes *hairy* and *even-skipped* (*eve*) are expressed in two stripes before gastrulation (Choe and Brown, 2007; Davis and Patel, 2002; El-Sherif et al., 2012; Patel et al., 1994; Sommer and Tautz, 1993). One En and one *wingless* stripe were detected at the same stage (Brown et al., 1994b; Davis and Patel, 2002; Nagy and Carroll, 1994; Patel et al., 1994). In a long-germ beetle, *Callosobruchus maculatus*, six *eve* primary stripes were evident before gastrulation (Patel et al., 1994), while four *eve* primary stripes were present in late blastoderm *Dermestes frischi* embryos (Patel et al., 1994), similar to what we observed for *prd*.

To our knowledge, this is the first demonstration of RNAi function in dermestids. Dermestid beetles include 500-700 species worldwide. *D. maculatus* (common name skin beetle), has been widely used for skeletonizing dead animals (Graves, 2005). It is a worldwide pest for the stored meat industry and also the silk industry because it slaughters silkworm cocoons (Shaver and Kaufman, 2009; Veer et al., 1996). Various dermestid species feed on stored meat, stored grain, silk, cheese, poultry, natural or synthetic fiber and pollen (Shaver and Kaufman, 2009). Because of their large numbers and their ability to occupy such diverse habitats, different beetle species have become economically significant pests for agriculture, forests, fabric, and stored food supplies, thus impacting both households and industry (Bouchard et al., 2009; Gullan and Cranston, 2010). The use of RNAi as a highly specific and safe method to control insect pests shows promise in a number of different taxa (Huvenne and Smagghe, 2010). Our studies suggest that RNAi will be a viable strategy for control of dermestid pests.

Protein motifs mix and match in Pax family members

D. melanogaster prd was the founding member of the metazoan Pax family of transcription factors, part of the genetic toolkit directing animal development (Bopp et al., 1986; Carroll et al., 2005; Frigerio et al., 1986). Pax family members have taken on diverse roles in embryonic development, organogenesis and have been implicated in a number of human cancers (Buckingham and Relaix, 2007; Degnan et al., 2009; Noll, 1993; Wang et al., 2008). Pax family proteins are characterized by the presence of multiple protein domains, including a paired domain (PD) composed of a bipartite DNA binding domain, (PAI and RED domains separated by a linker region), an octapeptide (OP), and a paired-type homeodomain (PTHD) (Jun and Desplan, 1996). Members of different Pax subfamilies contain different combinations of these protein domains, or even truncated versions of individual domains, imparting diversity in both structure and function to this gene family (Baumgartner et al., 1987; Bopp et al., 1986; Bopp et al., 1989; Breitling and Gerber, 2000; Friedrich, 2015; Frigerio et al., 1986; Paixão-Côrtes et al., 2015; Underhill, 2012). For example, *D. melanogaster* Pox-meso and Pox-neuro have the PD but lack a HD (Bopp et al., 1989). Phylogentic analyses suggest that *Pax* genes fall into distinct subfamilies, with *prd* a member of the *Pax3/7* group (Friedrich, 2015; Paixão-Côrtes et al., 2015). Pax3/7 family members generally contain a PD, OP and HD and are represented by both *prd* and the closely related *gsb* and *gsb-n* genes in *D. melanogaster*, with only *prd* involved in pair-rule segmentation in *D. melanogaster* (Baumgartner et al., 1987; Bopp et al., 1986; Burri et al., 1989; Frigerio et al., 1986; Gutjahr et al., 1993a; Gutjahr et al., 1993b; Li and Noll, 1993; Nüsslein-Volhard and Wieschaus, 1980).

Although both the PD and HD are shared by all these genes, the OP is present in Gsb and Gsb-n but not in Prd (Baumgartner et al., 1987; Frigerio et al., 1986). Similarly, in *T. castaneum* and *A. mellifera*, the OP motif is present in Gsb and Gsb-n but not in Prd and also is not found in the only *N. vitripennis* Pax3/7 family member (Choe and Brown, 2007; Keller et al., 2010). However, the OP is found in many other Pax proteins: e.g., insect Gsb/Gsb-n, Shaven, Pox-meso and Pox-neuro (Keller et al., 2010) and mammalian Pax 1/9 and Pax 2/5/8 (Stuart et al., 1994). Phylogenetic analysis suggests that the OP was a feature of ancestral Pax proteins. The presence of the OP in Gsb and Gsb-n but not in Prd of extant insects suggests that during Pax3/7 evolution, the OP was lost in an ancestral Prd ortholog. Therefore, the absence of the OP serves as a signature motif for identification of *prd* orthologs (Keller et al., 2010; Noll, 1993). In this study, of the three *prd* family member genes isolated, only one lacked the OP (Figures 2-5, 2-6). Expression and functional results demonstrated it to be a bona fide *prd* ortholog (Figures 2-7, 2-8, 2-9, 2-10), consistent with the utility of using the OP motif as a signature to distinguish among *prd* family members.

Pax3/7 function in panarthropods

Pax3/7 family members have been isolated from a broad range of arthropod groups and from the outgroups, Onychophora and Tardigrada. Expression studies suggest a conserved role in segmentation with segmentally expressed stripes seen for *Pax3/7* genes from crustaceans, chelicates, myriapods, two onychophorans and a tardigrade, suggesting that the ancestral function in segmentation was of the segment polarity type, affecting every segment (Davis et al., 2005; Franke et al., 2015; Gabriel

and Goldstein, 2007; Green and Akam, 2013; Janssen and Budd, 2013; Janssen et al., 2011; Schoppmeier and Damen, 2005a). Indications of a pair-rule type expression are seen in the millipede, *Glomeris marginata*, where the *Pax3/7* family gene *pairberry1* (*pby-1)* is expressed in stripes in the head and anterior thorax. Although these stripes arise almost simultaneously, their intensity alternates in every other segment (Janssen et al., 2011; Janssen et al., 2012). In the two-spotted spider mite (Chelicerata: *Tetranychus urticae*), delayed appearance of alternating stripes of a *Pax3/7* is reminiscent of pair-rule-type expression (Davis et al., 2005; Dearden et al., 2002). However, it is only in Pancrustacea, or possibly hexapods, that a clear PR-like expression pattern of *Pax3/7* genes is observed (Davis et al., 2001). The *Schistocerca americana* ortholog *pby-1* is expressed in a pair-rule-like pattern before it is expressed segmentally (Davis et al., 2001). Although a role for Pax3/7 in PR patterning may thus have arisen before the origin of holometabolous insects, it is in this clade that PR expression and function has been most extensively documented.

A detailed comparison of the expression of *Dmac-prd* to that seen for *prd* in other holometabolous insects shows similarities and differences within this large clade. *Dmac-prd* expression is initiated as a single stripe in the blastoderm (Figure 2-7A). In *T. castaneum*, *prd* expression also begins as a single stripe in the presumptive mandibular segment (Choe and Brown, 2007). Unlike *prd* in these two beetles, *D. melanogaster* Prd first is expressed in a broad anterior region that then resolves into a broad stripe (Gutjahr et al., 1993a). Posterior *Dmac-prd* stripes appear sequentially in an anterior to posterior fashion in the blastoderm embryo to generate a total of 4 primary stripes before gastrulation (Figure 2-7D). Sequential addition of *prd* stripes in

the blastoderm was also detected in *A. mellifera* and *N. vitripennis* (Keller et al., 2010; Osborne and Dearden, 2005). This anterior to posterior progression of stripe formation in the blastoderm was also reported for other pair-rule genes in *T. castaneum*, *N. vitripennis a* and *O. fasciatus* (El-Sherif et al., 2012; Erezyilmaz et al., 2009; Rosenberg et al., 2014). In contrast to this, in *D. melanogaster*, the primary Prd stripes 4 and 7 are expressed earlier than stripes 3, 5, 6 and 8 (Gutjahr et al., 1993a). Thus, even though Prd stripes do not appear simultaneously in long-germ *D. melanogaster*, they do not arise sequentially from the posterior end.

The remaining primary *Dmac-prd* stripes are added from the posterior region during germ band elongation (Figure 2-7), as in *T. castaneum* (Choe and Brown, 2007; Davis et al., 2001). As in other species, including *D. melanogaster*, the primary *prd* stripes in *D. maculatus* split into two secondary stripes (Figure 2-7E-G, P-R). As seen in *A. mellifera*, we did not detect any difference in the intensity or width within pairs of stripes, although differences were reported for *T. castaneum, N. vitripennis* and *D. melanogaster* (Choe and Brown, 2007; Davis et al., 2001; Gutjahr et al., 1993a; Keller et al., 2010; Osborne and Dearden, 2005). Therefore, to date, there is no obvious correlation between this feature and germ band mode. During germ band elongation, anterior *Dmac-prd* stripes fade while stripes in posterior abdominal segments display strong expression (Figure 2-7K-N). This feature is shared in *T. castaneum* and *A. mellifera* (Choe and Brown, 2007; Osborne and Dearden, 2005), but equally expressed segmental *prd* stripes without fading of anterior stripes were observed in late blastoderm and fully elongated *N. vitripennis* and *D. melanogaster* germ band embryos (Gutjahr et al., 1993a; Keller et al., 2010). Since *A. mellifera*, *N.*

vitripennis and *D. melanogaster* exhibit a long-germ mode of segmentation, while *T. castaneum* and *D. maculatus* show short- and intermediate-germ modes, such fading of anterior *prd* stripes during later embryogenesis cannot be correlated with germ band mode. Later during development, *Dmac-prd* is strongly expressed in gnathal segments (Figure 2-7O). This late *prd* expression pattern appears to be a common feature in insects examined so far, suggesting a conserved function for *prd* in head development (Aranda et al., 2008; Gutjahr et al., 1993a; Keller et al., 2010; Osborne and Dearden, 2005; Vanario-Alonso et al., 1995). In sum, although there is some divergence suggesting subtle modulation of *prd* expression, the early striped expression, the splitting of primary *prd* stripes, and the late head expression appear to be shared throughout insect taxa.

Dmac-prd *functions as a pair-rule gene*

As seen in other RNAi knockdown experiments, both *Dmac-prd* pRNAi and eRNAi resulted in a graded series of defects. Two non-overlapping target regions were used to perform pRNAi and both gave similar results, suggesting that effects were specific. In pRNAi experiments, the penetrance dropped rapidly within one-week of injection (Figure 2-9A). pRNAi in *T. castaneum* displayed relatively high penetrance after weeks (Bucher et al., 2002). Whether this difference is specific to *Dmac-prd* or a general feature of RNAi in *D. maculatus* remains to be determined.

Both eRNAi and pRNAi produced defective larvae with fused segmental boundary/boundaries between T2/T3 (parasegment 5, ps5), A1/A2 (ps7), A3/A4 (ps9), A5/A6 (ps11), A7/A8 (ps13). In this graded series, larvae displayed segmentation defects with different levels of severity (Figures 2-8 and 2-9C). One

parasegment (A5/A6) was more sensitive to RNAi, even with low levels of knockdown (Figure 2-9B), as has also been reported in other species for pair-rule mutation or knockdown (Coulter and Wieschaus, 1988; Erezyilmaz et al., 2009). En expression was reduced or completely lost in odd-numbered segments in ~ 50% of *Dmac-prd* dsRNA injected embryos and ~ 60% of pRNAi offspring (Figure 2-10). Together, these findings suggest that *Dmac-prd* functions as a pair-rule segmentation gene in odd-numbered parasegments by activating *en* expression. This function is shared with short-germ *T. castaneum* and long-germ *D. melanogaster* (Choe and Brown, 2007; Choe et al., 2006; DiNardo and O'Farrell, 1987; Maderspacher et al., 1998), and thus appears to be conserved, irrespective of the mode of segmentation.

2.6 Conclusions

Here we have established basic approaches necessary to use *D. maculatus* as a new insect model system. Methods are available not only for basic research approaches but also for developing alternative and safe methods for control of dermestid pests. *D. maculatus* represents the diverse clade of Coleoptera and displays an intermediate-germ mode of segment addition, making it a good system for comparative studies with shorter-germ *T. castaneum* and long-germ *D. malanogaster*. These comparative studies were initiated here by the isolation and characterization of the *D. maculatus* ortholog of *prd*. Consistent with the role of *prd* in *D. melanogaster* and *T. castaneum*, *prd* functions as a pair-rule segmentation gene in *D. maculatus.* Thus, *prd* appears to be a ‘core’ pair-rule gene that retains pair-rule function in a

range of insects that display variation in the function of other pair-rule genes and in the mode of segment addition.

Chapter 3: Rearing and double-stranded RNA-mediated gene knockdown in the hide beetle, *Dermestes maculatus*

[Published: Xiang, Reding and Pick, *JoVE*, 2016]

3.1 Abstract

Advances in genomics have raised the possibility of probing biodiversity at an unprecedented scale. However, sequence alone will not be informative without tools to study gene function. The development and sharing of detailed protocols for the establishment of new model systems in laboratories, and for tools to carry out functional studies, is thus crucial for leveraging the power of genomics. Coleoptera (beetles) are the largest clade of insects and occupy virtually all types of habitats on the planet. In addition to providing ideal models for fundamental research, studies of beetles can have impacts on pest control as they are often pests of households, agriculture, and food industries. Detailed protocols for rearing and maintenance of *D. maculatus* laboratory colonies and for carrying out dsRNA-mediated interference in *D. maculatus* are presented. Both embryonic and parental RNAi procedures—including apparatus set up, preparation, injection, and post-injection recovery—are described. Methods are also presented for analyzing embryonic phenotypes, including viability, patterning defects in hatched larvae, and cuticle preparations for unhatched larvae. These assays, together with *in situ* hybridization and immunostaining for molecular markers, make *D. maculatus* an accessible model system for basic and applied research. They further provide useful information for establishing procedures in other emerging insect model systems.

3.2 Introduction

In 1998, Fire and Mello reported that double-stranded RNA (dsRNA) can induce inhibition of gene function in *Caenorhabditis elegans* (Fire et al., 1998). This response triggered by dsRNA was named RNA interference (RNAi), and such RNAi-mediated gene silencing was reported to be conserved in animals, plants, and fungi (Cogoni et al., 1996; Kennerdell and Carthew, 1998; Napoli et al., 1990; Svoboda et al., 2000; Wianny and Zernicka-Goetz, 2000; Zimmermann et al., 2006). In plants and some animals, RNAi functions systemically, meaning that the effect can spread to other cells/tissues where dsRNA is not directly introduced (reviewed in (Grishok, 2005; Jose and Hunter, 2007; van Roessel and Brand, 2004). Scientists have made use of this endogenous cellular RNAi response by designing dsRNAs to target genes of interest, thereby knocking down gene function without directly manipulating the genome (reviewed in (Agrawal et al., 2003; Dorsett and Tuschl, 2004; Hammond et al., 2001; Hannon, 2002).

RNAi is a powerful tool for functional studies with the following advantages: First, even with minimal gene sequence information, a gene can be targeted using RNAi. This is especially important for studies of non-model organisms lacking genomic or transcriptomic data. Second, in organisms where the RNAi response is robustly systemic, RNAi-mediated gene knockdown can be performed at almost any developmental stage. This feature is very useful for studying the function of pleiotropic genes. Third, in some cases, RNAi effects spread to the gonads and progeny, such that phenotypes are observed in offspring (Bucher et al., 2002; Grishok

et al., 2000). This phenomenon, known as parental RNAi (pRNAi), is especially advantageous for genes impacting embryonic development, as numerous offspring produced by a single injected parent can be examined without direct manipulation of eggs. For these reasons, pRNAi is the method of choice. However, if pRNAi is ineffective, for example for genes required for oogenesis, then embryonic RNAi (eRNAi) must be used. Fourth, RNAi can be used to generate the equivalent of an allelic series in that the amount of dsRNA delivered can be varied over a range to produce weak to strong defects. Such a gradation of phenotypes can be helpful for understanding gene function when the gene is involved in a complex process and/or complete loss of function is lethal. Fifth, delivery of dsRNA is generally easy and feasible, especially in animals showing robust systemic RNAi responses. dsRNA can be introduced by microinjection (Fire et al., 1998; Kennerdell and Carthew, 1998), feeding/ingestion (Timmons and Fire, 1998; Turner et al., 2006), soaking (Eaton et al., 2002; Tabara et al., 1998), and virus/bacteria-mediated delivery (Travanty et al., 2004; Whitten et al., 2016). Sixth, unlike some gene targeting/editing methods, there is no need to screen for organisms carrying the mutation or to carry out genetic crosses to generate homozygotes when using RNAi. Therefore, compared to many other techniques for studying gene function, RNAi is fast, inexpensive, and can be applied for large-scale screens (Dönitz et al., 2015; Schmitt-Engel et al., 2015; Ulrich et al., 2015).

The broad utility of RNAi provides means to carry out functional studies in a wide range of organisms, expanding the range of species available for study beyond the traditional model systems for which genetic tools have been developed. For

example, studies using non-model systems are required to give insights into the evolution of genes and gene networks by comparing the functions of orthologs from species representing different development modes or exhibiting distinct morphological features (Angelini and Kaufman, 2004; Choe et al., 2006; Lynch et al., 2010; Tenlen et al., 2013). These types of studies will provide a better understanding of biological diversity, with impacts for both applied and basic research.

Being the largest animal group on the planet, insects provide a great opportunity to explore the mechanisms underlying diversity. Additionally, insects are generally small, have short life cycles, high fecundity, and are easy to rear in the lab. In the past two decades, RNAi has been successfully applied in insects spanning orders, including Diptera (true flies) (Kennerdell and Carthew, 1998), Lepidoptera (butterflies and moths) (Quan et al., 2002), Coleoptera (beetles) (Brown et al., 1999; Bucher et al., 2002), Hymenoptera (sawflies, wasps, ants and bees) (Lynch et al., 2006), Hemiptera (true bugs) , Isoptera (termites) (Zhou et al., 2008), Blattodea (cockroaches) (Ciudad et al., 2006), Orthoptera (crickets, grasshoppers, locusts, and katydids) (Mito et al., 2005) and Phthiraptera (lice) (Yoon et al., 2011). Successful application of RNAi has provided functional data for studies of patterning in early embryogenesis (anterior-posterior axis (Lynch et al., 2006), dorsal-ventral axis (Lynch et al., 2010), segmentation (Choe et al., 2006; Rosenberg et al., 2014)), sex determination (Hasselmann et al., 2008; Shukla and Palli, 2012), chitin/cuticle biosynthesis (Arakane et al., 2005), ecdysone signaling (Cruz et al., 2006), social behavior (Guidugli et al., 2005), and more. RNAi methods developed for different insect species may be of additional benefit in that they are likely to be useful for pest

control (reviewed in (Huvenne and Smagghe, 2010; Price and Gatehouse, 2008; Zhang et al., 2013)). RNAi effects will be gene-specific as well as species-specific, as long as non-conserved regions are chosen for targeting. For beneficial insect species like honeybees and silkworms, targeting genes vital for the survival of viruses or parasites to control infection may provide a novel strategy to protect these species (Kanginakudru et al., 2007; Paldi et al., 2010).

Dermestes maculatus (*D. maculatus*), common name hide beetle, is distributed worldwide except for Antarctica. As a holometabolous insect, the *D. maculatus* life cycle includes embryonic, larval, pupal, and adult stages (Figure 3-1). Because it feeds on flesh, *D. maculatus* is used in museums to skeletonize dead animals and forensic entomologists can use it to estimate time of death (Magni et al., 2015; Zanetti et al., 2015). *D. maculatus* feeds on animal products including carcasses, dried meat, cheese, and the pupae/cocoons of other insects and thus causes damage to households, stored food, and the silk, cheese, and meat industries (Shaver and Kaufman, 2009; Veer et al., 1996). Applying RNAi in this beetle could provide an efficient and environmentally friendly way to minimize its economic impact. Our lab has used *D. maculatus* as a new model insect to study segmentation (Chapter 2). In addition to being amenable to lab rearing, *D. maculatus* is of interest for basic research as it is an intermediate-germ developer, making it a useful species to study the transition between short- and long-germ development.

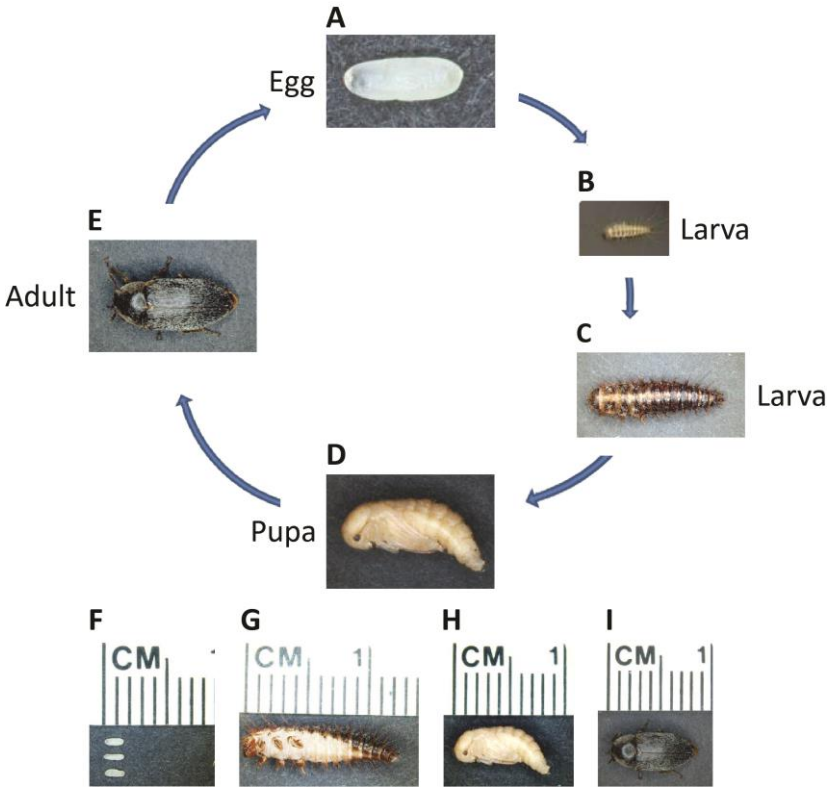

Figure 3-1. Life cycle of *D. maculatus*. Photographs of *D. maculatus* at different life stages, as indicated. The life cycle from egg to adult takes three weeks at 30 ºC but longer at lower temperatures. (A, F) Freshly laid embryos are white to light yellow and oval, approximately 1.5 mm in length. Embryogenesis takes ~55 h at 30 °C. (B, C and G) Larvae have dark pigmented stripes and are covered with setae. Larvae go through several instars depending on the environment and their length can extend up to over 1 cm. (D, H) Young pupae are light yellow. Pupation takes ~5-7 days at 30 °C. (E, I) Shortly after eclosion, dark pigmentation appears over the adult beetle body. Adults can live up to several months and one female can lay hundreds of embryos over her lifetime.

Previously, we showed that RNAi is effective in knocking down gene function in *D. maculatus* (Chapter 2). Here our experience rearing *D. maculatus* colonies in the laboratory is shared along with step-by-step protocols for both embryonic and parental RNAi set-up, injection, post-injection care, and phenotypic analysis. The dsRNA-mediated gene knockdown and analysis methods introduced here not only

provide detailed information for addressing questions in *D. maculatus*, but also have potential significance for applying RNAi in other non-model beetle/insect species.

3.3 Protocol

3.3.1 *Rearing of* D. maculatus

Note: A breeding colony of *D. maculatus*, was set up in the authors' lab using adults and larvae purchased commercially. The species identity was verified using DNA barcoding (Chapter 2).

3.3.1.1 To set up a new cage in the lab, spread a thin layer of wood shavings into a medium-size insect cage (30.5x19x20.3 cm). Place an ~ 10x6x3 cm chunk of Styrofoam in the cage to let larvae hide for pupation. Add 20-50 beetles (either adults or late instar larvae). Beetles will hide in the wood shavings.

3.3.1.2 Add wet cat food in a petri dish or a weighing boat. Cover the cage with mesh cloth and place the cage in an incubator (Figure 3-2).

Figure 3-2. *D. maculatus* lab colony. Photograph of a typical *D. maculatus* insect cage is shown. Wood shavings are spread to let the beetles hide. Cat food is added in a small petri dish or weighing boat. Styrofoam is placed into the cage as a refuge for final instar larvae to pupate. The cage shown here is 30.5x19x20.3 cm and houses a few hundred larvae, pupae, and adults.

3.3.1.3 For maintaining a breeding colony in the lab, set the temperature between 25 and 30 °C. *D. maculatus* grow faster at higher temperatures, but this also promotes the growth of fungus and mites. To maintain a healthy colony, use 25-28 °C for regular stock maintenance and 30 °C for rapidly expanding the colony. The life cycle takes approximately three weeks to four months depending on environmental factors (Zanetti et al., 2015).

3.3.1.4 Leave eggs in the cage to mature. To expand the colony, establish new cages with eggs (collected as described in Section 2), larvae, or adults, as above. *D. maculatus* lay eggs throughout the cage, especially near the food source.

3.3.1.5 Replace wet cat food about twice a week. Due to the unpleasant odor

of wet cat food, alternative food sources were also tested (see Discussion).

3.3.2 *Embryo collection*

3.3.2.1 To set up a collection, separate at least 50 males and 50 females from the colony. Young adults are best. Place adults in a mini-sized cage (17.8x10.2x12.7 cm) without wood shavings. Add cat food in a weighing boat.

3.3.2.2 Before starting collection, check the cage carefully for any embryos present and remove them. Put a stretched cotton ball into the cage, and leave the cage in a 30 °C incubator. After the appropriate time window, the cotton ball will be ready for embryo collection.

3.3.2.3 Fold a piece of black construction paper (A4 size) in half to create a crease, and then unfold.

3.3.2.4 Remove the stretched cotton ball from the cage. Remove adults from the cotton ball and put them back into the cage.

3.3.2.5 While pinching the stretched cotton ball very gently, tear it apart slowly into thin cotton filaments to let the eggs fall onto the black paper.

Note: *D. maculatus* embryos are fragile and hard to see in cotton. They can be easily crushed if holding the cotton ball too firmly.

3.3.3 *dsRNA preparation*

3.3.3.1 DNA template preparation for dsRNA synthesis

3.3.3.1.1 Run 4-6 50 µL PCR reactions using primers containing T7 promoter sequences at both 5’ ends to amplify DNA template according to manufacturer’s protocol.

3.3.3.1.2 Purify PCR product using a commercial PCR purification kit, following manufacturer's instructions. The ideal final concentration of DNA template is ≥100 ng/µL.

3.3.3.2 Injection buffer preparation

3.3.3.2.1 Prepare 100 mL of injection buffer (0.1 mM NaH_2PO_4, 5 mM KCl). Adjust pH to 6.8 with 5M NaOH.

3.3.3.2.2 Store aliquots at -20 °C.

3.3.3.3 dsRNA synthesis

3.3.3.3.1 Set up a reaction in a 0.2 mL PCR tube on ice and carry out an *in vitro* transcription reaction with T7 polymerase, following manufacturer's instructions, using ~500 ng template per reaction.

3.3.3.3.2 Incubate the tube at 37 °C overnight.

3.3.3.3.3 Digest the DNA template with DNase, following manufacturer's instructions.

3.3.3.3.4 Heat the tube to 94 °C and hold at 94 °C for 3 min.

3.3.3.3.5 To anneal the dsRNA, slowly cool the tube by 1 °C/min until it reaches 45 °C after 1 h.

Note: Steps 3.3.3.3.2 through 3.3.3.3.5 can be performed in a PCR cycler.

3.3.3.3.6 To ethanol precipitate dsRNA, add 280 µL of RNase free water to 20 µL of reaction to adjust to a final volume of 300 µL. Add 30 µL of 3 M NaOAc (pH 5.2) and 650 µL of ethanol. Place tube in -20 °C freezer overnight.

3.3.3.3.7 After centrifuging at 15,682 × g for 30 min at 4 °C, wash the

dsRNA pellet with 70% ethanol. Dry pellet and dissolve in 20 µL injection buffer.

3.3.3.3.8 Measure the concentration of the dsRNA using a spectrophotometer at A_{260}. The ideal concentration is 3–5 µg/µL. Check the quality by running 5 µL of a 1:25 dilution dsRNA on a 1% agarose gel at 90 V for 30 min. A single band of expected size will be readily visible.

3.3.3.3.9 Store the dsRNA at -20 °C or colder.

Note: For every RNAi knockdown experiment, include a control dsRNA, which would not be expected to impact the process being studied. *gfp* dsRNA is an excellent control for most experiments. Prepare and inject the control dsRNA side-by-side with the experimental dsRNA.

3.3.4 *Injection apparatus setup*

Note: See Figure 3-3

3.3.4.1 Assembly of microinjector and micromanipulator

3.3.4.1.1 Connect nitrogen or other air supply to the pressure input of a pneumatic pump instrument. If a pneumatic pump is not available, apply pressure using a 50 mL syringe connected to fine tubing.

3.3.4.1.2 Connect a foot switch to the remote connector of the pump to control the eject pressure flow.

3.3.4.1.3 Attach a glass capillary holder to the eject pressure port of the pump with tube.

3.3.4.1.4 Fix the capillary holder on a micromanipulator close to a

dissecting microscope.

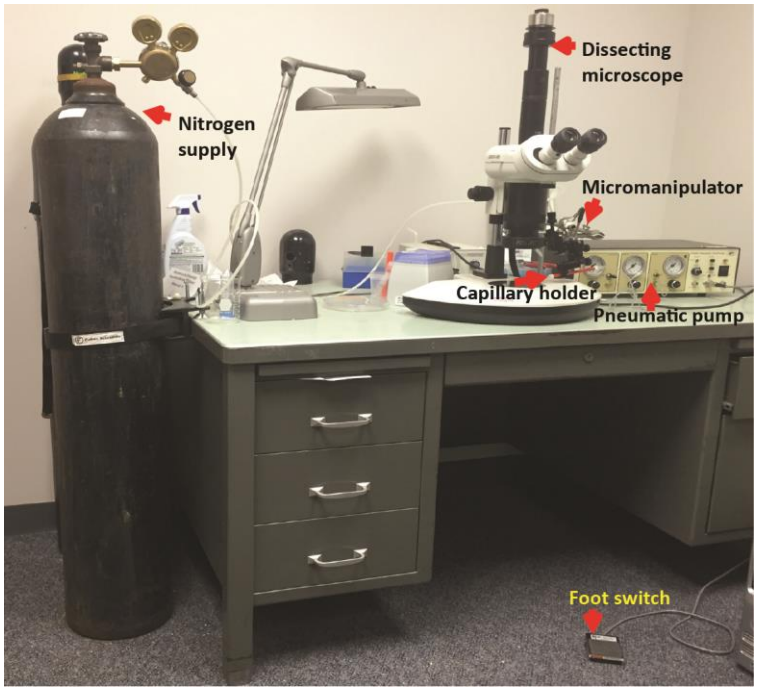

Figure 3-3. Injection apparatus. Photograph of the dissection microscope and micromanipulator used to inject *D. maculatus* embryos is shown. Nitrogen supply is connected to the pressure input port of a pneumatic pump. Glass capillary holder is connected to the eject pressure port of the pump. Foot switch is connected to the pump.

3.3.5 *Embryonic RNAi*

Note: Figure 3-4 shows a flowchart of *D. maculatus* embryonic RNAi.

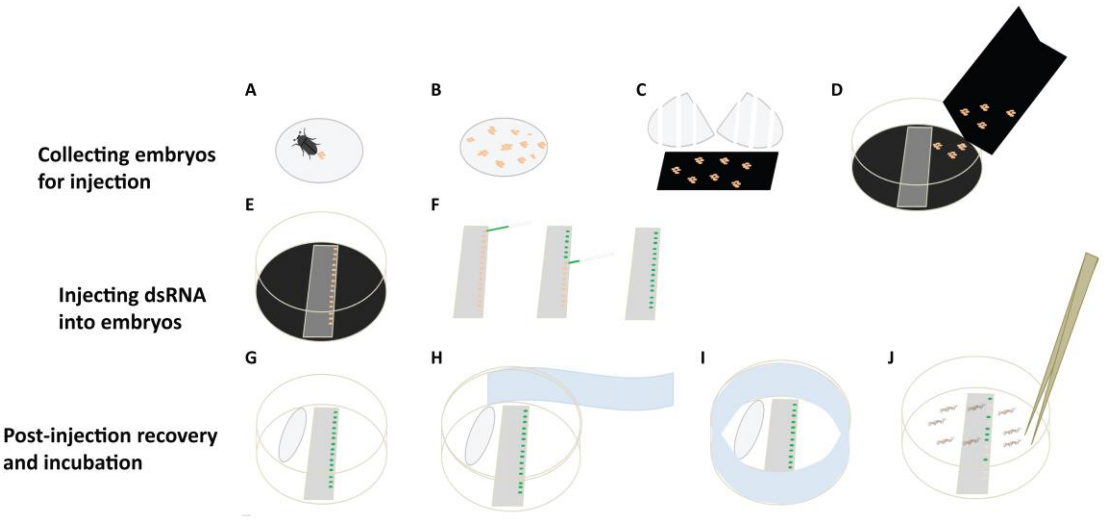

Figure 3-4. A flowchart for *D. maculatus* embryonic RNAi. (A-D) Collecting embryos for injection. Females lay embryos (orange) in cotton balls (grey circle). Separate embryos from cotton balls and let them drop onto a piece of black construction paper. White bars indicate tears in cotton ball. Transfer embryos to a collecting petri dish lid, lined with black paper. (E, F) Injecting dsRNA into embryos. Align embryos on slides on double stick tape and inject them individually under a dissecting microscope. Needle with green food dye is shown. (G-J) Post-injection recovery and incubation. Place a wet cotton ball in the petri dish to provide humidity. Cover the petri dish and wrap it with sealing film (light blue). Place the petri dish in an incubator and remove hatched larvae for phenotypic analysis.

3.3.5.1 eRNAi preparation

3.3.5.1.1 Prepare an embryo collecting petri dish lid (90 mm). Place a piece of black filter paper to cover the inside of the lid. Put a standard microscope slide on the black paper.

3.3.5.1.2 Dilute dsRNA to appropriate concentration with injection buffer. 2-3 µg/µL is recommended for initial experiments. Always keep dsRNA on ice prior to injection.

3.3.5.1.3 Add food coloring at 1:40 dilution to the dsRNA and pipette gently several times to mix well.

3.3.5.2 Collecting embryos for injection

Note: At 25 °C, nuclei in embryos 6-8 h After Egg Laying (AEL) migrate towards the egg periphery. A cellular blastoderm is established within 8-10 h AEL (Chapter 2). To ensure embryos prior to cellular blastoderm stage are used for injection, 0-3 h AEL embryos are recommended for use. Embryo collection, preparation, and injection usually take less than 2 h if the glass capillaries are in good shape. Therefore, the whole process can be completed within 5 h AEL.

3.3.5.2.1 Collect embryos as described in steps 3.3.2.2-3.3.2.5.

3.3.5.2.2 Tap the black construction paper to transfer embryos into collecting petri dish lid.

3.3.5.2.3 Stick double-sided tape along the edge of the slide.

3.3.5.2.4 Using a paint brush, align the embryos on the tape perpendicular to the slide edge with the anterior or posterior to the end. Note that anterior and posterior ends of early embryos are not readily distinguishable, thus on average half will be injected at the posterior end which is ideal.

3.3.5.3 Loading the dsRNA into the glass capillary

3.3.5.3.1 Take up 2-4 µL of dsRNA into a 20 µL microloader pipette tip.

3.3.5.3.2 Insert the tip into a pre-pulled glass capillary and gently pipette the dsRNA solution into the capillary (referred to as needle) and gently pipette the dsRNA solution into the capillary. Needles are prepared from commercial glass capillaries using a micropipette puller. An example of an ideal pulled needle is shown in Figure 3-5. The length and taper of needles may need to be optimized after injection trials.

3.3.5.3.3 Fix the glass capillary into the glass capillary holder.

3.3.5.3.4 Assemble the capillary holder into the micromanipulator.

3.3.5.4 Injecting dsRNA into embryos

3.3.5.4.1 Carefully transfer the slide with embryos onto the stage of the dissecting microscope.

3.3.5.4.2 Move the slide to bring one embryo to the center of the field and focus microscope.

3.3.5.4.3 Position the tip of the capillary with the micromanipulator while looking into the dissecting microscope. Bring the tip close to the end of the first embryo in the row.

3.3.5.4.4 Switch on the nitrogen or other air supply.

3.3.5.4.5 Set the solenoid input selector switch to vacuum.

3.3.5.4.6 Adjust the eject pressure regulator to 10-15 psi. Pressure may need to be adjusted depending on the apparatus.

3.3.5.4.7 Open the capillary if necessary. Once the tip is open, the colored dsRNA solution will fill the tip.

3.3.5.4.8 Move the capillary tip forward to puncture the embryo. If the pressure setting is ideal, no embryonic fluid will flow into the capillary.

3.3.5.4.9 Step on the foot switch to eject dsRNA solution into the embryo until an appropriate amount of solution is ejected. Figure 3-5 shows examples of embryo morphology after appropriate and inappropriate amounts of solution have been injected.

3.3.5.4.10 Keep the capillary tip inside the embryo for ~2 s, then remove

it.

3.3.5.4.11 Move the capillary to the next embryo and repeat steps 3.3.5.4.8-3.3.5.4.10 until all embryos are injected. Change glass capillary if it gets clogged or breaks.

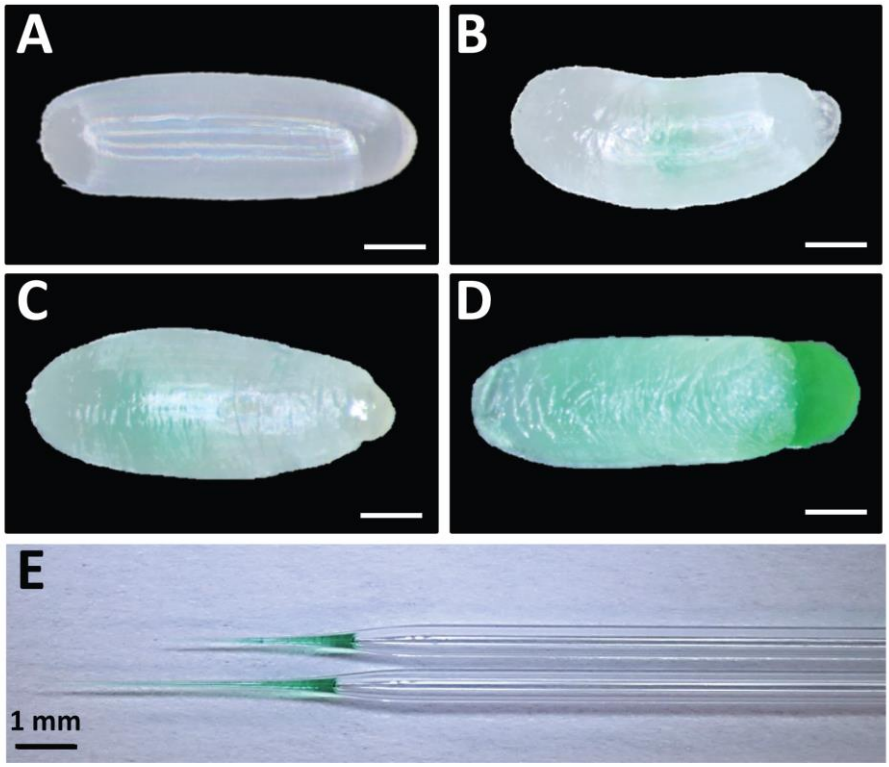

Figure 3-5. Good vs. bad embryonic injection examples. (A) Uninjected embryo. (B) Embryo injected with too little dsRNA. (C) Embryo injected with appropriate amount of dsRNA. (D) Broken embryo with overflowing dsRNA caused by over-injection. Food coloring was added to dsRNA for visualization. (E) Examples of pulled capillary tubes used as needles for injection. Note the taper and tip length for two examples of functional needles. Scale bars for A-D represent 200 μm.

3.3.5.5 Post-injection recovery and incubation

3.3.5.5.1 After injection, place the slide in a petri dish.

3.3.5.5.2 Add a wet cotton ball to the petri dish. Do not let the cotton ball touch the slide.

3.3.5.5.3 Cover the petri dish and wrap it with sealing film. Label the

dish with the name of the dsRNA, concentration, date, time, and number of injected embryos.

3.3.5.5.4 Place the petri dish in a 30 °C incubator until the embryos hatch.

3.3.6 *Parental RNAi*

3.3.6.1 Isolating pupae for pRNAi

3.3.6.1.1 Collect pupae from the colony.

3.3.6.1.2 Sort male and female pupae under microscope (see Figure 3-6). Keep them in two separate petri dishes in a 30 °C incubator in a 30 °C incubator to ensure that no mating occurs prior to injection.

3.3.6.1.3 Check every day for eclosed adults. Pupation usually takes 5-7 days at 30 °C.

3.3.6.1.4 Transfer eclosed males and females (see Figure 3-6) to two separate petri dishes and feed them cat food every other day until they are ready for injection.

3.3.6.1.5 Proceed to injection once there are enough females and males at appropriate age. Females 4 to 8 days post-eclosion are best. For a typical analysis, 8-12 females are used. An equal number of males are needed for mating (Fontenot et al., 2015).

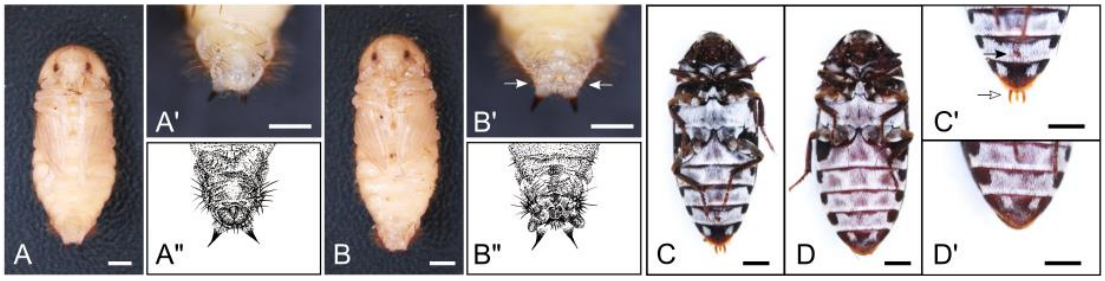

Figure 3-6. Male and female adults and pupae. (A) Ventral view of a male pupa. (A') Magnification of posterior part of A. (A") Illustration of male pupa genitalia. (B) Ventral view of a female pupa. (B') Magnification of posterior part of B. Female pupae have two genital papillae (white arrows). (B") Illustration of female pupa genitalia. (C) Ventral view of a male adult. (C') Magnified view of posterior part of C. Note that male adults have trident-like genitalia and a circular lobe-like structure on the 4th sternite (white and black arrows, respectively). (D) Ventral view of a female adult. (D') Magnified view of posterior part of D. For all panels, scale bars indicate 1 mm. This figure panel was prepared by Katie Reding.

3.3.6.2 Injecting dsRNA into female abdomen

3.3.6.2.1 Prepare dsRNA on ice (3.3.5.1.2 and 3.3.5.1.3).

3.3.6.2.2 Attach a 32-gauge needle to a 10 µL syringe.

3.3.6.2.3 Anaesthetize females on CO_2 stage.

3.3.6.2.4 Load dsRNA solution into the syringe without taking up any air.

3.3.6.2.5 Hold a female ventral side up with one hand and hold the syringe with the other.

3.3.6.2.6 Gently penetrate the segmacoria (membrane) between sternites 2 and 3 with the tip of the needle. Figure 3-7 shows a female during injection. If the needle does not penetrate the tissue easily, angle the needle upward and slowly press down. Insert approximately 2 mm of the needle into the body.

3.3.6.2.7 Check the syringe scale while slowly pushing the plunger, injecting ~2 µL per female.

3.3.6.2.8 After injecting, hold the needle still for at least 5 s before removing it from the female's abdomen.

3.3.6.2.9 Transfer the injected females to a petri dish (90 mm) and feed

with cat food.

3.3.6.2.10 Label the petri dish with the dsRNA name, amount injected, date, and number of females.

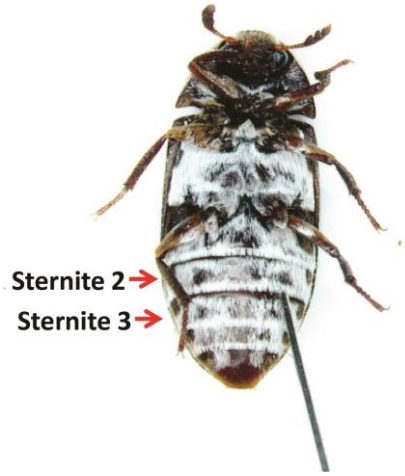

Figure 3-7. A female during injection. Females are anesthetized and placed ventral side up. A needle penetrating the segmacoria between the 2nd and 3rd sternites to inject dsRNA is shown.

3.3.6.3 Post-injection recovery and mating

3.3.6.3.1 Incubate the petri dish in a 30 °C incubator.

3.3.6.3.2 After 24 h, transfer injected females to a mini cage.

3.3.6.3.3 Add to the cage an equal number of uninjected young males, and label the cage.

3.3.6.3.4 Add a weighing boat with cat food into the cage.

3.3.6.3.5 Leave the cage in a 30 °C incubator to allow mating. After 24 h, females should start to lay eggs and embryos can be collected daily or at required time intervals.

3.3.7 *Phenotypic analysis after RNAi*

Note: At 30 °C, it takes ~55 h for eggs to hatch (Zanetti et al., 2015).

3.3.7.1 eRNAi viability analysis

3.3.7.1.1 Calculate hatch rate by comparing the number of hatched larvae to the total number of injected embryos. Be sure to include a negative control injection as embryos may be harmed or killed by the injection procedure. Typical hatch rates vary from 30% - 60%. Beware of hatched larvae eating unhatched eggs.

3.3.7.2 pRNAi viability analysis

Note: if female viability is impacted by the gene targeted by RNAi, females injected with specific dsRNA but not negative control dsRNA will begin to die. If egg production or egg laying is impacted, females will exhibit partial or complete sterility. Score female survival compared to negative controls or compare total number of eggs laid by experimental and control females (3.3.7.2.3).

3.3.7.2.1 Set up embryo collection following step 3.3.2.2.

3.3.7.2.2 After 24 h, collect embryos following steps 3.3.2.4-3.3.2.5.

3.3.7.2.3 Count the total number of the embryos.

3.3.7.2.4 Transfer the embryos to a 90 mm petri dish. Label the petri dish with the type of RNAi, collection date, and number of embryos.

3.3.7.2.5 Incubate the embryos in a 30 °C incubator until they hatch. Since hatched larvae feed on unhatched embryos, check the petri dish frequently and separate hatched larvae from unhatched embryos using

forceps (see Discussion).

3.3.7.2.6 Count the number of hatched embryos and calculate the hatch rate.

3.3.7.3 Examining cuticle defects in hatched larvae

3.3.7.3.1 Collect hatched larvae in a 1.5 mL microcentrifuge tube.

3.3.7.3.2 In a fume hood, add 1 mL of Fixation Solution.

3.3.7.3.3 Leave the microcentrifuge tube at 4 °C at least overnight to let the solution penetrate the larval tissue.

3.3.7.3.4 To visualize, remove as much fixative from the tube as possible.

3.3.7.3.5 Rinse larvae at least three times with PBST.

3.3.7.3.6 Transfer larvae to a multi-well glass plate with PBST using a P-1000 pipette tip with the end cut off to widen it.

3.3.7.3.7 Under a dissecting microscope, stretch larvae using forceps to examine defects. It is critical to stretch out larvae to examine defects as their bodies contract in fixative.

3.3.7.4 Examining cuticle defects in unhatched larvae

Note: This is useful for examination of early embryonic phenotypes, especially for embryos that do not survive to hatching.

3.3.7.4.1 For pRNAi, add PBST into the petri dish (3.3.7.2.4) and transfer unhatched embryos to a 1.5 mL microcentrifuge tube using a P-1000 pipette tip with the end cut off. For eRNAi, add PBST into the petri dish (3.3.5.5.4), brush unhatched embryos off the microscope slide

and transfer them to a microcentrifuge tube.

3.3.7.4.2 Fix the embryos and rinse them with PBST for visualization following steps 3.3.7.3.2-3.3.7.3.6.

3.3.7.4.3 Using forceps, dissect embryos out of the eggshell under a dissecting microscope in PBST.

3.3.7.4.4 Transfer the embryos back to 1.5 mL microcentrifuge tube (~200 µL of embryos in each tube).

3.3.7.4.5 Remove as much solution as possible.

3.3.7.4.6 Add 1 mL of 90% lactic acid/10% EtOH. Leave the centrifuge tube in a 60 °C incubator at least overnight.

Note: Embryos can be left at 60 °C for several days.

3.3.7.4.7 To mount the embryos, pipette them onto a microscope slide using a P-1000 pipette tip with the end cut off.

3.3.7.4.8 Manually position the embryos with forceps to an ideal orientation.

3.3.7.4.9 Cover the embryos with a cover-slip and visualize under microscope using DIC.

3.3.7.5 Examining cellular and molecular defects

Note: This is useful for investigating the underlying causes of cuticle phenotypes or lethality that is not accompanied by cuticle defects.

3.3.7.5.1 For pRNAi, separate embryos from cotton balls at appropriate development stage and transfer them into an embryo collecting basket. The collection basket can be the same or similar to that used for

Drosophila embryo collections. The egg basket can be made from a 25 mL plastic scintillation vial with the bottom of the vial removed, and a circle cut out of the lid (roughly 1 cm diameter). A circle of super fine mesh about 2.5 cm in diameter is placed inside the lid, and the scintillation vial is then screwed on and used upside-down. As the mesh can be easily removed once the embryos are washed, the mesh is immersed in a microcentrifuge tube with water to recover any embryos sticking to the mesh.

3.3.7.5.2 For eRNAi, at appropriate stage, add PBST to the petri dish. Brush the embryos off the microscope slide and transfer them to an embryo collecting basket.

Fixation, *in situ* hybridization, antibody staining, and nuclear staining protocols can be found in Chapter 2.

3.4 Representative results

The authors' lab has used RNAi technology to study the functional evolution of genes regulating segmentation in insects Chapter 2 and (Heffer et al., 2013). While all insects are segmented, the genes regulating this process appear to have diverged during insect radiations (Aranda et al., 2008; Choe et al., 2006; Dawes et al., 1994; Erezyilmaz et al., 2009; Heffer et al., 2010; Mito et al., 2007; Patel et al., 1992; Rosenberg et al., 2014; Stuart et al., 1991; Wilson and Dearden, 2012). Genetic screens in *Drosophila* identified a set of nine pair-rule segmentation genes that are responsible for promoting the formation of body segments (Guichet et al., 1997;

Jürgens et al., 1984; Nüsslein-Volhard and Wieschaus, 1980; Nüsslein-Volhard et al., 1984; Wakimoto and Kaufman, 1981; Wieschaus et al., 1984b; Yu et al., 1997). Here, the ortholog of one of these genes, *paired* (*prd*), is used to document the utility of RNAi for studying gene function in *D. maculatus*.

eRNAi and pRNAi were each effective in demonstrating roles for *Dmac-prd* in segment formation in this species. 2-3 µg/µL of dsRNA designed to target *Dmac-prd* (Figure 3-8B, D and F) was compared to *gfp* dsRNA, injected as negative control (Figure 3-8A, C and E).

Control offspring hatched with one pigmented stripe per segment. Neighboring pigmented stripes were separated by a non-pigmented gap (Figure 3-8A). After *prd* pRNAi, affected offspring hatched with fused neighboring pigmented stripes, indicating segmental boundaries were defective (Figure 3-8B). Depending on phenotypic severity, one or several fusions were detected in affected larvae. Nevertheless, fusions consistently appeared at the boundary regions between T2/T3, A1/A2, A3/A4, A5/A6, A7/A8, indicating pair-rule-like defects. Cuticle phenotypes after *prd* knockdown showed loss of abdominal segments as well as shortened body length (Figure 3-8D). Engrailed (En) antibody staining was performed to examine molecular defects in early embryos after *prd* knockdown. While control embryos showed striped En expression with equal intensity in every segment (Figure 3-8E), reduced En expression was detected in alternate stripes in offspring from *Dmac-prd* dsRNA injected females (asterisks in Figure 3-8F). The pattern of reduced En expression is consistent with the defective cuticle pattern observed in affected

hatched larvae. For more detailed results of phenotypes after *prd* knockdown in *D. maculatus*, see Chapter 2.

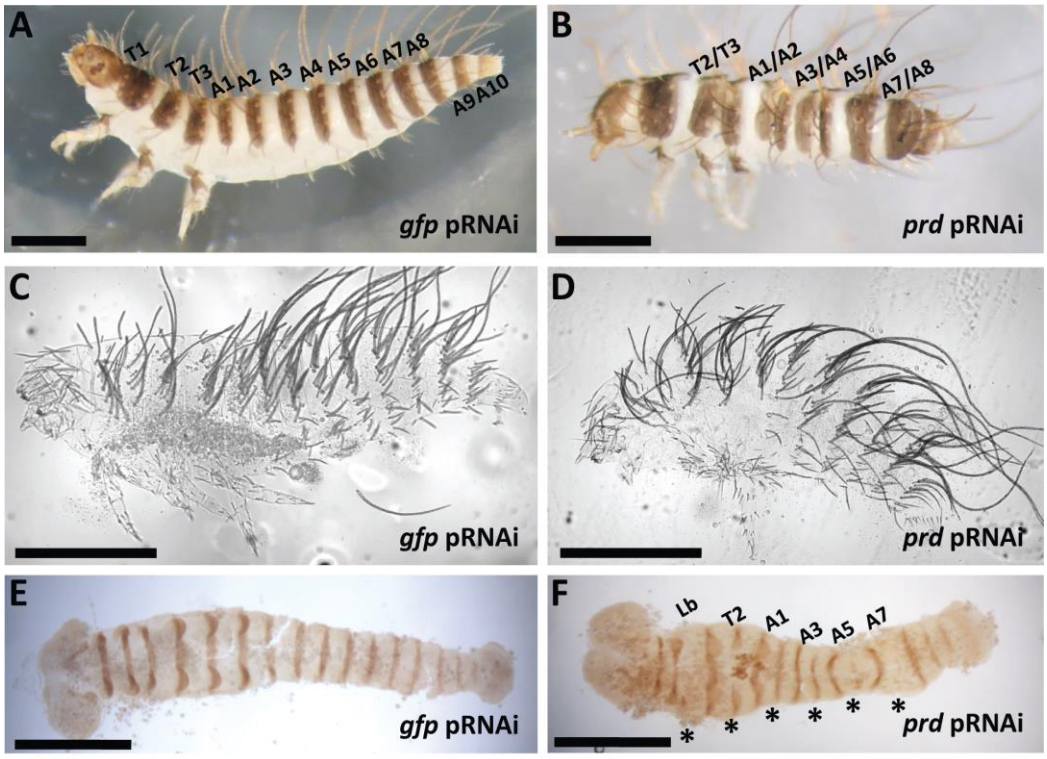

Figure 3-8. Representative phenotypes after *Dmac-prd* pRNAi. (A) Control injection. Lateral view of a hatched wild type-like *gfp* pRNAi offspring with three thoracic segments and ten abdominal segments. Each segment has setae and pigmented stripes. (B) Lateral view of a hatched *prd* pRNAi offspring. The gap between labeled neighboring pigmented stripes is narrowed or completely missing. (C) Cuticle phenotype of an unhatched control wild type-like embryo. (D) Cuticle phenotype of an unhatched *prd* pRNAi offspring with fewer abdominal segments. (E,F) Dissected germband from: (E) Control, *gfp* pRNAi has evenly expressed En in every segment. (F) *prd* pRNAi, En expression is reduced in alternate segments (asterisks). For all panels, scale bars indicate 500 μm.

3.5 Discussion

While a small number of sophisticated model systems (mice, flies, worms) were developed during the 20th century, the 21st century has seen a wave of new animal systems being developed in labs throughout the world. These new systems

allow scientists to address comparative, evolutionary questions that cannot be probed using only the 'standard' model systems. This deployment of new models requires the rapid development of methods for lab culturing, gene identification, and functional approaches in new species. Here, procedures for rearing *D. maculatus* in the lab and step-by-step protocols for embryonic RNAi, parental RNAi, and phenotypic analysis in this beetle were presented. The goal is that these descriptions encourage others to use *D. maculatus* in their own experiments and to make use of the approaches presented here to develop additional new model species.

While *D. maculatus* lab colonies are incredibly easy to maintain, one limitation of rearing this species is the unpleasant odor of the wet cat food given to the beetles as their source of food. To avoid this, alternative foods such as whey/soy protein powder, cheese, ground dog food, and powdered milk, were tested with or without wet cotton to alter humidity. Ground dog food was the most effective alternative and can be used for regular colony feeding. Survival was excellent (>90%) from egg to adult in cages reared on just dry dog food in 80% relative humidity, with or without wet cotton added. However, supplementing this diet with wet cat food when collecting eggs to increase fecundity may be necessary when collecting large numbers of eggs. If dog food is used, old food should be removed regularly, as conditioned dog food was found to inhibit egg laying (Fontenot et al., 2015). Dog food kibbles (K.R., preliminary results), cork, wood, paper, and other materials can also be used as refuges (Fontenot et al., 2014). Interestingly, biodegradation of Styrofoam using mealworm beetle larvae has been reported (Yang et al., 2015). Therefore, this was tested for *D. maculatus* larvae. Young *D. maculatus* larvae

survived until adulthood with only Styrofoam or asbestos-containing materials and wet cotton (data not shown) but whether they eat and digest those materials remains to be determined.

This report is the first detailed protocol for carrying out functional genetic studies in *D. maculatus.* The use of RNAi here represents an expansion of this technique to a new model system. Several specific observations are worth noting with respect to RNAi knockdown experiments in *D. maculatus* and other non-model species. First, to guarantee that RNAi will be effective in *D. maculatus,* the same strain of *D. maculatus* used here should be employed. There is evidence from *Tribolium castaneum* that different strains show variation in RNAi phenotypes (Dönitz et al., 2015; Kitzmann et al., 2013), and mutant phenotypes often show dependence on genetic background in model species (Chandler et al., 2014; Doetschman, 2009; Montagutelli, 2000). Also, there is anecdotal evidence for strain-dependence in other protocols, including *in situ* hybridization. Second, appropriate timing of injection is critical for successful RNAi in *D. maculatus*. Somewhat counterintuitively, the segmacoria is most easily penetrated after the cuticle has completely sclerotized, at least two days after eclosion. Therefore, virgin females 4-8 days after eclosion should be used. Older females experience lower fecundity than newly eclosed females and thus are not appropriate for injection. Third, injected dsRNA may get pushed out by the inner pressure of the female abdomen. To minimize the possibility of losing a large amount of dsRNA after injection, hold the needle in the abdomen for ~5 s after injection and then remove it slowly (3.3.6.2.8). Meanwhile, avoid pressing the female's abdomen during or shortly after injection. To

circumvent biased results caused by this issue, inject at least 8 females for each dsRNA to get enough offspring (~200 embryos daily) for phenotypic analysis. Fourth, high egg yield is important for providing unbiased data for phenotypic analysis after injection. On average, each *D. maculatus* female produces approximately 35-55 embryos daily. Egg yield depends on population size, female age, humidity, food availability, temperature, (data not shown) and other environmental factors (Fontenot et al., 2015). Usually, females lay more at 30 °C than 25 °C. Fifth, unhatched embryos can be cannibalized by hatched larvae. As hatched larvae are usually wild-type-like or only mildly affected, while unhatched embryos are usually more severely affected, this habit of *D. maculatus* larvae can cause biased results in a quantitative phenotypic analysis. Therefore, removal of hatched larvae as early as possible is strongly recommended.

Our lab has focused on *D. maculatus* segmentation, although many aspects of this species—including physiology, ecology, and pest control—are of great interest. For studying embryogenesis and segmentation, a series of darkly pigmented stripes on the dorsal side of *D. maculatus* larvae can serve as a natural marker for abnormal development. Also, characteristic setae rooted on the pigmented stripes of larvae can be used as an indication of segments. These morphological features, together with the finding that mildly or moderately affected embryos can survive to hatching, are advantages of the *D. maculatus* model to study the mechanisms involved in patterning the basic body plan.

Finally, the importance of carrying out highly controlled experiments—including a negative control such as *gfp* dsRNA and testing two non-overlapping

target regions for each gene—is critical avoid misinterpretation due to effects of injection per se and to off-target effects. For *D. maculatus*, 4-6 µg (2 µL of 2 or 3 µg/µL) dsRNA were injected into each female and the dsRNA was 200-250 bp long. Amounts and other details of the protocol may need to be optimized if targeting genes functioning later in development or in different physiological/metabolic processes. Previous discoveries showed that RNAi effects can be passed on to subsequent generations beyond the F1 generation in *C. elegans* (Grishok et al., 2000). A minority of hatched *D. maculatus* larvae with segmentation defects due to RNAi can survive until adulthood and can reproduce. Preliminary experiments failed to reveal obvious defects in the F2 generation. Future studies may reveal transgenerational effects of RNAi in this species.

Chapter 4: Conservation and variation of pair-rule patterning mechanisms revealed in *Dermestes maculatus*

[Xiang, Reding, Heffer and Pick, Submitted]

4.1 Abstract

A set of pair-rule segmentation genes (PRGs) promote the formation of alternate body segments in *Drosophila melanogaster* (*Drosophila*). Expression and/or functional studies indicate that many PRGs function in segmentation outside of *Drosophila*, although the precise cohort of genes varies, and the specific roles of individually conserved genes varies as well. While *Drosophila* embryos are long germ, with segments specified more-or-less simultaneously at the blastoderm stage, most other insects and arthropods add segments sequentially as the germband elongates (short or intermediate germ mode). The hide beetle, *Dermestes maculatus*, represents an intermediate state between short and long germ development and was therefore chosen to examine conservation and variation in the expression and function of PRGs. Here we show that eight of nine *Drosophila* PRG orthologs are expressed in stripes in *Dermestes*. RNAi revealed functional conservation for five PRGs, while others vary. *Dmac-eve*, *-odd* and *-run* play roles in both germband elongation and PR-patterning, while *slp*, similar to *prd*, functions exclusively as a classical PRG. *Dmac-prd* and *-slp* double RNAi offspring developed asegmentally but did not fail to elongate, indicating functional decoupling of elongation and segment formation. Generally, extensive cell death prefigured cuticle defects, suggesting a conserved mechanism of PRG action. In addition, an organized region with high mitotic activity

near the margin of the segment addition zone, likely contributes to truncation of *eve*^{RNAi} embryos. Our results suggest that the same mechanisms promote formation of segments in both blastoderm-specified and sequentially added tissue, with a subset of PRGs having additional roles in elongation in sequentially-segmenting species.

4.2 Introduction

As segmentation is a shared feature of all arthropods, mechanisms controlling it would be expected to be largely shared among diverse members of this clade. The regulation of segmentation has been studied extensively in the model insect, *Drosophila*, where genes act hours before segments actually form, pre-figuring and determining the patterns of segmentation that unfold during later stages of embryogenesis (Akam, 1987; Ingham, 1988; Lawrence, 1992). The *Drosophila* segmentation genes fall into three broad classes that act sequentially: gap genes specify units of several segments in width, pair-rule genes (PRGs) specify parasegmental units, followed by segment polarity genes, which define the anterior and posterior compartments of each segment (Gilbert, 2010; Nüsslein-Volhard et al., 1987; Nüsslein-Volhard and Wieschaus, 1980). In recent years, the advent of molecular genetic approaches in diverse insects has enabled comparative studies of regulatory mechanisms functioning in other species, usually using the *Drosophila* model as a starting point (Abzhanov et al., 1999; Angelini et al., 2005; Liu and Kaufman, 2005b; Peel et al., 2005; Williams and Nagy, 2017). These types of comparative studies of segmentation genes have revealed that they are present in genomes throughout Insecta, as well as more distant arthropods, but the

morphological events leading to the formation of segments in most arthropods differ significantly from that in *Drosophila* (Davis and Patel, 2002; Peel et al., 2005). *Drosophila* are long germ insects (Krause, 1939) in which all segments are specified more or less simultaneously in the blastoderm ("simultaneous segmentation" (Davis and Patel, 2002). In contrast, other arthropods and most insects add posterior segments sequentially after the blastoderm stage, during which only a small number of anterior segments are specified ("sequential segmentation" (Davis and Patel, 2002; Peel et al., 2005). Sequentially segmenting arthropods can be subdivided into short and intermediate germ band developers, based upon the number of segments specified at blastoderm (Davis and Patel, 2002).

The studies summarized above reflect two paradoxes: first, the presence of morphological segments is ubiquitous but the way in which these segments develop varies, suggesting greater constraint on segment existence than the mechanisms leading to their formation. Second, genes utilized in the most derived mode of segmentation, long germ development seen in *Drosophila*, are present in animals that form segments by an alternate route, and so must be at least to some extent, re-purposed, a prime example of Developmental System Drift (True and Haag, 2001). In *Drosophila*, a set of nine PRGs interact to establish repeated segments along the anterior-poster axis. Most *Drosophila* PRGs are expressed in striped patterns - 'PR-stripes' - at the blastoderm stage in the primordia of the alternate segmental regions missing in mutant embryos (Akam, 1987; Lawrence, 1992). PR-like expression of PRG orthologs has been reported in a number of arthropods, but their functions have

been analyzed only in a handful insects (Choe et al., 2006; Liu and Kaufman, 2005a; Mito et al., 2007; Nakao, 2015; Rosenberg et al., 2014; Wilson and Dearden, 2012).

In the flour beetle, *Tribolium castaneum* (*Tribolium, Tc*), which is a short germ insect, though expressed in striped patterns, knockdowns of *even-skipped (eve)*, *odd-skipped* (*odd)* and *runt* (*run)* produced truncated phenotypes instead of PR-like phenotypes (Choe and Brown, 2009; Choe et al., 2006). In addition, unlike *Drosophila*, *Tc-odd* and *-eve* were shown to be part of a wave-like clock mechanism, responsible for addition of segments sequentially during germ band elongation, similar to the segmentation clock seen in vertebrates (El-Sherif et al., 2012; Sarrazin et al., 2012). In hemimetabolous *Gryllus bimaculatus* (*Gryllus*) and *Oncopeltus fasciatus* (*Oncopeltus*), *eve* RNAi caused disorganized and/or truncated thorax and abdomen (Liu and Kaufman, 2005a; Mito et al., 2007). In *Gryllus*, after *eve* knockdown, PR-like defects were detected only in the anterior region (Mito et al., 2007). These findings revealed that, in these sequentially segmenting species, some PRG orthologs function differently, at least during posterior germ band elongation. Surprisingly, in two model species in Hymenoptera, whose long germ segmentation mode is thought to have evolved independently from *Drosophila*, PRG orthologs still show functional divergence: morpholino knockdown of *eve*, *odd* and *h* resulted in loss of abdomen in *Nasonia vitripennis* while *eve*, *ftz* and *run* are required for maternal patterning in *Apis mellifera* (Rosenberg et al., 2014; Rosenberg et al., 2009; Wilson and Dearden, 2012).

Here, we studied the expression and function of the cohort of nine *Drosophila* PRG orthologs in the intermediate germ beetle, *Dermestes maculatus.* Eight of the

nine are expressed in stripes in blastoderm stage embryos and in the elongating germ band. PR-like defects were seen for *sloppy paired* (*slp*) RNAi knockdown, indicating it functions exclusively in PR patterning, as previously reported after *Dmac-paired* (*prd*) knockdown (Chapter 2). RNAi knockdown of *Dmac-eve*, *odd* and *run* resulted in truncated embryos, indicating a role in germ band elongation, as was seen in *Tribolium* (Choe et al., 2006). PR-like defects in moderate knockdown of these genes demonstrated *Drosophila*-like roles in PR-patterning. Milder PR-like phenotypes were observed for *fushi tarazu* (*ftz*) and *hairy* (*h*) knockdown, impacting formation of the abdomen more broadly. Simultaneous knock down of *prd* and *slp* resulted in elongated germ bands with no Engrailed (En) stripes and lacking segment borders, indicating that germ band elongation and PR patterning are decoupled processes. Patterns of apoptosis seen after knockdown of each PRG ortholog generally prefigured the observed phenotypes, seen long ago for *Drosophila* PR phenotypes (Ingham et al., 1985; Magrassi and Lawrence, 1988), although we also observed disruptions in mitotic patterns. Based upon this, we propose that PRGs, in addition to regulating specific target genes, have an evolutionarily conserved function in promoting cell viability.

4.3 Methods and materials

Animal rearing and PRG ortholog isolation

A *D. maculatus* colony has been maintained in our lab for over three years, as described (Chapter 2 and 3). 0-1 day AEL embryos (30 °C) were homogenized in TRIzol (Invitrogen) using a disposable RNase-free plastic tissue grinder (Fisher

Scientific). Total RNA was extracted using a Qiagen RNeasy mini kit (Qiagen). After genomic DNA removal with RNase-free DNase (Qiagen), total RNA was purified using RNeasy spin columns. RNA quality and concentration were determined by spectrophotometry and gel electrophoresis. Embryonic cDNA was prepared using a QuantiTect Reverse Transcription kit (Qiagen). Forward and reverse degenerate primers targeting conserved protein motifs were either designed by ourselves or from previous literature (Damen et al., 2005; Damen et al., 2000); primer sequences available upon request). Motifs were: ***eve***, Homeodomain; ***odd***, Zn-finger double domain and RNA helicase (UPF2 interacting domain); ***run***, Runt domain; ***h***, basic helix-loop-helix; ***slp***, fork head domain; ***opa***, Zn-finger domain; ***ftz***, homeodomain (Ftz-specific N-terminal arm and conserved region QIKIWFQN); ***ftz-f1***, (conserved motifs in first Zn-finger, FF1 box and AF2 domain). After a gene-specific region had been isolated by degenerate PCR, 3' RACE was performed to isolate additional gene sequence using the FirstChoice RLM-RACE kit (Ambion). Generally, two rounds of PCR were performed to increase specificity. Additional amplification was performed if necessary to isolate sequence at least to the stop codon and usually including 3'UTR. To ensure that the separately isolated regions correspond to a single gene, gene specific primers including the regions isolated by both degenerate PCR and 3' RACE were used to amplify cDNA and products were sequenced. Figure 4-1 shows the schematic representation of the genes. Restriction enzyme cutting sites were also included at the 5' end of both primers for insertion into KS vectors. Constructs were then used as templates for *in situ* probe and dsRNA synthesis. All gene sequences are shown in Appendix II.

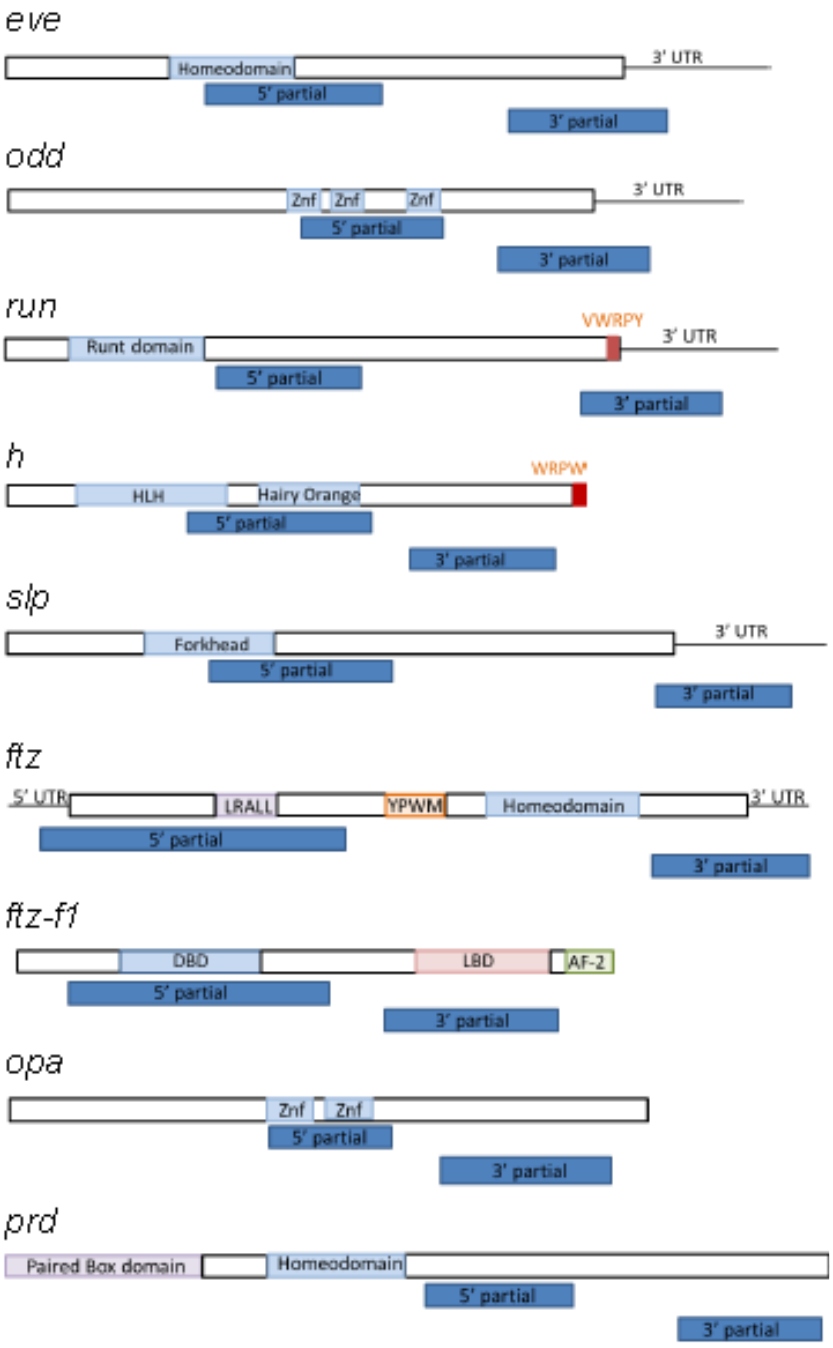

Figure 4-1. **Gene regions targeted by *Dmac*-PRG ortholog RNAi.** Schematic drawings of genes examined in this study (not to scale). Conserved domains/motifs are shown for each *Dermestes* PRG ortholog. Two dsRNAs targeting non-overlapping regions were used to ensure specificity (dark blue boxes). 5' partial dsRNAs targeted upstream coding regions, while 3' partial dsRNAs targeted downstream coding region, sometimes including partial 3' UTR. For each gene knockdown, experiments using two dsRNAs gave very similar phenotypes, including defective patterns shown in hatched larvae, though the penetrance and severity varied.

Phylogenetic analysis

To identify PRG orthology, phylogenetic analysis was performed as described in (Rosenberg et al., 2014). Homologous protein sequences from other species were trimmed to align with the partial *D. maculatus* PRG ortholog sequence we isolated. Multiple sequence alignment was carried out using MUSCLE (Edgar, 2004). Phylogenetic analysis was carried out using RAxML at CIPRES science gateway (http://www.phylo.org/index.php/portal/) (Miller, 2010; Stamatakis, 2006; Stamatakis et al., 2008). Trees were visualized using Dendroscope (Huson and Scornavacca, 2012).

RNAi

RNAi was carried out according to Chapter 3. Two non-overlapping target regions were chosen for each gene to ensure effects were specific (Figure 4-1, dark blue boxes). *gfp* dsRNA was used as negative control. DNA templates for dsRNA synthesis were amplified from above KS constructs with gene specific primers containing T7 promoter sequence at both 5' ends. Complementary ssRNA was synthesized using MEGAscript T7 Transcription kit (Ambion) and then annealed to make dsRNA. After ethanol precipitation, dsRNA was dissolved in injection buffer (0.1 mM NaH_2PO_4, 5 mM KCl, pH 6.8). For parental RNAi, ~2 µl of 3 µg/µl was injected into 8-10 females for each dsRNA. After ~24 hr recovery at 30 °C, injected females were mated with uninjected young males for 1 day before embryo collection. Data reported in Table 4-1 were compiled from embryos laid on the 3rd and the 4th day after dsRNA injection, as frequency of phenotypes decreased dramatically after

the 5th day (see also Chapter 2). For embryonic RNAi, pre-blastoderm stage embryos were injected. After injection, embryos were held at 30 °C until hatching.

Gene expression and phenotypic analysis

Analysis of gene expression patterns was carried out following previously discribed protocols (Chapter 2). Phenotypic analysis of embryos and larvae was carried out as described (Chapter 3). For antibody staining and SYTOX Green nuclear staining, after eggshell removal, fixed embryos were incubated in primary antibody at 4°C overnight (mouse 4D9 anti-Engrailed 1:5 (Developmental Studies Hybridoma Bank); rabbit anti-cleaved *Drosophila* Dcp-1 1:100 (Cell signaling, #Asp216); rabbit anti-phospho Histone H3 (PH3) 1:200 (EMD Millipore, #06-570) and secondary antibody at room temperature for 2 hours (biotinylated anti-mouse antibody 1:500 (Vector Laboratories; #BA-9200); biotinylated goat anti-rabbit 1:200 (Vector Laboratories; #BA-1000); Alexa Fluor 488 goat anti-rabbit 1:200 (Thermo Fisher Scientific; #A11008). SYTOX Green staining was performed by 20 min room temperature incubation in SYTOX Green 1: 1000 (Thermo Fisher Scientific; #S7020). Blocking with 1% BSA and 1% NGS in PBS for one hour at room temperature was included for Dcp-1 and PH3 antibody staining. Embryos were visualized under microscopy (Olympus SZX12, Leica SP5X, Leica 501007, Zeiss SteREO Discovery. V12 or Zeiss Axio Imager. M1). Image stacking used CombineZP and merged images were prepared using Photoshop if necessary. For analysis of ovarian morphology, ovaries were dissected from injected females and transferred to cold PBS immediately. After 20 min fixation in 4% PFA and several

PBS/PBST washes, ovaries were incubated in Alexa Fluor 488 phalloidin 1:200 (Life technologies, #A12379) at 4 °C overnight. Ovaries were then placed on slides in 70% glycerol with DAPI and visualized with Leica 501007 microscopy.

qPCR for knockdown validation and gene expression examination

To verify gene knockdown after RNAi, 0-6 hour AEL embryos from dsRNA-injected females were collected on the 3rd day after injection and aged for another 2 hours at 30 °C to reach late blastoderm to late germ band stages (Chapter 2) when PRGs are relatively highly expressed. RNA was extracted as described above. cDNA synthesis was performed using an iScript cDNA synthesis kit (BioRad) following manufacturer's instructions. 1 µg of total RNA was used for each reverse transcription reaction. To avoid amplifying dsRNA instead of endogenous mRNA transcripts, primers used for amplification did not completely overlap the RNAi target regions. All amplicons' sizes were below 200 bp. Two reference genes, COI and 16s rRNA, were included when performing qPCR reactions to normalize Ct values. A 1:10 dilution of cDNA generated from 20 µl reverse transcription reaction was used as template for qPCR using a Roche LightCycler 480 with SYBR Green Master Mix with settings: 95 °C incubation, 10 min; 60 °C annealing temp. Abs Quant/Fit Points analysis was used to calculate Ct value. To calculate relative expression of the gene of interest in pRNAi offspring to *gfp* pRNAi offspring, we used the $2^{-\Delta\Delta Ct}$ method. For each RNAi knockdown, three biological replicates were performed and mean and standard error were calculated.

4.4 Results

4.4.1 Dermestes *PRG orthologs show PR-like expression with distinct features*

Dermestes maculatus orthologs of *Drosophila* pair-rule genes (PRGs) were isolated by degenerate PCR and 3' RACE. Phylogenetic analysis demonstrated that each *Dermestes* PRG ortholog clustered closely with its *Tribolium* counterpart (Figure 4-2). Expression of each gene was examined by *in situ* hybridization to staged *Dermestes* embryos.

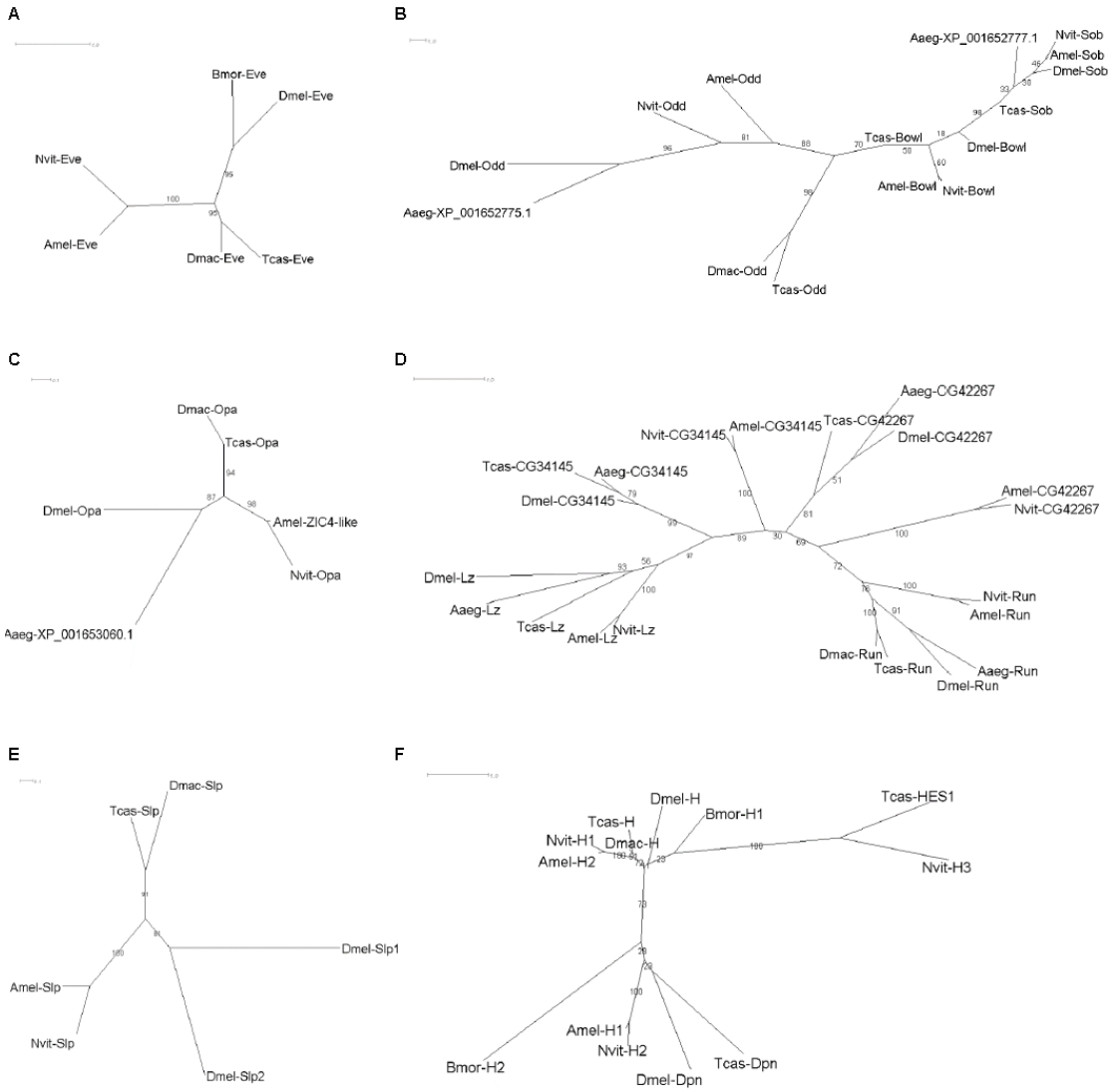

Figure 4-2. Phylogenetic analyses of isolated *Dermestes* PRG orthologs. Phylogenetic analyses of *eve* (A), *odd* (B), *opa* (C), *run* (D), *slp* (E) and *h* (F) protein sequences. Isolated individual *Dermestes* PRG orthologs closely grouped with counterparts in *Tribolium*. Bootstrap values (1,000 replicates) are shown adjacent to branches. Abbreviations: *Dmac*: *Dermestes maculatus*; *Dmel*: *Drosophila melanogaster*; *Tcas*: *Tribolium castaneum*; *Nvit*: *Nasonia vitripennis*; *Amel*: *Apis mellifera*; *Bmor*: *Bombyx mori*; *Aaeg*: *Aedes aegypti*.

Dmac-eve, -odd and *-run* striped expression arose at the blastoderm stage with primary stripes emerging sequentially from cap-like expression in the posterior region. Stripes arose in an anterior-to-posterior order (Figures 4-3 and 4-4). As new stripes emerged posteriorly, the more anterior stripes refined (Figure 4-4A-D, G-J, M-P). Prior to gastrulation, there were at least four primary stripes of each of these genes (Figure 4-4D, J, P). During gastrulation, and as the germ band elongated, posterior stripes were added sequentially while anterior stripes faded gradually (Figures 4-3 and 4-4).

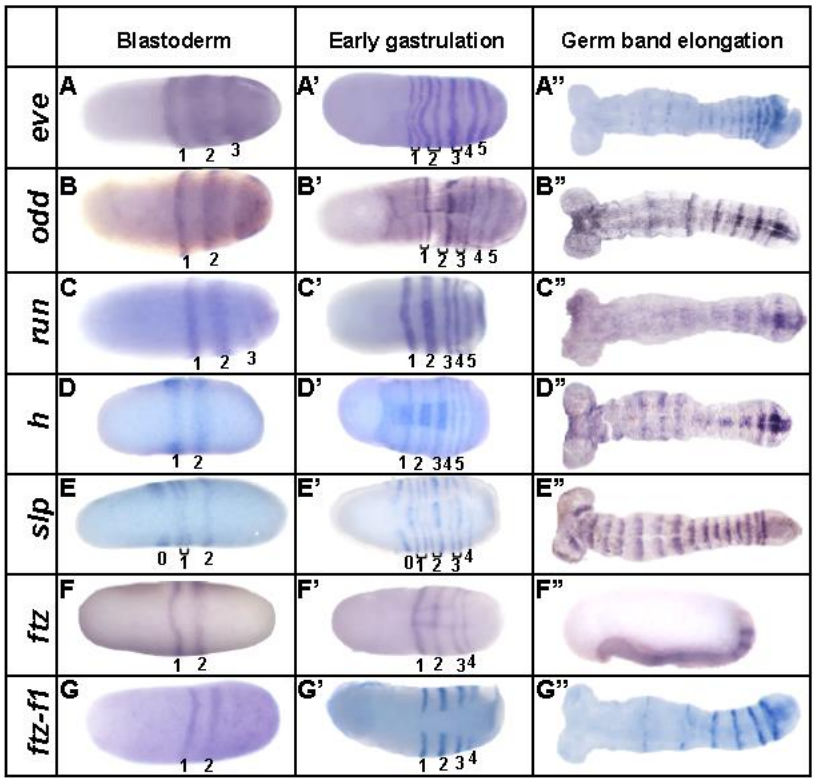

Figure 4-3. *Dermestes* PRG orthologs are expressed in stripes. *Dermestes* embryos at blastoderm, early gastrulation, and germ band elongation stages are shown to represent developmental stages of interest. Embryos at early gastrulation were identified by the appearance of the ventral furrow using SYTOX Green (not shown). (A) The first *Dmac-eve* primary stripe has refined as a transverse stripe in the center of this blastoderm stage embryo. The second *Dmac-eve* primary stripe is fuzzy and broad. A third *Dmac-eve* stripe is resolving from cap-like expression in the posterior end. (A') At the onset of gastrulation, 5 *Dmac-eve* primary stripes have emerged. The anterior three have split into secondary stripes (brackets). (A'') *Dmac-eve* stripes fade in anterior segments during germ band elongation. Strong expression is seen in posterior segments. (B) 2 *Dmac-odd* primary stripes are clearly detectable, along with cap-like expression in the posterior. (B') By early gastrulation, 5 primary stripes and 3 intercalated secondary *Dmac-odd* stripes have emerged. (B'') *Dmac-odd* primary and secondary stripes alternate in intensity in growing germ band, with fading anterior expression. (C) 3 *Dmac-run* stripes have arisen in this blastoderm stage embryo. Weak cap-like expression is seen in the posterior end. (C') In total, 5 *Dmac-run* stripes have emerged at early gastrulation, with the first and the second ones showing broader expression. (C'') During germ band elongation, anterior *Dmac-run* expression fades as weak expression is seen at the posterior end of the germ band. (D) Blastoderm stage embryo showing 2 *Dmac-h* stripes. (D') An embryo at early gastrulation with at least 5 *Dmac-h* primary stripes. The second primary stripe has split into two thin secondary stripes. (D'') Strong *Dmac-h* stripes are seen in the most posterior two segments and faint *Dmac-h* expression is seen in the anterior as the germ band elongates. (E) 3 *Dmac-slp* stripes in a blastoderm stage embryo. The most

anterior stripe marks the future antennae, thus is referred to as "stripe 0". Secondary stripes has emerged for *Dmac-slp* stripe 1 (bracket). (E') Stripe 0, 4 *Dmac-slp* primary stripes and 3 secondary stripes present at the beginning of gastrulation. (E'') Segmental *Dmac-slp* stripes show equal intensity with fuzzy anterior borders in elongating germ band. (F) A blastoderm stage embryo with two *Dmac-ftz* stripes. (F') 4 *Dmac-ftz* stripes at early gastrulation stage. (F'') Strong *Dmac-ftz* expression is detectable in posterior segments. (G) Lateral *Dmac-ftz-f1* expression in 2 stripes in a blastoderm stage embryo. (G') 4 *Dmac-ftz-f1* stripes are clearly visible but not expressed in the ventral furrow. (G'') A growing germ band stage embryo with fading *Dmac-ftz-f1* expression in the anterior. Strong striped *Dmac-ftz-f1* expression appears in the posterior. All embryos are oriented: anterior, left.

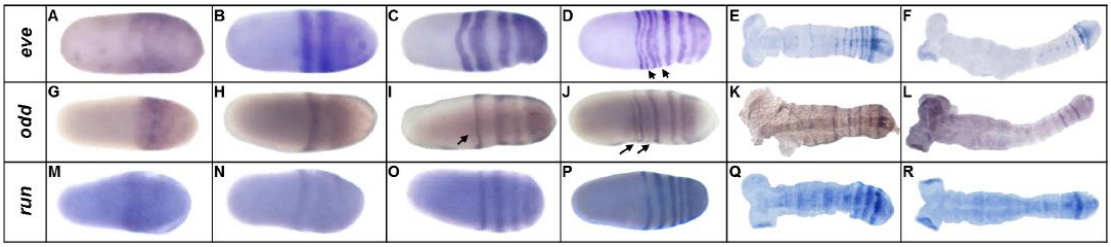

Figure 4-4. Expression of *Dmac-eve, odd,* and *run*. *In situ* hybridization was carried out for *Dmac-eve* (A-F), *Dmac-odd* (G-L) or *Dmac-run* (M-R). Embryos from early blastoderm to late germ band elongation are shown; anterior, left. (A) Initial *Dmac-eve* expression in the posterior half of the embryo. (B) The first *Dmac-eve* stripe has settled in the center, and the second has resolved from the posterior cap-like expression. (C) 3 *Dmac-eve* primary stripes and posterior cap-like expression. (D) Embryo at late blastoderm stage with 4 *Dmac-eve* primary stripes and an emerging fifth stripe. Arrows indicate splitted secondary stripes. (E) Mid-germ band stage embryo showing fading *Dmac-eve* stripes in the anterior. (F) Strong *Dmac-eve* in newly patterned posterior segments in late germ band stage embryo. (G) *Dmac-odd* early expression in the posterior. (H) The first *Dmac-odd* primary stripe has appeared and weak posterior expression is visible. (I) Embryo with 3 primary *Dmac-odd* stripes and posterior cap-like expression. Arrow shows a weak secondary stripe anterior to the first primary stripe. (J) 2 weak *Dmac-odd* secondary stripes (arrows) have emerged while the fourth primary stripe is resolving from the posterior. (K) Growing germ band with *Dmac-odd* primary and secondary stripes. Note that intensity alternates between primary and secondary stripes. (L) Extended germ band with *Dmac-odd* stripes in posterior segments. (M) *Dmac-run* early broad expression. (N) Embryo showing the first stripe and weak posterior expression of *Dmac-run*. (O) 3 *Dmac-run* stripes and posterior cap-like expression. (P) 4 *Dmac-run* stripes and an emerging fifth stripe. (Q) Mid-germ band stage embryo with faint anterior expression and 3 posterior stripes. (R) Late-germ band stage embryo with one clear posterior *Dmac-run* stripe.

For *Dmac-eve,* secondary segmental stripes appeared by splitting of the primary stripes (Figure 4-4D, arrows). For *Dmac-odd*, one secondary stripe was added *de novo* anterior to each primary stripe (Figure 4-4I, J, arrows). The intensity alternated between pairs of *Dmac-odd* secondary and primary stripes throughout late blastoderm and germ band elongation stages with secondary stripes remaining weaker than primary stripes (Figure 4-4J-L). In contrast to both *eve* and *odd,* secondary stripes were not observed for *Dmac-run* (Figure 4-3C', C''; 4-4O-R). Dot-like expression of *Dmac-run*, likely in the central nervous system (CNS), was detected in fully elongated germ bands (not shown).

In contrast to *eve, odd* and *run*, *Dmac-h* was first observed broadly in the center of the embryo, with no obvious posterior cap-like expression (FA). Two primary stripes resolved from this broad expression (Figures 4-5B; 4-3D). Weak expression at the anterior edge of the head lobes was also seen in these early stage embryos (FB). Additional stripes were added sequentially from the posterior half; at least five primary stripes were detected at early gastrulation (FD). Secondary stripes arose by splitting of most primary stripes (Figure 4-3D', stripe 2, 3). As the germ band elongated, additional stripes emerged from the posterior end (FE, F). The striped pattern was maintained through mid-germ band stages, but then faded quickly (Figure 4-3D''; 4-5G). As in *Tribolium*, expression of *h* was also detected along the midline (FG, (Aranda et al., 2008).

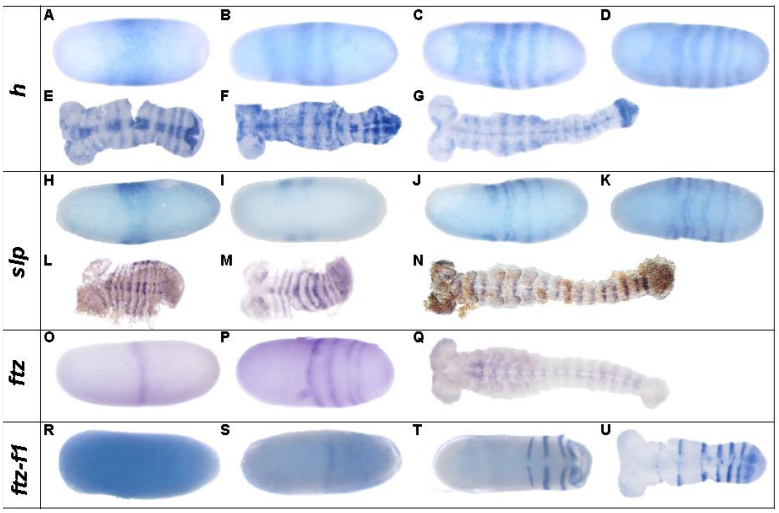

Figure 4-5. Expression of *Dmac-h, slp, ftz* and *ftz-f1*. *In situ* hybridization was carried out for *Dmac-h* (A-G), *Dmac-slp* (H-N), *Dmac-ftz* (O-Q), or *Dmac-ftz-f1* (R-U). Embryos from early blastoderm to late germ band elongation are shown; anterior, left. (A) *Dmac-h* is initially expressed in a broad region in the center then (B) resolves into stripes. (C-F) Posterior stripes are added sequentially at both blastoderm and germ band elongation stages. (G) *Dmac-h* striped expression fades during germ band elongation and midline expression appears in late germ band stages. (H) Lateral *Dmac-slp* striped expression in a broad central stripe. (I) Two distinct stripes emerge from this broad region. (J-M) Posterior *Dmac-slp* stripes arise from the posterior and secondary stripes appear in the anterior. (N) Striped expression of *Dmac-slp* persists until late germ band stage. Note that the gold color in this embryo is background from the yolk. (O) *Dmac-ftz* is first detectable as a single, central stripe. (P) 4 *Dmac-ftz* stripes were present prior to gastrulation. (Q) *Dmac-ftz* CNS expression in late germ band stages. (R) Uniform *Dmac-ftz-f1* expression in an early embryo. (S) One *Dmac-ftz-f1* stripe in the center. (T) *Dmac-ftz-f1* stripes during gastrulation. Note that expression was absent from the ventral furrow. (U) Embryo with 6 well-defined *Dmac-ftz-f1* stripes and a newly arising 7th stripe at the posterior.

Similar to *Dmac-h, Dmac-slp* was first expressed in a broad stripe in the center of embryo, and later resolved into two stripes with stronger expression laterally (Figure 4-5H, I). The first stripe remained strong only on the lateral sides, later contributing to expression in the head lobes. Secondary striped expression appeared anterior to the first primary stripe, as a new primary stripe emerged posterior to it (Figure 4-3E). Additional stripes appeared sequentially from the posterior region of

the embryo and intercalated secondary stripes appeared between primary stripes, generating seven *Dmac-slp* stripes (four primary, except stripe 0 in antennae) at early gastrulation (Figure 4-3E'; 4-5J, K). Unlike many other *Dmac*-PRG orthologs, anterior *Dmac-slp* stripes remained strongly expressed in each segment during germ band elongation, although they became broader with slightly fuzzy anterior borders (Figure 4-3E''; 4-5L-N). There was no obvious intensity difference among stripes in elongated germ bands.

Dmac-ftz was first expressed as a single stripe in the center of the embryo (Figure 4-5O). A second, clear stripe appeared next, posterior to the first stripe (Figure 4-3F). Later, more stripes were added sequentially from the posterior half of the embryo. In total, there were four stripes detectable at early gastrulation, with the first stripe appearing most intense (Figure 4-3F'). Posterior stripes appeared and anterior striped expression became weak and fuzzy as the germ band elongated. At mid- to late germ band stages, strong striped expression was detectable only in the most posterior segments (Figure 4-3F''). In later stage embryos, when segments were well established, *Dmac-ftz* was expressed segmentally, likely in the CNS (Figure 4-5Q). No secondary segmental striped expression was detected throughout early embryogenesis. *Dmac-ftz-f1*, whose ortholog encodes an Ftz cofactor in *Drosophila*, was first expressed uniformly in pre-blastoderm stage embryos (Figure 4-5R); this early ubiquitous expression of *ftz-f1* is conserved in *Drosophila* and *Tribolium* (Heffer et al., 2012; Yussa et al., 2001). Maternally deposited *Dmac-ftz-f1* was also confirmed by RT-PCR (not shown). Later, expression of *Dmac-ftz-f1* was similar to that of *Dmac-ftz* with one single stripe appearing first and posterior stripes arising

sequentially from the posterior half of the embryo, as ubiquitous expression faded (Figures 4-5S and 4-3G). Four *Dmac-ftz-f1* stripes were present at early gastrulation (Figure 4-3G'). These stripes differed from other PRG stripes in that no expression was detected on the dorsal side or in the ventral furrow region (Figure 4-3G'). Striped expression persisted through gastrulation, but gradually faded in an anterior-to-posterior fashion as the germ band elongated (Figure 4-3G''; 4-5T, U). *Dmac-ftz-f1* was also expressed in the distal leg tips and head appendages in late stage embryos (not shown). *Dmac-odd-paired* (*opa*) showed only marginal expression with faint segmental-like stripes in the embryo rudiment during gastrulation (not shown).

In sum, except for *opa*, *Dermestes* PRG orthologs were expressed in primary PR like-patterns, with stripes added sequentially from the posterior. For each of them, there were four or five primary stripes established at the onset of gastrulation. For several genes (*eve, odd, h, slp*), secondary stripes developed later, either by splitting (*eve* and *h*) or *de novo* (*odd* and *slp*). Additional stripes were added from the posterior during germ band elongation, with more anterior stripes fading concurrently, except for *Dmac-slp*, which maintained segmental stripes throughout the germ band stages.

4.4.2 *Knockdown of* Dmac-eve, -odd *or* -run *reveals dual roles in segment formation*

Parental RNAi (pRNAi) was used to test the function of *Dmac*-PRG orthologs. Knock down (verified by qRT-PCR, Figure 4-6) is expected to vary in individual embryos, generating phenocopies of an allelic series, allowing us to examine defects in both hatched (less severely affected) and unhatched (more severely affected) offspring. Average egg yield, hatch rate and penetrance after each

knockdown are shown in Table 4-1. *Dmac-eve*, *-odd* and *-run* knockdown did not affect egg yield; however, the hatch rates were decreased compared to the control group (*gfp* dsRNA injection; Table 4-1). A graded series of defects were observed in hatched larvae after these knockdowns.

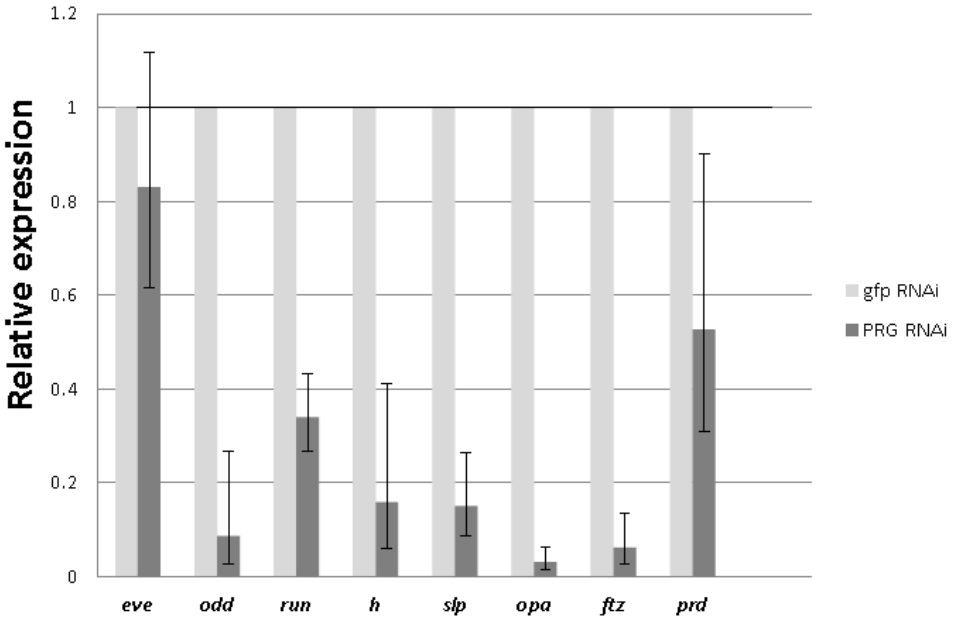

Figure 4-6. Validation of knockdown using qPCR. *Dermestes* embryos between blastoderm and late germ band stages from RNAi treated females were collected for qPCR analysis. Expression levels of the target gene, as indicated, in control group (*gfp* RNAi) was normalized to 1.0 (light gray bars). Relative expression levels of target genes in experimental groups (PRG ortholog RNAi) was calculated using the $2^{-\Delta\Delta Ct}$ method (dark gray bars). Three biological replicates were carried out for each RNAi. Error bars indicate standard error.

Table 4-1. Summary of egg yield, hatch rate and penetrance after *Dermestes* PRG RNAi. Embryos were collected daily starting on the 3rd day after injection for four consecutive days. Here we present data from the first two collections (the 3rd and the 4th day after injection) as it includes the majority of hatched offspring with defects. For each PRG RNAi, two dsRNA targeting different regions (5' and 3') were used to ensure RNAi effect specificity.

	Average daily egg yield per female	Hatch rate	Penetrance (hatched larvae with segmentation defects)
gfp dsRNA control 1st	24	83.7% (241/288)	0% (0/241)
gfp dsRNA control 2nd	33.7	46.6% (220/472)	0% (0/220)
eve 5' dsRNA	33.5	16.0% (96/602)	51.0% (49/96)
eve 3' dsRNA	44.2	24.0% (212/884)	12.7% (27/212)
odd 5' dsRNA	39.7	11.8% (84/714)	20.2% (17/84)
odd 3' dsRNA	40.2	13.7% (110/803)	23.6% (26/110)
run 5' dsRNA	32.0	10.2% (72/703)	48.6% (35/72)
run 3' dsRNA	44.3	23.7% (189/797)	29.6% (56/189)
h 5' dsRNA	18.25	46.6% (136/292)	0% (0/136)
h 3' dsRNA	40.0	27.2% (239/879)	12.6% (30/239)
slp 5' dsRNA	35.1	14.6% (113/773)	44.2% (50/113)
slp 3' dsRNA	32.2	14.2% (55/386)	85.5% (47/55)

For *Dmac-eve*, defects including abnormalities within segment(s) and/or fusion at segmental boundaries were observed for one or more segments in different larvae (Figure 4-7B). Defects occurred frequently at the boundaries between T3/A1, A2/A3, A4/A5, A6/A7, A8/A9 and neighboring regions, suggestive of pair-rule-like patterning (Figure 4-7B'). Similarly, defective segment(s) and/or fused adjacent segments were observed after *Dmac-odd* knockdown (Figure 4-7C). Fusions after *Dmac-odd* RNAi were generally milder than those seen for *Dmac-eve* knockdown, with loss of only portions of non-pigmented regions evident. Interestingly, pigmented stripes sometimes were disrupted by non-pigmented tissue (Figure 4-8A, arrow). In other cases, the T2 leg was deformed with duplicated claw or thickened paddle-like structures at the tip (Figure 4-8B). These are reminiscent of *Drosophila odd* mutants, which display mirror-image duplications (Coulter and Wieschaus, 1988). Overall, for *Dmac-odd*, defects occurred most frequently in T2, A1, A5, A7 segments (Figure 4-7C'). *Dmac-run* knockdown produced defects including segment fusions and deletions in hatched larvae (Figure 4-7D), sometimes accompanied by a deformed leg with duplicated claw or thickened structure (Figure 4-7D, arrow). Extra pigmented regions were also observed in larvae, indicating partial segmental duplication (not

shown). Defects occurred frequently at T2, A1, A5, A7, A9 and neighboring regions (Figure 4-7D').

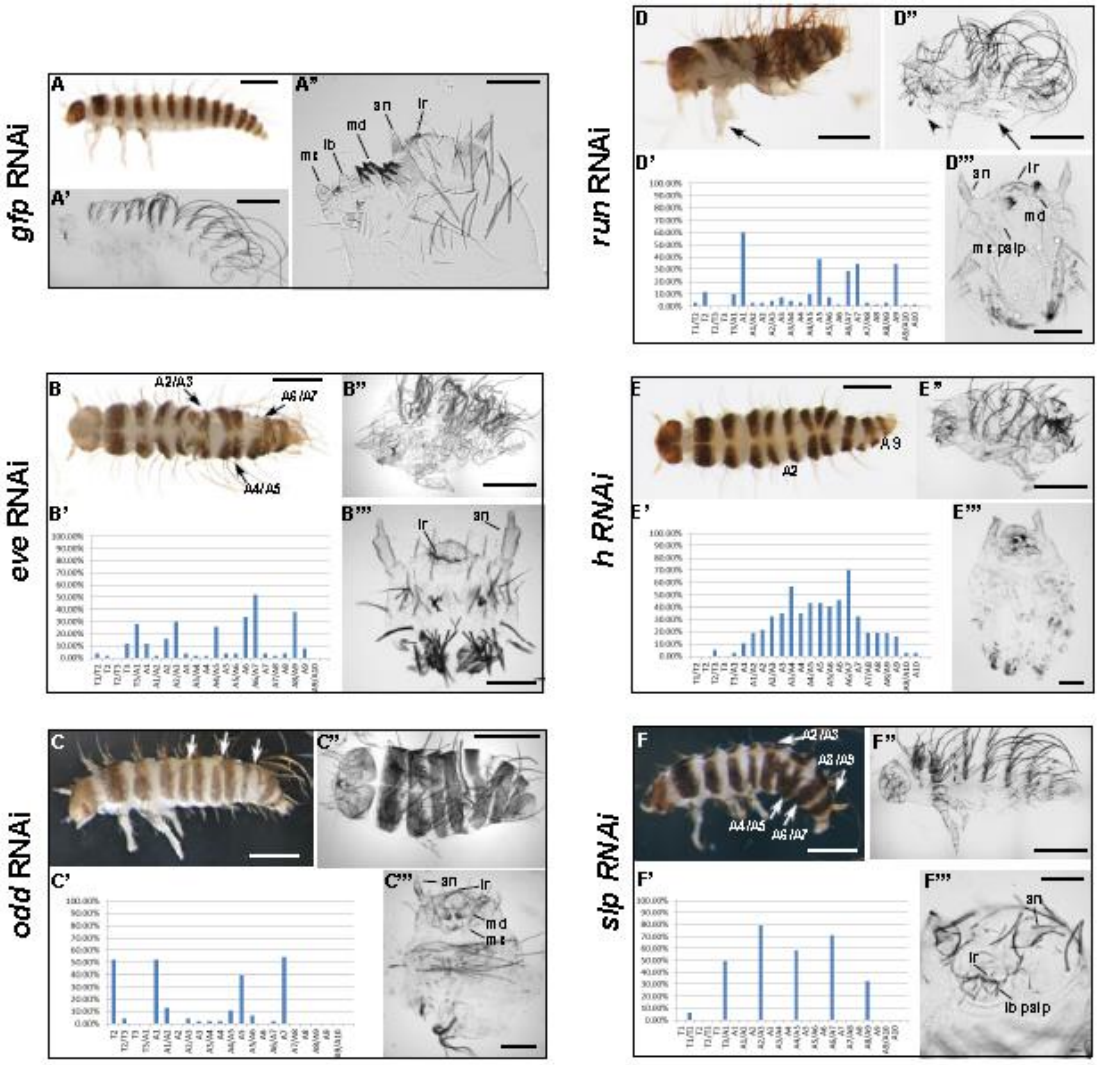

Figure 4-7. Truncated embryos and pair-rule defects after *Dermestes* PRG ortholog knockdowns. Offspring of pRNAi for control *gfp* or *Dmac*-PRG ortholog, as indicated. The second panel in each composite indicates (Y-axis) the frequency of defects seen in (X-axis) hatched larval segments, anterior to posterior, as indicated. (A, A') Control *Dermestes* larvae have 3 thoracic segments and 10 abdominal segments. (A) Hatched larva with pigmented stripes on head and every trunk segment. (A') Cuticular preparation of unhatched larva without pigmentation. (A'') Head close-up shows antennae, labrum, mandibles, maxillae and labium. (B-B'') <u>*Dmac-eve* pRNAi.</u> (B) Moderately affected hatched larva with multiple fused segments (arrows). (B') T3/A1, A2/A3, A4/A5, A6/A7, A8/A9, and neighboring regions were most frequently affected. (B'') Unhatched larva with shortened body length. (B''') Spherical cuticle of a severely affected unhatched larva consists of only head, with antenna and labrum. (C-C''') <u>*Dmac-odd* pRNAi</u>. (C) Hatched larva with

only two pairs of legs and several partially fused segments (arrows). (C') T2, A1, A5, and A7 were most commonly affected. (C'') Unhatched larva with short body and fewer segments. (C''') Severely affected unhatched offspring with head and some thoracic structure. (D-D''') *Dmac-run* pRNAi. (D) Hatched *Dmac-run* pRNAi larva has fewer segments and a deformed leg with duplicated claw (arrow). (D') T2, A1, A5, A7, A9, and adjacent regions most frequently affected. (D'') Unhatched, shortened larva with duplicated claw (arrow) and leg-like maxilla (arrowhead). (D''') 'Head only' cuticle lacking partial maxillary and labium structures. (E-E''') *Dmac-h* pRNAi. (E) Hatched larva with irregular segmentation between A2 and A9. (E') Regions between A1 and A9 most frequently affected. (E'', E''') Unhatched larva with head and thoracic segments, but little or no segmented abdomen. (F-F''') *Dmac-slp* pRNAi. (F) Hatched larva with several fused adjacent segments (arrows). (F') T3/A1, A2/A3, A4/A5, A6/A7, and A8/A9 most frequently affected. (F'') Unhatched larvae with fewer trunk segments and only one pair of legs. (F''') Unhatched larval head missing mandibles and maxillae. Scale bars represent 100 µm for A'', B''', C''', D''', E''' and F''', or 500 µm for all other panels.

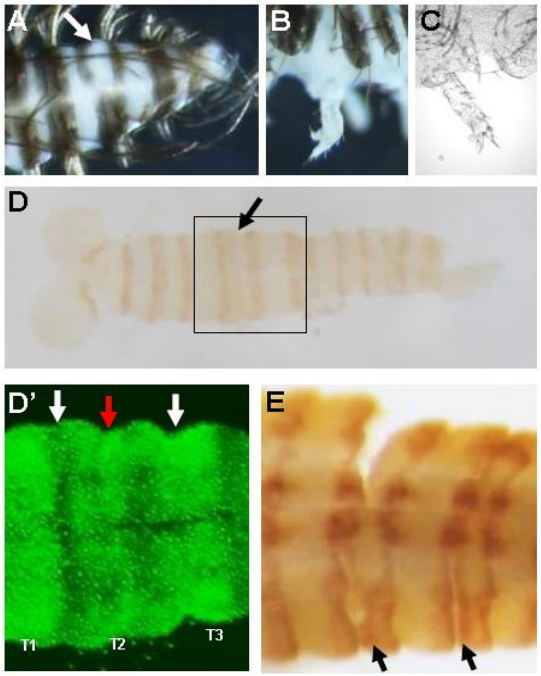

Figure 4-8. *Dmac-odd* RNAi results in duplication phenotypes. Offspring of *Dmac-odd* dsRNA-injected females were analyzed. (A) Hatched larva with pigmented stripe disrupted by non-pigmented tissue (arrow). (B) Duplicated claw of T2 in hatched larva. (C) Duplicated claw of T2 leg in unhatched larva. (D) En expression in germ band elongation stage embryo. Arrow indicates an extra weak En stripe between T1 and T2 stripes. (D') SYTOX Green staining of the boxed region in (D). White arrows indicate segmental boundaries. Red arrow shows an extra

segmental furrow. (E) Arrows show clear extra En stripes in embryo after germ band retraction.

Phenotypes observed in unhatched offspring were more severe, as would be expected. For *Dmac-eve* knockdown, moderately affected unhatched larvae included some gnathal and trunk structures, but the overall body length was dramatically shortened (Figure 4-7B''). The most severely affected ones were composed of only a small, spherical anterior structure with antennae and labrum, lacking mandible, maxilla or labium, referred to as 'head-only' (Figure 4-7B'''). After *Dmac-odd* knockdown, moderately affected unhatched larvae had significantly shortened body lengths with fewer trunk segments (Figure 4-7C''). Severely affected, unhatched larvae had head, one or two thoracic segments, and drastically shortened, asegmental posterior trunks; the labium seemed to be missing (Figure 4-7C'''). As in hatched larvae, deformed T2 legs or duplicated claws were sometimes observed (Figure 4-8C). Moderately affected unhatched larvae after *Dmac-run* knockdown had significantly shortened body length with fewer trunk segments (Figure 4-7D''). Occasionally, maxillae-to-leg-like transformation was observed (Figure 4-7D'', arrowhead). Duplicated claws were found (Figure 4-7D'', arrow), as in hatched larvae. Severely affected offspring appeared to be 'head-only,' similar to severe cuticle phenotype after *Dmac-eve* knockdown, with wild type-like antennae, labrum, and mandible but missing the labium and partial maxillary structures (Figure 4-7D''').

In sum, knockdown of *Dmac-eve, -odd,* or *-run* revealed two classes of defects. In more severe cases, unhatched larvae displayed severe "head-only" (*eve*,

run) or "anterior-only" (*odd*) embryos. In milder cases, larvae hatched, displaying pair-rule like defects (*eve, run, odd*), along with occasional mirror image duplications (*run, odd*). This indicates that these three genes function in at least two phases of segmentation patterning in *Dermestes*: formation of an elongating germ band and subdivision of organized tissue into metameric units.

4.4.3 *Additional PRG orthologs play roles in segmentation in* Dermestes

Unlike the two classes of defects described above, *Dmac-h*, *-slp*, *-ftz* or *-ftz-f1* RNAi produced distinct outcomes. *Dmac-h* pRNAi resulted in disruption of consecutive abdominal segments in ~12% of hatched larvae (Figure 4-7E). *Dmac-h* pRNAi caused defects in the entire abdominal region instead of a pair-rule-like or other specific register (Figure 4-7E'). In unhatched larvae with severe defects, truncated embryos displayed head and some thoracic segments with little (Figure 4-7E'') or almost no (Figure 4-7E''') abdominal structure.

Knockdown of *Dmac-slp* produced a range of defects, with mildly affected larvae hatching with one fusion between two neighboring segments (not shown) and moderately affected larvae displaying several fusions (Figure 4-7F). Very often, T1 and/or T3 legs were missing or deformed in hatched larvae (not shown). The observed fusions occurred between T1/T2, T3/A1, A2/A3, A4/A5, A6/A7 and A8/A9 segmental boundaries (Figure 4-7F'), complementary to the pattern produced after *Dmac-prd* RNAi (Chapter 2 and 3). Unhatched larvae only had one pair of legs, with shorter body length and fewer segments (Figure 4-7F''). The head also showed some defects with missing mandibles, maxillae and partial labium (Figure 4-7F'''). These

results suggest a *Drosophila*-like pair-rule function for *Dmac-slp*, and the overall defects after *Dmac-slp* knockdown are more severe than our previously reported PR-defects after *Dmac-prd* knockdown (Chapter 2).

For *Dmac-ftz* pRNAi, only 2 out of over 500 hatched larvae showed fusion of segments, despite knockdown of *Dmac-ftz* to ~6% of wild type levels (Figure 4-6). After injection of dsRNA directly into embryos (embryonic RNAi, eRNAi), 5%-11% of injected embryos had fused or missing segments (Figure 4-9A, B). Fusion of segments was detected with a pair-rule-like register, usually between A1/A2, A3/A4, A5/A6, A7/A8, as revealed by anti-Engrailed staining (see below). The pattern was complimentary to that after *Dmac-eve* mild knockdown (Figure 4-7B'). However, the low penetrance of segmentation defects after eRNAi, and the absence of detectable defects after pRNAi, indicate that knockdown of *Dmac-ftz* is tolerated, perhaps due to redundancy with another PRG ortholog.

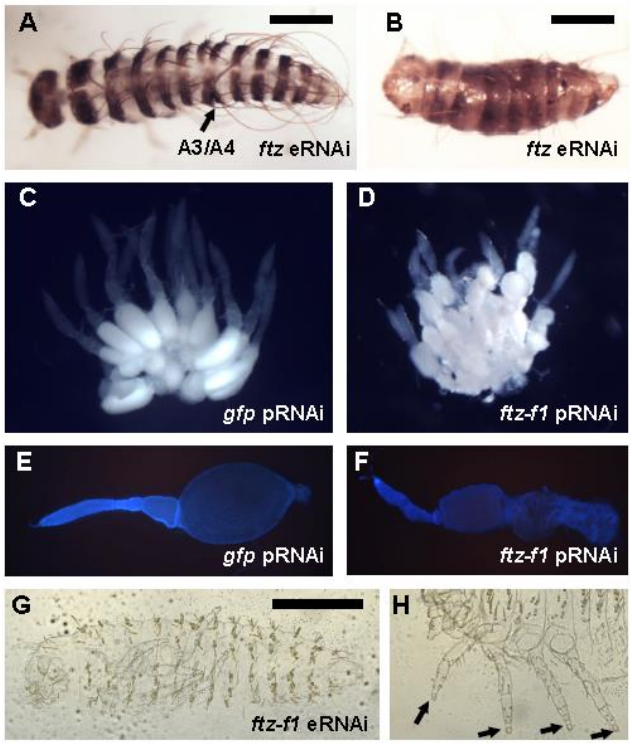

Figure 4-9. Phenotypes after *Dmac-ftz* and *ftz-f1* RNAi. (A, B) Hatched offspring after *Dmac-ftz* eRNAi. (A) Mildly affected embryo with single segmental fusion (arrow). (B) Severely affected larva with shortened body length and fewer segments. (C-H) Phenotypes after *Dmac-ftz-f1* pRNAi or eRNAi. (C, E) Wild type-like ovaries from *gfp* dsRNA injected female. (C) Large, oval shaped, developing oocyte in each ovariole. (E) DAPI staining of dissected ovariole reveals large oocyte. (D, F) Ovaries from *Dmac-ftz-f1* dsRNA-injected females. (D) Small primary oocytes clustered in each ovariole. No mature oocyte is visible. (F) Dissected ovariole show shrunken oocyte. (G) Unhatched larva from *Dmac-ftz-f1* injected female has normal number of segments without any obvious segmentation defect. (H) Arrows indicate truncated distal ends of legs. Scale bars represent 500 µm.

In contrast to the genes described above, RNAi failed to provide convincing evidence for roles of *Dmac-ftz-f1* in segmentation. pRNAi for *Dmac-ftz-f1* blocked oogenesis (Figure 4-9C-F) such that embryos could not be analyzed. Surprisingly, eRNAi did not result in any obvious segmentation defects, although PR-defects were observed in *Tribolium* using a similar approach (Heffer et al., 2012). Cuticle phenotypes of unhatched embryo showed well-patterned metameric segments with shortened setae all over the body (Figure 4-9G). Claws and head appendages were blunt-ended, consistent with *Dmac-ftz-f1* expression in tip primordia and demonstrating activity of the dsRNA (Figure 4-9H). Finally, no obvious defects were observed for *Dmac-opa* pRNAi, despite knockdown to ~3% of wild type levels (Figure 4-6). Analysis of genetic mutants for *Dmac-ftz-f1*, *opa* and *ftz* will be necessary to definitively determine their roles.

4.4.4 *Expression of* engrailed *suggests PR-like functions of* Dermestes *PRG orthologs*

PRGs in *Drosophila* and *Tribolium* regulate segment formation in part by controlling the expression of *engrailed* (*en*) at the border of each segment (Choe and Brown, 2009; DiNardo and O'Farrell, 1987; Jaynes and Fujioka, 2004). We therefore

examined En expression in early stage control (*gfp* dsRNA) and PRGs RNAi offspring. Segmental striped En was detected after *gfp* RNAi in embryos at early and late germ band elongation stages (Figure 4-10A, A'). In severely affected offspring of *Dmac-eve* dsRNA-injected females, En was only expressed in antennal segments (Figure 4-10B). In less severely affected embryos with relatively elongated germ bands, En stripes were reduced or undetectable in alternate segments (Figure 4-10B', asterisks). After *Dmac-odd* pRNAi, truncated embryos showed fuzzy and enlarged En striped expression (Figure 4-10C). Less severely affected embryos with relatively elongated germ bands displayed abnormally spaced, 'paired' En stripes (Figure 4-10C'), similar to previous findings in *Drosophila* (Mullen and DiNardo, 1995). Extra En stripes were frequently detected between pairs of En stripes (Figure 4-8D, E, arrows), and extra segmental furrows were observed in the region where ectopic En was expressed (Figure 4-8D', red arrow). Offspring of *Dmac-run* dsRNA-injected females included truncated embryos with En expression in only antenna and mandibular segments (Figure 4-10D), while less severely affected embryos with relatively elongated germ bands expressed fused En stripes (Figure 4-10D'). After *Dmac-h* pRNAi, many embryos stopped developing at very early stages (no divided nuclei in the center, not shown). No clear En striped expression was detected in truncated embryos (Figure 4-10E). For *Dmac-slp* pRNAi, En expression was undetectable or decreased in alternate segments (Figure 4-10F, F', asterisks). After *Dmac-ftz* eRNAi, ~ 25% of embryos showed reduced En expression in a pair-rule-like alternate segment pattern (Figure 4-10G, asterisks), although the overall En expression at the posterior end of the germ band was weak. In sum, these results

indicate that - with possible exceptions of *ftz-f1* and *opa* (data not shown) - all of the *Dmac*-PRG orthologs are required for proper *en* expression, with most of them behaving similarly to their *Drosophila* counterparts.

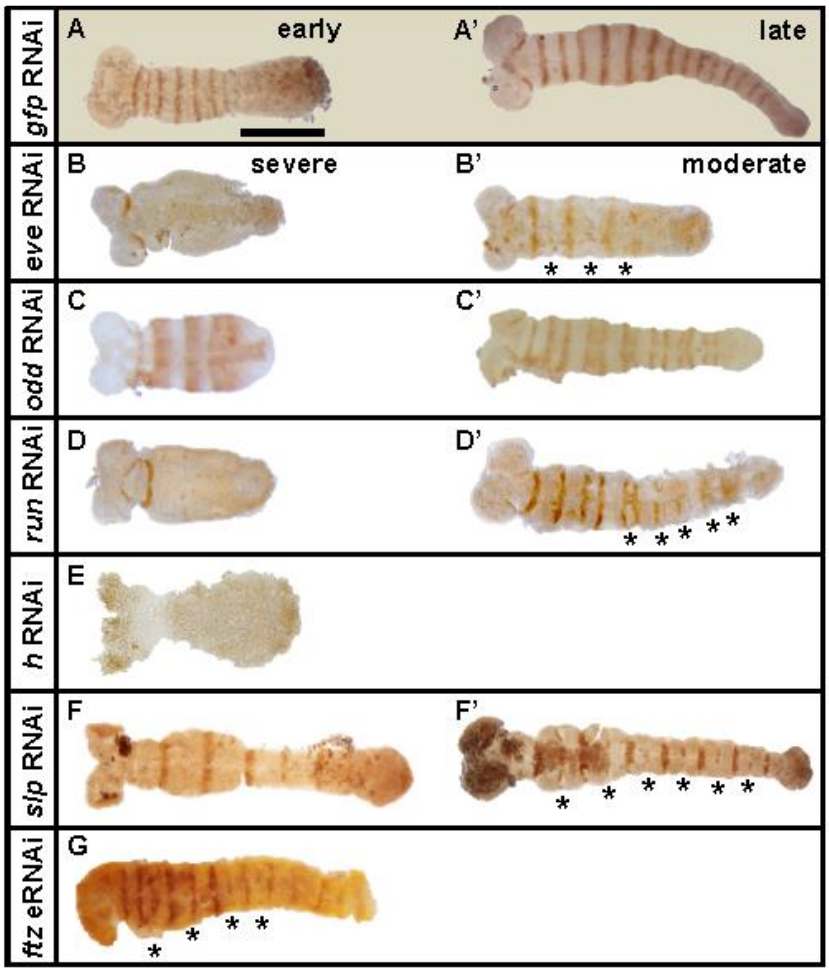

Figure 4-10. En expression altered after *Dermestes* PRG knockdown. (A, A') Control embryo (from *gfp* dsRNA-injected female) shows En stripes with equal intensity in every segment at early or late germ band elongation stages. (B) *Dmac-eve* pRNAi, severely affected embryo with truncated, asegmental germ band only has antennal En expression; (B') less severely affected embryo shows reduced En in alternate stripes (asterisks). (C) *Dmac-odd* pRNAi, severely affected embryo with truncated germ band has enlarged En stripes; (C') "paired" En stripes detected in moderately affected embryo. (D) *Dmac-run* pRNAi, severely affected embryo. En only detected in antennal and mandibular segments; (D') Fused En stripes visible in moderately affected offspring (asterisks). (E) *Dmac-h* pRNAi. No striped En detectable. (F) *Dmac-slp* RNAi. Alternate En stripes absent or (F') reduced (asterisks). (G) *Dmac-ftz* eRNAi. Alternate En stripes weak or absent. Scale bars represent 500 µm.

4.4.5 *Knockdown of* Dermestes *PRGs results in increased apoptosis*

In *Drosophila*, cell death contributes to patterning defects in PRG mutants (Ingham et al., 1985; Magrassi and Lawrence, 1988). To further characterize the role of *Dmac* PRG orthologs, we examined cell death patterns in control and pRNAi-embryos by performing antibody staining against an apoptosis marker, cleaved Dcp-1 (Figure 4-11A-F). Very little apoptotic activity was detected in offspring of *gfp* dsRNA-injected females from early stages to late germ band elongation (not shown). When segmental grooves were clear, only a weak apoptotic signal was detected in the head lobes and posterior germ band ends (Figure 4-11A).

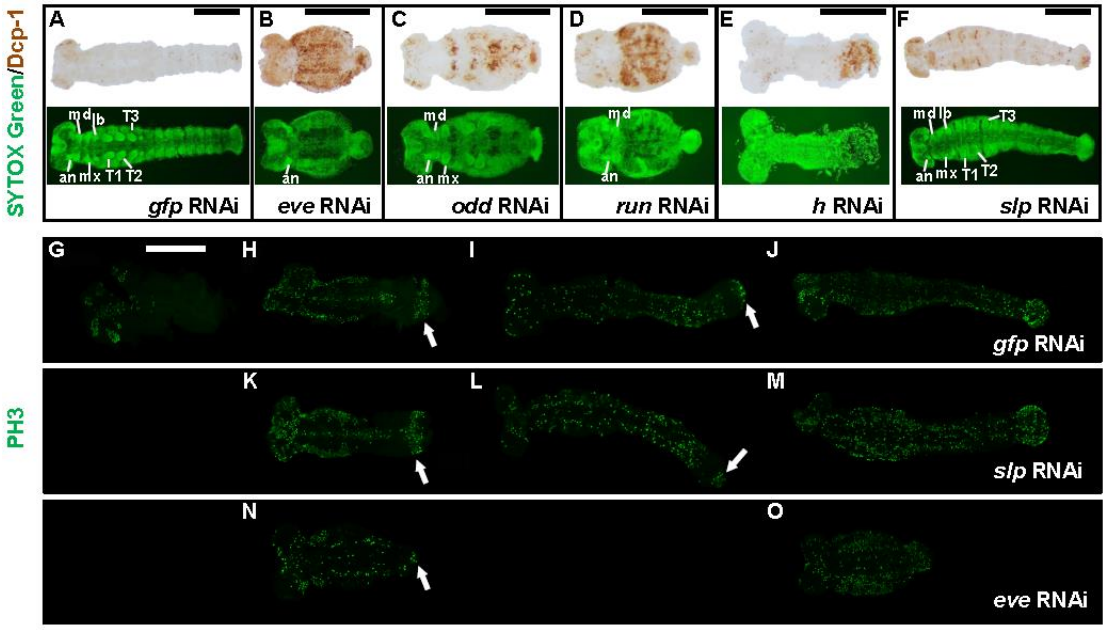

Figure 4-11. Increased apoptosis and disrupted mitosis after *Dermestes* PRG knockdown. (A-F) Dcp-1 (top panels) and SYTOX Green nuclear stainings (bottom panels) in pRNAi offspring. (A) As in untreated wildtype embryos (not shown), apoptosis detected in the head and posterior at low levels after germ band elongation. At this stage, primordial appendages are visible. (B) *Dmac-eve* RNAi. Increased apoptosis detected in the trunk. Antennae primordia, but no appendages, visible. (C) *Dmac-odd* pRNAi. Increased apoptosis in trunk region of early embryo. Antennal, mandible, maxillary and some thoracic primordia are detectable. (D) *Dmac-run*

pRNAi. Extensive apoptosis in center of embryo; only antennal and mandible appendages present. (E) *Dmac-h* pRNAi. High apoptotic activity at the posterior end. (F) *Dmac-slp* pRNAi. Striped apoptosis signals concentrated in alternate compartments in extended germ band stage embryo. (G-O) PH3 staining was used to monitor mitosis. (G-J) *gfp* pRNAi. (G) Mitotic cells clustered in head lobes at early germ band elongation stage. (H) As germ band elongates, increased mitosis signal was detected in the head and along the anterior and central trunk. In the posterior, mitotic cells are arranged in striped pattern (arrow). (I) Concentrated mitotic activity persists in the posterior end in embryo at late germ band elongation stage (arrow). (J) High mitotic activity all along the embryo at later stage. (K-M) *Dmac-slp* pRNAi. PH3 staining very similar to control. Concentrated mitosis signal present in the posterior (arrows in K, L). (N,O) *Dmac-eve* pRNAi. (N) Embryo during germ band elongation has fewer mitotic cells without a clear striped-like arrangement in the posterior. (O) Later stage *Dmac-eve* RNAi embryo with extensive mitotic activity throughout. Scale bars represent 500 µm.

Dmac-eve, *-odd* and *-run* pRNAi produced truncated embryos with extensive apoptosis. For *Dmac-eve* RNAi, severely affected embryos showed high apoptotic activity almost uniformly throughout the embryo (Figure 4-11B). *Dmac-odd* pRNAi displayed less apoptosis in the trunk and striped apoptotic signals were detected in the anterior (Figure 4-11C). These results are consistent with the finding that the cuticle defects after *Dmac-odd* RNAi were milder than *Dmac-eve* RNAi. For *Dmac-run* pRNAi, again, extensive apoptosis was detected uniformly in the trunk (Figure 4-11D). A concentrated region with apoptosis activity in the posterior end was detected in *Dmac-h* RNAi embryos (Figure 4-11E). For *Dmac-slp* knockdown, at the time when segmental furrows appeared, apoptosis was detected in alternate compartments, in a pair-rule-like pattern (Figure 4-11F). Together, apoptosis patterns matched morphological defects (Figure 4-7), indicating that cell death is involved in causing the defects after *Dermestes* PRGs knockdown.

4.4.6 *Knockdown of* Dmac-eve *causes disruption of posterior mitotic activity*

Cell proliferation has been documented in the posterior growth zone in annelids and some basal arthropods (Scholtz, 1993; Shankland and Seaver, 2000). Although recent work has suggested that germ band elongation in sequentially segmenting insects is mainly driven by cell rearrangement rather than cell division (Nakamoto et al., 2015), we examined mitotic figures in *Dermestes* embryos using an antibody against phospho-Histone H3 (PH3; Figure 4-11G-O; 4-12). In *gfp* pRNAi control embryos, mitosis was detected as nuclei divided in the syncytial blastoderm (Figure 4-12A'). There was no mitotic activity detected in the embryonic rudiment in late blastoderm stage embryos (Figure 4-12B'). During gastrulation and early germ band elongation, mitosis was detected in patches in the head lobes, and in some regions of the trunk (Figure 4-12C'-E'; 4-11G). In mid-germ band stage embryos, mitotic activity expanded and a localized region with high mitotic activity was evident in the segment addition zone (SAZ) (Figure 4-11H, arrow). This region retained mitotic activity throughout germ band elongation (Figure 4-11I, arrow). In fully elongated germ band embryos that had developed segmental furrows, mitosis was detected throughout the embryo, with stronger activity in the posterior end (Figure 4-11J).

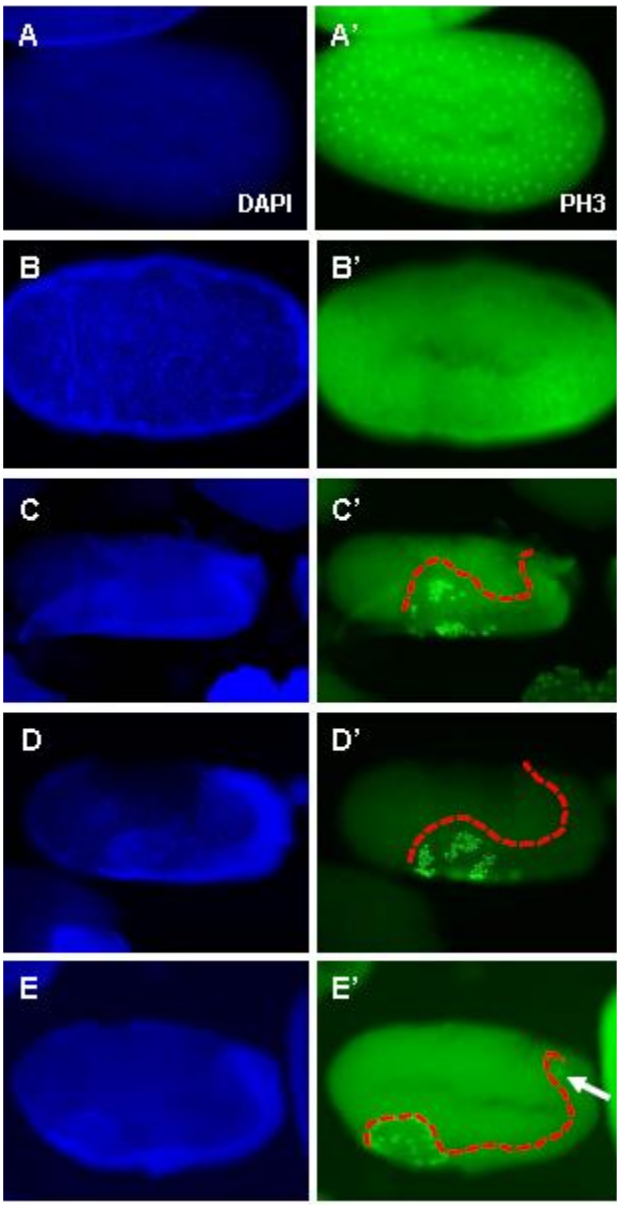

Figure 4-12. Mitotic activity in early *Dermestes* embryos. (A-E) DAPI staining was carried out for visualization of nuclei. (A'-E') Mitotic activity was examined using anti-PH3 antibody. (A, A') Dividing nuclei in a syncytial blastoderm. (B, B') No detectable mitosis in embryo at late blastoderm stage. (C, C' and D, D') Embryos at early germ band stages show mitosis in the head region. (E, E') Mitotic cell is detected in the posterior region as the germ band elongates (arrow). Dashed red line in C'-E' outlines the germ band.

To examine effects of PRG orthologs that function exclusively in pair-rule patterning vs. those that also play a role in elongation, mitosis was examined in

Dmac-slp and *Dmac-eve* pRNAi embryos, respectively. Patterns of mitosis after *Dmac-slp* knockdown did not appear different from *gfp* RNAi controls. Localized mitotically active regions were detected during germ band elongation in patterns similar to controls (Figure 4-11K, L, arrow). Mitotic activity was normal in the head and trunk regions; however, the posterior domain showing high levels of mitosis in controls and *Dmac-slp* embryos had little mitotic activity after knockdown of *Dmac-eve*, with only a few mitotic cells evident (Figure 4-11N, arrow). These cells were also not as well organized as those in *gfp* RNAi control and *Dmac-slp* RNAi embryos at comparable stages. Extensive mitosis was detected almost uniformly in later stage, shortened *eve* RNAi embryos (Figure 4-11O). In sum, these results indicate that there is a localized region within the SAZ with high mitotic activity during *Dermestes* germ band elongation. While there was little effect on mitosis of *Dmac-slp* knockdown, mitosis in the SAZ was greatly reduced and mitotic cells were not well organized in *Dmac-eve* knockdown embryos.

4.4.7 Dmac-prd *and* -slp *double knockdown produces elongated but asegmental germ band*

The results presented above and previously (Chapter 2) suggest that, in contrast to other *Dmac* PRG orthologs, *Dmac-slp* and *-prd* function exclusively in PR segmentation, apparently required for the patterning of alternate sets of body segments. To test this, we simultaneously knocked down *Dmac-slp* and *Dmac-prd* (double pRNAi, Figure 4-13). Examination of cuticle preparations revealed dramatically shortened larvae, lacking overt signs of segmentation (Figure 4-13A, B).

Remnants of segments were suggested by residual setae. There were no obvious leg structures, and all gnathal segments (mandible, maxillae and labium) were missing; only antennae and labrum were evident in head regions. In severely affected embryos, there was no striped En expression in the germ band at late elongated stages (Figure 4-13C) and embryo morphology, as indicated by SYTOX Green staining, revealed no clear segmental furrows or grooves (Figure 4-13C'). In some embryos, reduced En expression (Figure 4-13D) together with fused adjacent segments (Figure 4-13D') indicated a milder phenotype. The defects were more obvious in the posterior region in even-numbered segments (asterisks, Figure 4-13D, D'). This milder pattern is consistent with our findings that, *Dmac-slp* knockdown produced more severe PR defects than *Dmac-prd* knockdown. In late stage embryos, after germ band retraction, there was only residual En expression along the midline (Figure 4-13F). No segmental grooves, gnathal, or leg appendages were evident (Figure 4-13F'). Strong apoptotic signals were detected almost uniformly at elongated germ band stages (Figure 4-13G), but germ band elongation per se seemed unaffected. Extensive apoptotic activity persisted after germ band retraction (Figure 4-13H).

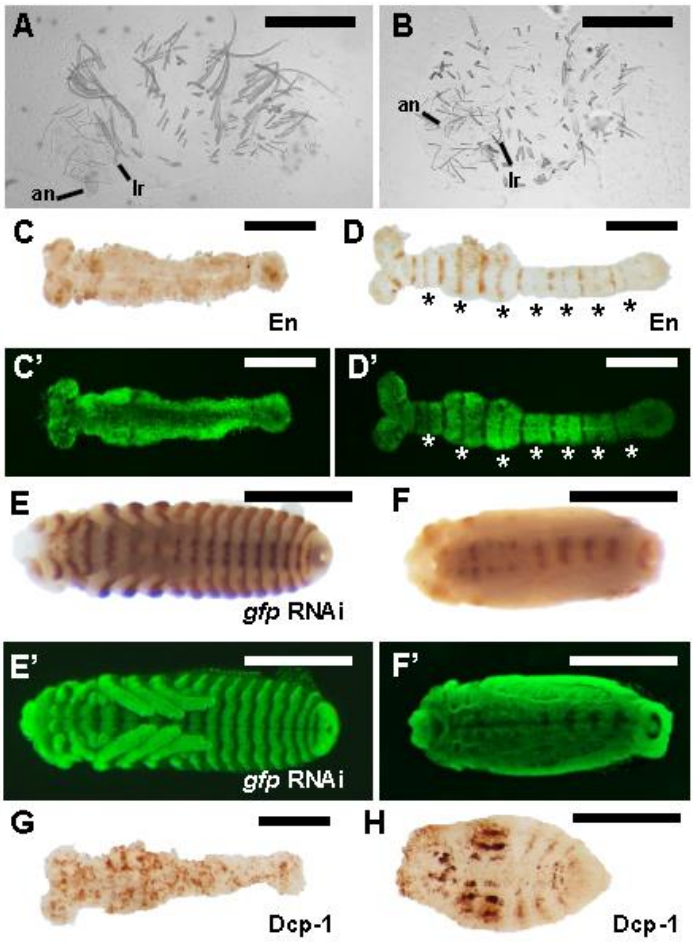

Figure 4-13. *Dmac-prd* and *-slp* double RNAi produces asegmental embryos. (A, B) Significantly shortened unhatched larvae after double *Dmac-prd*, *-slp* pRNAi. Only antenna and labrum are visible. No gnathal appendages or legs are presented. (C) No striped-like En expression detected in elongated germ band in severely affected embryo. (D) Moderately affected embryo shows reduced En expression. Reduction is more obvious for even-numbered En stripes (asterisks). (C', D') SYTOX Green staining of embryos in (C) and (D) for visualization of embryo morphology. Note that there are no obvious segmental grooves in (C') and fused adjacent segments in (D'), indicating overt lack of segmentation or milder segmentation defects, respectively. (E) Striped En expression at the posterior border of each segment in control embryos. (F) Only residual En expression along midline after double knockdown. (E', F') SYTOX Green staining of embryos in (E) and (F) for visualization of embryo morphology. (G, H) Dcp-1 antibody staining for apoptosis in elongated germ band stage and later stage embryo. Note that there is almost uniform apoptosis signal in elongated germ band (G). Scale bars represent 500 µm.

4.5 Discussion

Dermestes has fewer posterior segments added after gastrulation than its well studied beetle counterpart, *Tribolium,* representing an intermediate state between ancestral short and derived long germ modes. Here, we examined the expression and functions of PRG orthologs in *Dermestes.* Eight of nine orthologs of *Drosophila* PRGs were found to be expressed in PR-like stripes and seven are involved in segmentation. *eve*, *run*, and *odd* function in both posterior elongation and PR segmentation; *slp* and *prd* function exclusively in PR segmentation; *h* has a role in posterior patterning while *ftz* has a mild PR-like function. Consistent with cuticular defects, expression of En was disrupted after RNAi knockdown of each of these genes. In addition, as in *Drosophila*, these PRGs were shown to promote cell viability. Knockdown of *Dmac-eve,* but not *Dmac-slp,* disrupted mitotic activity in the SAZ in elongating germ bands. Simultaneous knockdown of *Dmac-slp* and *-prd* produced elongated but asegmental embryos, confirming their exclusive roles as "core" PRGs, specifying the formation of alternate segmental regions in both segments patterned in blastoderm and elongating germ band.

Variation in PRG orthologs in holometabolous insects

The PRGs, originally isolated in *Drosophila*, are largely conserved in arthropod genomes and many function in segmentation (reviewed in (Peel et al., 2005). Sequential segmentation is thought to be ancestral but long germ, with roughly simultaneous specification of segments, has arisen independently multiple times in holometabolous insects (Davis and Patel, 2002; Liu and Kaufman, 2005b; Lynch et

al., 2012). While most PRGs are expressed in stripes in blastoderm embryos in *Drosophila*, cap-like expression of *eve, odd* and *run* in the SAZ in sequentially segmenting *Tribolium* was observed and this expression correlates with the failure of embryos to elongate after knockdown of these gene (Choe et al., 2006; El-Sherif et al., 2012; Rosenberg et al., 2014; Sarrazin et al., 2012). In this species, PR stripes arise at the posterior end of the embryo and move anteriorly, generating a 'final' pattern of *Drosophila*-like PR stripes, with expression in alternate segmental units. In addition, in an independently derived long germ insect, *Nasonia*, at least some PR stripes were shown to arise in an anterior-to-posterior order (Keller et al., 2010; Rosenberg et al., 2014). In contrast, in *Drosophila*, PR-stripes arise in different orders for different genes, with no anterior-to-posterior bias (Yu and Pick, 1995). Here we found that a sequentially segmenting species with an intermediate germ mode share features seen for all of these other species: *Dermestes* display posterior cap-like expression of *eve*, *odd*, and *run*, which likely reflects a clock mechanisms shared with *Tribolium* (El-Sherif et al., 2012; Sarrazin et al., 2012). In addition, blastoderm stripes arose sequentially, similar to what was seen in *Nasonia* (Rosenberg et al., 2014). Finally, secondary stripes, generated for several PRGs in both *Drosophila* and sequentially segmenting species were seen in *Dermestes*. Specifically, secondary segmental stripes were observed for *Dmac-eve*, *-odd*, *-h*, and *-slp,* which emerged either by splitting (*eve* and *h*) or *de novo* (*odd* and *slp*). Subtle differences in expression were also observed. For example, secondary stripes are not seen in *Drosophila* for *hairy* but were seen in *Dermestes* as well as in *Tribolium*. For *eve*, secondary stripes are seen in both *Drosophila* and *Dermestes* but they are added *de*

novo in *Drosophila* and arise by splitting in *Dermestes* and its beetle counterpart, *Tribolium* (Brown et al., 1997; Frasch and Levine, 1987; Macdonald et al., 1986; Patel et al., 1994). More drastic differences in expression were seen for *opa* and *ftz-f1*. *Dmel-opa* is expressed ubiquitously and is required for the pair-rule segmentation (Benedyk et al., 1994; Jürgens et al., 1984). In *Dermestes*, marginal segmental stripes of *opa* were all that could be detected. In *Drosophila*, Ftz-F1 expressed ubiquitously (Yussa et al., 2001), while in *Dermestes*, as well as in *Tribolium* (Heffer et al., 2013), PR-like stripes were observed. Finally, intensities of primary and secondary stripes alternated only for *Dmac-odd*, while primary stripes exhibit stronger expression in *Drosophila* for other genes as well (Clark and Akam, 2016) and *Dmac-slp* differed from other PRGs in *Drosophila* and *Dermestes* in that anterior stripes did not fade in elongating germ bands. Together these results suggest loss of a posteriorly biased expression of PRGs in the evolution of long germ insects but, in addition, reveal extensive fine-tuning of regulatory mechanisms controlling PR expression in multiple lineages.

Two distinct modes of PRG function in segmentation

Knockdown of either *Dmac-slp* or *–prd* caused PR-like segmentation defects exclusively, consistent with their functions as "core" PR genes. Similar PR-like defects were seen after RNAi knockdown of these genes in *Tribolium* and *slp* and *prd* were the only pair-rule genes identified in a *Tribolium* mutant screen (Choe and Brown, 2007; Choe et al., 2006; Maderspacher et al., 1998). Knockdown of a second group of genes, *Dmac-eve*, *-odd* or *-run*, produced two distinct classes of defect:

mildly or moderately affected offspring usually hatched, showing PR-like defects, while severely affected offspring, mostly unhatched, had defects in elongation and cuticles were composed of head or anterior regions only. These findings suggest two independent modes of PRG activity are required for segment formation: First, formation of an elongating germ band and Second, subdivision of organized tissue into metameric units. The latter, 'classic' PR patterning, occurs in both blastoderm-patterned tissue and in tissue specified as the germ band elongates. Mode 1 requires *Dmac-eve*, *-odd*, and *-run*, as previously reported for *Tribolium* (Choe et al., 2006). Mode 2 also requires *Dmac-eve*, *-odd*, and *-run*, as well as the core PRGs *Dmac-slp* and *-prd*. These findings suggest that the same mechanism is used for segment-specification in segments patterned during blastoderm and germ band elongation stages. The idea that some PRGs function in both germ band elongation and PR patterning in insects was proposed previously (Choe et al., 2006). However, a classic PR patterning role can be concealed by severely truncated phenotypes, and/or if the identity of lost segment cannot be easily determined because lack of reliable markers, as the case in the cricket, *Gryllus* (Mito et al., 2005). Here, we circumvented these issues by quantitative examination of moderate cuticle defects in hatched larvae after *Dmac-eve*, *-odd* and *-run* knockdown. PR-like roles were revealed by compiling moderate defects seen in individual larvae (Figure 4-14) and confirmed by the observation of irregular *en* expression in young embryos.

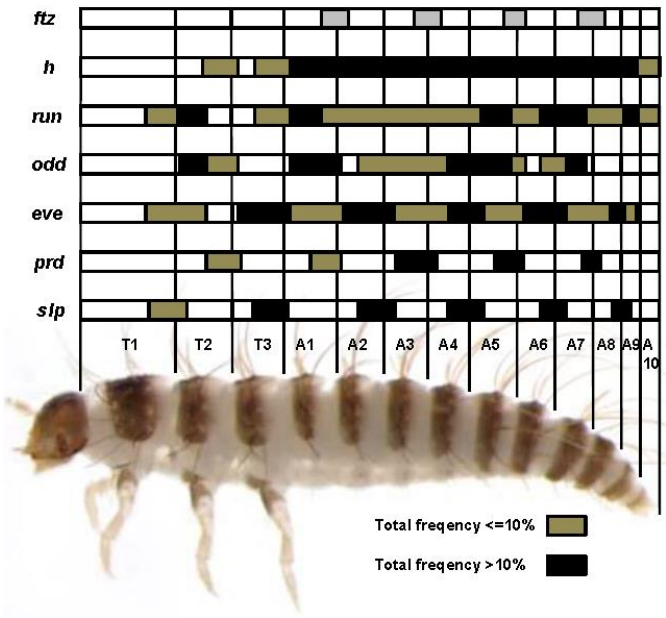

Figure 4-14. *Dermestes* PRG orthologs required for elongation and PR-like segmentation. Schematic representation of defective patterns after PRGs RNAi in *D. maculatus*. Results are based on defective patterns in affected hatched larvae after pRNAi, except for *ftz* (eRNAi, gray bars). Black bars indicate regions affected at high frequency (>10%) while tan bars show regions affected at low frequency (≤10%). For genes playing dual roles in *Dermestes* segmentation (*eve*, *odd*, *run*), black bars alone show PR-like phenotypes in moderately affected offspring (most are hatched), while black and tan bars together indicate severely affected, truncated offspring (unhatched). Note that PR-like defects seen for *slp* and *prd* pRNAi, as well as between *ftz* eRNAi and *eve* pRNAi, are complimentary.

Simultaneous knockdown of *Dmac-prd* and *-slp* produced embryos with no segmental boundaries across gnathal, thoracic and abdominal regions, but germ band elongation was not impaired. This supports the notion that germ band elongation and segmentation patterning are decoupled modes. Similarly, elongated but unsegmented posterior tissue was reported in crustaceans when Notch signaling was disrupted pharmacologically (Williams et al., 2012). Though the defects are (probably) caused by different mechanisms, these findings suggest that decoupling of germ band elongation and segment formation may reflect an ancestral state.

Cellular defects after Dermestes *PRG knockdown*

To begin to address the mechanisms underlying PRG action in elongation and segment formation, we analyzed patterns of cell death after PRG knockdown. Our experiments revealed increased apoptosis in these embryos, in patterns generally corresponding to the observed mutant phenotypes, suggesting that a major and shared role of PRGs is to control cell viability. Cell death has been reported in *Drosophila* when genes crucial for embryonic or later, larval stage patterning are mutated (Bonini and Fortini, 1999; Hughes and Krause, 2001; Ingham et al., 1985; Jäckle et al., 1985; Klingensmith et al., 1989; Magrassi and Lawrence, 1988; Werz et al., 2005; White and Lehmann, 1986). Although cell death was implicated in PR-patterning in *Drosophila* many years ago, its molecular basis has still not been elucidated. In *Drosophila* imaginal discs, cell surface proteins are required for maintaining cell viability (Milán et al., 2002). Interestingly, some cell surface proteins are downstream targets of PRGs during germ band elongation (Paré et al., 2014), and the crosstalk between cell surface proteins and PRGs might be conserved among arthropods (Benton et al., 2016). It will be interesting to further investigate the underlying mechanisms, such as identifying PRGs targets for supporting cell viability, understanding how mis-specified cells are recognized and by which program they execute cell death.

In addition to increased apoptosis, knockdown of *Dmac-eve* resulted in abnormal mitotic patterns. This suggests a role for mitosis in the elongation of the germ band, which requires *Dmac-eve* function. These abnormalities in mitosis were

not seen for *Dmac-slp* knockdown, consistent with *slp* and *prd* playing no role in elongation of the germ band. However, Nakamoto et al. provided strong evidence that mitosis is not required for germ band elongation in *Tribolium*, and those results are likely to extend to *Dermestes* (Nakamoto et al., 2015). Therefore, future experiments will be needed to determine the causes and consequences of these abnormal mitotic patterns. Until now, our understanding of cell division in the SAZ is limited by lack of understanding of cell dynamics and appropriate tools (Williams and Nagy, 2017). However, we have little information about the roles of mitotic cells in *Dermestes* SAZ during germ band elongation and segmentation specification. We note that in wild type embryos, and unaffected by *Dmac-slp* knockdown, we observed a concentrated region with high mitotic activity posterior to a mitotically-silent region (Figure 4-11). Unpublished but cited work suggests that a similar pattern is present in other species representing distinct arthropod branches (Williams and Nagy, 2017).

Divergent expression and function of some PRGs

In contrast to the relatively conserved roles in PR patterning for the five genes discussed above (*Dmac-eve, -odd, -run, -slp, -prd*), four genes that are required for segmentation and *en* expression in *Drosophila*, showed either no defects after knockdown (*opa, ftz-f1*) or clear defects but with low penetrance (*ftz, h*). *opa* is a PRG in *Drosophila* but is expressed ubiquitously in the trunk in embryos. Recent data suggests that *opa* modulates the function of other PRGs in *Drosophila* (Clark and Akam, 2016). pRNAi of *Dmac-opa* did not produce obvious segmentation defects and its expression was marginal. Few other functional studies have been performed

for *opa* orthologs in other insect species, but it did not function in segmentation in *Tribolium* (Choe et al., 2006).

The PRG *ftz-f1*, which is expressed ubiquitously in *Drosophila*, is expressed in stripes and has pair-rule function in *Tribolium* (Heffer et al., 2012). As multiple attempts targeting *ftz* didn't give segmentation phenotype, Ftz-F1 appears to function without Ftz as a partner in *Tribolium* (Choe et al., 2006; Stuart et al., 1991). In *Dermestes,* we did not detect PR-like segmentation defects in *D. maculatus*. In this case, it is possible that a role for *Dmac-ftz-f1* provided by maternally deposited transcript was ineffectively targeted in injected embryos, thus masking a role for this gene in segmentation.

pRNAi for *Dmac-h* and *-ftz* produced embryonic defects with variable and low penetrance. The two PRGs are well studied in *Drosophila* and have interesting and distinct evolutionary histories. Vertebrate *h* orthologs are involved in somitogenesis and their oscillating expression is activated by Notch/Delta signaling (Pourquié, 1999, 2003). Therefore, there is a particular interest to investigate *h* function in arthropods for deep homology of segmentation mechanism between vertebrates and arthropods. Variable functions of *h* have been reported in several hemimetabolous and holometabolous insects (Aranda et al., 2008; Choe et al., 2006; Pueyo et al., 2008; Rosenberg et al., 2014; Wilson and Dearden, 2012). While results from basal arthropods indicate Notch/Delta pathway is required for segmentation (Schoppmeier and Damen, 2005b; Stollewerk et al., 2003), debate still remains in basal insect (Kainz et al., 2011; Pueyo et al., 2008). Here, we showed disrupted

abdominal segmentation after *Dmac-h* pRNAi, but only in a small percentage of embryos. Similarly, effects of *Dmac-ftz* were poorly penetrant. *ftz* arose as a *Hox* gene and retains *Hox*-like expression in many arthropods but acquired PR-expression in insect lineages (Heffer et al., 2010; Hughes and Kaufman, 2002c). As mentioned above, *ftz* is not involved in segmentation in short germ beetle, *Tribolium*. We propose that these low penetrance effects, seen for both *h* and *ftz,* reflect marginal requirements for these genes in segmentation, perhaps due to partial redundancy with other PRGs. Their situation in *Dermestes,* and perhaps other beetles, may thus represent an intermediate evolutionary stage, in which they retain the freedom to functionally diverge. In lineages leading to *Drosophila*, each of these genes has become essential for pair-rule patterning: in *A. melifera*, *ftz* may have taken on a *bcd*-like role in head patterning (Wilson and Dearden, 2012), while outside of the holometabolous insects, *ftz* may play no role in segmentation (Dawes et al., 1994) and *h* may be restricted to a role in Notch/Delta signaling. It may also be of significance that a major role of *h* in *Drosophila* is to regulate *ftz* expression (Carroll and Scott, 1986; Howard and Ingham, 1986; Ish-Horowicz and Pinchin, 1987). Thus, these two genes became interdependent in a lineage in which they are both absolutely required for segmentation. Future studies will examine the re-wiring underlying these types of changes in PR-gene function during evolution.

Chapter 5: **Conclusions and future directions**

Here I have established methods for lab rearing, gene orthologs isolation, gene expression and functional studies in an intermediate germ beetle, *Dermestes maculatus*. Compared with its short germ counterpart, *T. castaneum, D. maculatus* has more anterior segments patterned before gastrulation. If an ancestral mechanism involving *eve, run* and *odd* only accounts for specifying segments after gastrulation, we would expect less severe defects with missing fewer posterior segments after these gene knockdown in *D. maculatus*. However, we were surprised to find that severely truncated defects after *Dmac-eve, -run* and *-odd* knockdown were highly similar to previously reported defects after *eve, run* and *odd* knockdown in *T. castaneum* (Choe et al., 2006). Therefore, these three genes are necessary for adding segments during both blastoderm and germ band stages in both beetles with distinct segmentation modes. Sequentially establishing segments in an anterior-to-posterior order appears to be conserved in beetles. Long germ beetles have (almost) all the segments patterned before gastrulation. It would be interesting to carry out the same study on segmentation patterning in a long germ beetle species, such as *Callsobruchus maculatus*. If *C. maculatus* patterns segments sequentially at both blastoderm and germ band elongation stages, it would support previous hypotheses that long germ segmentation mode evolved independently in different lineages. Moreover, it would show that diverse strategies are used for achieving long germ modes in different lineages.

PRG functions are divergent in different insects. To understand how the PRG regulatory network re-wired during evolution, the interactions among PRGs need to

be unraveled. We examined the expression level changes of PRG ortholog after each knockdown. However, our attempts failed as the results varied a lot among three replicates, thus we didn't get definitive conclusions regarding genetic interactions among PRG orthologs in *D. maculatus*. In the future, investigating if there is overlapping or mutually exclusive expression between PRG orthologs may give some clues about genetic interactions among PRG regulatory network. Further examination of PRG expression patterns after each PRG knockdown would provide more direct evidence.

It would be interesting to study cellular dynamics in the posterior region in elongating germ bands. Despite previous studies on segmentation in sequentially segmenting species, our knowledge about the cellular dynamics is still quite limited (Williams and Nagy, 2017). A well-organized high mitotic activity region in SAZ posterior to a low mitotic activity region was reported here in *D. maculatus*. Very similar observations were reported in the milkweed bug *Oncopeltus* and a crustacean *Thamnocephalus platyurus* (Auman et al., 2017; Williams and Nagy, 2017). Now, the hypothesis is that mitosis in the SAZ in elongating germ band generates an undifferentiated cell pool for future segments, while cells are specified in the low mitotic activity region for making a new segment (Auman et al., 2017). This hypothesis remains to be tested.

From our RNAi results, we noticed a significant difference between the duration of gene knockdown in *D. maculatus* and *T. castaneum*. The duration time in *D. maculatus* after RNAi is only a few days. However, the RNAi effects in *T. castaneum* last over weeks (Bucher et al., 2002). Such divergence among species

implies that there are different RNAi mechanisms even within this single order. Many factors may have impact on the duration of RNAi effect such as the mechanisms for dsRNA uptake, maintenance, amplification and removal. There might be possible compensatory mechanisms yielding more gene products to counteract the RNAi effect in some species. Future experiments are required to address these questions.

Appendx I. List of Primers

Part I: Primers for *COI* amplification
target size ~700 bps
LCO1490 5′-GGTCAACAAATCATAAAGATATTGG
HCO2198 5′-TAAACTTCAGGGTGACCAAAAAATCA

Part II: Primers for degenerate PCR

Gene	Primer sequence	Target motif in *T. castaneum*
prd	*prd*-deg1 F 5′-GGNGGNGTNTTYATHAAYGG	GGVFING
	prd-deg1 R 5′-RTTNSWRAACCANACYTG	QVWFSN
	prd-deg2 F: 5′-MARATHGTNGARATGGC	KIVEMA
	prd-deg2 R 5′-RTANACRTCNGGRTAYTG	QYPDIY
eve	DEG*eve*F 5'- TAYMGNACNGCNTTYACNMG	YRTAFTR
	DEG*eve*R 5'- RTTYTGRAACCANACYTTDAT	IKVWFQN
odd	*odd*-fw 5' AARAARSARTTYATHTGYAARTWYTGY	KRQFICK
	odd-bw 5' TGNGTYTTNARRTTNGMNCKYTGRTTR	NQRSNLK
run	*run*-fw-1 5' RCNRYNATGAARAAYCARGTNGC	AVMKNQ
	run-bw 5' CKNGGYTCNCKNGGNCCRTC	DGPREPR
	run-fw-2 5' MRNTTYAAYGAYYTNMGNTTYGTNGG	KFNDLRF
h	*h*-fw 5' AARCCNATHATGGARAARMGNMG	KPIMEKR
	h-bw-1 5' YTGNARRTTYTGNARRTGYTTNAC	VKHLQN
	h-bw-2 5' GTYWTYTCNARDATRTCNGCYTTYTC	EKADILE
slp	*slp*-fw 5' AARCCNCCNTWYWSNTAYAAYGC	KPPYSYN
	slp-bw 5' TTNCCNGTNGTNCCNCCDATRAA	FIGGSTG
opa	*opa*-fwNEW 5' CAYGTNGGNGGNCCNGARTGYAC	HVGGPEC
	opa-bwNEW 5' RTGNACYTTCATRTGYTTNCKNAR	LRKHMK

Part III: Gene specific primers for 3'RACE

prd:
1st round primers
*Dmac-prd*3'RACEouter 5'AGAAACAGGCTCGATTCGTC (ETGSIR)
*Dmac-prd*3'RACEinner 5' GATCGTCTCGTCAAGGAAGG (DRLVKE)
2nd round primers
*Dmac-prd*3'end-outer 5' TTAGCTGGTGGCATTCAAAA (LAGGIQN)
*Dmac-prd*3'end-inner 5' AAGCTCTGTTGGTGCTGGTT (SSVGAG)

eve:
*Dmac-eve*3'RACEouter 5' GCGTTTGGAAAAAGAGTTCTAC (RLEKEFY)
New*Dmac-eve*3'RACEouter 5' CAAAGAAAACTATGTGTCCAGACC (KENYVSR)

odd:
Dmac-odd3'RACEouter 5' ACTGACGAACGCCCATATTC (TDERPY)
*Dmac-odd*3'RACEinner 5' CAGCAAAGAGAAGCCATTCA (SKEKPF)

run:
*Dmac-run*3'RACEouter 5' GTTGCGACATACACCAAAGC (VATYTK)
*Dmac-run*3'RACEinner 5' CACCAAAGCCATCAAAGTCA (TKAIKV)

h:
1st round primers
*Dmac-h*3'RACEouter ATGGAGAAGAGGCGAAGG (MEKRRR)
*Dmac-h*3'RACEinner CTGAATGAACTCAAAACCCTCA (LNELKTL)
2nd round primers
Dmac-FURTHER*hairy*3'RACEouter 5' AGTTGGACGTTTTCCTGGACTA (VGRFPGL)
Dmac-FURTHER*hairy*3'RACEinner 5' ATAACAGCTCAACAGCAACAGC (ITAQQQQ)

slp:
*Dmac-slp*3'RACEouter 5' CATGCGCAACTTCCCTTATT (MRNFPY)
*Dmac-slp*3'RACEinner 5' CGTTAAAGTTCCGCGTCATT (VKVPRH)

opa:
NEW*Dmac-opa*3'RACEouter 5' TGGTCAATCACATCAGAGTGC (LVNHIRV)
*Dmac-opa*3'RACEinner 5' TCGCCAGAAGTGAAAACCTC (FARSEN)
NEW*Dmac-opa*3'RACEinner 5' CGGATAGGAAGAAGCATTCG (SDRKKH)

Part IV: Primers for verification and cloning

Gene	Primer sequence	R.E site	Note
prd	5’ ccgctcgagGTCTCGTCAAGGAAGGGATTT	XhoI	LVKEGI-YGWY*, 1120 bp
	5’ gctctagaGCTGGTTCATTAATACCAACCATAG	XbaI	
eve	5' ccgctcgagGCTGGCGCGTTTGGAAAA	XhoI	LARLEK - 95 bp downstream of stop codon, 729 bp
	5' cgcggatccTTTCGCCTATTTCCCTCGGA	BamHI	
odd	5' ccggaattcACTGACGAACGCCCATATTC	EcoRI	TDERPYS - 132 bp downstream of stop codon, 645 bp
	5' cgcggatccGCGAGAGAGATCTCATTGTTCG	BamHI	
run	5' ccggaattcCACCAAAGCCATCAAAGTCA	EcoRI	TKAIKV - 181 bp downstream of stop codon, 911 bp
	5' cgcggatccAAGAACATTGGACAGACTTGTAGAC	BamHI	
h	5' ccggaattcCGCCGACATCCTAGAAAAG	EcoRI	ADILEK - IRKNEP, 660 bp
	5’ cgcggatccGGGTTCGTTCTTGCGTATCA	BamHI	
slp	5’ ccggaattcCCTCAACGGCATCTACGAAT	EcoRI	LNGIYE - 221 bp downstream of stop codon, 963 bp
	5' cgcggatccTGCGATCGTGTGCTCTTTTA	BamHI	
opa	5' ccgctcgagTGGTCAATCACATCAGAGTGC	Xhol	LVNHIRV - EWYVSCQ, 470 bp
	5' gctctagaCTGGCAGGAAACGTACCACT	XbaI	

Part V: Primers for amplifying templates for dsRNA synthesis

dsRNA Name	Primer sequence	Target size	Target region
gfp	Forward: 5’ taatacgactcactatagggagaTTCACTGGAGTTGTCCCAAT Reverse: 5’	723 bp	FTGVVPI-FVTAAG

	taatacgactcactatagggagaCCCAGCAGCTGTTACAAACT		
***Dmac-prd* 5'**	Forward: 5' taatacgactcactatagggagaTTCAACTCCATACGCACCAA Reverse: 5' taatacgactcactatagggagaTGATGAACTCGGTTGCACAT	256 bp	STPYAP-VQPSSS
***Dmac-prd* 3'**	Forward: 5' taatacgactcactatagggagaAGTGCCAATAGCAACAGCAA Reverse: 5' taatacgactcactatagggagaCCGAAGGTTTTTGATGGATT	254 bp	SANSNS-NPSKTF
***Dmac-eve* 5'**	Forward: 5' taatacgactcactatagggagaCGCGTTTGGAAAAAGAGTTC Reverse: 5' taatacgactcactatagggagaATAATGCAGCGGCAAAGTCT	236 bp	RLEKEF - TLPLHY
***Dmac-eve* 3'**	Forward: 5' taatacgactcactatagggagaCACGTATCGCCAACACATTC Reverse: 5' taatacgactcactatagggagaGCCTATTTCCCTCGGACTATG	244 bp	HVSPTH - 91 bp downstream of stop codon
***Dmac-odd* 5'**	Forward: 5' taatacgactcactatagggagaACTGACGAACGCCCATATTC Reverse: 5' taatacgactcactatagggagaCGTCAGCAGATGCGTTTTTA	249 bp	TDERPY - KTHLLT
***Dmac-odd* 3'**	Forward: 5' taatacgactcactatagggagaGCCTCAACAAGAAATCGTGA Reverse: 5' taatacgactcactatagggagaCGAACTTTTCGAATTTGTGG	251 bp	PQQEIV - 112 bp downstream of stop codon
***Dmac-run* 5'**	Forward: 5' taatacgactcactatagggagaGATATGGATTGCCAGGGATG Reverse: 5' taatacgactcactatagggagaAACCATTTGGCGGTACAAAG	237 bp	YGLPGM - FVPPNG
***Dmac-run* 3'**	Forward: 5' taatacgactcactatagggagaGCGCGAAAGAGCATT	256 bp	ARKSIL - 172 bp

	TTAAC Reverse: 5' taatacgactcactatagggagaGGACAGACTTGTAGACTCCGACT		downstream of stop codon
Dmac-h 5'	Forward: 5' taatacgactcactatagggagaCATCCTAGAAAAGGCCGACA Reverse: 5' taatacgactcactatagggagaAGGATGTGGACCTGAACCTG	258 bp	ILEKAD - QVQVHI
Dmac-h 3'	Forward: 5' taatacgactcactatagggagaGTGTCCAATTAGTGCCCACA Reverse: 5' taatacgactcactatagggagaGGAAAGTGGTTTCTGCATGG	248 bp	VQLVPT - MQKPLS
Dmac-slp 5'	Forward: 5' taatacgactcactatagggagaCAAGGATGGCAAAATTCGAT Reverse: 5' taatacgactcactatagggagaCCGAAAGGATTCACCTGGTA	251 bp	QGWQNS YQVNPF
Dmac-slp 3'	Forward: 5' taatacgactcactatagggagaCCTCTTCAAACCCGTACCAG Reverse: 5' taatacgactcactatagggagaTGCGATCGTGTGCTCTTTTA	258 bp	LFKPVP - 218 bp downstream of stop codon
Dmac-opa 5'	Forward: 5' taatacgactcactatagggagaTGGTCAATCACATCAGAGTGC Reverse: 5' taatacgactcactatagggagaGCGAATGCTTCTTCCTATCC	195 bp	VNHIRV - DRKKHS
Dmac-opa 3'	Forward: 5' taatacgactcactatagggagaTCGCTGAGGAAGCATATGAA Reverse: 5' taatacgactcactatagggagaCTGGCAGGAAACGTACCACT	247 bp	SLRKHM - WYVSCQ
Dmac-ftz 5'	Forward: 5' taatacgactcactatagggagaGACACAGGCGACTGCAAAT Reverse: 5' taatacgactcactatagggagaTAACTGCCGGTGTTGGTGTA	673 bp	45 bp upstream of start site - TPTPAV

Dmac-ftz 3'	Forward: 5' taatacgactcactatagggagaCACTGAAGACATCAACATGAATCAG Reverse: 5' taatacgactcactatagggagaAGAGCTCTTCGCGTAAAAATAAG	233 bp	TEDINMNQ - 40 bp downstream of stop codon
Dmac-ff1 5'	Forward: 5' taatacgactcactatagggagaGGACGCGTCGTATTTGTTTT Reverse: 5' taatacgactcactatagggagaATGATCATGGAGGTGTGTGG	735 bp	DASYLF - PHTSMI
Dmac-ff1 3'	Forward: 5' taatacgactcactatagggagaGCAGAACTTACTTTATGGACTC Reverse: 5' taatacgactcactatagggagaCTTCTGGGTAACATGAAATG	512 bp	QNLLYGL - ISLYPE

Part VI: Primers for qPCR

Gene name	Sequence	Primer length	Target product size
eve	Forward: CATGTCGGAAATCCATCGGT	20 bp	117 bp
	Reverse: GCCGCTTAGGTTGAGGTTTA	20 bp	
odd	Forward: CCCAACAATCGGAAGCAAAC	20 bp	99 bp
	Reverse: TCAAATCTAGGCAGGTGGATG	21 bp	
run	Forward: TCTGAGGATGAAGATATCGATGTTG	25 bp	88 bp
	Reverse: CAGGATGTTGGATTTCTTGCAG	22 bp	
h	Forward: ATCAAGGGAAGCAGGAAGTG	20 bp	104 bp
	Reverse: CTGTTGCTGTTGAGCTGTTATC	22 bp	
slp	Forward: CTTTTAAGCGCACGATGGTTC	21 bp	97 bp
	Reverse: TTCGGATATAGGCCCACAAAC	21 bp	
prd	Forward: AATGAAGGCGGGTCTGATTG	20 bp	93 bp
	Reverse: TAGCTGATGTGCGGTGAAAG	20 bp	
opa	Forward: CCTCCGACAAGCCGTATAATTG	22 bp	136 bp
	Reverse: TCCTCTCCATCGCTTTCATAATG	23 bp	
ftz	Forward: ACCAACACCGGCAGTTATAC	20 bp	146 bp
	Reverse: GTCTTGTCCTTTTACCACCATG	22 bp	
ff1	Forward: CACGACGTCACCTCATTCC	19 bp	116 bp
	Reverse: CCTGCACAAAGTCCCTGATAA	21 bp	

COI	Forward: TGGAGGAGCTTCTGTTGATTTA	22 bp	76 bp
	Reverse: GTTTACTGCTCCAAGAATTGAAGA	24 bp	
16s rRNA	Forward: ATGAATGGCTAGACGAGAGAAATAG	25 bp	106 bp
	Reverse: ACTCTATAGGGTCTTCTCGTCTTT	24 bp	

Appendix II. Isolated *D. maculatus* Gene Sequences

COI

```
aactttatatttcatctttggagcatgagcaggtatagtaggaacatccctaagaatacta
  T   L   Y   F   I   F   G   A   W   A   G   M   V   G   T   S   L   S   M   L
attcgaacagaattaggtatacctggatctctaattggtgacgatcaaatttttaatgta
 I   R   T   E   L   G   M   P   G   S   L   I   G   D   D   Q   I   F   N   V
attgttacagctcatgcatttattataatttttttcatagtaatacctattataattggt
 I   V   T   A   H   A   F   I   M   I   F   F   M   V   M   P   I   M   I   G
ggatttggaaattgattagttccattaatattaggagctcctgatatagcatttccccga
 G   F   G   N   W   L   V   P   L   M   L   G   A   P   D   M   A   F   P   R
ataaataatataagattttgacttcttccaccatctttatctcttttattaataagaaga
 M   N   N   M   S   F   W   L   L   P   P   S   L   S   L   L   L   M   S   S
atggtagaaagaggagcaggaacaggatgaacagtttatccacccctatcagctaatatt
 M   V   E   S   G   A   G   T   G   W   T   V   Y   P   P   L   S   A   N   I
gcacatggaggagcttctgttgatttagcaatttttagattacatcttgcaggaatttct
 A   H   G   G   A   S   V   D   L   A   I   F   S   L   H   L   A   G   I   S
tcaattcttggagcagtaaactttattactacagtaattaatatacgatcaaaaggaata
 S   I   L   G   A   V   N   F   I   T   T   V   I   N   M   R   S   K   G   M
actcctgatcgaatacctttatttgtttgatcagtagcaattactgctttactactactt
 T   P   D   R   M   P   L   F   V   W   S   V   A   I   T   A   L   L   L   L
ttatctctaccagttcttgctggagcaattacaatattattaactgatcgaaatctaaat
 L   S   L   P   V   L   A   G   A   I   T   M   L   L   T   D   R   N   L   N
acttcattctttgatcctgcaggaggtggagatcctattctttatcaacacttattc
 T   S   F   F   D   P   A   G   G   G   D   P   I   L   Y   Q   H   L   F
```

prd

```
attaaaatcgtcgagatggcggcggctggtgtaagaccgtgtgtcgtctcaagacagtta
 I   K   I   V   E   M   A   A   A   G   V   R   P   C   V   V   S   R   Q   L
agggtgtctcatggatgtgtcagcaaaattctcaacagatatcaagaaacaggctcgatt
 R   V   S   H   G   C   V   S   K   I   L   N   R   Y   Q   E   T   G   S   I
cgtcccggagtcatcggtggttcgaaaccaagagtggcaactccggaagtagaaaaccgt
 R   P   G   V   I   G   G   S   K   P   R   V   A   T   P   E   V   E   N   R
attgagcaatataagcgtgaaaatccatcaattttcagttgggaaattcgcgatcgtctc
 I   E   Q   Y   K   R   E   N   P   S   I   F   S   W   E   I   R   D   R   L
gtcaaggaagggatttgtgacagaagtacagccccgagtgtctcggcgatttcccgcctt
 V   K   E   G   I   C   D   R   S   T   A   P   S   V   S   A   I   S   R   L
ttgcgtgggaaaggtgcagattgtgaagataagtcgtcggacaatgaaggcgggtctgat
 L   R   G   K   G   A   D   C   E   D   K   S   S   D   N   E   G   G   S   D
tgcgacagtgaacctgggatcccattgaaaaggaaacagagaagatctcggaccactttc
 C   D   S   E   P   G   I   P   L   K   R   K   Q   R   R   S   R   T   T   F
accgcacatcagctagacgaattagaaaaagcttttgagagaactcaatatcctgatatc
 T   A   H   Q   L   D   E   L   E   K   A   F   E   R   T   Q   Y   P   D   I
tacaccagagaagagctggcccaaagaaccaagttgactgaagctagaatacaggtttgg
 Y   T   R   E   E   L   A   Q   R   T   K   L   T   E   A   R   I   Q   V   W
ttcagcaacagaagggcgagactacgaaaacagttggcttcaacatcatcttcttacaca
 F   S   N   R   R   A   R   L   R   K   Q   L   A   S   T   S   S   S   Y   T
cctttaggtgttgtcagtggtccatacaccacccctttcaactccatacgcaccaattgga
 P   L   G   V   V   S   G   P   Y   T   T   P   S   T   P   Y   A   P   I   G
caatcaattagcgaaggaagttttgtaacaacatcaacaacgtctaccaatcaaatgaca
 Q   S   I   S   E   G   S   F   V   T   T   S   T   T   S   T   N   Q   M   T
gaactgtacccaagccatggtcattctacttcaccaaacttacctttgacaactcataat
 E   L   Y   P   S   H   G   H   S   T   S   P   N   L   P   L   T   T   H   N
```

```
ccgtattcaacacattccatatatcagacttcaaacattaacaatatcatgccaatgaca
 P  Y  S  T  H  S  I  Y  Q  T  S  N  I  N  N  I  M  P  M  T
accatgacaaccccaagctcccttaactcgcatgtgcaaccgagttcatcacctatcaac
 T  M  T  T  P  S  S  L  N  S  H  V  Q  P  S  S  S  P  I  N
cccttagctggtggcattcaaaacctaagccaaagctctgttggtgctggttacaaagaa
 P  L  A  G  G  I  Q  N  L  S  Q  S  S  V  G  A  G  Y  K  E
gaaaaccaagtgaccgaatcatcaagtccaggaattcaacagcagacttacactaacatg
 E  N  Q  V  T  E  S  S  S  P  G  I  Q  Q  Q  T  Y  T  N  M
ccgcctacaccaacaagcatggtgacaattctaggacctaacagtgccaatagcaacagc
 P  P  T  P  T  S  M  V  T  I  L  G  P  N  S  A  N  S  N  S
aatgaacctagttgtactgaagttagtagcaacaacaataatctgcaacatctcaaccac
 N  E  P  S  C  T  E  V  S  S  N  N  N  N  L  Q  H  L  N  H
caatggtcaacggccccaatgccacgccagcccagtccaacaaacctaaaccaaccactt
 Q  W  S  T  A  P  M  P  R  Q  P  S  P  T  N  L  N  Q  P  L
tctacaactctaggccaaattggacaacaactaggagtgcattcccaaactctatcgagc
 S  T  T  L  G  Q  I  G  Q  Q  L  G  V  H  S  Q  T  L  S  S
tttggccaaaacagccttcacacttatggaacccataatccatcaaaaaccttcggccac
 F  G  Q  N  S  L  H  T  Y  G  T  H  N  P  S  K  T  F  G  H
caaccattctatggttggtattaa
 Q  P  F  Y  G  W  Y  -
```

gsb

```
ctagtgattaagatcgttgaaatggcagccgccggaatccggccctgtgtcatttcgcga
 L  V  I  K  I  V  E  M  A  A  A  G  I  R  P  C  V  I  S  R
caactccgggtttctcatgggtgcgtttccaaaattctgaaccgctaccaagaaaccgga
 Q  L  R  V  S  H  G  C  V  S  K  I  L  N  R  Y  Q  E  T  G
agcatcagacctggggttattggtggctcgaaaccgagggttgcaactgctgaagttgag
 S  I  R  P  G  V  I  G  G  S  K  P  R  V  A  T  A  E  V  E
gccagaattgagcagttgaaaaagcagcaacctgggatattttcgtatgaaataagggat
 A  R  I  E  Q  L  K  K  Q  Q  P  G  I  F  S  Y  E  I  R  D
aagctgataaaggagggcatttgcgataagaattcagctccttctgtcagttcaatcagc
 K  L  I  K  E  G  I  C  D  K  N  S  A  P  S  V  S  S  I  S
agattgttgcgaggcggaagaagagacgacgctgacagaaagaatcattccatcgatggc
 R  L  L  R  G  G  R  R  D  D  A  D  R  K  N  H  S  I  D  G
attttaggcccaaattcttcgtgcgaagaaagtgatactgaatccgaacctgggataccg
 I  L  G  P  N  S  S  C  E  E  S  D  T  E  S  E  P  G  I  P
ttgaagaggaagcagcgtcgttccagaacgacctttactggggagcaattggaagcttta
 L  K  R  K  Q  R  R  S  R  T  T  F  T  G  E  Q  L  E  A  L
gaacgcgctttcggaaggacccagtaccccgacgtctataat
 E  R  A  F  G  R  T  Q  Y  P  D  V  Y  N
```

gsb-n

```
attaagatcgtggaaatggctgcagctggaatacggccgtgtgttatttcacgtcagctt
 I  K  I  V  E  M  A  A  A  G  I  R  P  C  V  I  S  R  Q  L
agggtttcgcatggttgtgtatcgaaaatattgaatcgctatcaagaaacaggcagcatc
 R  V  S  H  G  C  V  S  K  I  L  N  R  Y  Q  E  T  G  S  I
cgacctggggttattgggggctctaagccaagagtcgcgactccagaagtcgaggctaga
 R  P  G  V  I  G  G  S  K  P  R  V  A  T  P  E  V  E  A  R
attgagcaaatcaaaagacaacaacccaccatattctcctgggaaatacgagagaagctt
 I  E  Q  I  K  R  Q  Q  P  T  I  F  S  W  E  I  R  E  K  L
atcaaagaaggagtcgccgatcctccgagtgtttcttctatcagtcgcctcttaagaggt
 I  K  E  G  V  A  D  P  P  S  V  S  S  I  S  R  L  L  R  G
ggtggaagacgcgacgatcctgatggcaagaaagattacaccatcgacggcatccttggg
 G  G  R  R  D  D  P  D  G  K  K  D  Y  T  I  D  G  I  L  G
ggtcgagaagaagacagcgatacagaatctgagccagggattccgctgaagcggaagcaa
 G  R  E  E  D  S  D  T  E  S  E  P  G  I  P  L  K  R  K  Q
```

```
cgcaggtcgaggacaacattttcaggggaacaactggaagctttggaacgagctttcgga
 R  R  S  R  T  T  F  S  G  E  Q  L  E  A  L  E  R  A  F  G
aggactcagtatcccgacgtatataatcac
 R  T  Q  Y  P  D  V  Y  N  H
```

eve

```
cggacggcgttcacgcgggatcagctggcgcgtttggaaaaagagttctacaaagaaaac
 R  T  A  F  T  R  D  Q  L  A  R  L  E  K  E  F  Y  K  E  N
tatgtgtccagacctaggcgctgtgaactcgcggcgcaattaaacctcccggaaagcacc
 Y  V  S  R  P  R  R  C  E  L  A  A  Q  L  N  L  P  E  S  T
atcaaagtctggttccaaaataggaggatgaaggataagagacagaggctggcgattgct
 I  K  V  W  F  Q  N  R  R  M  K  D  K  R  Q  R  L  A  I  A
tggccatacgcggcggtgtacaccgatccagcttttgctgcctcaattctgcacgccgcc
 W  P  Y  A  A  V  Y  T  D  P  A  F  A  A  S  I  L  H  A  A
gctcagactttgccgctgcattatgcgcctccgcccccgatgtactcgcataattatcca
 A  Q  T  L  P  L  H  Y  A  P  P  P  P  M  Y  S  H  N  Y  P
cgttatcatccgtatactggttttggggttccgcagcatgtcggaaatccatcggtgacg
 R  Y  H  P  Y  T  G  F  G  V  P  Q  H  V  G  N  P  S  V  T
gctccgccgatgctcaaccatcagcttccgccgatccccacgaccataccacaaccccaa
 A  P  P  M  L  N  H  Q  L  P  P  I  P  T  T  I  P  Q  P  Q
ctgccttcaggcctaaacctcaacctaagcggcctagacttcggcccttcatcatacccc
 L  P  S  G  L  N  L  N  L  S  G  L  D  F  G  P  S  S  Y  P
aaattcacgactcaaacccaccaccacgtatcgccaacacattcgcccgtcgcctcagaa
 K  F  T  T  Q  T  H  H  H  V  S  P  T  H  S  P  V  A  S  E
ctcagcctcagccccccctgtccacgacggcttattaatcccctcgcgaacctcccccgaa
 L  S  L  S  P  P  V  H  D  G  L  L  I  P  S  R  T  S  P  E
cgaacaacgctcccggaaaagccgaaactgttcaaaccctacaaatccgaagcgtaaccg
 R  T  T  L  P  E  K  P  K  L  F  K  P  Y  K  S  E  A  -
ccggcacgctccgcaaacagaaaatgtgattttaatattatttagtagtcgataataatt
tattgtacatagtccgagggaaataggcgaaagagattgttattatattgtttctttaat
attatgtctttaagatggattttctttgtaaatagttcttgtatagctgtgattttaatt
tttgtaaatagttttaatacttattttcaatgctgtggattttccttgatggaacgcata
atttgtattaagacaggaataaatgaatatatcttacgtaaaaaaaaaaaaa
```

odd

```
gaacgcacccacactgacgaacgcccatattcgtgcgacatctgcggaaaagccttcaga
 E  R  T  H  T  D  E  R  P  Y  S  C  D  I  C  G  K  A  F  R
agacaagaccatctcagagatcacagatacatccacagcaaagagaagccattcaaatgc
 R  Q  D  H  L  R  D  H  R  Y  I  H  S  K  E  K  P  F  K  C
ggcgaatgcggaaagggtttctgccaatcgcgaactttggccgtccacaagattttgcac
 G  E  C  G  K  G  F  C  Q  S  R  T  L  A  V  H  K  I  L  H
atggaagaatcgccgcataaatgccccgtttgcaacaggagcttcaatcagcgctcgaat
 M  E  E  S  P  H  K  C  P  V  C  N  R  S  F  N  Q  R  S  N
ttaaaaacgcatctgctgacgcacacagaacgtccgctcgaatgcaatatgtgctctcaa
 L  K  T  H  L  L  T  H  T  E  R  P  L  E  C  N  M  C  S  Q
ttattcacgtcctacaacgatttgaaaacgcacgaactgcgacatatgccccaacaatcg
 L  F  T  S  Y  N  D  L  K  T  H  E  L  R  H  M  P  Q  Q  S
gaagcaaaccaaacacctccgccgccgcctcaacaagaaatcgtgatgctaacaacgccg
 E  A  N  Q  T  P  P  P  P  P  Q  Q  E  I  V  M  L  T  T  P
ccatcgccatccacctgcctagatttgacgacgaaaaagctcgaggacgaaaagccggcg
 P  S  P  S  T  C  L  D  L  T  T  K  K  L  E  D  E  K  P  A
aaaaaacctctgggcttcagcatagaggaaatcatgaagcgataaagcattccgccgcca
 K  K  P  L  G  F  S  I  E  E  I  M  K  R  -
aaaataatgccaaagacccctctacctctctctttcttttgttccttctcccccgccgg
caagactgagaaagttaccacaaattcgaaaagttcgaacaatgagatctctctcgc
```

run

```
gttgcgacatacaccaaagccatcaaagtcaccgtcgatggtccgcgagaaccaagaacc
 V  A  T  Y  T  K  A  I  K  V  T  V  D  G  P  R  E  P  R  T
aaatcaaatttccagtatggatatggattgccagggatgccaggagctttcaatcccttt
 K  S  N  F  Q  Y  G  Y  G  L  P  G  M  P  G  A  F  N  P  F
ttgctcaaccctggatggtttgatgctgcttatatttcttatgcgtggcctgattatttc
 L  L  N  P  G  W  F  D  A  A  Y  I  S  Y  A  W  P  D  Y  F
cgcagcagacctgctggtggacttcctcaaaatattcatccaagtttgatgaaagaaaca
 R  S  R  P  A  G  G  L  P  Q  N  I  H  P  S  L  M  K  E  T
ccgcctttgcctcaacctcctcgggagttttatcagccgcaaggcttccagcaaagcttt
 P  P  L  P  Q  P  P  R  E  F  Y  Q  P  Q  G  F  Q  Q  S  F
gtaccgccaaatggtttagttccacctttttcgccgccaagtgatatccctaaatctttt
 V  P  P  N  G  L  V  P  P  F  S  P  P  S  D  I  P  K  S  F
gataatttccatcttcggcctgtgcctccttcgccctttagaacaactcagtttacgtgtt
 D  N  F  H  L  R  P  V  P  P  S  P  L  E  Q  L  S  L  R  V
tccccagtttcaaacgcgcaaagtatgagtccccaaactcaagatcgcgacatgaggatc
 S  P  V  S  N  A  Q  S  M  S  P  Q  T  Q  D  R  D  M  R  I
aactcaaccgtcgatcaacaatcagaagattctgaggatgaagatatcgatgttgtcaaa
 N  S  T  V  D  Q  Q  S  E  D  S  E  D  E  D  I  D  V  V  K
tctgccttcgtccctatcaaacccgctagtttaatgctgcaagaaatccaacatcctgat
 S  A  F  V  P  I  K  P  A  S  L  M  L  Q  E  I  Q  H  P  D
tctacagttgaagataaagaaacgatacgtgttaaatgcgaactcaaagcgccgagtgcg
 S  T  V  E  D  K  E  T  I  R  V  K  C  E  L  K  A  P  S  A
cgaaagagcattttaacatcgccgtcgacaacaaaactgcagccccaaaaccaaaccaaa
 R  K  S  I  L  T  S  P  S  T  T  K  L  Q  P  Q  N  Q  T  K
acagtttggaggccctattaatatttgagagcatcaaagaagcgatctgtgtatagacaa
 T  V  W  R  P  Y  -
ttttgcgtgtaaatatttgtataaacgtgacgcgatagtatttatattatagtaattgt
aaatgttgtaaatatttgtaaaaaagatgatctatttaacactgtttcatagtcggagtc
tacaagtctgtccaatgttctt
```

h

```
atggagaagaggcgaagggcccgcatcaacaattgtctgaatgaactcaaaaccctcatc
 M  E  K  R  R  R  A  R  I  N  N  C  L  N  E  L  K  T  L  I
ttagacgctatgaaaaaagaccccgcccgacattccaaattagagaaggccgacattctc
 L  D  A  M  K  K  D  P  A  R  H  S  K  L  E  K  A  D  I  L
gagatgactgtgaagcatttgcaaaatcttcaaaggcaacaagccgcgatttcggcggcc
 E  M  T  V  K  H  L  Q  N  L  Q  R  Q  Q  A  A  I  S  A  A
actgatccagctgtactcaacaagtttagggccggtttcagcgagtgtgcgagcgaagtt
 T  D  P  A  V  L  N  K  F  R  A  G  F  S  E  C  A  S  E  V
ggacgttttcctggactagagccggtggttaaacgtcgccttctgcagcacctcgctaat
 G  R  F  P  G  L  E  P  V  V  K  R  R  L  L  Q  H  L  A  N
tgcttgaatcaagggaagcaggaagtggcttcgcaggttcaggtccacatccttcccagc
 C  L  N  Q  G  K  Q  E  V  A  S  Q  V  Q  V  H  I  L  P  S
cccggcgacaatgttggcggccaaaatgtgataacagctcaacagcaacagcctaatggg
 P  G  D  N  V  G  G  Q  N  V  I  T  A  Q  Q  Q  Q  P  N  G
attattttgagtaacggtaacggcggcggtgtccaattagtgcccacacgtttgcccaac
 I  I  L  S  N  G  N  G  G  G  V  Q  L  V  P  T  R  L  P  N
ggggatatcgccctagttttgcccacgtctgcgaccacgacacccacctcgacacctagc
 G  D  I  A  L  V  L  P  T  S  A  T  T  T  P  T  S  T  P  S
agcagctcgccactacccctcctcgtcccgataccatcgcgaacagcctcaacggcttca
 S  S  S  P  L  P  L  L  V  P  I  P  S  R  T  A  S  T  A  S
gcgtcgtcatcatcatcctcccactattcaccctcaaacagtcccgaacccatggacacg
 A  S  S  S  S  S  S  H  Y  S  P  S  N  S  P  E  P  M  D  T
ctcaattacaacccacccatgcagaaaccactttccttagtgatacgcaagaacgaaccc
 L  N  Y  N  P  P  M  Q  K  P  L  S  L  V  I  R  K  N  E  P
```

```
gtcgaagaagagaaaccctggaggccgtggtga
 V  E  E  E  K  P  W  R  P  W  -
```

slp

```
aagaggttgaccctcaacggcatctacgaatatatcatgcgcaacttcccttattaccgc
 K  R  L  T  L  N  G  I  Y  E  Y  I  M  R  N  F  P  Y  Y  R
gagaataagcaaggatggcaaaattcgatcagacacaatttgagtttgaacaaatgtttc
 E  N  K  Q  G  W  Q  N  S  I  R  H  N  L  S  L  N  K  C  F
gttaaagttccgcgtcattatgatgatcctggcaaaggtaattactggatgttagatcct
 V  K  V  P  R  H  Y  D  D  P  G  K  G  N  Y  W  M  L  D  P
tctgctgaagacgtttttattggtggcacgacggggaaattgcggcgaagatcgacggcg
 S  A  E  D  V  F  I  G  G  T  T  G  K  L  R  R  R  S  T  A
gcgtctaggtctagattggctgcttttaagcgcacgatggttcttggtgccgccggtatg
 A  S  R  S  R  L  A  A  F  K  R  T  M  V  L  G  A  A  G  M
taccaggtgaatccttttcggcggtgctccttacaatccgtttgtgggcctatatccgaat
 Y  Q  V  N  P  F  G  G  A  P  Y  N  P  F  V  G  L  Y  P  N
ccggctttattagcgtcggcaatgtaccaccaacaaaggtacggcagcaatccgtatttt
 P  A  L  L  A  S  A  M  Y  H  Q  Q  R  Y  G  S  N  P  Y  F
caaccatcggttttggctaaaccaacaccgataccggcagcggttgcggctgccgccacg
 Q  P  S  V  L  A  K  P  T  P  I  P  A  A  V  A  A  A  A  T
tccgcaactcaagcgttcagcatggaaaggctgttggcacccagcgaggcggctacaaac
 S  A  T  Q  A  F  S  M  E  R  L  L  A  P  S  E  A  A  T  N
tttttacgccaccaccatcaaccgcctccaggtttagatatataccaggctggcattaga
 F  L  R  H  H  H  Q  P  P  P  G  L  D  I  Y  Q  A  G  I  R
ttaccgctgcaattccctccaagccacccgcagcatctgcaaccgcaacaccaccaccag
 L  P  L  Q  F  P  P  S  H  P  Q  H  L  Q  P  Q  H  H  H  Q
cagcacgcgttgtcaccttcaagcagctctagctcgccagagccgcgcaatgaaaacctc
 Q  H  A  L  S  P  S  S  S  S  S  S  P  E  P  R  N  E  N  L
ttcaaacccgtaccagtgataacgcgacaaagttgaaaatcatcacgacaaagactttcg
 F  K  P  V  P  V  I  T  R  Q  S  -
tccccagtgattgatctcatcacaccaccctcgaagtaacataaacgtccacatcgcaca
cacacccacacactttcacccctaacttattatggactaactaactcgtaactgtgttt
ttaattaatttgtgtatatataagctagacagctggctgtaaaacttttgtatataaaag
agcacacgatcgcaagcgaaaagtgttgtaacgcatattgtaaatattgtaaatgattgt
tttctttttgtatatatcgcctatacatatataatatatggattattttaataaataga
tatgactggaaaaaaaaaaa
```

opa

```
aaatataaactggtcaatcacatcagagtgcacacgggcgaaaagccgtttccatgtccg
 K  Y  K  L  V  N  H  I  R  V  H  T  G  E  K  P  F  P  C  P
ttccccggctgcggcaaagtcttcgccagaagtgaaaacctcaaaatacacaaaaggacg
 F  P  G  C  G  K  V  F  A  R  S  E  N  L  K  I  H  K  R  T
cataccggcgagaagccgttcaagtgcgagttcgagggctgcgataggcggtttgccaat
 H  T  G  E  K  P  F  K  C  E  F  E  G  C  D  R  R  F  A  N
tcgtcggataggaagaagcattcgcacgtgcacacctccgacaagccgtataattgtcgc
 S  S  D  R  K  K  H  S  H  V  H  T  S  D  K  P  Y  N  C  R
gtggctggttgcgacaagtcgtacacccacccgtcgtcgctgaggaagcatatgaaggtg
 V  A  G  C  D  K  S  Y  T  H  P  S  S  L  R  K  H  M  K  V
cacgggtgttcggggaggtcgccgccgcattatgaaagcgatggagaggagtcgaattcg
 H  G  C  S  G  R  S  P  P  H  Y  E  S  D  G  E  E  S  N  S
tcctcggctggtagcatttcggtggcggctagtccgcatgttggcgtcgcggctcctcag
 S  S  A  G  S  I  S  V  A  A  S  P  H  V  G  V  A  A  P  Q
gtccaggttcaagtgccggcgacggcggctgccctcagcgagtggtacgtttcctgccag
 V  Q  V  Q  V  P  A  T  A  A  A  L  S  E  W  Y  V  S  C  Q
acgacgccagcgccggacgcgctcggtggcctcgccggccacttcggccagctgcaccac
 T  T  P  A  P  D  A  L  G  G  L  A  G  H  F  G  Q  L  H  H
```

```
cacaccggcgcggccaccgcctactgatgacacgccacccccttcggaagacgaccaagat
 H  T  G  A  A  T  A  Y  -
ctctaccctcaccgccaccatcaaaacaggacgacgcgactgtgaaaaccgcgtgcgtct
ataagacgagtgatataaaccgagtgccccgaactaaagacattctaaaatcagccacaa
ctgcacactttcaacaaggacgcggcgaattatgaaaaaaaaaaaaaa
```

Scr

```
attccgcagatctatccatggatgaagagagtacatttgggccaaagtactgttaatgca
 I  P  Q  I  Y  P  W  M  K  R  V  H  L  G  Q  S  T  V  N  A
aatggggagacaaaaagacaaaggacatcttatacacgctaccaaactttggagttggaa
 N  G  E  T  K  R  Q  R  T  S  Y  T  R  Y  Q  T  L  E  L  E
aaagagttccattttaatcgttaccttacccgccgacgacgtatcgagatcgcgcacgca
 K  E  F  H  F  N  R  Y  L  T  R  R  R  R  I  E  I  A  H  A
ctttgcttaacagaaagacagataaaaatctggttccagaaccgccgcatgaaatggaaa
 L  C  L  T  E  R  Q  I  K  I  W  F  Q  N  R  R  M  K  W  K
aaggaacataagatggccagtatgaatatcgttccttaccacatgtctccttacggacat
 K  E  H  K  M  A  S  M  N  I  V  P  Y  H  M  S  P  Y  G  H
ccctatcaatttgacttgcatcctagtcagtttgcacatcttgctacttaggatgctttt
 P  Y  Q  F  D  L  H  P  S  Q  F  A  H  L  A  T  -
gtctcatactcgtttttataggtatttttatttttatttttgtttgtatctatttttgtcg
cggctttattaacttatagcacttttttatgtaatatctgtttatgtttgcatgatttgta
aatattgttgcgctaacaacaagcaaattcggaaatatacagggagacactgataatgtg
cttaaatgcgcacaccttgtaattaataacttttgaataaaacaaagaacataactgtc
attaccaaaaataaaaatttattaaattaaatatttcttaaatgttattgaaatctttta
aatttttattgttctttgagttatgataattaattacatttacgtttctaaaattgttaa
aaaaaacagtcaaatcaaacaaaatcaaatagaatgttgttttgtaaatatgtgaatata
ttaattttatcttaaaatttaaaaaaatatgaaattgttaagttatattactgctagttt
tcatttcttacttttttgttaaaacatcattgattctgttatttattatttttaagtatg
tatgtaggatttaaaaccatttttgcttcccatattgttaattttgaatagaataaaaa
tagaaatcaaaaagttaaaaaaaaaaaa
```

Antp

```
gattccgcagatctacccgtggatgaggagtcagtttgaaagaaaaaggggccgccaaacg
  I  P  Q  I  Y  P  W  M  R  S  Q  F  E  R  K  R  G  R  Q  T
tatacgcgctaccaaacgctggaattagagaaggaatttcattttaacaggtaccttact
 Y  T  R  Y  Q  T  L  E  L  E  K  E  F  H  F  N  R  Y  L  T
cgacggcgacgcatagaaatcgcacatgcattgtgtttgaccgaaaggcagatcaaaatc
 R  R  R  R  I  E  I  A  H  A  L  C  L  T  E  R  Q  I  K  I
tggttccaga
 W  F  Q
```

***pb* (*proboscipedia*)**

```
gattccacagatatatccatggatgaaagaaaaaaagaccacccgaaaaagtagtcaacaa
  I  P  Q  I  Y  P  W  M  K  E  K  K  T  T  R  K  S  S  Q  Q
gaaaatggacttccacggaggttgagaactgcgtatacaaatacacagctattggaattg
 E  N  G  L  P  R  R  L  R  T  A  Y  T  N  T  Q  L  L  E  L
gaaaaggaatttcatttcaacaaatatctttgccggcctaggcgaattgaaattgcagcg
 E  K  E  F  H  F  N  K  Y  L  C  R  P  R  R  I  E  I  A  A
tcgttagatcttacggaaagacaggtgaaagtgtggtttcagaaccggcgcaatcact
 S  L  D  L  T  E  R  Q  V  K  V  W  F  Q  N  R  R  N  H
```

abd-A (*abdominal-A*)

```
gattccgcaaatttatccatggatgtcaattacagattggatgagcccatttgaccgtgtc
  I   P   Q   I   Y   P   W   M   S   I   T   D   W   M   S   P   F   D   R   V
gtgtgcggtgagtacaatggtccgaatggttgtcctcggagacggggaagacaaacatac
 V   C   G   E   Y   N   G   P   N   G   C   P   R   R   R   G   R   Q   T   Y
acgcgatttcaaacattggaattagagaaagaatttcattttaatcattatttgacgcga
 T   R   F   Q   T   L   E   L   E   K   E   F   H   F   N   H   Y   L   T   R
cggcgacgtattgaaatagcgcacgccttatgtttaacagaaaggcagataaaaatatgg
 R   R   R   I   E   I   A   H   A   L   C   L   T   E   R   Q   I   K   I   W
ttccagaaccgccgaatcactagt
 F   Q   N   R   R   I   T   S
```

Dfd (*Deformed*)

```
gattccgcagatctacccgtggatgcgaaaagtacacgtggccggtgcttcgaacggttcc
  I   P   Q   I   Y   P   W   M   R   K   V   H   V   A   G   A   S   N   G   S
ttcacacctggaatggaacctaagagacaacgcacggcatacacgaggcatcaaattttg
 F   T   P   G   M   E   P   K   R   Q   R   T   A   Y   T   R   H   Q   I   L
gaactggaaaaagagtttcactacaacagatacttgactcgcagaagacgaatagaaata
 E   L   E   K   E   F   H   Y   N   R   Y   L   T   R   R   R   R   I   E   I
gcacacacgctggtgctttcagagagacaaattaaaatctggttccaaaaccgacgaaat
 A   H   T   L   V   L   S   E   R   Q   I   K   I   W   F   Q   N   R   R   N
c
```

Ubx (*Ultrabithorax*)

```
gattccgcagatatatccgtggatggccatagcaggtgcaaacggacttcgacgaagaggt
  I   P   Q   I   Y   P   W   M   A   I   A   G   A   N   G   L   R   R   R   G
cgtcagacgtatacaagataccagacattagagttggaaaaggaatttcacacgaaccac
 R   Q   T   Y   T   R   Y   Q   T   L   E   L   E   K   E   F   H   T   N   H
tatctaacacggcggaggcgaattgaaatggcacatgccttatgtctaacagaaagacag
 Y   L   T   R   R   R   R   I   E   M   A   H   A   L   C   L   T   E   R   Q
attaaaatttggtttcagaatcggngtaatcact
 I   K   I   W   F   Q   N   R   X   N   H
```

caudal (*cad*)

```
aagacgcggacgaaggacaaataccgagtcgtgtacacggaccatcaaagaatagaattg
 K   T   R   T   K   D   K   Y   R   V   V   Y   T   D   H   Q   R   I   E   L
gagaaagaatttacttttaacaatcagtacattacaatccgccgtaaaagtgaactcgcg
 E   K   E   F   T   F   N   N   Q   Y   I   T   I   R   R   K   S   E   L   A
gcaactttaggtctctccgaaaggcaaattaagatctggttccaaaacaggcgcgcaaaa
 A   T   L   G   L   S   E   R   Q   I   K   I   W   F   Q   N   R   R   A   K
caacgcaagcaagtcaagaagcgcaacgaagaaaagaaccaacttgaaaatcaaattact
 Q   R   K   Q   V   K   K   R   N   E   E   K   N   Q   L   E   N   Q   I   T
cagcaacagcagacgccaaattacaacatgtatcaaaatcagcaaagtcttcttcagcaa
 Q   Q   Q   Q   T   P   N   Y   N   M   Y   Q   N   Q   Q   S   L   L   Q   Q
cagcaccaacagatgcagcagttagccgccgtggctaattcagcgcctagcagcagccct
 Q   H   Q   Q   M   Q   Q   L   A   A   V   A   N   S   A   P   S   S   S   P
attctgaattcgataatgccaacgtcaccacagagcatagcaacatctcacatttccatg
```

```
 I  L  N  S  I  M  P  T  S  P  Q  S  I  A  T  S  H  I  S  M
gatcatataaaatgtgaacctgaacccatggcatgatcatttttataaaatgatcgacac
 D  H  I  K  C  E  P  E  P  M  A  -
agatatccacaatagtggatgcaggccggataaaacactaataattcaattcaattattg
gcaagtgcaattttccagtgcaatttgaagcattgtttaactttagtaataattataata
tatttagtcagttgagcttcccacattaactttatgtaattataacttgtaaagaatgtt
ttaaacgtgtttgctgactccagactgcagatcggagtttgctgcatgattctagctatt
acctaattgttttctaaattantaccttacttggttagatataatttaaaatgttacga
tatantttgttattagagagtgtgattgtatgtgaagatgggattttatttatataanag
tgtggtcatagagagtgttcaataataaaaataaatantttattaataaaaaaaaaaa
```

en

```
gacaagcggccgcggacagcattttcaggagcccaactagcacgtttaaaacatgaattc
 D  K  R  P  R  T  A  F  S  G  A  Q  L  A  R  L  K  H  E  F
gctgaaaaccgatacttgaccgaacgtcgacgccagcaactaagtgcggaacttggttta
 A  E  N  R  Y  L  T  E  R  R  R  Q  Q  L  S  A  E  L  G  L
aacgaagcccaaatcaaaatctggttccaaaacaaaagggcaaaaattaaaaaagcttca
 N  E  A  Q  I  K  I  W  F  Q  N  K  R  A  K  I  K  K  A  S
ggtcaaaagaatcctttagctttacaacttatggcacaaggtttgtacaatcattcaaca
 G  Q  K  N  P  L  A  L  Q  L  M  A  Q  G  L  Y  N  H  S  T
gtcgcatgcgacgaagaagatatgccaataagttcttaatagtcaaacttcagaaattaa
 V  A  C  D  E  E  D  M  P  I  S  S  -
cgaattttctaagtagatctcactaaatgtatattgtacaaaatttatttatgcgtatat
tttttaaaataaagtgtatataacatagcataataaataagcattgagcatgtaattcgc
tactttacattttcgtgcttaagcttatttctgtttgtagattagattgcaaagttttaa
atgtaaataatcatcgtagcaaattattcctttgtttataaaccagtgaaaattttactt
ttaacttgtttatattttaaatgatttgtattttattcgagccttataaatagactgatt
tgtatttaatagtgtgatgtgcaatgtattgttattaagtattactcgtatgtaaataaa
tggattataagtatttgaaataaatttgttctaccataaaaaaaaaaaaactaaggggggg
g
```

Appendix III. Detailed Embryo Fixation and *in situ* Hybridization Protocol

Part I: *D. maculatus* Embryo Fixation Protocol

1. Prepare a collecting basket with a small piece of mesh in the center.

2. Transfer appropriately staged embryos to the basket.

3. Treat embryos with 50% bleach for four minutes. Stir occasionally.

4. Rinse with tap water three times and embryo wash buffer once (8g NaCl, 500 µl of Triton X-100 in 2L dH_2O). Make sure to wash all embryos off the wall of the vial to the center of the mesh.

5. Transfer the mesh to a 1.5 ml Eppendorf tube with 1 ml of dH_2O using forcep. (Note: use ~ 200 µl of embryos in each tube. If there are too many embryos, split them to more tubes.)

6. Remove the mesh once most embryos are off the mesh.

7. Submerge the tube with embryos in boiling water for 3 minutes.

8. Transfer the tube to ice immediately and let it stay on ice for 7 minutes.

9. Remove dH_2O without losing embryos.

10. Add 500 µl of heptane and 500 µl of 4% PFA (paraformaldehyde).

11. Fix the embryos on the shaker at high speed (250 rpm) for 20 minutes.

12. Remove the aqueous phase (PFA, lower layer) without sucking up embryos.

13. Add 800 µl of 100% MeOH. Cap the tube and shake it vigorously for 20 seconds.

14. Flick the tube gently to let the embryos sink to the bottom. Note: If most embryos are still floating around, shake the tube for another 20 seconds.

15. Remove as much solution as possible without losing any embryos.

16. Rinse twice with 800 µl of 100% MeOH. Make sure to rinse embryos off the wall of the vial.

17. Add 800 µl of 100% MeOH and store the tube at -20° C.

The embryos will be dissected in PBST to remove the eggshell before in situ hybridization or antibody staining.

Part II: Whole Mount *D. macµlatus* Embryo in situ Hybridization with Digoxigenin-labeled Probe

Rinse means invert tube several times. Wash/rock means leave tube on nutator for certain time period.

Day 1

1. Remove 1.5 ml Eppendorf microcentrifuge tube from freezer. Each tube should contain ~ 200 µl embryos.

2. Remove MeOH, and rinse once with 500 µl of MeOH.

3. Remove, rinse once with 500 µl of MeOH/PBST 1:1.

4. Remove, rinse three times with 500 µl of PBST.

5. Transfer embryos to a multi-well glass plate using a P1000 pipette tip with the end cut off.

6. To remove eggshell, hand-dissect embryos in PBST using Dumont #5 forceps.

7. Transfer embryos back to a 1.5 ml Eppendorf microcentrifuge tube.

8. After all the embryos sink to the bottom, remove as much PBST as possible without losing any embryos.

9. Rinse twice with PBST.

10. Remove, add 500 µl of 4% PFA, Rock for 25 min.

11. Remove PFA, rinse once with 500 µl of PBST.

12. Remove, wash three times with PBST (5 min each). * At this time turn on heat block, set the temperature to 95° C.

13. Remove most PBST but keep embryos immersed in PBST. Heat the microcentrifuge tube with embryos in heat block for 5 min (95° C). *After this, switch the heat block temperature setting to 90° C.

14. Rinse once with 500 µl of Hybridization solution (Hyb. Sol.)/PBST 1:1.

15. Remove, rinse once with 500 µl of Hyb. Sol.

16. Remove, add Hyb. Sol. 500 µl and incubate in 60° C hybridization oven for 30 min.

17. Repeat Step 16.

18. Heat the probe (1 to 50 dilution in Hyb. Sol., 200 µl in total) at 90° C in heat block for 5 min. Transfer it to ice immediately.

19. Take the microcentrifuge tube out of the oven. Remove as much Hyb. Sol. as possible without losing any embryos.

20. Add the probe. Flick the tube gently a few times and incubate it at 60° C overnight (~ 16 hours).

Day 2

1. Carefully remove probe. Rinse once with 500 µl of Hyb. Sol.

2. Remove, add 1 ml of Hyb. Sol., rock for 20 min at 60° C.

3. Remove, add 1 ml of Hyb. Sol./PBST 1:1, rock for 20 min at 60° C.

4. Remove, wash 4X5 min in PBST at 60° C.

5. Remove, add 1 ml of 1:2000 anti-dig-AP, FAB-fragment antibody (diluted in PBST).

6. Incubate for 1 hour at room temperature (R.T.).

The following steps are all carried out at R. T.

7. Remove, rinse once with 500 µl of PBST.

8. Remove, wash 4X10 min with PBST.

9. Remove, wash in 500 µl of staining buffer for 5 min.

10. Remove, add 1 ml color reaction buffer (4.5 µl of NBT 100 mg/ml and 3.5 µl of BCIP 50 mg/ml in 1 ml of staining buffer).

11. Rock in dark, check color change every 10 min in multi-well glass dish under microscope.

12. Rock until color develops to ideal intensity. Stop reaction by adding 500 µl of PBST.

13. Remove solution. Rinse three times with PBST.

14. Wash with PBST 3X5 min.

15. Wash with MeOH/PBST 1:1 for 5 min.

16. Rinse twice with MeOH.

17. Rinse once with EtOH.

18. Rinse twice with MeOH.

19. Wash with MeOH/PBST 1:1 for 5 min.

20. Wash with PBST for 3X5 min. * Embryos can be saved in PBST at 4° C for days before visualization.

To visualize embryos:

Embryos at pre-blastoderm, blastoderm and gastrulation stages can be visualized directly in PBST under dissecting microscope.

Germ band needs to be dissected out from surrounding yolk with forceps. To mount, germ band is transferred onto microscope slide with either a P200 tip (end cut off) or with forceps. After removing the remaining PBST, add 70% glycerol (in 0.1 M Tris pH 8.0) on to microscope slide and flatten germ band carefully with forceps. Cover with a coverslip and then proceed to visualization using microscope.

20XSSC (1L)

175.3 g NaCl

88.2 g Sodium citrate

adjust pH to 7.0

store at R.T.

Hybridization Solution (50 ml)

50% Formanmide	25 ml
5XSSC	12.5 ml of 20X
100 ug/ml Salmon Sperm DNA	500 µl
50 ug/ml Heparin	250 µl
0.1% Tween 20	50 µl

dH_2O	11.7 ml

store at 4° C

Staining Buffer (50 ml)

100 mM NaCl	1 ml of 5M
50 mM $MgCl_2$	2.5 ml of 1 M
100 mM Tris pH 9.5	46.45 ml
0.1% Tween 20	50 µl

store at R.T.

Part 3: Troubleshooting and comments on protocol

1. If a lot of embryos at the blastoderm stage are not intact or many germ bands have been fragmented after fixation, hand shaking might be too vigorously. Try to reduce shaking time or shake less vigorously.

2. Poor fixation might result if there are too many embryos in each individual Eppendorf tube. Try to split embryos into more tubes.

3. Fixation still works without the heating and cooling treatments. But the space between the eggshell and the embryo might be small for hand-dissection if you skip this step.

4. We have tried several ways to get around the requirement for hand-dissection to remove the eggshell but they were unsuccessful. These included extending bleach treatment time and using ice cold MeOH during fixation.

5. For in situ hybridization, the color starts to show up after ~ 15 minutes and develops within an hour. a) If the staining becomes dark very quickly or shows strong

background, try to use more diluted probe. b) If the staining is still weak after one hour, remove solution and add fresh NBT/BCIP solution. Also, using less diluted probe might help.

Appendix IV. List of Materials

Name of Material/ Equipment	Company	Catalog Number	Comments/Description
***Dermestes maculatus* live beetles**	Our lab or Carolina Biological Supply	#144168	Our lab strain was verified by COI barcoding; strain variation from Carolina cannot be ruled out
Wet cat food	Fancy Feast		Chunks of meat with gravy. Can buy at most pet food and grocery stores
Dry dog food	Purina Puppy Chow		Can buy at most pet food and grocery stores
Insect cage (size medium, 30.5x19x20.3 cm)	Exo Terra	PT2260	For colony maintenance. Can use larger cage if needed
Insect cage (size mini, 17.8x10.2x12.7 cm)	Exo Terra	PT2250	For embryo collection
Petri dish	VWR	89038-968	
Cotton ball	Fisher	22-456-883	
Megascript T7 transcription kit	Fisher	AM1334	For 40 reactions
Pneumatic pump	WPI	PV830	
Capillary holder	WPI		
Micromanipulator	NARISHIGE	MN-151	
Black filter paper (90 mm)	VWR	28342-010	
Food coloring (green)	McCormick		
Borosilicate glass capillary	Hilgenberg	1406119	
Needle puller (micropipette puller)	Sutter Instrument Co.	P-97	
Microscope glass slide	WorldWide Life Sciences Division	41351157	
Sealing film (Parafilm M)	Fisher	13-374-12	
Model 801 Syringe (10 µl)	Hamilton	7642-01	

Needle (32-gauge)	Hamilton	7762-05	
Fixation Solution (Pampel's)	BioQuip Products, Inc.	1184C	Toxic, needs to be handled in fume hood
Forcep (DUMONT #5)	Fine Science Tools	11252-30	
Cover slip (24X50 mm, No. 1.5)	Globe Scientific	1415-15	
Eppendorf Femtotips Microloader pipette tip	Fisher	E5242956003	
Dissecting microscopy for embryo injection	Leica	M420	
Dissecting microscopy for larval phenotypic visualization	Zeiss	SteREO Discover. V12	
DIC microscopy	Zeiss	AXIO Imager. M1	

Appendix V. Criteria for Identifying Segmentation Defects

WT-like segments: pigmented stripes separated by non-pigmented region (below)

Fusion of neighboring segments: reduced non-pigmented region (below, A and B). Sometimes largely or completely missing non-pigmented region, a broad pigmented stripe is present (below, C)

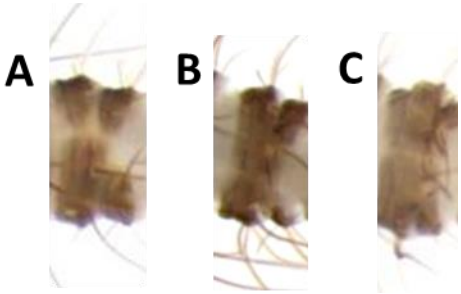

Duplication: very often identified by duplicated claw (below, A and B). Very occasionally, duplicated pigmented region is detected (below, C)

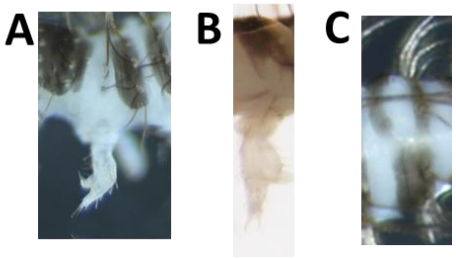

Deletion/disruption: identified by disrupted pigmentation (below)

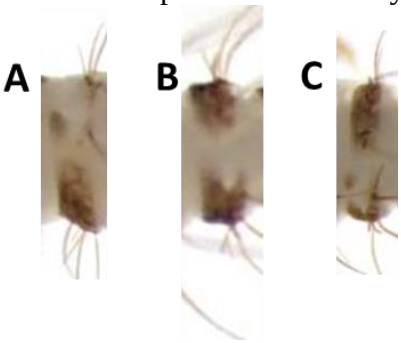

References

Abzhanov, A., Popadic, A., and Kaufman, T.C. (1999). Chelicerate Hox genes and the homology of arthropod segments. Evol Dev *1*, 77-89.

Agrawal, N., Dasaradhi, P.V., Mohmmed, A., Malhotra, P., Bhatnagar, R.K., and Mukherjee, S.K. (2003). RNA interference: biology, mechanism, and applications. Microbiol Mol Biol Rev *67*, 657-685.

Akam, M. (1987). The molecular basis for metameric pattern in the Drosophila embryo. Development *101*, 1-22.

Akam, M. (1989). Drosophila development: making stripes inelegantly. Nature *341*, 282-283.

Akam, M., and Dawes, R. (1992). More than one way to slice an egg. Curr Biol *2*, 395-398.

Angelini, D.R., and Kaufman, T.C. (2004). Functional analyses in the hemipteran Oncopeltus fasciatus reveal conserved and derived aspects of appendage patterning in insects. Dev Biol *271*, 306-321.

Angelini, D.R., Liu, P.Z., Hughes, C.L., and Kaufman, T.C. (2005). Hox gene function and interaction in the milkweed bug Oncopeltus fasciatus (Hemiptera). Dev Biol *287*, 440-455.

Arakane, Y., Muthukrishnan, S., Kramer, K.J., Specht, C.A., Tomoyasu, Y., Lorenzen, M.D., Kanost, M., and Beeman, R.W. (2005). The Tribolium chitin synthase genes TcCHS1 and TcCHS2 are specialized for synthesis of epidermal cuticle and midgut peritrophic matrix. Insect Mol Biol *14*, 453-463.

Aranda, M., Marques-Souza, H., Bayer, T., and Tautz, D. (2008). The role of the segmentation gene *hairy* in *Tribolium*. Dev Genes Evol ***218***, 465-477.

Auman, T., Vreede, B.M.I., Weiss, A., Hester, S.D., Williams, T.A., Nagy, L.M., and Chipman, A.D. (2017). Dynamics of growth zone patterning in the milkweed bug Oncopeltus fasciatus. Development.

Bateson, W. (1894). Materials for the Study of Variation Treated with Especial Regard to Discontinuity in the
Origin of Species (London: Macmillan).

Baumgartner, S., Bopp, D., Burri, M., and Noll, M. (1987). Structure of two genes at the gooseberry locus related to the paired gene and their spatial expression during Drosophila embryogenesis. Genes Dev *1*, 1247-1267.

Bely, A.E., and Weisblat, D.A. (2006). Lessons from leeches: a call for DNA barcoding in the lab. Evol Dev *8*, 491-501.

Benedyk, M.J., Mullen, J.R., and DiNardo, S. (1994). odd-paired: a zinc finger pair-rule protein required for the timely activation of engrailed and wingless in Drosophila embryos. Genes Dev *8*, 105-117.

Benton, M.A., Akam, M., and Pavlopoulos, A. (2013). Cell and tissue dynamics during Tribolium embryogenesis revealed by versatile fluorescence labeling approaches. Development *140*, 3210-3220.

Benton, M.A., Pechmann, M., Frey, N., Stappert, D., Conrads, K.H., Chen, Y.T., Stamataki, E., Pavlopoulos, A., and Roth, S. (2016). Toll Genes Have an Ancestral Role in Axis Elongation. Curr Biol *26*, 1609-1615.

Binner, P., and Sander, K. (1997). Pair-rule patterning in the honeybee Apis mellifera: Expression of even-skipped combines traits known from beetles and fruitfly. Dev Genes Evol *206*, 447-454.
Blair, S.S. (2008). Segmentation in animals. Curr Biol *18*, R991-995.
Bonini, N.M., and Fortini, M.E. (1999). Surviving Drosophila eye development: integrating cell death with differentiation during formation of a neural structure. Bioessays *21*, 991-1003.
Bopp, D., Burri, M., Baumgartner, S., Frigerio, G., and Noll, M. (1986). Conservation of a large protein domain in the segmentation gene paired and in functionally related genes of Drosophila. Cell *47*, 1033-1040.
Bopp, D., Jamet, E., Baumgartner, S., Burri, M., and Noll, M. (1989). Isolation of two tissue-specific Drosophila paired box genes, Pox meso and Pox neuro. EMBO J *8*, 3447-3457.
Bouchard, P., Grebennikov, V., Smith, A.B.T., and Douglas, H. (2009). Biodiversity of Coleoptera (Blackwell Publishing).
Breitling, R., and Gerber, J.K. (2000). Origin of the paired domain. Dev Genes Evol *210*, 644-650.
Brena, C., and Akam, M. (2013). An analysis of segmentation dynamics throughout embryogenesis in the centipede Strigamia maritima. BMC Biol *11*, 112.
Brown, S., and Denell, R. (1996). Segmentation and dorso-ventral patterning in *Tribolium 7*, 8.
Brown, S.J., Hilgenfeld, R.B., and Denell, R.E. (1994a). The beetle Tribolium castaneum has a fushi tarazu homolog expressed in stripes during segmentation. Proc Natl Acad Sci U S A *91*, 12922-12926.
Brown, S.J., Mahaffey, J.P., Lorenzen, M.D., Denell, R.E., and Mahaffey, J.W. (1999). Using RNAi to investigate orthologous homeotic gene function during development of distantly related insects. Evol Dev *1*, 11-15.
Brown, S.J., Parrish, J.K., Beeman, R.W., and Denell, R.E. (1997). Molecular characterization and embryonic expression of the even-skipped ortholog of Tribolium castaneum. Mech Dev *61*, 165-173.
Brown, S.J., Patel, N.H., and Denell, R.E. (1994b). Embryonic expression of the single Tribolium engrailed homolog. Dev Genet *15*, 7-18.
Brown, S.J., Shippy, T.D., Miller, S., Bolognesi, R., Beeman, R.W., Lorenzen, M.D., Bucher, G., Wimmer, E.A., and Klingler, M. (2009). The red flour beetle, Tribolium castaneum (Coleoptera): a model for studies of development and pest biology. Cold Spring Harb Protoc *2009*, pdb.emo126.
Bucher, G., Scholten, J., and Klingler, M. (2002). Parental RNAi in Tribolium (Coleoptera). Curr Biol *12*, R85-86.
Buckingham, M., and Relaix, F. (2007). The role of Pax genes in the development of tissues and organs: Pax3 and Pax7 regulate muscle progenitor cell functions. Annu Rev Cell Dev Biol *23*, 645-673.
Burri, M., Tromvoukis, Y., Bopp, D., Frigerio, G., and Noll, M. (1989). Conservation of the paired domain in metazoans and its structure in three isolated human genes. EMBO J *8*, 1183-1190.
Campos-Ortéga, J.A., and Hartenstein, V. (1997). The embryonic development of Drosophila melanogaster (Springer).

Carroll, S.B., Grenier, J.K., and Weatherbee, S.D. (2005). From DNA to diversity : molecular genetics and the evolution of animal design, 2nd edn (Malden, MA: Blackwell Pub.).
Carroll, S.B., and Scott, M.P. (1986). Zygotically active genes that affect the spatial expression of the fushi tarazu segmentation gene during early Drosophila embryogenesis. Cell *45*, 113-126.
Chandler, C.H., Chari, S., Tack, D., and Dworkin, I. (2014). Causes and consequences of genetic background effects illuminated by integrative genomic analysis. Genetics *196*, 1321-1336.
Cheatle, Jarvela, A.M., and Pick, L. (2015). Evo-Devo: discovery of diverse mechanisms
regulating development. 50th
anniversary volume of Current Topics in Developmental Biology.
Chipman, A.D., and Akam, M. (2008). The segmentation cascade in the centipede Strigamia maritima: involvement of the Notch pathway and pair-rule gene homologues. Dev Biol *319*, 160-169.
Chipman, A.D., Arthur, W., and Akam, M. (2004). A double segment periodicity underlies segment generation in centipede development. Curr Biol *14*, 1250-1255.
Choe, C.P., and Brown, S.J. (2007). Evolutionary flexibility of pair-rule patterning revealed by functional analysis of secondary pair-rule genes, paired and sloppy-paired in the short-germ insect, Tribolium castaneum. Dev Biol *302*, 281-294.
Choe, C.P., and Brown, S.J. (2009). Genetic regulation of engrailed and wingless in Tribolium segmentation and the evolution of pair-rule segmentation. Dev Biol *325*, 482-491.
Choe, C.P., Miller, S.C., and Brown, S.J. (2006). A pair-rule gene circuit defines segments sequentially in the short-germ insect Tribolium castaneum. Proc Natl Acad Sci U S A *103*, 6560-6564.
Ciudad, L., Piulachs, M.D., and Bellés, X. (2006). Systemic RNAi of the cockroach vitellogenin receptor results in a phenotype similar to that of the Drosophila yolkless mutant. FEBS J *273*, 325-335.
Clark, E. (2017). Dynamic patterning by the Drosophila pair-rule network reconciles long-germ and short-germ segmentation (bioRxiv), pp. 1-62.
Clark, E., and Akam, M. (2016). Odd-paired controls frequency doubling in Drosophila segmentation by altering the pair-rule gene regulatory network. Elife *5*.
Cogoni, C., Irelan, J.T., Schumacher, M., Schmidhauser, T.J., Selker, E.U., and Macino, G. (1996). Transgene silencing of the al-1 gene in vegetative cells of Neurospora is mediated by a cytoplasmic effector and does not depend on DNA-DNA interactions or DNA methylation. EMBO J *15*, 3153-3163.
Copf, T., Rabet, N., Celniker, S.E., and Averof, M. (2003). Posterior patterning genes and the identification of a unique body region in the brine shrimp Artemia franciscana. Development *130*, 5915-5927.
Coulter, D.E., Swaykus, E.A., Beran-Koehn, M.A., Goldberg, D., Wieschaus, E., and Schedl, P. (1990). Molecular analysis of odd-skipped, a zinc finger encoding segmentation gene with a novel pair-rule expression pattern. EMBO J *9*, 3795-3804.

Coulter, D.E., and Wieschaus, E. (1988). Gene activities and segmental patterning in Drosophila: analysis of odd-skipped and pair-rule double mutants. Genes Dev *2*, 1812-1823.
Cruz, J., Mané-Padrós, D., Bellés, X., and Martín, D. (2006). Functions of the ecdysone receptor isoform-A in the hemimetabolous insect Blattella germanica revealed by systemic RNAi in vivo. Dev Biol *297*, 158-171.
Damen, W.G. (2004). Arthropod segmentation: why centipedes are odd. Curr Biol *14*, R557-559.
Damen, W.G., Janssen, R., and Prpic, N.M. (2005). Pair rule gene orthologs in spider segmentation. Evol Dev *7*, 618-628.
Damen, W.G., Weller, M., and Tautz, D. (2000). Expression patterns of hairy, even-skipped, and runt in the spider Cupiennius salei imply that these genes were segmentation genes in a basal arthropod. Proc Natl Acad Sci U S A *97*, 4515-4519.
Davis, G.K., D'Alessio, J.A., and Patel, N.H. (2005). Pax3/7 genes reveal conservation and divergence in the arthropod segmentation hierarchy. Dev Biol *285*, 169-184.
Davis, G.K., Jaramillo, C.A., and Patel, N.H. (2001). Pax group III genes and the evolution of insect pair-rule patterning. Development *128*, 3445-3458.
Davis, G.K., and Patel, N.H. (2002). Short, long, and beyond: molecular and embryological approaches to insect segmentation. Annu Rev Entomol *47*, 669-699.
Dawes, R., Dawson, I., Falciani, F., Tear, G., and Akam, M. (1994). Dax, a locust Hox gene related to fushi-tarazu but showing no pair-rule expression. Development *120*, 1561-1572.
Dearden, P.K., Donly, C., and Grbić, M. (2002). Expression of pair-rule gene homologues in a chelicerate: early patterning of the two-spotted spider mite Tetranychus urticae. Development *129*, 5461-5472.
Degnan, B.M., Vervoort, M., Larroux, C., and Richards, G.S. (2009). Early evolution of metazoan transcription factors. Curr Opin Genet Dev *19*, 591-599.
Denell, R. (2008). Establishment of tribolium as a genetic model system and its early contributions to evo-devo. Genetics *180*, 1779-1786.
DiNardo, S., and O'Farrell, P.H. (1987). Establishment and refinement of segmental pattern in the Drosophila embryo: spatial control of engrailed expression by pair-rule genes. Genes Dev *1*, 1212-1225.
Doe, C.Q., Smouse, D., and Goodman, C.S. (1988). Control of neuronal fate by the Drosophila segmentation gene even-skipped. Nature *333*, 376-378.
Doetschman, T. (2009). Influence of genetic background on genetically engineered mouse phenotypes. Methods Mol Biol *530*, 423-433.
Donoughe, S., and Extavour, C.G. (2016). Embryonic development of the cricket Gryllus bimaculatus. Dev Biol *411*, 140-156.
Dorsett, Y., and Tuschl, T. (2004). siRNAs: applications in functional genomics and potential as therapeutics. Nat Rev Drug Discov *3*, 318-329.
Driever, W., and Nüsslein-Volhard, C. (1988). The bicoid protein determines position in the Drosophila embryo in a concentration-dependent manner. Cell *54*, 95-104.
Driever, W., Siegel, V., and Nüsslein-Volhard, C. (1990). Autonomous determination of anterior structures in the early Drosophila embryo by the bicoid morphogen. Development *109*, 811-820.

Dönitz, J., Schmitt-Engel, C., Grossmann, D., Gerischer, L., Tech, M., Schoppmeier, M., Klingler, M., and Bucher, G. (2015). iBeetle-Base: a database for RNAi phenotypes in the red flour beetle Tribolium castaneum. Nucleic Acids Res *43*, D720-725.
Eaton, B.A., Fetter, R.D., and Davis, G.W. (2002). Dynactin is necessary for synapse stabilization. Neuron *34*, 729-741.
Eckert, C., Aranda, M., Wolff, C., and Tautz, D. (2004). Separable stripe enhancer elements for the pair-rule gene hairy in the beetle Tribolium. EMBO Rep *5*, 638-642.
Edgar, R.C. (2004). MUSCLE: multiple sequence alignment with high accuracy and high throughput. Nucleic Acids Res *32*, 1792-1797.
El-Sherif, E., Averof, M., and Brown, S.J. (2012). A segmentation clock operating in blastoderm and germband stages of Tribolium development. Development *139*, 4341-4346.
El-Sherif, E., and Levine, M. (2016). Shadow Enhancers Mediate Dynamic Shifts of Gap Gene Expression in the Drosophila Embryo. Curr Biol *26*, 1164-1169.
Erezyilmaz, D.F., Kelstrup, H.C., and Riddiford, L.M. (2009). The nuclear receptor E75A has a novel pair-rule-like function in patterning the milkweed bug, *Oncopeltus fasciatus*. Dev Biol ***334***, 300-310.
Fire, A., Xu, S., Montgomery, M.K., Kostas, S.A., Driver, S.E., and Mello, C.C. (1998). Potent and specific genetic interference by double-stranded RNA in Caenorhabditis elegans. Nature *391*, 806-811.
Foe, V.E., Odell, G.M., and Edgar, B.A. (1993). Mitosis and Morphogenesis in the *Drosophila* Embryo: Point and Counterpoint, Vol 1 (University of Cambridge).
Folmer, O., Black, M., Hoeh, W., Lutz, R., and Vrijenhoek, R. (1994). DNA primers for amplification of mitochondrial cytochrome c oxidase subunit I from diverse metazoan invertebrates. Mol Mar Biol Biotechnol *3*, 294-299.
Fontenot, E.A., Arthur, F.H., and Hartzer, K.L. (2014). Effect of diet and refugia on development of *Dermestes maculatus* DeGeer reared in a laboratory. Journal of Pest Science *88*, 113-119.
Fontenot, E.A., Arthur, F.H., and Hartzer, K.L. (2015). Oviposition of *Dermestes maculatus* DeGeer, the hide beetle, as affected by biological and environmental conditions. Journal of Stored Products Research *64*, 154-159.
Franke, F.A., Schumann, I., Hering, L., and Mayer, G. (2015). Phylogenetic analysis and expression patterns of Pax genes in the onychophoran Euperipatoides rowelli reveal a novel bilaterian Pax subfamily. Evol Dev *17*, 3-20.
Frasch, M., and Levine, M. (1987). Complementary patterns of even-skipped and fushi tarazu expression involve their differential regulation by a common set of segmentation genes in Drosophila. Genes Dev *1*, 981-995.
Friedrich, M. (2015). Evo-Devo gene toolkit update: at least seven Pax transcription factor subfamilies in the last common ancestor of bilaterian animals. Evol Dev *17*, 255-257.
Frigerio, G., Burri, M., Bopp, D., Baumgartner, S., and Noll, M. (1986). Structure of the segmentation gene paired and the Drosophila PRD gene set as part of a gene network. Cell *47*, 735-746.
Gabriel, W.N., and Goldstein, B. (2007). Segmental expression of Pax3/7 and engrailed homologs in tardigrade development. Dev Genes Evol *217*, 421-433.

Gergen, J.P., and Wieschaus, E.F. (1985). The localized requirements for a gene affecting segmentation in Drosophila: analysis of larvae mosaic for runt. Dev Biol *109*, 321-335.
Gilbert, S.F. (2010). Developmental Biology, Ninth edition edn (Sinauer).
Goltsev, Y., Hsiong, W., Lanzaro, G., and Levine, M. (2004). Different combinations of gap repressors for common stripes in Anopheles and Drosophila embryos. Dev Biol *275*, 435-446.
Goto, T., Macdonald, P., and Maniatis, T. (1989). Early and late periodic patterns of even skipped expression are controlled by distinct regulatory elements that respond to different spatial cues. Cell *57*, 413-422.
Graves, R. (2005). Beetles & Bones: Care, Feeding, and Use of Dermestid Beetles (Jillett Publications).
Grbic, M., Nagy, L.M., Carroll, S.B., and Strand, M. (1996). Polyembryonic development: insect pattern formation in a cellularized environment. Development *122*, 795-804.
Grbić, M., and Strand, M.R. (1998). Shifts in the life history of parasitic wasps correlate with pronounced alterations in early development. Proc Natl Acad Sci U S A *95*, 1097-1101.
Green, J., and Akam, M. (2013). Evolution of the pair rule gene network: Insights from a centipede. Dev Biol *382*, 235-245.
Grimaldi, D., and Engel, M.S. (2005). Evolution of the insects, 1st Edition edn (Cambridge University Press).
Grishok, A. (2005). RNAi mechanisms in Caenorhabditis elegans. FEBS Lett *579*, 5932-5939.
Grishok, A., Tabara, H., and Mello, C.C. (2000). Genetic requirements for inheritance of RNAi in C. elegans. Science *287*, 2494-2497.
Grossniklaus, U., Pearson, R.K., and Gehring, W.J. (1992). The Drosophila sloppy paired locus encodes two proteins involved in segmentation that show homology to mammalian transcription factors. Genes Dev *6*, 1030-1051.
Guichet, A., Copeland, J.W., Erdelyi, M., Hlousek, D., Zavorszky, P., Ho, J., Brown, S., Percival-Smith, A., Krause, H.M., and Ephrussi, A. (1997). The nuclear receptor homologue Ftz-F1 and the homeodomain protein Ftz are mutually dependent cofactors. Nature *385*, 548-552.
Guidugli, K.R., Nascimento, A.M., Amdam, G.V., Barchuk, A.R., Omholt, S., Simões, Z.L., and Hartfelder, K. (2005). Vitellogenin regulates hormonal dynamics in the worker caste of a eusocial insect. FEBS Lett *579*, 4961-4965.
Gullan, P.J., and Cranston, P.S. (2010). The insects: an outline of Entomology (Oxford, UK: Blackwell Publishing).
Gutjahr, T., Frei, E., and Noll, M. (1993a). Complex regulation of early paired expression: initial activation by gap genes and pattern modulation by pair-rule genes. Development *117*, 609-623.
Gutjahr, T., Patel, N.H., Li, X., Goodman, C.S., and Noll, M. (1993b). Analysis of the gooseberry locus in Drosophila embryos: gooseberry determines the cuticular pattern and activates gooseberry neuro. Development *118*, 21-31.

Gutjahr, T., Vanario-Alonso, C.E., Pick, L., and Noll, M. (1994). Multiple regulatory elements direct the complex expression pattern of the Drosophila segmentation gene paired. Mech Dev *48*, 119-128.
Hammond, P.M. (1992). Global Biodiversity": status of the Earth's living resources.
Hammond, S.M., Caudy, A.A., and Hannon, G.J. (2001). Post-transcriptional gene silencing by double-stranded RNA. Nat Rev Genet *2*, 110-119.
Handel, K., Grünfelder, C.G., Roth, S., and Sander, K. (2000). Tribolium embryogenesis: a SEM study of cell shapes and movements from blastoderm to serosal closure. Dev Genes Evol *210*, 167-179.
Hannon, G.J. (2002). RNA interference. Nature *418*, 244-251.
Harding, K., Hoey, T., Warrior, R., and Levine, M. (1989). Autoregulatory and gap gene response elements of the even-skipped promoter of Drosophila. EMBO J *8*, 1205-1212.
Hasselmann, M., Gempe, T., Schiøtt, M., Nunes-Silva, C.G., Otte, M., and Beye, M. (2008). Evidence for the evolutionary nascence of a novel sex determination pathway in honeybees. Nature *454*, 519-522.
Hedges, S.B., Marin, J., Suleski, M., Paymer, M., and Kumar, S. (2015). Tree of life reveals clock-like speciation and diversification. Mol Biol Evol *32*, 835-845.
Heffer, A., Grubbs, N., Mahaffey, J., and Pick, L. (2013). The evolving role of the orphan nuclear receptor ftz-f1, a pair-rule segmentation gene. Evol Dev *15*, 406-417.
Heffer, A., Shultz, J.W., and Pick, L. (2010). Surprising flexibility in a conserved Hox transcription factor over 550 million years of evolution. Proc Natl Acad Sci U S A *107*, 18040-18045.
Heffer, A.M., Mahaffey, J.W., and Pick, L. (2012). Characterization of Tribolium ftz-f1 reveals dynamic roles during embryogenesis. Evol Dev, Submitted.
Hiromi, Y., and Gehring, W.J. (1987). Regulation and function of the Drosophila segmentation gene fushi tarazu. Cell *50*, 963-974.
Hiromi, Y., Kuroiwa, A., and Gehring, W.J. (1985). Control elements of the Drosophila segmentation gene fushi tarazu. Cell *43*, 603-613.
Howard, K., and Ingham, P. (1986). Regulatory interactions between the segmentation genes fushi tarazu, hairy, and engrailed in the Drosophila blastoderm. Cell *44*, 949-957.
Howard, K., Ingham, P., and Rushlow, C. (1988). Region-specific alleles of the Drosophila segmentation gene hairy. Genes Dev *2*, 1037-1046.
Hughes, C.L., and Kaufman, T.C. (2002a). Exploring myriapod segmentation: the expression patterns of even-skipped, engrailed, and wingless in a centipede. Dev Biol *247*, 47-61.
Hughes, C.L., and Kaufman, T.C. (2002b). Exploring the myriapod body plan: expression patterns of the ten Hox genes in a centipede. Development *129*, 1225-1238.
Hughes, C.L., and Kaufman, T.C. (2002c). Hox genes and the evolution of the arthropod body plan. Evol Dev *4*, 459-499.
Hughes, C.L., Liu, P.Z., and Kaufman, T.C. (2004). Expression patterns of the rogue Hox genes Hox3/zen and fushi tarazu in the apterygote insect Thermobia domestica. Evol Dev *6*, 393-401.

Hughes, S.C., and Krause, H.M. (2001). Establishment and maintenance of parasegmental compartments. Development *128*, 1109-1118.
Hunt, T., Bergsten, J., Levkanicova, Z., Papadopoulou, A., John, O.S., Wild, R., Hammond, P.M., Ahrens, D., Balke, M., Caterino, M.S., *et al.* (2007). A comprehensive phylogeny of beetles reveals the evolutionary origins of a superradiation. Science *318*, 1913-1916.
Huson, D.H., and Scornavacca, C. (2012). Dendroscope 3: an interactive tool for rooted phylogenetic trees and networks. Syst Biol *61*, 1061-1067.
Huvenne, H., and Smagghe, G. (2010). Mechanisms of dsRNA uptake in insects and potential of RNAi for pest control: a review. J Insect Physiol *56*, 227-235.
Ingham, P.W. (1988). The molecular genetics of embryonic pattern formation in Drosophila. Nature *335*, 25-34.
Ingham, P.W., Howard, K.R., and Ish-Horowicz, D. (1985). Transcription pattern of the *Drosophila* segmentation gene *hairy*. Nature *318*, 439-445.
Ingham, P.W., and Martinez-Arias, A. (1986). The correct activation of Antennapedia and bithorax complex genes requires the fushi tarazu gene. Nature *324*, 592-597.
Ish-Horowicz, D., and Pinchin, S.M. (1987). Pattern abnormalities induced by ectopic expression of the Drosophila gene hairy are associated with repression of ftz transcription. Cell *51*, 405-415.
Janssen, R., and Budd, G.E. (2013). Deciphering the onychophoran 'segmentation gene cascade': Gene expression reveals limited involvement of pair rule gene orthologs in segmentation, but a highly conserved segment polarity gene network. Dev Biol *382*, 224-234.
Janssen, R., Budd, G.E., Prpic, N.M., and Damen, W.G. (2011). Expression of myriapod pair rule gene orthologs. Evodevo *2*, 5.
Janssen, R., and Damen, W.G. (2006). The ten Hox genes of the millipede Glomeris marginata. Dev Genes Evol *216*, 451-465.
Janssen, R., Damen, W.G., and Budd, G.E. (2012). Expression of pair rule gene orthologs in the blastoderm of a myriapod: evidence for pair rule-like mechanisms? BMC Dev Biol *12*, 15.
Janssens, H., Siggens, K., Cicin-Sain, D., Jiménez-Guri, E., Musy, M., Akam, M., and Jaeger, J. (2014). A quantitative atlas of Even-skipped and Hunchback expression in Clogmia albipunctata (Diptera: Psychodidae) blastoderm embryos. Evodevo *5*, 1.
Jarvis, E., Bruce, H.S., and Patel, N.H. (2012). Evolving specialization of the arthropod nervous system. Proc Natl Acad Sci U S A *109 Suppl 1*, 10634-10639.
Jaynes, J.B., and Fujioka, M. (2004). Drawing lines in the sand: even skipped et al. and parasegment boundaries. Dev Biol *269*, 609-622.
Jose, A.M., and Hunter, C.P. (2007). Transport of sequence-specific RNA interference information between cells. Annu Rev Genet *41*, 305-330.
Jun, S., and Desplan, C. (1996). Cooperative interactions between paired domain and homeodomain. Development *122*, 2639-2650.
Jäckle, H., Rosenberg, U.B., Preiss, A., Seifert, E., Knipple, D.C., Kienlin, A., and Lehmann, R. (1985). Molecular analysis of Krüppel, a segmentation gene of Drosophila melanogaster. Cold Spring Harb Symp Quant Biol *50*, 465-473.
Jürgens, G., Wieschaus, E., Nüsslein-Volhard, C., and Kluding, H. (1984). Mutations affecting the pattern of the larval cuticle in *Drosophila melanogaster*. II. Zygotic loci

on the third chromosome. Wilhelm Roux's archives of developmental biology *193*, 283-295.
Kainz, F., Ewen-Campen, B., Akam, M., and Extavour, C.G. (2011). Notch/Delta signalling is not required for segment generation in the basally branching insect Gryllus bimaculatus. Development *138*, 5015-5026.
Kanginakudru, S., Royer, C., Edupalli, S.V., Jalabert, A., Mauchamp, B., Prasad, S.V., Chavancy, G., Couble, P., Nagaraju, J., and Chandrashekaraiah (2007). Targeting ie-1 gene by RNAi induces baculoviral resistance in lepidopteran cell lines and in transgenic silkworms. Insect Mol Biol *16*, 635-644.
Keller, R.G., Desplan, C., and Rosenberg, M.I. (2010). Identification and characterization of Nasonia Pax genes. Insect Mol Biol *19 Suppl 1*, 109-120.
Kennerdell, J.R., and Carthew, R.W. (1998). Use of dsRNA-mediated genetic interference to demonstrate that frizzled and frizzled 2 act in the wingless pathway. Cell *95*, 1017-1026.
Kilchherr, F., Baumgartner, S., Bopp, D., Frei, E., and Noll, M. (1986). Isolation of the *paired* gene of *Drosophila* and its spatial expression during early embryogenesis. Nature *321*, 493-499.
Kitzmann, P., Schwirz, J., Schmitt-Engel, C., and Bucher, G. (2013). RNAi phenotypes are influenced by the genetic background of the injected strain. BMC Genomics *14*, 5.
Klingensmith, J., Noll, E., and Perrimon, N. (1989). The segment polarity phenotype of Drosophila involves differential tendencies toward transformation and cell death. Dev Biol *134*, 130-145.
Klingler, M., and Gergen, J.P. (1993). Regulation of runt transcription by Drosophila segmentation genes. Mech Dev *43*, 3-19.
Kornberg, T. (1981). Engrailed: a gene controlling compartment and segment formation in Drosophila. Proc Natl Acad Sci U S A *78*, 1095-1099.
Kosman, D., Mizutani, C.M., Lemons, D., Cox, W.G., McGinnis, W., and Bier, E. (2004). Multiplex detection of RNA expression in Drosophila embryos. Science *305*, 846.
Kosman, D., and Small, S. (1997). Concentration-dependent patterning by an ectopic expression domain of the Drosophila gap gene knirps. Development *124*, 1343-1354.
Kraft, R., and Jäckle, H. (1994). Drosophila mode of metamerization in the embryogenesis of the lepidopteran insect Manduca sexta. Proc Natl Acad Sci U S A *91*, 6634-6638.
Krause, G. (1939). Die Eitypen der Insekten. Biol Zentralbl, 495-536.
Lawrence, P.A. (1992). The Making of a Fly: The Genetics of Animal Design (Blackwell Scientific, Oxford, UK).
Lewis, E.B. (1978). A gene complex controlling segmentation in Drosophila. Nature *276*, 565-570.
Li, X., and Noll, M. (1993). Role of the gooseberry gene in Drosophila embryos: maintenance of wingless expression by a wingless--gooseberry autoregulatory loop. EMBO J *12*, 4499-4509.
Liu, P., and Kaufman, T.C. (2009). Dissection and fixation of large milkweed bug (Oncopeltus) embryos. Cold Spring Harb Protoc *2009*, pdb.prot5261.

Liu, P.Z., and Kaufman, T.C. (2004). hunchback is required for suppression of abdominal identity, and for proper germband growth and segmentation in the intermediate germband insect Oncopeltus fasciatus. Development *131*, 1515-1527.
Liu, P.Z., and Kaufman, T.C. (2005a). even-skipped is not a pair-rule gene but has segmental and gap-like functions in Oncopeltus fasciatus, an intermediate germband insect. Development *132*, 2081-2092.
Liu, P.Z., and Kaufman, T.C. (2005b). Short and long germ segmentation: unanswered questions in the evolution of a developmental mode. Evolution and Development *7*, 629-646.
Liu, W., Yang, F., Jia, S., Miao, X., and Huang, Y. (2008). Cloning and characterization of Bmrunt from the silkworm Bombyx mori during embryonic development. Arch Insect Biochem Physiol *69*, 47-59.
Lorenzen, M.D., Berghammer, A.J., Brown, S.J., Denell, R.E., Klingler, M., and Beeman, R.W. (2003). piggyBac-mediated germline transformation in the beetle Tribolium castaneum. Insect Mol Biol *12*, 433-440.
Lynch, J.A., Brent, A.E., Leaf, D.S., Pultz, M.A., and Desplan, C. (2006). Localized maternal orthodenticle patterns anterior and posterior in the long germ wasp Nasonia. Nature *439*, 728-732.
Lynch, J.A., El-Sherif, E., and Brown, S.J. (2012). Comparisons of the embryonic development of Drosophila, Nasonia, and Tribolium. Wiley Interdiscip Rev Dev Biol *1*, 16-39.
Lynch, J.A., Peel, A.D., Drechsler, A., Averof, M., and Roth, S. (2010). EGF signaling and the origin of axial polarity among the insects. Curr Biol *20*, 1042-1047.
Macdonald, P.M., Ingham, P., and Struhl, G. (1986). Isolation, structure, and expression of even-skipped: a second pair-rule gene of Drosophila containing a homeo box. Cell *47*, 721-734.
Maderspacher, F., Bucher, G., and Klingler, M. (1998). Pair-rule and gap gene mutants in the flour beetle Tribolium castaneum. Dev Genes Evol *208*, 558-568.
Magni, P.A., Voss, S.C., Testi, R., Borrini, M., and Dadour, I.R. (2015). A Biological and Procedural Review of Forensically Significant Dermestes Species (Coleoptera: Dermestidae). J Med Entomol *52*, 755-769.
Magrassi, L., and Lawrence, P.A. (1988). The pattern of cell death in fushi tarazu, a segmentation gene of Drosophila. Development *104*, 447-451.
Martinez-Arias, A., and Lawrence, P.A. (1985). Parasegments and compartments in the Drosophila embryo. Nature *313*, 639-642.
Miller, M.A., Pfeiffer, W., and Schwartz, T. (2010). Creating the CIPRES Science Gateway for inference of large phylogenetic trees. In Proceedings of the Gateway Computing Environments Workshop (GCE) (New Orleans), pp. 1-8.
Milán, M., Pérez, L., and Cohen, S.M. (2002). Short-range cell interactions and cell survival in the Drosophila wing. Dev Cell *2*, 797-805.
Misof, B., Liu, S., Meusemann, K., Peters, R.S., Donath, A., Mayer, C., Frandsen, P.B., Ware, J., Flouri, T., Beutel, R.G., *et al.* (2014). Phylogenomics resolves the timing and pattern of insect evolution. Science *346*, 763-767.
Mito, T., Kobayashi, C., Sarashina, I., Zhang, H., Shinahara, W., Miyawaki, K., Shinmyo, Y., Ohuchi, H., and Noji, S. (2007). *even-skipped* has gap-like, pair-rule-

like, and segmental functions in the cricket *Gryllus bimaculatus*, a basal, intermediate germ insect (Orthoptera). Dev Biol *303*, 202-213.
Mito, T., Sarashina, I., Zhang, H., Iwahashi, A., Okamoto, H., Miyawaki, K., Shinmyo, Y., Ohuchi, H., and Noji, S. (2005). Non-canonical functions of hunchback in segment patterning of the intermediate germ cricket Gryllus bimaculatus. Development *132*, 2069-2079.
Mito, T., Shinmyo, Y., Kurita, K., Nakamura, T., Ohuchi, H., and Noji, S. (2011). Ancestral functions of Delta/Notch signaling in the formation of body and leg segments in the cricket Gryllus bimaculatus. Development *138*, 3823-3833.
Miya, K., and Kobayashi, Y. (1974). The embryonic development of Atrachya menetriesi Faldermann (Coleoptera, Chrysomelidae), 2: Analyses of early development by ligation and low temperature treatment. Journal of the Faculty of Agriculture - Iwate University *12*, 39-55.
Montagutelli, X. (2000). Effect of the genetic background on the phenotype of mouse mutations. J Am Soc Nephrol *11 Suppl 16*, S101-105.
Mouchel-Vielh, E., Blin, M., Rigolot, C., and Deutsch, J.S. (2002). Expression of a homologue of the fushi tarazu (ftz) gene in a cirripede crustacean. Evol Dev *4*, 76-85.
Mullen, J.R., and DiNardo, S. (1995). Establishing parasegments in Drosophila embryos: roles of the odd-skipped and naked genes. Dev Biol *169*, 295-308.
Nagaso, H., Murata, T., Day, N., and Yokoyama, K.K. (2001). Simultaneous detection of RNA and protein by in situ hybridization and immunological staining. J Histochem Cytochem *49*, 1177-1182.
Nagy, L., Riddiford, L., and Kiguchi, K. (1994). Morphogenesis in the early embryo of the lepidopteran Bombyx mori. Dev Biol *165*, 137-151.
Nagy, L.M., and Carroll, S. (1994). Conservation of wingless patterning functions in the short-germ embryos of Tribolium castaneum. Nature *367*, 460-463.
Nakamoto, A., Hester, S.D., Constantinou, S.J., Blaine, W.G., Tewksbury, A.B., Matei, M.T., Nagy, L.M., and Williams, T.A. (2015). Changing cell behaviours during beetle embryogenesis correlates with slowing of segmentation. Nat Commun *6*, 6635.
Nakao, H. (2010). Characterization of Bombyx embryo segmentation process: expression profiles of engrailed, even-skipped, caudal, and wnt1/wingless homologues. J Exp Zool B Mol Dev Evol *314*, 224-231.
Nakao, H. (2012). Anterior and posterior centers jointly regulate Bombyx embryo body segmentation. Dev Biol *371*, 293-301.
Nakao, H. (2015). Analyses of interactions among pair-rule genes and the gap gene Krüppel in Bombyx segmentation. Dev Biol *405*, 149-157.
Napoli, C., Lemieux, C., and Jorgensen, R. (1990). Introduction of a Chimeric Chalcone Synthase Gene into Petunia Results in Reversible Co-Suppression of Homologous Genes in trans. Plant Cell *2*, 279-289.
Noll, M. (1993). Evolution and role of Pax genes. Curr Opin Genet Dev *3*, 595-605.
Nüsslein-Volhard, C., Frohnhöfer, H.G., and Lehmann, R. (1987). Determination of anteroposterior polarity in Drosophila. Science *238*, 1675-1681.
Nüsslein-Volhard, C., Kluding, H., and Jürgens, G. (1985). Genes affecting the segmental subdivision of the Drosophila embryo. Cold Spring Harb Symp Quant Biol *50*, 145-154.

Nüsslein-Volhard, C., and Wieschaus, E. (1980). Mutations affecting segment number and polarity in Drosophila. Nature *287*, 795-801.
Nüsslein-Volhard, C., Wieschaus, E., and Kluding, H. (1984). Mutations affecting the pattern of the larval cuticle in *Drosophila melanogaster*. I.Zygotic loci on the second chromosome. Wilhelm Roux's archives of developmental biology *193*, 267-282.
Osborne, P.W., and Dearden, P.K. (2005). Expression of Pax group III genes in the honeybee (Apis mellifera). Dev Genes Evol *215*, 499-508.
Paixão-Côrtes, V.R., Salzano, F.M., and Bortolini, M.C. (2015). Origins and evolvability of the PAX family. Semin Cell Dev Biol.
Paldi, N., Glick, E., Oliva, M., Zilberberg, Y., Aubin, L., Pettis, J., Chen, Y., and Evans, J.D. (2010). Effective gene silencing in a microsporidian parasite associated with honeybee (Apis mellifera) colony declines. Appl Environ Microbiol *76*, 5960-5964.
Papillon, D., and Telford, M.J. (2007). Evolution of Hox3 and ftz in arthropods: insights from the crustacean Daphnia pulex. Dev Genes Evol *217*, 315-322.
Paré, A.C., Vichas, A., Fincher, C.T., Mirman, Z., Farrell, D.L., Mainieri, A., and Zallen, J.A. (2014). A positional Toll receptor code directs convergent extension in Drosophila. Nature *515*, 523-527.
Patel, N.H., Ball, E.E., and Goodman, C.S. (1992). Changing role of *even-skipped* during the evolution of insect pattern formation. Nature ***357***, 339-342.
Patel, N.H., Condron, B.G., and Zinn, K. (1994). Pair-rule expression patterns of even-skipped are found in both short- and long-germ beetles. Nature *367*, 429-434.
Peel, A.D., Chipman, A.D., and Akam, M. (2005). Arthropod segmentation: beyond the Drosophila paradigm. Nat Rev Genet *6*, 905-916.
Posnien, N., Schinko, J., Grossmann, D., Shippy, T.D., Konopova, B., and Bucher, G. (2009). RNAi in the red flour beetle (Tribolium). Cold Spring Harb Protoc *2009*, pdb.prot5256.
Pourquié, O. (1999). Notch around the clock. Curr Opin Genet Dev *9*, 559-565.
Pourquié, O. (2003). The segmentation clock: converting embryonic time into spatial pattern. Science *301*, 328-330.
Pourquié, O. (2011). Vertebrate segmentation: from cyclic gene networks to scoliosis. Cell *145*, 650-663.
Price, D.R., and Gatehouse, J.A. (2008). RNAi-mediated crop protection against insects. Trends Biotechnol *26*, 393-400.
Pueyo, J.I., Lanfear, R., and Couso, J.P. (2008). Ancestral Notch-mediated segmentation revealed in the cockroach Periplaneta americana. Proc Natl Acad Sci U S A *105*, 16614-16619.
Quan, G.X., Kanda, T., and Tamura, T. (2002). Induction of the white egg 3 mutant phenotype by injection of the double-stranded RNA of the silkworm white gene. Insect Mol Biol *11*, 217-222.
Ramos, R.G., Machado, L.C., and Moda, L.M. (2010). Fluorescent visualization of macromolecules in Drosophila whole mounts. Methods Mol Biol *588*, 165-179.
Richards, S., Gibbs, R.A., Weinstock, G.M., Brown, S.J., Denell, R., Beeman, R.W., Gibbs, R., Bucher, G., Friedrich, M., Grimmelikhuijzen, C.J., *et al.* (2008). The genome of the model beetle and pest Tribolium castaneum. Nature *452*, 949-955.

Rohr, K.B., Tautz, D., and Sander, K. (1999). Segmentation gene expression in the mothmidge Clogmia albipunctata (Diptera, psychodidae) and other primitive dipterans. Dev Genes Evol *209*, 145-154.
Rosenberg, M.I., Brent, A.E., Payre, F., and Desplan, C. (2014). Dual mode of embryonic development is highlighted by expression and function of *Nasonia* pair-rule genes. Elife ***3***, e01440.
Rosenberg, M.I., Lynch, J.A., and Desplan, C. (2009). Heads and tails: evolution of antero-posterior patterning in insects. Biochim Biophys Acta *1789*, 333-342.
Sander, K. (1976). Specification of the basic body pattern in insect embryogenesis. Advances in Insect Physiology *12*, 125-238.
Sarrazin, A.F., Peel, A.D., and Averof, M. (2012). A segmentation clock with two-segment periodicity in insects. Science *336*, 338-341.
Savard, J., Tautz, D., Richards, S., Weinstock, G.M., Gibbs, R.A., Werren, J.H., Tettelin, H., and Lercher, M.J. (2006). Phylogenomic analysis reveals bees and wasps (Hymenoptera) at the base of the radiation of Holometabolous insects. Genome Res *16*, 1334-1338.
Schmidt-Ott, U., and Lynch, J.A. (2016). Emerging developmental genetic model systems in holometabolous insects. Curr Opin Genet Dev *39*, 116-128.
Schmitt-Engel, C., Schultheis, D., Schwirz, J., Ströhlein, N., Troelenberg, N., Majumdar, U., Dao, V.A., Grossmann, D., Richter, T., Tech, M., *et al.* (2015). The iBeetle large-scale RNAi screen reveals gene functions for insect development and physiology. Nat Commun *6*, 7822.
Schneuwly, S., Klemenz, R., and Gehring, W.J. (1987). Redesigning the body plan of Drosophila by ectopic expression of the homoeotic gene Antennapedia. Nature *325*, 816-818.
Scholtz, G. (1993). Teloblasts in decapod embryos: an embryonic character reveals the monophyletic origin of freshwater crayfishes (Crustacea, Decapoda). Zoologischer Anzeiger *230*, 45-54.
Schoppmeier, M., and Damen, W.G. (2005a). Expression of Pax group III genes suggests a single-segmental periodicity for opisthosomal segment patterning in the spider Cupiennius salei. Evol Dev *7*, 160-169.
Schoppmeier, M., and Damen, W.G. (2005b). Suppressor of Hairless and Presenilin phenotypes imply involvement of canonical Notch-signalling in segmentation of the spider Cupiennius salei. Dev Biol *280*, 211-224.
Schroeder, M.D., Pearce, M., Fak, J., Fan, H., Unnerstall, U., Emberly, E., Rajewsky, N., Siggia, E.D., and Gaul, U. (2004). Transcriptional control in the segmentation gene network of Drosophila. PLoS Biol *2*, E271.
Schröder, R., Jay, D.G., and Tautz, D. (1999). Elimination of EVE protein by CALI in the short germ band insect Tribolium suggests a conserved pair-rule function for even skipped. Mech Dev *80*, 191-195.
Schönauer, A., Paese, C.L., Hilbrant, M., Leite, D.J., Schwager, E.E., Feitosa, N.M., Eibner, C., Damen, W.G., and McGregor, A.P. (2016). The Wnt and Delta-Notch signalling pathways interact to direct pair-rule gene expression via caudal during segment addition in the spider Parasteatoda tepidariorum. Development *143*, 2455-2463.

Shankland, M., and Seaver, E.C. (2000). Evolution of the bilaterian body plan: what have we learned from annelids? Proc Natl Acad Sci U S A *97*, 4434-4437.
Shaver, B., and Kaufman, P.E. (2009). Common name: hide beetle. http://entnemdept.ufl.edu/creatures/misc/beetles/hide_beetle.htm.
Shukla, J.N., and Palli, S.R. (2012). Sex determination in beetles: production of all male progeny by parental RNAi knockdown of transformer. Sci Rep *2*, 602.
Sommer, R.J., and Tautz, D. (1993). Involvement of an orthologue of the Drosophila pair-rule gene hairy in segment formation of the short germ-band embryo of Tribolium (Coleoptera). Nature *361*, 448-450.
Stahi, R., and Chipman, A.D. (2016). Blastoderm segmentation in Oncopeltus fasciatus and the evolution of insect segmentation mechanisms. Proc Biol Sci *283*.
Stamatakis, A. (2006). RAxML-VI-HPC: maximum likelihood-based phylogenetic analyses with thousands of taxa and mixed models. Bioinformatics *22*, 2688-2690.
Stamatakis, A., Hoover, P., and Rougemont, J. (2008). A rapid bootstrap algorithm for the RAxML Web servers. Syst Biol *57*, 758-771.
Stollewerk, A., Schoppmeier, M., and Damen, W.G. (2003). Involvement of Notch and Delta genes in spider segmentation. Nature *423*, 863-865.
Stuart, E.T., Kioussi, C., and Gruss, P. (1994). Mammalian Pax genes. Annu Rev Genet *28*, 219-236.
Stuart, J.J., Brown, S.J., Beeman, R.W., and Denell, R.E. (1991). A deficiency of the homeotic complex of the beetle *Tribolium*. Nature ***350***, 72-74.
Svoboda, P., Stein, P., Hayashi, H., and Schultz, R.M. (2000). Selective reduction of dormant maternal mRNAs in mouse oocytes by RNA interference. Development *127*, 4147-4156.
Tabara, H., Grishok, A., and Mello, C.C. (1998). RNAi in C. elegans: soaking in the genome sequence. Science *282*, 430-431.
Telford, M.J. (2000). Evidence for the derivation of the Drosophila fushi tarazu gene from a Hox gene orthologous to lophotrochozoan Lox5. Curr Biol *10*, 349-352.
Tenlen, J.R., McCaskill, S., and Goldstein, B. (2013). RNA interference can be used to disrupt gene function in tardigrades. Dev Genes Evol *223*, 171-181.
Timmons, L., and Fire, A. (1998). Specific interference by ingested dsRNA. Nature *395*, 854.
Travanty, E.A., Adelman, Z.N., Franz, A.W., Keene, K.M., Beaty, B.J., Blair, C.D., James, A.A., and Olson, K.E. (2004). Using RNA interference to develop dengue virus resistance in genetically modified Aedes aegypti. Insect Biochem Mol Biol *34*, 607-613.
Treisman, J., Gonczy, P., Vashishtha, M., Harris, E., and Desplan, C. (1989). A single amino acid can determine the DNA binding specificity of homeodomain proteins. Cell *59*, 553-562.
True, J.R., and Haag, E.S. (2001). Developmental system drift and flexibility in evolutionary trajectories. Evol Dev *3*, 109-119.
Turner, C.T., Davy, M.W., MacDiarmid, R.M., Plummer, K.M., Birch, N.P., and Newcomb, R.D. (2006). RNA interference in the light brown apple moth, Epiphyas postvittana (Walker) induced by double-stranded RNA feeding. Insect Mol Biol *15*, 383-391.

Ulrich, J., Dao, V.A., Majumdar, U., Schmitt-Engel, C., Schwirz, J., Schultheis, D., Ströhlein, N., Troelenberg, N., Grossmann, D., Richter, T., *et al.* (2015). Large scale RNAi screen in Tribolium reveals novel target genes for pest control and the proteasome as prime target. BMC Genomics *16*, 674.
Underhill, D.A. (2012). PAX proteins and fables of their reconstruction. Crit Rev Eukaryot Gene Expr *22*, 161-177.
van der Zee, M., Berns, N., and Roth, S. (2005). Distinct functions of the Tribolium zerknüllt genes in serosa specification and dorsal closure. Curr Biol *15*, 624-636.
van Roessel, P., and Brand, A.H. (2004). Spreading silence with Sid. Genome Biol *5*, 208.
Vanario-Alonso, C.E., O'Hara, E., McGinnis, W., and Pick, L. (1995). Targeted ribozymes reveal a conserved function of the Drosophila paired gene in sensory organ development. Mech Dev *53*, 323-328.
Veer, V., Negi, B.K., and Rao, K.M. (1996). Dermestid beetles and some other insect pests associated with stored silkworm cocoons in India, including a world list of dermestid species found attacking this commodity. Journal of Stored Products Research *32*, 69-89.
Verd, B., Clark, E., Anton, C., and Johannes, J. (2016). A damped oscillator imposes temporal order on posterior gap gene
expression in Drosophila (bioRxiv).
Wakimoto, B.T., and Kaufman, T.C. (1981). Analysis of larval segmentation in lethal genotypes associated with the antennapedia gene complex in Drosophila melanogaster. Dev Biol *81*, 51-64.
Wakimoto, B.T., Turner, F.R., and Kaufman, T.C. (1984). Defects in embryogenesis in mutants associated with the antennapedia gene complex of Drosophila melanogaster. Dev Biol *102*, 147-172.
Wang, Q., Fang, W.H., Krupinski, J., Kumar, S., Slevin, M., and Kumar, P. (2008). Pax genes in embryogenesis and oncogenesis. J Cell Mol Med *12*, 2281-2294.
Wangler, M.F., Yamamoto, S., and Bellen, H.J. (2015). Fruit flies in biomedical research. Genetics *199*, 639-653.
Werz, C., Lee, T.V., Lee, P.L., Lackey, M., Bolduc, C., Stein, D.S., and Bergmann, A. (2005). Mis-specified cells die by an active gene-directed process, and inhibition of this death results in cell fate transformation in Drosophila. Development *132*, 5343-5352.
White, R.A., and Lehmann, R. (1986). A gap gene, hunchback, regulates the spatial expression of Ultrabithorax. Cell *47*, 311-321.
Whitten, M.M., Facey, P.D., Del Sol, R., Fernández-Martínez, L.T., Evans, M.C., Mitchell, J.J., Bodger, O.G., and Dyson, P.J. (2016). Symbiont-mediated RNA interference in insects. Proc Biol Sci *283*.
Wianny, F., and Zernicka-Goetz, M. (2000). Specific interference with gene function by double-stranded RNA in early mouse development. Nat Cell Biol *2*, 70-75.
Wieschaus, E., Nusslein-Volhard, C., and Kluding, H. (1984a). Krüppel, a gene whose activity is required early in the zygotic genome for normal embryonic segmentation. Dev Biol *104*, 172-186.
Wieschaus, E., Nüsslein-Volhard, C., and Jürgens, G. (1984b). Mutations affecting the pattern of the larval cuticle in Drosophila *melanogaster*. *III. Zygo*tic loci on the X-

chromosome and fourth chromosome. Wilhelm Roux's archives of developmental biology *193*, 296-307.
Williams, T., Blachuta, B., Hegna, T.A., and Nagy, L.M. (2012). Decoupling elongation and segmentation: notch involvement in anostracan crustacean segmentation. Evol Dev *14*, 372-382.
Williams, T.A., and Nagy, L.M. (2017). Linking gene regulation to cell behaviors in the posterior growth zone of sequentially segmenting arthropods. Arthropod Struct Dev.
Wilson, M.J., and Dearden, P.K. (2012). Pair-rule gene orthologues have unexpected maternal roles in the honeybee (*Apis mellifera*). PLoS One *7*, e46490.
Xu, H., and O'Brochta, D.A. (2015). Advanced technologies for genetically manipulating the silkworm Bombyx mori, a model Lepidopteran insect. Proc Biol Sci *282*.
Xu, J., Tan, A., and Palli, S.R. (2010). The function of nuclear receptors in regulation of female reproduction and embryogenesis in the red flour beetle, Tribolium castaneum. J Insect Physiol *56*, 1471-1480.
Xu, X., Xu, P.X., Amanai, K., and Suzuki, Y. (1997). Double-segment defining role of even-skipped homologs along the evolution of insect pattern formation. Dev Growth Differ *39*, 515-522.
Yang, Y., Yang, J., Wu, W.M., Zhao, J., Song, Y., Gao, L., Yang, R., and Jiang, L. (2015). Biodegradation and Mineralization of Polystyrene by Plastic-Eating Mealworms: Part 1. Chemical and Physical Characterization and Isotopic Tests. Environ Sci Technol *49*, 12080-12086.
Yoon, K.S., Strycharz, J.P., Baek, J.H., Sun, W., Kim, J.H., Kang, J.S., Pittendrigh, B.R., Lee, S.H., and Clark, J.M. (2011). Brief exposures of human body lice to sublethal amounts of ivermectin over-transcribes detoxification genes involved in tolerance. Insect Mol Biol *20*, 687-699.
Yu, Y., Li, W., Su, K., Yussa, M., Han, W., Perrimon, N., and Pick, L. (1997). The nuclear hormone receptor Ftz-F1 is a cofactor for the Drosophila homeodomain protein Ftz. Nature *385*, 552-555.
Yu, Y., and Pick, L. (1995). Non-periodic cues generate seven ftz stripes in the Drosophila embryo. Mech Dev *50*, 163-175.
Yussa, M., Lohr, U., Su, K., and Pick, L. (2001). The nuclear receptor Ftz-F1 and homeodomain protein Ftz interact through evolutionarily conserved protein domains. Mech Dev *107*, 39-53.
Zanetti, N.I., Visciarelli, E.C., and Centeno, N.D. (2015). The Effect of Temperature and Laboratory Rearing Conditions on the Development of Dermestes maculatus (Coleoptera: Dermestidae). J Forensic Sci.
Zhang, H., Li, H.C., and Miao, X.X. (2013). Feasibility, limitation and possible solutions of RNAi-based technology for insect pest control. Insect Sci *20*, 15-30.
Zhang, Z.-Q. (2011). Animal biodiversity: An introduction to higher-level classification and taxonomic
richness. Zootaxa, 6.
Zhou, X., Wheeler, M.M., Oi, F.M., and Scharf, M.E. (2008). RNA interference in the termite Reticulitermes flavipes through ingestion of double-stranded RNA. Insect Biochem Mol Biol *38*, 805-815.

Zimmermann, T.S., Lee, A.C., Akinc, A., Bramlage, B., Bumcrot, D., Fedoruk, M.N., Harborth, J., Heyes, J.A., Jeffs, L.B., John, M., *et al.* (2006). RNAi-mediated gene silencing in non-human primates. Nature *441*, 111-114.